Polymer Microspheres for Vaccine Delivery

by

Justin Hanes

B.S. Chemical Engineering
University of California at Los Angeles, 1991

Submitted to the Department of Chemical Engineering
in partial fulfillment of the requirements for the degree of

DOCTOR OF PHILOSOPHY IN CHEMICAL ENGINEERING

AT THE

MASSACHUSETTS INSTITUTE OF TECHNOLOGY

SEPTEMBER 1996

Signature of Author _____
Department of Chemical Engineering
June 28, 1996

Certified by _____
Robert Langer
Kenneth J. Germeshausen Professor of Chemical
and Biomedical Engineering
Thesis Supervisor

Accepted by _____
Robert E. Cohen
Professor of Chemical Engineering
Chairman, Committee for Graduate Students

Polymer Microspheres for Vaccine Delivery

by

Justin Hanes

Submitted to the Department of Chemical Engineering on
June 28, 1996 in partial fulfillment of the requirements
for the degree of Doctor of Philosophy in Chemical Engineering

Abstract

The overall goal of this thesis was to develop polymeric controlled release delivery systems which could be administered either by injection or by inhalation that, by sustaining the delivery of vaccine antigens over extended periods of time, may reduce the number of vaccine doses required to achieve successful immunization (i.e., protection against infection). Poly(D,L-lactic-*co*-glycolic acid) (PLGA) and poly(anhydride-*co*-imides) were chosen as two candidate biodegradable polymers to study for vaccine delivery. PLGA is known to be very safe and is currently FDA approved for use in biodegradable surgical sutures and in various controlled release products, whereas poly(anhydride-*co*-imides) are able to incorporate derivatives of adjuvants into their polymeric backbone and therefore may be ideally suited as a matrix for vaccine antigen delivery.

In initial studies, micrometer-sized PLGA spheres (microspheres) containing a model vaccine were prepared using a double-emulsification procedure and characterized with respect to their degradation process with the ultimate goal of gaining a more thorough understanding of polymer erosion and macromolecule release from porous bulk-eroding microspheres. Recombinant glycoprotein 120 strain MN (gp120, MW ≈ 104,000), a well-characterized protein under investigation as a prophylactic vaccine for HIV-1, was used as a model antigen. Subsequently, a theoretical model based on these studies was developed for predicting the time evolution of total mass, mean molecular weight and drug release for PLGA microspheres containing a macromolecular drug, such as a protein or peptide. The use of the model is illustrated by comparison with erosion and release data from PLGA microspheres loaded with gp120.

PLGA microspheres containing a model vaccine (gonadotropin releasing hormone conjugated to tetanus toxoid, GnRH-TT) were prepared and used to immunize rats to test the ability of controlled release microspheres to reduce the number of injections needed for successful immunization. Microspheres were as effective in a single dose in eliciting systemic antibody levels as the standard three-dose immunization schedule.

To improve patient compliance and potentially decrease the cost of mass immunization programs we sought to develop vaccines that could be delivered without skilled medical personnel or the use of needles. To this end, porous PLGA microspheres were developed, some of which incorporate a major component of

lung surfactant, L,α-phosphatidylcholine dipalmitoyl (DPPC), as a method of antigen delivery to the lung via inhalation. The use of relatively light (porous) microspheres permits more efficient aerosolization and longer-lived, deep-lung-depositing PLGA aerosols; the use of DPPC further improves the performance of dry powder PLGA microsphere formulations by rendering them even more porous. Greater than 60% of DPPC-containing porous PLGA microspheres were delivered to the lung of rats in *in vivo* aerosolization studies compared with only 22% of non-porous PLGA microspheres of comparable size.

Many antigens are very poorly immunogenic, i.e., it is difficult to induce a strong immune response to them even with a well-designed controlled release system. Therefore, the final portion of this thesis was dedicated to the development of new polymers designed specifically for vaccine delivery in that they contain derivatives of adjuvants built into their backbone. To accomplish this goal, a series of anhydride-*co*-imide terpolymers based on trimellitylimido-L-tyrosine (TMA-Tyr), sebacic acid (SA), and 1,3-bis(carboxyphenoxy)propane (CPP) [poly(TMA-Tyr:SA:CPP)] was synthesized. It is desirable to incorporate tyrosine into the backbone of the polymer system due to its inherent ability to enhance the immune response to vaccine antigens. CPP and SA were copolymerized with the tyrosine derivative, TMA-Tyr, in order to develop a polymer with suitable material properties for drug delivery (e.g., high molecular weight, amorphous, and good solubility in low-boiling organic solvents), as well as to provide a series of polymers capable of a wide range of degradation and antigen release properties. Subsequently, these new polymers were used to prepare polymer microspheres capable of the controlled release of macromolecules (such as bovine serum albumin) for periods ranging from days to over one month. A close correlation between protein release and polymer weight loss was observed, suggesting a release mechanism controlled mainly by polymer erosion.

The degradation properties of poly(TMA-Tyr:SA:CPP) microspheres and *in vivo* acute toxicity of the polymer are also reported. TMA-Tyr:SA:CPP terpolymers were well-tolerated in acute toxicity studies in rats, and therefore show promise as biomaterials for vaccine delivery.

Thesis Supervisor: Robert Langer
Title: Kenneth J. Germeshausen Professor of Chemical and Biomedical Engineering

Dedicated to my wife, Molly

mother, Jayne

and

father, Harry

Acknowledgments

Special thanks to Bob Langer for his guidance and inspiration. He is truly an amazing man worthy of all the awards and honors he receives and, on a personal level, is caring and understanding. I would also like to thank him for sending me to Hawaii and Nice! It has been a pleasure and honor to work with him, and learn from him, the past several years. Thanks to my thesis committee: Linda Griffith-Cima, Bryan Roberts, and George Siber for their help, guidance, and many useful comments and discussions. Special thanks to George for welcoming me into his lab to do cell-culture experiments at the Dana-Farber Cancer Institute at Harvard.

I also am grateful to the many members of LangerLabs that I have known throughout the past few years. I thank Masatoshi Chiba for his help, friendship, and many scientific discussions over sushi in Porter Square. Thanks to David Edwards for being a stud (it is just that simple - the man is a genius). Denise Barrera, Doug Kline, and Smadar Cohen for getting me started. Rick (Medium-man) Batycky, Carmen Evora, Patrice Hildgen, Burkhard Kriwet, Giovanni Caponetti, and Jeff Hrkach for collaborations, friendship, and scientific discussions. Hongming Chen for many hours of useful discussions on vaccine delivery and for her rendition of "Kung Fu Fighting" - she's fast as lightening. Karen "Shaq" Foo for being nice and for being too chicken to shoot in water-polo when she's wide open. Giovanni Caponetti and Joe Siedel for being there to absorb most of the Cheeto-boy jokes and for our much-needed golf breaks. Tani "Ottoman" Chen for spinning the dope tunes. Tani's footprint is still on my back from the time he finally was fed up with me lingering at MIT and was forced to kicked me out of the office we shared. I hope Shaq gets my desk! I also thank Mark and Erin Johnson for friendship and taking care of "the monster" so that Molly and I could get away. Scott Coleman for his quick wit and (not-so-quick) laboratory help. Actually, Scott was great in the lab - too bad he wasn't much help to DKE's basketball team! (Just kidding fellas - truce?). Maria-Teresa Perrachia (don't think I would forget you, hon'!) for being a great friend, showing Molly and I around her beautiful hometown, Parma, Italy, and for feeding me every time I opened my mouth. And, of course, Pam Brown for running the show - she will be my first free-agent signing if/when I go into academics.

I also had a life, albeit limited, outside of MIT during my graduate-school years. I am grateful to have met dozens of great people and to have made many

good friends. Among those that I have not already mentioned, I would like to thank Mark Powers for being a great friend, roommate, and for busting the deuce before me - he and Karen Foo were especially terrific during the stretch drive of this thesis; Tom Bratkovich for the friendship and roomie thing and for going nuts with me at the Bull-Pen over UCLA games; and Phil Cali for the friend and roomie stuff, his scrumptious sauce, and for juicin' at six in the morning right outside my bedroom door (his rendition of "Baby-Man" is also much appreciated). I will also never forget the many nights Tom, Phil and I spent playing three-man poker with plenty of "cold-cock" malt liquor on hand to make it more interesting. Thanks to Bobby Padera for getting Karen Foo through the first year of classes and for his deadly backdoor cuts to the hoop. Joanne Curley and Cormac Kissane for comedy relief and all the timely pints of Guinness. Lloyd Johnston because now I have a place to stay in Australia - he also has a pretty wicked change-up. Jeff Hrkach for friendship, taking care of Sam, and for owning the paint for four years. Admiral Bill (medium-sized county) Stock-tone for his tasty margaritas and an entertaining radio show on Friday afternoons. Chris Dowd for being a good friend and for his uncanny ability to get a shot off every time he touches the basketball. Colin Wolden and Rick Batycky for friendship and for carrying me in 3-on-3 volleyball. Mark Prausnitz for helping me be a better public speaker and for his clever plan to get us a free hotel in Maui for three days. Jeff Cleland, Mike Powell, Eilene Duenas, Amy Lim, and many others at Genentech for their help, collaboration, and a nice place to stay in while I was visiting them (I hope they see this and invite me back!). And last, but not least, the people of Charlestown, MA for their hospitality.

Finally, and most importantly, I would like to thank my family, starting with the Sarber's for their support and for being great in-laws. Special thanks to John and Phyl for providing Molly and me with a great resort in Coronado, CA to visit several times a year. Brant and Carol Sarber for feeding Molly and me all the time - *Eat at Island Pasta!* Kurt and Betty Sarber for hours of tennis lessons and for being so much fun. My uncle Weaver for being a role model to me early in life (whether or not that's a good thing is still being debated). My aunt Marilynn for voting with me to see action movies instead of drippy love stories, and for being so supportive. My sister, Holly, for helping to raise me, giving me history, writing, and math lessons when I was four years old, and for having her friends protect me when I was a kid. My father for being my best man and best friend. My mom for taking me to Judo, raising me, and for making a stupid little kid believe in himself. Most of all, thanks to my wife, Molly, for her unconditional and unwavering love and support.

Table of Contents

List of Figures

List of Tables

1 Introduction

When Edward Jenner began injecting an extract of cowpox lesions into patients to prevent smallpox infection in the late eighteenth century, little could he have known how his crude inoculation would revolutionize the science of disease prevention and control. Since those humble beginnings, the science of vaccination has both spurred and adapted biotechnological advances in order to produce vaccines that are efficacious and safe.

Recent developments in the fields of protein sequencing and genetic engineering have engendered the subunit vaccine approach in which the whole-killed or attenuated infectious agents often present in vaccine preparations are replaced with a peptide or protein subunit known to elicit an effective immune response toward the parent organism. Because subunit vaccines consist of well-characterized molecules, often produced by recombinant DNA technology, and do not contain the disease-causing agent, their safety profiles are superior to conventional whole-organism vaccines in which the absence of viable infectious agents must constantly be validated. This is of particular relevance as vaccines for more serious illnesses, such as Hepatitis and HIV, are developed. Unfortunately, the improvement in safety afforded by subunit vaccines often comes at the expense of efficacy. Subunit vaccines are frequently poorly immunogenic, necessitating several booster injections in order to achieve the desired antibody response and a more frequent vaccination schedule.

In the administration of any vaccine program (subunit or conventional) the number and frequency of injections required for protection can become a crucial factor to its success. More booster injections translates into more patient visits, and patient compliance becomes a limiting factor. Usually this was considered in terms of

vaccination programs in developing countries where, even if the problems of inadequate storage and improper vaccination practices [1] could be overcome to ensure potent vaccine doses were correctly administered, the population can be nomadic or difficult to reach by health authorities. As a result, millions of people die each year in developing countries from diseases for which there exists an known vaccine, such as tetanus, measles, and pertussis [1-3]. However, recent experience has shown that patient compliance can be problematic even with conventional vaccines in an industrialized country such as the United States. Witness the recent outbreaks of measles among large numbers of unvaccinated children below five years of age and in unsuccessfully vaccinated children of school- and college-age [4]. In response to these recent epidemics, the Advisory Committee on Immunization Practices (ACIP) has set a goal for the year 2000 of 90% of children fully vaccinated (four doses of diphtheria, tetanus and pertussis, three doses of oral polio, three doses of *Haemophilus influenzae* and one dose of measles, mumps and rubella) by age two; studies show, however, that the target far exceeds the practice to date [5]. Opportunities to immunize children during contact with health-care workers (such as at hospital emergency wards) was cited as a means of improving the vaccine coverage, but in one study almost 40% of adults accompanying children to a pediatric emergency department provided inaccurate information about their measles immunization history [6]. Finally, the increase in patient visits to attain complete coverage will increase the cost of vaccination, whether it be through a private health-care provider, a local health clinic, or through subsidized mass vaccination programs on a state or national level.

Clearly, from the standpoint of disease prevention and economics, there is a demonstrated need to reduce the number of injections required for the newly developed subunit vaccines as well as the existing traditional vaccines. More important, as subunit vaccines for diseases more serious than measles are developed and the consequences of incomplete protection include death, their efficacy must be improved to as close to 100%

as possible. The primary strategy for achieving these goals is improvement of the immunogenicity of the infectious agent or subunit (the *antigen*) through the use of immunological adjuvants.

Controlled release antigen delivery systems offer an exciting addition to existing adjuvants for vaccination [2, 7, 8]. In fact, the investigation of controlled release formulations for vaccine delivery is a top priority of the World Health Organization due to their potential for reducing the number of injections required for successful vaccination. These systems slowly leak antigen into the tissues of a vaccinated individual while simultaneously serving as a repository for unreleased antigen, a phenomenon known as the depot theory of adjuvant action [9, 10]. Although the modes of action of adjuvants are not completely understood, according to the depot theory, subsequently released antigen behaves as a secondary stimulus to the sensitizing action of the antigen released earlier, often leading to a dramatic increase in protective antibody production [11].

Controlled release systems are already used in humans as "depots" to deliver an array of drugs and hormones [8] Such systems may have a tremendous impact on immunization programs since they can be designed to deliver controlled amounts of antigen continuously or in spaced pulses at predetermined rates [12-14], while simultaneously protecting undelivered antigen from rapid degradation *in vivo*. Controlled release microspheres have also shown considerable potential for oral [15-20] and pulmonary [21] immunization. The ability to deliver antigens via one of these routes would be a major advance in vaccinology as it would simplify and reduce the cost of vaccine administration. Other potential advantages of polymeric controlled release systems include: lower dosage requirements, leading to a decreased probability for adverse side effects and decreased cost; localized or targeted delivery of antigen to antigen presenting cells or the lymphatic system; more than one antigen may be encapsulated, facilitating the design of a formulation that can immunize an individual

against more than one disease, or against several epitopes of a given pathogen in a single injection; and improved patient compliance. In addition, controlled release systems may eventually reduce the number of vaccine doses required for successful vaccination to a single-injection, thus reducing the cost of immunization programs while increasing coverage.

The major accomplishments of this thesis include: (1) preparation and characterization of vaccine-containing polymer microspheres using FDA-approved lactic-*co*-glycolic acid polymers (PLGA) capable of releasing microgram quantities of vaccine in a predictable manner for extended periods of time; (2) development of a mathematical model to predict important microsphere parameters during their degradation and vaccine release, including polymer molecular weight and vaccine release kinetics; (3) demonstration that PLGA microspheres are able to reduce the number of shots to one necessary for successful immunization against a model vaccine that normally requires three doses; (4) use of PLGA polymers to produce porous microspheres capable of being delivered via the pulmonary route, a first step toward needle-free vaccines and the use of pulmonary administration to achieve heightened levels of immunity in the mucosal surfaces of the body (the site of entrance of most pathogens into the body); (5) synthesis and characterization of new polymers containing vaccine-adjuvant derivatives (tyrosine derivatives) in an attempt to engineer new polymers specifically for vaccine delivery; (6) preparation of injectable microspheres from these new tyrosine-containing polymers capable of delivering nanogram to milligram quantities of a model protein antigen over the period of days to several weeks; and (7) characterization of the degradation properties of microspheres made with these new polymers and preliminary biocompatibility studies on the polymers *in vivo*.

2 Vaccine Adjuvants

2.1 Classical Adjuvants

An adjuvant is a compound administered with the antigen, or which provides a mode of presentation of antigen, which enhances the immune response toward that antigen. The mechanisms of adjuvant action are complex, and as more is discovered about their effects on the immune system, the less likely it appears that a few theories will be able to explain the actions of the entire spectrum of adjuvant/antigen combinations. For simplicity, adjuvant action may be broken down into two general categories: (i) direct stimulatory effect on the immune system and (ii) method of antigen presentation to the immune system.

An example of the former category is muramyl dipeptide (MDP), a component of a peptidoglycan found in the cell wall of several mycobacterium strains used as adjuvants. MDP is the minimum monomeric structure which retains the adjuvanticity of the parent peptidoglycan. A water-soluble molecule, MDP has been found to interact with a variety of cells of the immune system, including B cells, T cells and macrophages. On the cellular level, MDP has a broad spectrum of activity, including mitogenicity and polyclonal B cell activation. The activity and specificity of MDP can be changed by modifications in its structure; for example, replacement of L-alanine with D-alanine causes immunosuppression. This relationship between structure and function is viewed as evidence that interactions between immune cell receptors and MDP are an integral part of its action [11].

Many adjuvants, however, do not appear to have direct interactions with immunocompetent cells. Rather, these adjuvants are hypothesized to act by affecting

the manner in which the immune system interacts with antigen. Aluminum-containing compounds such as aluminum hydroxide are the adjuvants most widely used in human vaccines and the only ones currently approved by the FDA. Antigen is adsorbed onto an aluminum hydroxide suspension and is thus injected in the context of an antigen-aluminum complex. Aluminum adsorbates have been hypothesized to work primarily by a "depot" effect by which adsorbed antigen is kept at the injection site [9] or within the peripheral lymph nodes [22] for extended periods of time and is available for more efficient processing by immunocompetent cells. Although the persistence of antigen does seem to play a role in the adjuvanticity of the aluminum salts, the depot theory has been found to be only one aspect of what appears to be a complex process involving interactions of antigen, adjuvant and the immune system [11]. For example, the antigen's conformation in association with the aluminum compound is expected to have a dramatic effect on its interaction with antigen-presenting cells. Similarly, the capacity of these cells to uptake and process antigen is directly influenced by the aluminum compounds themselves. Alum adjuvants have been found to increase the circulation of lymphocytes through draining lymphoid tissue [23], induce the production of plasma cell-containing granulomas at the injection site [11] and increase the uptake of antigen by macrophages and the resultant antigen-induced T-cell proliferation [24]. These effects, in conjunction with the depot effect, all result in more efficient processing of antigen by the immune system.

However, alum adjuvants suffer from several drawbacks which limit their commercial utility and may render them unsuitable for use in some subunit vaccines. Compared with other adjuvants, alum is a relatively weak adjuvant [25] and may not be able to sufficiently enhance the immune response toward a poorly immunogenic antigen. This problem is especially relevant to subunit vaccines. Physicochemical and morphological differences in alum vaccines due to batch-to-batch variation [26] and aging [27] can cause variability in the immune response which must be overcome by

repeated injections, in part defeating the purpose of including the adjuvant in the first place.

A family of more potent adjuvants which also utilize a depot effect are Freund's adjuvants, which are water-in-oil emulsions. Incomplete Freund's Adjuvant (IFA) consists of aqueous antigen emulsified in a low viscosity, low specific gravity mineral oil with an added emulsifier. IFA is hypothesized to act in a similar manner to aluminum compounds, but its superior adjuvanticity may be due to several factors. Because antigen may be released from within a water-in-oil emulsion more slowly than from alum [28], the depot effect of IFA is apparently more prolonged than alum. Additionally, the non-metabolizable mineral oil component of IFA is more inflammatory than alum and thus may be more potent in its stimulation of immune cells. The importance of this aspect of IFA is demonstrated when other metabolizable oils, such as peanut oil, are substituted for mineral oil; both the adjuvanticity and the intensity of local reactions were reduced [29-31]. IFA was used in an influenza vaccine in Great Britain which was withdrawn from the market after a low incidence of cyst or abscess formation at the injection site was observed [31]. Although the United States armed forces also utilized an IFA-containing influenza vaccine, no water-in-oil emulsion vaccine has ever been licensed for use in the general population in the United States [11].

Complete Freund's Adjuvant (CFA), which is IFA containing killed mycobacteria, demonstrates how the depot and immunostimulatory effects of a water-in-oil emulsion can be combined to maximize adjuvanticity. CFA was developed after Freund used mineral oil to increase the immune response to mycobacteria, the bacterium responsible for tuberculosis [32]. Subsequent studies found that killed mycobacteria-mineral oil combination could increase the immune response toward other antigens when injected in a water-in-oil emulsion and led to the development of both CFA and IFA. Analysis of the immune-stimulating properties of the bacterium

demonstrated that they are localized within the cell wall. Finally, the adjuvanticity of the whole bacterium was isolated to the subunit MDP (discussed above), which is the minimum adjuvant-active structure of the cell wall [33]. In an CFA vaccine, the mineral oil-mycobacteria phase attracts and stimulates a variety of immune cells, including macrophages, dendritic cells and lymphocytes [30], while the depot effect of the emulsion ensures that antigen is continuously present. This combination made CFA the strongest first-generation adjuvant in most applications. Unfortunately, the immunostimulatory effect of mineral oil emulsions is due in large part to a heightened local inflammatory reaction, which in the case of CFA is severe enough to cause granuloma formation, ulceration and pain at the injection site as well as systemic effects such as fever [11]. For these reasons, CFA is unsuitable for human or veterinary vaccines, and even its use in experimental animals is increasingly being restricted.

Experience with aluminum-based and Freund's adjuvants demonstrates several concepts of vaccination. Sustained delivery of antigen has been shown to improve the immune response when compared to a bolus injection of an aqueous preparation of antigen. In addition, while concomitant stimulation of the immune system via the vehicle (an aluminum adsorbate or water-in-oil emulsion) further strengthens the immune response, the magnitude of the adjuvant effect practically achievable is limited by local inflammatory reactions. Given the importance of the depot effect to the function of many adjuvants, it is not surprising that one of the first applications of the technology of controlled delivery of macromolecules from polymer systems was in the development of single-step vaccination systems.

2.2 Polymeric Sustained Delivery Systems

By releasing small amounts of macromolecules over sustained periods of time ranging from days to years, polymeric controlled release systems are able to greatly

improve the depot effect crucial to the working of adjuvants such as alum and Freund's. An advantage of these systems is that the dose and release rate can be varied by changing various parameters of each system. This allows the antigen to be reproducibly delivered according to the kinetics for optimum immune response, while antigen release from emulsions and alum adsorbates is expected to be of much shorter duration, more variable, and less easily controlled.

The first polymeric controlled delivery vaccination systems were developed with the concept of using a polymer purely as a matrix to achieve a desired release profile, with no direct effect of the polymer on the immune system desired (immuno-inert). Pellets were fabricated from poly(ethylene-vinyl acetate), a non-bioerodible polymer shown to be inert and biocompatible in previous controlled release applications, loaded with several different protein antigens and implanted subcutaneously in both mice [34] and rabbits [35]. In each case, an adjuvant effect over two injections of antigen in saline was seen, in some cases comparable to two injections of antigen in CFA.

Subsequent efforts with immuno-inert polymers sought to improve the interaction of antigen and immune system by two methods: 1) the size scale of the delivery vehicle was reduced from millimeters to microns, and 2) a bioerodible polymer (most often polyesters of lactic and glycolic acid) was employed as the matrix. These microparticular systems display many advantages over the larger implantable geometries. From a practical standpoint, particles smaller than 100 μm in diameter can be readily injected while larger systems must be surgically implanted. Because the polymer matrix is designed to erode under physiologic conditions by polymer hydrolysis and solubilization of the degradation products, device removal, usually by an invasive surgical procedure, is unnecessary. In addition, smaller microparticles, those in the size range of 1 - 10 μm, are readily phagocytosed by macrophages [36-38], the cell principally responsible for initiating the cascade of events leading to an effective humoral (i.e., antibody-mediated) immune response. Thus antigen may remain

protected by the delivery system until its targeted delivery to an antigen-presenting cell, avoiding the necessity for immediate release/desorption from the system and possible degradation. The reduced particle size and choice of a bioerodible polymer also give greater flexibility in the release kinetics possible for a given antigen dose. By such methods as varying the copolymer composition and molecular weight [39] and the fabrication conditions [13], bioerodible polymer microparticles can be designed to release antigen continuously or in a discrete pulses over long periods of time. Finally, the most commonly used bioerodible lactic/glycolic acid polyesters (PLGA) have been approved by the FDA for clinical use in a number of applications such as resorbable surgical sutures [40, 41] and sustained release of leuprolide acetate (Lupron Depot) [42].

The characteristics of bioerodible microparticle delivery systems described above make them promising candidates for use as efficacious vaccines as well as excellent tools for probing the effects of antigen release patterns and vaccine formulation parameters on the immune response. For example, Eldridge and coworkers [43] used a PLGA microsphere delivery system for staphylococcal enterotoxin B toxoid which consisted of small (1-10 μm) and larger (20-50 μm) particles administered together. The mixture of the two size ranges was able to elicit a strong secondary immune response far surpassing those resulting from the administration of either size range alone or of antigen and alum. These results support the rationale of using smaller particles, which have been found to be taken up by macrophages, to generate the primary antibody response and primed memory B cells. The larger microspheres, which cannot be phagocytosed, release their antigen more slowly and provide the long-term persistent levels of antigen which stimulate a strong, sustained secondary antibody response. A pulsatile release pattern, which mimics antigen levels obtained with multiple injections, was shown to be attainable with a single injection in a study with tetanus toxoid [14]. After one injection of a mixture of PLGA microspheres of different sizes, monomer ratios, antigen loading and method of preparation (coacervation vs. spray drying), a

strong initial antigen dose with two subsequent booster doses at 1 and 3 months was delivered. For certain strongly immunogenic antigens, this system, by reproducing the antigen levels achieved clinically with multiple injections, may provide a viable one-step vaccination system.

Polymers other than PLGA have also been used in microparticulate vaccine systems, such as gelatin [44] and microencapsulated liposomes (MEL) [45]. In the latter system, liposomes loaded with a model antigen were incorporated into ionically crosslinked alginate polymer microspheres. By protecting the liposomes from rapid degradation and clearance from the injection site, the polymer microcapsules acted as a depot for antigen and resulted in a 3 to 4-fold improvement in the antibody levels over those obtained with unencapsulated liposomes. These and other applications show that bioerodible microparticulate vaccine systems have a great potential for success in reducing the number of booster injections required for a variety of antigens.

2.3 Adjuvant-Active Polymeric Delivery Systems

In all of the microparticulate antigen delivery systems discussed above, the polymer acts merely as a matrix (depot) to allow sustained antigen release or protection and is postulated to have little or no direct effect on the immune system. If the adjuvants such as Freund's or alum are used as the paradigm of adjuvant action, the strongest adjuvants combine the antigen depot effect with a direct immunostimulatory or immunoenhancing effect. By comparison, if a polymeric microparticulate vaccine system could be designed so that the delivery system is itself immunoenhancing and releases antigen according to the optimal profile, the resulting immune response should be increased beyond that obtained with an immuno-inert release system. If so, the extra immune response obtained may be the key to eliciting sufficiently high and persistent levels of antibody for successful immunization, particularly for poorly immunogenic

antigens such as subunit vaccines. Since microparticulate delivery systems can be targeted to interact with different components of the immune system by varying their size, adjuvant-active microparticles could be designed to be phagocytosed by antigen-presenting cells and then interact with them in a specific manner while releasing antigen. Because the response of the immune system is different - subtly or grossly - for every antigen, the versatility of polymeric microparticulate release systems can be exploited to tailor a unique adjuvant-active microparticulate vaccine for each of any number of diverse antigens.

Research into this emerging field has concentrated on a variety of strategies for producing adjuvant-active polymeric microparticles. A variety of adjuvant-active microparticulate vaccine systems are discussed below. Although the ultimate goal of this research is to produce a viable vaccine, the results also provide further insight into the complex mechanisms of adjuvanticity.

2.3.1 Poly(methylmethacrylates) and Derivatives

Based on their clinical use in surgery and dentistry, non-bioerodible polyacrylates were among the first polymers suggested for use as microparticular adjuvants [46]. In a series of studies, Kreuter and co-workers used a poly(methylmethacrylate) system with an average particle size of 50 to 300 nm to investigate the adjuvant effect with influenza virus and correlate it with a number of polymer physicochemical properties. Initial efforts showed that polymerization of methyl methacrylate monomer by gamma irradiation in the presence of influenza virions resulted in a greater adjuvant effect than adsorption of the virions onto previously fabricated microparticles [47]. Coating of the virion by monomer and polymer during the polymerization process is proposed as an explanation for this

phenomenon, since no virion features can be seen on the particle surface by scanning electron microscopy [48].

The source of the adjuvanticity of this polymer system is not known. The monomer, methyl methacrylate, has been found to cause a severe inflammatory response with cell destruction and abscess formation when injected at a 1% concentration and a less intense response at 0.1% [25]. In contrast to CFA, a strong adjuvant which is hypothesized to act by a similarly intense inflammatory effect, methyl methacrylate actually suppresses the immune response when added to conventional and poly(methyl methacrylate) influenza vaccines [25]. Although repeated washing and final lyophilization were used to remove residual monomer after polymerization, it is possible that a small amount of residual monomer may cause a sub-acute inflammatory response which acts to attract and/or activate immune cells. The basis of the interactions of the poly(methyl methacrylate) particles with these cells is also not clear. Particle size was found to have a profound effect on adjuvanticity, with particles greater than 800 nm showing little or no effect [25]; this may be indicative of direct cell-particle interactions. Studies of the fate of poly(methyl methacrylate) nanoparticles after intravenous administration showed that they were taken up by the liver, spleen and bone marrow [49]. However, after intramuscular [49] or subcutaneous [50] administration, the particles remained at the injection site.

Further studies were performed by adsorbing antigen onto already prepared microparticles and correlating polymer and microparticle properties with the observed adjuvanticity. As with the copolymerized virion preparations, smaller particles were more adjuvant-active [51]. The authors note, however, that the surface area increases with decreasing particle size, an effect which is critical for systems where antigen is adsorbed. In order to investigate the effect of polymer hydrophobicity, copolymer particles of MMA with varying ratios of hydroxyethyl methacrylate (a more hydrophilic monomer) were prepared, as were particles of poly(ethylcyanoacrylate) or

poly(butylcyanoacrylate). In general, adjuvanticity increased with hydrophobicity as measured by contact angle or hydrophilic monomer content. Since cell adhesion and uptake by macrophages is improved for more hydrophobic systems, this conclusion may be considered further evidence that phagocytosis by immune cells plays a part in the poly(methyl methacrylate) vaccine system [52].

2.3.2 Non-ionic Block Copolymers

Block copolymers of poly(oxyethylene) (POE) and poly(oxypropylene) (POP) in a variety of structural configurations have been studied as potential adjuvants. Although not strictly particles per se, they have been used as vaccine adjuvants in microparticulate-like oil-in-water emulsions and are recognized for their utility in probing the mechanisms and physicochemical properties which underlie adjuvanticity.

Originally, triblock copolymers consisting of hydrophilic POE segments flanking a central hydrophobic POP segment were studied as adjuvants in aqueous suspensions [53]. By varying the lengths and proportions of the segments, polymers of varying hydrophile-lipophile balance (HLB) can be made. HLB is a parameter which is used to classify surfactants according to their relative hydrophobicity, with an HLB of 0 being hydrophobic (a spreading agent) and 18 hydrophilic (a solubilizer). These copolymers were tested as aqueous suspensions in mice for their ability to enhance primary and secondary antibody responses and delayed-type hypersensitivity (DTH) to sheep red blood cells and DNP-BSA. Two structurally similar copolymers of different molecular weight were found to be adjuvant-active toward different immune responses; the larger of the two, L121 (HLB = 0.5), enhanced the primary and secondary antibody responses toward both antigens, and the smaller copolymer, L101 (HLB = 1.0), showed adjuvant activity in the DTH reaction. Their similarities in structure but differences in action were taken as evidence that active sites on the molecule were not responsible for

stimulation of the immune system. Instead, an explanation based on the HLB was proposed to account for the fact that copolymers of higher HLB were either not adjuvant-active or suppressed the immune response [53].

Further studies utilized block copolymers in an oil-in-water emulsion system [54, 55]. Unlike in the water-in-oil emulsion adjuvants like Freund's, where antigen is concentrated within a dispersed aqueous phase, the copolymers were used to stabilize protein antigen within an oil phase and concentrate it on the droplet surface. Both L121 and L101 were found to stabilize BSA in the oil phase and improve the antibody response. L121 was a more potent adjuvant, but L101 induced more granuloma formation, which indicates that in this situation adjuvanticity cannot be completely explained by the strength of the inflammatory response. A hypothesis was presented that the oil droplet acts as a depot as well as a surface on which protein, copolymer and adsorbed host molecules (such as component C) can activate inflammatory mechanisms and be presented to the immune system in a favorable configuration [54].

To further investigate this hypothesis, triblock copolymers with POP chains flanking the POE chain (so-called reverse triblocks), octablock copolymers and triblock copolymers were tested in the oil-in-water system with a more complete characterization of the biological responses. Correlations between chemotaxis, complement activation, antigen retention at the injection site and adjuvanticity were observed. The more adjuvant-active systems also induced inflammatory responses characterized by local neutrophil infiltration and lymph node germinal center hyperplasia (a site of B-cell differentiation) as opposed to granuloma formation. From a structural standpoint, the reverse triblock copolymers showed a diminished adjuvanticity. In addition, a low HLB was found to be a necessary, but not sufficient, condition for adjuvanticity [55].

The surfaces formed by the non-ionic block copolymers were then studied by dispersing them in saline to observe the morphology or coating them onto supports for

physicochemical characterization and adsorptive behavior measurements. In comparison with the other copolymers, the most adjuvant-active copolymers were observed to form fibers with large surface area (instead of spheres) in saline, displayed more hydrophilic surfaces as determined by contact angle measurements, and adhered serum proteins less tightly. Those copolymers which induced granuloma formation were found to form crystalline surface domains that were toxic to macrophages. Copolymers with slight structural differences were used to demonstrate the effects of copolymer structure on surface properties. When the POE chains in a triblock copolymer were lengthened, the hydrophilic surface was destabilized because it was too mobile, and adsorbed proteins were shed from it. Changing the overall molecular size of a triblock copolymer but keeping the relative proportions constant changed the morphology from a fiber to a sphere because the shortened center POP chain could not fold enough to allow the hydrophilic POE chains to properly orient themselves to form a completely hydrophilic surface. This surface morphology change manifests itself in lower protein binding and lack of complement activation. Finally, antibody binding studies were used to show that antigen adsorbed onto the more hydrophilic surfaces was more accessible and thus its conformation was affected by the hydrophobicity of the surface [56].

These observations were taken as evidence that the orientation of non-ionic copolymer segments on the oil drop in the oil-in-water vaccine determines the type of surface formed and thereby influences both the orientation of antigen and adsorbed proteins and their interaction with the immune system. Therefore, the non-ionic block copolymers provide evidence that the surface morphology of an adsorption microparticulate vaccine system is another characteristic which may be investigated in order to optimize the desired immune response.

2.3.3 Tyrosine-based Adjuvants

2.3.3.1 L-Tyrosine and Its Simple Derivatives

L-tyrosine was first found to be adjuvant-active when used as an adsorbate for grass pollens as a vaccine-based treatment for hay fever [57]. Because of their low but finite water solubility (5 mg/L) [58], L-tyrosine particulates provide a relatively hydrophobic surface for antigen adsorption yet can easily be suspended in an aqueous environment. After subcutaneous injection in guinea pigs, significantly higher antibody levels were achieved with antigen-tyrosine adsorbates than with antigen in saline [57, 59]. Studies using intraperitoneal injections of radiolabeled antigen demonstrated that adsorbed antigen persisted at the injection site and its appearance in the bloodstream was delayed relative to antigen in saline [58].

L-tyrosine embodies many features which make it desirable as an adjuvant. Because it is a naturally occurring constituent of human and animal systems, the toxicity of compounds based on L-tyrosine is expected to be low. Furthermore, it is a relatively simple molecule yet has functional groups that allow a variety of chemical modifications. Indeed, the finding that L-tyrosine is adjuvant-active when used as a particulate adsorbate has been the genesis for a large volume of adjuvant research.

Since the general trend is that adjuvanticity increases with increasing hydrophobicity, simple N-acyl, O-acyl, amide and ester derivatives of L-tyrosine were tested in guinea pigs with the same grass pollen antigens [60]. The findings reproduced the correlation of hydrophobicity with adjuvanticity as the chain length of the derivative group was increased. Wheeler also found that as the hydrophobicity increased, so did the inflammatory response as measured by local lesions. In fact, the most adjuvant-active derivatives caused ulceration and were inappropriate for use in animal systems [60], evidence that the adjuvanticity of L-tyrosine and its derivatives

involves both the depot effect and immune stimulation via a local inflammatory response.

Interestingly, other researchers have shown good adjuvanticity with fewer problems with biocompatibility using the stearyl ester of L-tyrosine. Studies using recombinant hepatitis B surface antigen (HBsAg) in mice showed that stearyl L-tyrosine adsorbates produced an adjuvant effect stronger than alum in the secondary response [61]. Furthermore, antibodies of the IgG2a and IgG2b isotype were preferentially produced; these isotypes are associated with higher affinity and complement fixation [61], with the IgG2a isotype most efficient at antibody-dependent cell-mediated cytotoxicity [62]. Unlike the alum vaccine, the stearyl tyrosine adjuvant did not elicit anti-HBsAg IgE antibodies - a class of antibodies associated with immediate-type hypersensitivity [62]. Using other viral and bacterial antigens in combination with other ester analogs, Penney et al. [62] found that the adjuvant effect of stearyl tyrosine derivatives was quite antigen-specific. Stearyl tyrosine was comparable to alum with bacterial toxoids but better than alum with viral antigens. A non-aromatic derivative, stearyl glycyl glycine, was found to be more potent than stearyl tyrosine in some viral vaccines. This is noteworthy in that the adjuvant effect of tyrosine has often been explained by the presence of the aromatic moiety, which is known to be involved in T-cell recognition [63] and other immune responses [62]. The stearyl tyrosine derivative has been found to have low toxicity and pyrogenicity and does not cause granuloma formation [61], and in none of the above studies do the authors cite adverse local inflammatory reactions.

2.3.3.2 Dityrosine Monomers and Polymers

Because of the demonstrated adjuvanticity of L-tyrosine and its simple derivatives, more complex derivatives were studied for application in controlled release

of antigen. Kohn and Langer [64] synthesized a bioerodible dityrosine-based poly(iminocarbonate) for use in an implantable adjuvant-active vaccine delivery system. Such a system was envisioned to deliver antigen and enhance the immune response over an extended period of time, after which the device would degrade and be adsorbed by the body. As part of the characterization of their systems, the adjuvanticity of the monomer, *N*-benzyloxycarbonyl-L-tyrosyl-L-tyrosine hexyl ester (CTTH), in particulate form was assessed [65]. When used as an adsorbate for bovine serum albumin (BSA) in mice, CTTH was found to have an adjuvanticity comparable to that of CFA. There was no histopathological evidence of an acute or chronic inflammatory response toward CTTH particles, which were completely absent from the injection site after 56 weeks [65]. A controlled release device made of poly(CTTH-iminocarbonate) loaded with BSA was implanted subcutaneously in mice and the resulting antibody levels were compared with those from BSA/saline injections and BSA-loaded poly(bisphenyl-A-iminocarbonate) (poly(BPA)) implants. Poly(bisphenyl-A-iminocarbonate) is a polymer with the same polymerizing bond as poly(CTTH) and with similar *in vitro* BSA release profiles [66]. The antibody response from the poly(CTTH) device was superior to that of the injections or the poly(BPA) device. The intrinsic adjuvanticity of the CTTH monomer was promoted as a possible explanation for the superior adjuvanticity of the poly(CTTH) device [65].

In order to further investigate relationships between structure and adjuvanticity, a systematic investigation of the adjuvanticity of a series of dityrosine monomers and polymers when used as microparticulate adsorbates for BSA was undertaken [67]. The synthesis route of Kohn et al. [64] was used. Monomers and polymers with either benzyloxycarbonyl or t-butylcarbonyl N-terminal blocking groups, and with n-alkyl ester chains ranging from propyl to octyl, were prepared and purified to test the effect of increasing hydrophobicity on the immune response. Particulates were formed by

grinding the monomers or polymers in a mortar and pestle and sieving to less than 250 μm.

Monomer and polymer particulates were adsorbed with BSA and injected subcutaneously into mice, with BSA in saline and CFA as controls, and given as a booster injection after five weeks. In contrast to previous studies using both L-tyrosine derivatives [60] and polyacrylates [52], the derivatives with the shorter chain lengths, i.e. those which are less hydrophobic, showed the highest antibody response, in many cases statistically comparable to CFA. This trend is seen with both the monomers and the polymers. A possible explanation may lie in the size range of the particles studied. In the polyacrylate study, particles were less than 100 nm in diameter and thus easily phagocytosed by antigen-presenting cells, whereas the dityrosine particles were in the range of 50 to 250 μm and would not be expected to be taken up by immunocompetent cells. This means that antigen must be desorbed from the dityrosine particulate before it can be processed by the immune system. Therefore the enhancing effect of hydrophobicity on particle phagocytosis is not applicable to this system. Instead, the interactions of BSA and the particle surface become paramount. Adsorption of proteins onto hydrophobic surfaces is highly entropically driven and often irreversible [68, 69] and involves interactions with the hydrophobic regions of the protein [70]. In this case, a less hydrophobic surface might be expected to enhance BSA desorption, thereby leading to more continuous release of antigen at the injection site. Another aspect of antigen/particle interactions is the conformation of the adsorbed protein, as was the case with non-ionic block copolymers. A more hydrophilic surface may allow the adsorbed protein to assume a more favorable conformation for recognition by and stimulation of immune cells such as macrophages, T-cells and B-cells. Finally, as was shown in the studies of stearyl tyrosine derivatives, the effect can be highly antigen specific.

The adjuvanticity of the polymer particles does not appear to be caused by the release of intact monomer during polymer degradation. Iminocarbonate bonds can degrade via two pathways: 1) an acid-catalyzed pathway leading to transformation of the iminocarbonate bond to a carbonate bond; and 2) base-catalyzed iminocarbonate bond cleavage [66]. *In vitro* studies of dityrosine polymer particles and slabs at physiological pH show molecular weight decrease and the appearance of a carbonate shoulder on the IR spectrum, indicating that both pathways are operating. After a certain time period, the molecular weight reaches a plateau, corresponding to low oligomers, beyond which no further decrease is seen due to the stability of the carbonate bond at physiological pH. There is little or no weight loss, which would be an indication of solubilization of monomer or monomer degradation products. In fact, one year after particles were injected subcutaneously in mice, the polymers persisted at the site of injection while the monomers had disappeared completely [67].

Further development of dityrosine poly(iminocarbonate) systems, whether devices or particulates, requires improvement of the bioerodibility of the poly(iminocarbonate). One possible strategy is to influence the local pH to provide a more basic environment for polymer degradation and favor the base-catalyzed chain cleavage route. Another strategy could be to obtain polymer microparticles of a size that would be phagocytosed by antigen-presenting cells whose arsenal of degradation mechanisms would be expected to be more varied than simply pH-driven hydrolysis. These microparticles could be made as adsorbates or used to incorporate and release antigen in the same manner as the poly(lactic-glycolic acids). Toward that end, the synthesis reaction has recently been modified to increase the polymer molecular weight [71-74] so that conventional microparticulate manufacturing techniques can be applied. Naturally, the immune response toward a microparticular dityrosine system may be quite different from that seen with larger particles and remains to be seen.

2.3.3.3 Other Tyrosine-based Polymers

Poly(phosphates) of a variety of dityrosine and serine-tyrosine monomers have been synthesized and used as adsorbates for *Schistosoma japonicum* antigen [75]. The 10-μm particle adsorbates showed strong adjuvant activity comparable to CFA and antigen. Depending on the choice of blocking groups, degradation rates at physiological pH can vary from less than a week to much longer.

Due to the flexibility of polymerization of L-tyrosine-based compounds, there are almost limitless possibilities for novel L-tyrosine-containing polymers for use in microparticulate vaccine systems. As research into the L-tyrosine-mediated adjuvanticity expands the understanding of this phenomenon, polymer synthesis is expected to become more clearly directed by the desired degradation and release rates and physicochemical properties for a given application.

2.4 Incorporated Immunostimulants

A necessary aspect of any adjuvant-active microparticulate vaccination system is the delivery of antigen to the immune system over a sustained period of time. In most of the work described above, the adjuvant activity is built into the release matrix, usually a polymer. However, a less elegant but viable concept is to use the antigen delivery system itself to deliver soluble adjuvant simultaneously with antigen by incorporating them both within the release matrix. The continuous supply of antigen is available for processing and recognition by, and stimulation of, the immune system, while sustained levels of adjuvant in the vicinity of the antigen can directly stimulate such immune cells as macrophages, T-cells and B-cells. In fact, controlled release technology is tailor-made for the delivery of soluble adjuvants such as MDP, which is rapidly cleared from the body after a bolus injection [76]. The feasibility of controlled

delivery of an immunological adjuvant from a microparticulate system has been demonstrated with the release of a muramyl dipeptide derivative from PLGA microspheres for the purposes of macrophage anti-tumor activation [77]. In this work, the microspheres were designed to be phagocytosed, thereby localizing the adjuvant within the target cell. However, there is no reason why the components cannot be released extracellularly with a somewhat lower efficiency.

Preliminary work on systems of this type has been reported in the literature. In the development of an antifertility vaccine [30, 78], the formulation consists of PLGA microspheres loaded with the antigen (human chorionic gonadotropin) and nor-MDP as an adjuvant. A mixture of fast, moderate and slow release microspheres was prepared from polymers of different degradation rates and was able to stimulate antibody production for more than one year. Studies with injections of antigen and adjuvant showed that adjuvant was required during the initial immune response to elicit high antibody levels but that those levels could be sustained for up to a year thereafter with the delivery of antigen alone [30]. This finding simplifies further formulation in that the sustained delivery of adjuvant only needs to be guaranteed for the first few weeks after injection. This could be achieved by separate populations of antigen- and adjuvant-releasing microspheres designed for long- and short-term release, respectively. Additionally, a vaccine for human immunodeficiency virus type 1 (HIV-1) consisting of a subunit antigen, gp120, was encapsulated in PLGA microspheres with QS21, a purified component of a saponin adjuvant [79]. A single injection of the microsphere formulation is able to elicit higher neutralizing antibody levels than three injections of the solubilized components at much higher doses [80].

The advantages of this adjuvant strategy are its relative simplicity and the potential to use "off-the-shelf" polymers that are already in clinical use, such as PLGA. However, a key requirement is the availability of a soluble adjuvant whose immunological effects are appropriate for the antigen being delivered. Also, the

simultaneous delivery of two compounds by a release pattern which is efficacious for both involves a complex interplay of formulation parameters, such as dose and loading, polymer degradation behavior, and the chemical properties of the antigen and adjuvant. If the desired delivery patterns and doses for antigen and adjuvant are very different, optimization of their simultaneous delivery may not be practical.

2.5 Microparticulates for Mucosal Immunization

The mucosal surfaces, including the lungs, nose, and lining of the gastrointestinal (GI) tract, are the site of entry of most pathogens into the body. For this reason, the ability to induce high titers of secretory IgA (sIgA; along with IgG, sIgA is a dominant antibody subtype found on the mucosal surfaces) may be important for protection against challenge by many infectious agents. Parenteral injections of antigen are usually ineffective at stimulating production of sIgA, which is most effectively elicited by immunization of mucosal surfaces (e.g. pulmonary or oral administration). Mucosal administration of vaccines often leads to the induction of sIgA antibody production not only in the mucosa of the region immunized, but also in other mucosal surfaces of the body, including the gastrointestinal, genitourinary, and respiratory tracts. Furthermore, mucosal immunization (e.g., pulmonary or oral) offers the advantages of convenience and reduced cost of administration, and greater patient acceptance.

Since microspheres are taken up from the intestine by the Peyer's patches (PP), they have considerable potential as carriers for oral immunization [38, 81, 82]. The polymer wall of microspheres is expected to protect encapsulated vaccine from degradation by the low pH of the stomach and from proteolysis in the gut. Recent studies [15] have shown that orally administered microspheres containing SEB toxoid not only induced circulating IgM, IgG, and IgA anti-toxin antibody, but also a

disseminated mucosal IgA response in mice. In contrast, oral immunization with the same amount of fluid antigen resulted in minimal to absent antibody titers of all classes.

Microsphere size is also known to play a role in determining the type and quality of the immune response to oral immunization. Eldridge and coworkers showed that orally administered microspheres less than 10 μm in diameter are preferentially absorbed by the Peyer's patches in the GI tract and passed to the immune inductive environment of both the Peyer's patches and systemic lymphoid organs [15]. Time-course studies on the fate of the microspheres within the gut-associated lymphoid tissue showed that the majority of microspheres <5 μm in diameter were transported through the efferent lymphatics within macrophages, while the majority of those >5 μm in diameter remained in the Peyer's patches for up to 35 days [15]. This pattern of absorption and redistribution suggests that particle size may be a determinant in the type of immune response (i.e. circulating vs. mucosal) elicited by oral vaccination with antigen-containing microspheres. Microspheres with diameters <5 μm would be predicted to induce primarily a circulating immune response due to their propensity to disseminate into the systemic lymphoid tissues, while microspheres with diameters >5 μm would be expected to induce primarily a mucosal response because they remain in the IgA inductive environment of the Peyer's patches.

The extent of microsphere uptake by the Peyer's patches also seems to correlate with the effective hydrophobicity of the polymer used. Microspheres composed of polystyrene, poly(methyl methacrylate), poly(hydroxybutyrate), poly(D,L-lactide), poly(L-lactide), and of poly(D,L-lactide-*co*-glycolide) with various ratios of lactide to glycolide were all shown to be absorbed into the Peyer's patches [15]. However, the polymers with the greatest relative hydrophobicity [poly(styrene), poly(methyl methacrylate), and poly(hydroxybutyrate)] were absorbed most readily, while similar sized microspheres made of the relatively less hydrophobic polymers [poly(D,L-lactide), poly(L-lactide), and of poly(D,L-lactide-co-glycolide)] were also absorbed, but in lower

numbers. In contrast, very few or no microspheres made of ethyl cellulose, cellulose triacetate, or cellulose acetate hydrogen phthalate were taken up by the Peyer's patches.

Influenza virus proteins have also been encapsulated into microspheres and delivered orally in animals [19, 83, 84]. Mice given microencapsulated influenza A virus vaccine orally produced higher salivary IgA antibody titers which lasted longer (up to 4 months) than titers in mice given equivalent doses of free antigen [84]. Subsequently, it was shown that orally delivered microencapsulated influenza virus provided protection against viral challenge, and that the oral route boosted antibody titers which resulted from primary oral or systemic immunization [19].

Microencapsulated oral vaccines designed to protect against diarrhea induced by enterotoxigenic *E. coli* are also currently in the early stages of development. Encapsulation of a pilus protein (colonization factor antigen) in microspheres has been shown to preserve its immunogenicity upon oral administration and, subsequently, protection of rabbits from pathogen challenge has been demonstrated [16-18]. Systemic IgG and local mucosal IgA responses were elicited in animals following both intragastric and intraduodenal immunization.

Mucosal immunization has also shown a great deal of potential as a means of boosting the immune response to achieve a high level of local mucosal IgA antibody. For example, oral or intratracheal (i.t.) boosting of mice that received intraperitoneal (i.p.) primary immunizations with microencapsulated SEB toxoid was as effective at inducing disseminated mucosal IgA antitoxin antibodies as three oral doses in microspheres. On the other hand, soluble toxoid was ineffective for boosting [12]. In a subsequent study, Rhesus macaques that received two intramuscular (i.m.) primary immunizations, followed by i.t. boosting, were protected against aerosol challenge with lethal doses of SEB [85]. Monkeys receiving i.t. immunizations developed bronchial-alveolar wash anti-SEB toxin titers that were superior to those achieved by oral or i.m. boosting. This study also showed that i.m. priming with microencapsulated Simian

Immunodeficiency Virus (SIV), followed by either oral or i.t. boosting in microspheres, was capable of protecting 4 out of 6 monkeys from two vaginal challenges with 2 ID_{50} of $SIV_{mac}251$. Overall, these studies showed the potential of oral and i.t. immunization as a means of boosting the immune response generated by primary parenteral immunization.

Oral and intratracheal administration of microspheres have shown potential in the production of secretory and, to a somewhat lesser degree, circulating antibody. However, experience with controlled release systems administered via these routes of administration has been brief and no long-term studies have been done to determine the quality of protection that can be achieved. In addition, even with the use of microspheres to protect antigens from degradation in the gut and intestine, the oral route is still an inefficient way to deliver macromolecules such as subunit antigens. Further studies are needed to: (i) improve microsphere uptake in the intestine and (ii) improve the flow properties of microparticulate aerosols so that a reasonable dose of vaccine can be delivered via the pulmonary route. Studies to address the latter point are described in Chapter 7 of this thesis. In the very least, however, both oral and pulmonary administration may ultimately find use as methods of boosting the immune response to a previously parenterally administered vaccine formulation.

3 Materials and Methods

3.1 PLGA Microspheres Containing Water-Soluble Vaccines

3.1.1 Materials

Recombinant glycoprotein 120 strain MN (gp120), the envelope glycoprotein of human immunodeficiency virus type 1 (HIV-1), was supplied by Genentech, Inc., South San Francisco, CA. Poly(D,L-lactic-*co*-glycolic) acid with a molar ratio of 50:50 (PLGA 50:50, Resomer RG503) was from Boehringer Ingelheim (distributed by B.I. Chemicals, Montvale, NJ). Polyvinyl alcohol (PVA, M_W = 25,000, 88 mole % hydrolyzed) was from Aldrich Chemical Co., Milwaukee, WI. FITC-Dextran (M_W = 71,000) was from Sigma Chemical Company, St. Louis, MO. Methylene chloride was analytical grade.

3.1.2 Microsphere Preparation

A variation of the double-emulsion solvent-evaporation procedure [13, 86] was used to prepare microspheres containing water-soluble molecules. Briefly, 1.0 mL of an aqueous solution (with or without dissolved gp120 or FITC-Dextran) was emulsified into 3.0 g of polymer dissolved in 10.0 mL methylene chloride at 0°C using a vortex homogenizer (Virtis Cyclone) at 8000 RPM for 1 min. Subsequently, the first emulsion was pumped through a static mixer (Koch Engineering Co., Inc., Wichita, KS) along with an aqueous 5.0 % PVA solution at rates of 20 mL/min and 2000 mL/min, respectively, into a hardening bath (12 liters of double-distilled water at 4°C). The microspheres were stirred and allowed to harden for one to two hours at 4°C with a

sterile nitrogen flow over the top to facilitate methylene chloride evaporation. Subsequently, the microspheres were sieved using a 20 μm stainless steel sieve, and washed with 2 x 15 liters of 1 % aqueous Tween 20 solution at 4°C. The microspheres were collected by filtration and dried to constant weight by running a slow flow of dry nitrogen through them for 2-3 days. The microspheres were ground into a free-flowing powder with a mortar and pestle before use.

3.1.3 Protein Recovery from Microspheres

The amount of protein encapsulated in polymer microspheres (protein loading) was determined by digesting a known weight of microspheres in 0.1 N NaOH and determining the gp120 concentration by 1) protein assay (Micro-BCA assay, Pierce); and 2) solution absorbance at 280 nm.

3.1.4 Microsphere Size Distribution Analysis

Microsphere size distributions were determined using a Coulter Multisizer II (Coulter Electronics Limited, Luton, Beds, England). Approximately 10 drops Coulter type IA non-ionic dispersant were added, followed by 2 mL isoton II solution (Coulter), to 5-10 mg microspheres and the spheres were dispersed by brief vortex mixing. This suspension was added to 50 mL isoton II solution until the coincidence of particles was between 5 and 8 %. Greater than 50,000 particles were counted for each batch of spheres.

3.1.5 Microsphere Porosity

Microsphere and polymer porosity and density measurements were carried out by Porous Materials, Inc., Ithaca, NY. Helium pyncnometry was used to determine the density of the polymer. Non-mercury porosimetry was used to determine initial microsphere porosity (cc/g) and pore-size distribution.

3.1.6 Drug Distribution by Confocal Microscopy

For confocal microscopy, a few milligrams of microspheres containing FITC-Dextran as the drug were suspended in glycerin by brief probe sonication (Vibra-cell Model VC-250 Sonicator, 1/8" microtip probe, Sonics & Materials Inc., Danbury, CT) at output 4 (50W). A drop of the suspension was placed onto a glass slide and a glass cover slip was applied and held in place with finger nail polish. The suspension was allowed to settle for one hour before being viewed by confocal microscopy (Bio-Rad MRC-600 Confocal, Axioplan microscope). Drug distribution in microspheres was viewed before, and at various times during, *in vitro* degradation.

3.1.7 Microsphere Degradation: SEM Analysis

Microsphere morphology after preparation and at specific time points during *in vitro* degradation was observed by scanning electron microscopy (SEM) using a Stereoscan 250 MK3 microscope from Cambridge Instruments (Cambridge, MA) at 15 kV. Microspheres were freeze-dried, mounted on metal stubs with double-sided tape, and coated with gold prior to observation. The number of pores per unit area, N, on the surface of the spheres during degradation was estimated by examining SEM micrographs of degrading microspheres. The number of pores per sphere was counted visually on the visible hemispherical portion of at least 10 microspheres per time point.

The surface area of these hemispheres was calculated as equal to $2\pi r^2$, where r is the radius of the particle.

3.1.8 Microsphere Degradation: GPC analysis

Microspheres (10-30 mg) were degraded *in vitro* at 37°C in 5.0 mL 0.1M phosphate buffer, pH 7.2. There were two separate tubes of microspheres for each degradation time point. Seven time points were taken in all: t = 1 day, 4 days, 1 week, and then weekly for a total of 4 weeks. The sampling procedure was as follows: samples were removed from the incubator and centrifuged to collect the microspheres. The supernatant (containing degradation products) was removed and the pellet was washed with 5.0 mL double-distilled water. The microspheres were freeze-dried to a free flowing powder before being analyzed by gel permeation chromatography (GPC). For GPC analysis, the samples were dissolved completely in chloroform, filtered with a 0.45 μm filter, and eluted through a series of columns (Phenogel guard, linear, and 1000 Å columns, Phenomenex, Torrance, CA) using a Perkin Elmer isocratic LC 250 pump and LC30 differential refractive index detector (Perkin Elmer, Norwalk, CT). Molecular weights of the polymers were determined relative to narrow molecular weight polystyrene standards (Polysciences Inc., Warrington, PA) using Turbochem3 computer software on a DECpc 433 data station (Perkin Elmer).

3.1.9 Polymer Degradation: Polymer Mass Loss

For polymer mass loss studies, 10.0 mL of phosphate buffer (0.1M, pH 7.2) was added to each of 33 centrifugation tubes containing 250 mg of polymer. The tubes were incubated at 37°C on an orbital shaker. At various times the polymer was pelleted by centrifugation and the buffer was removed. The polymer sample was washed several

times with dd-H_2O, dried extensively under vacuum, and the solid was weighed. Each point represents the average of three samples.

3.1.10 Thermal Analysis

Thermal analysis was performed on degrading microspheres and on bulk polymer using a Perkin Elmer DSC-2 differential scanning calorimeter consisting of a DSC7 analyzer and TAC7/7 instrument controller. UNIX software was used on a DECpc 433 data station. An average sample weight of 5-10 mg was heated at heating rates ranging from 5 to 10°C/min under a flow of N_2 (30 psi).

3.1.11 *In Vitro* Release of gp120

For release experiments, 30.0 mg of microspheres were placed in a 2 mL round bottom centrifuge tube (Cryo Tubes, Nunc) and 1.0 mL of phosphate buffer containing 0.02% w/v Tween 20 (0.1 M, pH 7.2) was added. The samples were vortexed briefly at a moderate speed to disperse the spheres and placed on an orbital shaker at 37°C. To assure that sink conditions were maintained throughout the release study, the buffer was removed three times per week starting twenty-four hours after initiation of the release (i.e., day 1) by centrifuging the tube at 1500 RPM (19 cm rotor) for 5 min and collecting the supernatant. 1.0 mL fresh buffer was added, the tube was sealed, and the spheres were vortexed briefly and replaced on the orbital shaker. The collected release sample was stored at -80°C until analysis. Protein concentration of the samples was determined by protein assay (Micro-BCA Assay, Pierce, Rockford, IL) using gp120 solutions of known concentration for a standard curve. Due to the small amount of release buffer sample the micro-BCA assay was carried out on a micro-scale (50 µl sample + 50 µl BCA reagent mixture) in, for example, a 96-well low protein-binding

plate. It usually takes approximately twelve hours at room temperature before the color of the wells is intense enough to yield accurate values; the reaction was run until the absorbance of the highest standard was close to 0.9 at 560 nm. The plate was read with a plate reader at 560 nm. If more than one plate was run, a complete set of standards was run on each. All wells were done in duplicate. The "release profile" for blank microspheres was determined and subtracted from the corresponding release profile for loaded spheres to correct for interference of degradation products with the protein assay. All release samples were done in triplicate.

3.2 GnRH-TT Immunization

3.2.1 Materials

Gonadotropin releasing hormone conjugated to tetanus toxoid (GnRH-TT) was supplied by Dr. Yun-Yen Tsong at The Population Council, Center for Biomedical Research, New York, NY.

3.2.2 Determination of GnRH-TT Loading in Microspheres

An aliquot of microspheres (2.0 mg) was dissolved in 1.5 mL of acetone. After centrifugation (2000 *g*, 15 min), the residue was washed twice with 1.5 mL of acetone, collected by centrifugation, and dried. 0.5 mL of 0.01 N NaOH was added to the remaining protein and it was allowed to dissolve overnight. Protein concentration was determined by BCA protein assay (Pierce, Rockford, IL).

3.2.3 Immunization of Rats

Male Sprague-Dawley rats (275-300 g, Charles River Co., Wilmington, MA) were housed in temperature and light-controlled rooms, two animals per cage. The control group (n=8) was immunized with three intramuscular injections (at weeks 0, 4, and 8) of 100 μg GnRH-TT per rat per injection in 0.5 mL of vehicle containing 2.5% Pluronic L121 and 0.5% Tween 80 in 10 mM phosphate buffer saline. For the microsphere group (n=8), each rat was immunized with a single intramuscular injection (at week 0) of microspheres containing 200 μg GnRH-TT in addition to 100 μg soluble GnRH-TT in 0.5 mL of the saline-based injection vehicle used for the control group. Rats were bled from the tail vein at two week intervals. Sera was collected for determination of testosterone levels and anti-GnRH antibody titers.

I^{125}-GnRH (DuPont NEN, Boston, MA) was used as a tracer for determination of anti-GnRH antibody titers by radioimmunoassay (RIA) [87]. All assays were carried out in duplicate. 100 μl of radioactive tracer (about 15000 cpm) was added to 100 μl of diluted serum [1 to 100 dilution with 0.01M phosphate buffered saline (PBS) containing 1% bovine serum albumin] and the mix was incubated at room temperature for 20 hours. 200 μl of freshly prepared anti-γ-globulin (5 mg/mL in PBS) was added and mixed by vortex. 500 μl of 25% polyethylene glycol 8000 in PBS was added to each tube and centrifuged at 3000 *g* for 25 min. The supernatant was aspirated and the pellet was counted for 3 min in a gamma counter (Micromedic 4/6000 Plus automatic gamma counter). Anti-GnRH titers were calculated and expressed as nmol/L of serum based on the specific activity of the radioactive tracer as compared to a standard curve.

Serum testosterone levels were determined by RIA using a Coat-a-Count Total Testosterone Kit from Diagnostic Products Corp. (Los Angeles, CA). The sensitivity of the assays was 0.01-0.02 nmol/L. Duplicates of 50 μl aliquots of sera were used in each assay. Levels of testosterone were calculated relative to a standard curve using testosterone samples supplied with the kit.

3.3 PLGA Microspheres for Pulmonary Delivery

3.3.1 Materials

Poly(D,L-lactic-*co*-glycolic acid) with a molar ratio of 50:50 (PLGA 50:50, Resomer RG506) was obtained from Boehringer Ingelheim (distributed by B.I. Chemicals, Montvale, NJ). FITC-Dextran with an average molecular weight of 19,000, and L,α-phosphatidylcholine dipalmitoyl (DPPC) were purchased from Sigma Chemical Company, St. Louis, MO.

3.3.2 Microsphere Preparation

The double-emulsion solvent-evaporation procedure [13, 86] was modified to prepare microspheres for aerosolization. Briefly, 300 μl of an aqueous FITC-Dextran solution (50 mg/mL) was emulsified on ice into 4.0 mL polymer solution in methylene chloride (200 mg polymer) by sonication at output 3 (Model VC-250, Sonics & Materials Inc., Danbury, CT) using a microtip for 5-10 s to form the inner-emulsion. The first emulsion was poured into 100 mL 1.0 % aqueous PVA solution and homogenized (Silverson Homogenizer) at 6000 RPM using a 5/8" tip for 1 min to form the double emulsion. The microspheres were continuously stirred for 3 hours to allow hardening, collected by centrifugation, washed several times with double-distilled water, and freeze-dried into a freely flowing powder. Microspheres containing DPPC were prepared by dissolving DPPC in the polymer solution at 3 mg/mL prior to the initial emulsification.

3.3.3 Microsphere Characteristics

Particle size distributions were determined as described in section 3.1.4. Microsphere morphology was determined by scanning electron microscopy as described in section 3.1.7. Microsphere density and the density of the polymer was estimated by mercury intrusion and by helium pyncnometry, respectively, at Porous Materials, Inc. (Ithaca, NY). Microsphere porosity was determined by dividing the density of the porous microspheres by the density of the polymer phase and subtracting this value from one. Drug distribution within microspheres was determined by confocal microscopy as described in section 3.1.6.

3.3.4 Determination of Amount FITC-Dextran and DPPC Encapsulated

The amount of model drug, FITC-Dextran, encapsulated into microspheres was determined by dissolving 10.0 mg microspheres in 3.0 mL 0.8 N NaOH overnight at 37°C, filtering with a 0.45 μm filter (Millipore), and measuring the fluorescence relative to a standard curve (494 nm excitation and 525 nm emission) using a fluorimeter. The drug loading was determined by dividing the amount of FITC-Dextran encapsulated by the theoretical amount if it all were encapsulated. The amount of lung surfactant, DPPC, encapsulated into microspheres was determined by dissolving 10.0 mg of microspheres in chloroform and using the Stewart Assay [88] to determine DPPC concentration.

3.3.5 *In Vitro* Aerosolization and Inertial Deposition Behavior

The *in vitro* microparticle aerodynamic characteristics were studied using an Andersen Mark I Cascade Impactor (Andersen Samplers, Atlanta, GA) at an air flow rate of 28.3 l/min. The metal impaction plates were coated with a thin film of Tween 80 minimize particle bouncing [89]. Gelatin capsules (Eli Lilly) were charged with 20 mg

of microparticles and loaded into a Spinhaler inhalation device (Fisons, Bedford, MA). The aerosolization experiments were done in triplicate. In each experiment 10 inhalers were discharged for 30 seconds into the impactor. A 60-second interval was observed between every two consecutive aerosolizations. Fractions of microspheres deposited on each of nine stages, corresponding to stages 0 - 7 and the filter (F) of the impactor, were collected in volumetric flasks by carefully washing the plates with NaOH solution (0.8 N) in order to provide degradation of the polymer and complete dissolution of the fluorescent material. After 12 hours of incubation at 37°C, the solutions were filtered with a 0.45 μm filter and the amount of fluorescent material in each stage was measured at 494 nm (excitation) and 525 nm (emission) using a fluorimeter. Respirable fraction of the delivered dose was calculated according to the fluorescence measurements as percentages of the total fluorescence (i.e., that amount collected in stages 0 - Filter) compared with that collected in stages 2 - Filter of the Impactor.

3.3.6 *In Vivo* Particle Distribution Following Aerosolization in Rats

Male Sprague Dawley rats (150-200 g) were anesthetized using a mixture of ketamine (90 mg/kg) and xylazine (10 mg/kg). The anesthetized rat was placed ventral side up on a surgical table provided with a temperature controlled pad to maintain physiological temperature. The animal was cannulated above the carina with an endotracheal tube connected to a Harvard ventilator (Rodent Ventilator Model 683, South Natick, MA). The animal was force ventilated for 20 minutes at 300 mL/min. 50 mg of microspheres made with or without DPPC were introduced into the endotracheal tube. Following the period of forced ventilation, the animal was sacrificed and the lungs and trachea were separately washed using bronchoalveolar lavage as follows: a tracheal cannula was inserted, tied into place, and the airways were washed with 10 mL aliquots of phenol red-free Hanks balanced salt solution (Gibco, Grand Island, NY)

without Ca^{2+} and Mg^{2+} (HBSS). The lavage procedure was repeated until a total volume of 30 mL was collected. The lavage fluid was centrifuged (400 *g*) and the pellets collected and resuspended in 2 mL HBSS. 100 µl was removed for particle counting using a hemacytometer. The remaining solution was mixed with 10 mL of 0.4 N NaOH. After incubation at 37°C for 12 hours, the fluorescence of each solution was measured (wavelengths of 494 nm excitation, 525 nm emission) using a fluorimeter.

3.4 Poly(TMA-Tyr:SA:CPP) Synthesis

3.4.1 Materials

Trimellitic anhydride (TMA), L-tyrosine (Tyr), and sebacic acid (SA) were purchased from Aldrich Chemical Co. 1,3-bis(carboxyphenoxy)propane (CPP) was synthesized according to the method described by Conix [90]. Calcium carbonate (Mallinckrodt), barium oxide (EM science), and cadmium acetate hydrate (Aldrich Chemical Co.) were reduced to less than 50 µm particle size and dried in an oven at 140°C for 48 hours before use. Organic solvents were analytical grade.

3.4.2 Polymer Characterization

The molecular weight and polydispersity of the polyanhydrides were determined using a Perkin Elmer gel permeation chromatography (GPC) system equipped with a series 10 pump, 3600 data station, and an LC-25 refractive index detector (Perkin Elmer, Norwalk, CT). Samples were filtered and eluted in chloroform through a Phenogel 15µm column (Phenomenex, Torrance, CA) at a flow rate of 0.90 mL/min. The molecular weights were determined relative to polystyrene standards

(Polysciences, Warrington, PA) using CHROM2 and GPC5 computer software (Perkin Elmer).

Thermal analysis was performed using a Perkin Elmer DSC-2 differential scanning calorimeter consisting of a DSC7 analyzer and TAC7/7 instrument controllers. UNIX software was used on a DECpc 433 data station. An average sample weight of 5-10 mg was heated at heating rates ranging from 5 to 10°C/min under a flow of N_2 (30 psi).

Infrared (IR) spectroscopy was performed using a Nicolet Magna-IR 550 Spectrometer and Nicolet data station with OMNIC 1.20 software (Nicolet, Madison, WI). The samples were either film cast in chloroform onto an NaCl plate or ground and pressed into KBr pellets.

Elemental analysis (C/N/H/O) was performed by Galbraith Laboratories (Knoxville, TN).

^{1}H NMR (360 MHz) spectroscopy was performed by Spectral Data Services, Inc. (Champaign, IL). The composition of poly(TMA-Tyr:SA:CPP) was determined by using the ratio of the average intensities per proton of each of the monomers. Degree of oligomerization of acylated monomers was determined from the average intensity per proton of several representative peaks of the repeating unit and the methyl terminal protons of the acetic mixed anhydride end group.

Stability studies were performed in solid state and in anhydrous chloroform under inert atmosphere (Ar gas replaced) at 25, 4, and -20°C. The polymer molecular weight was followed by GPC with time.

3.4.3 Monomer Purification

TMA (130 g) was recrystallized from a 1:1 mixture of hot toluene and acetic anhydride (180 mL) three times before use. SA (60 g) was recrystallized three times

from ethanol (240 mL). L-tyrosine was purified by precipitation from a concentrated ammonia solution using glacial acetic acid several times before use. Briefly, tyrosine was dissolved in a large volume of ammonia, followed by slow addition of glacial acetic acid with vigorous stirring until the solution was slightly acidic (pH 6-7). The solution was kept cool using an external ice bath. The precipitated tyrosine was collected by filtration, washed extensively with water and methanol, and dried to constant weight under high vacuum. CPP was purified by extraction with acetone and ether before use.

3.4.4 Preparation of Trimellitylimido-L-tyrosine (TMA-Tyr)

TMA-Tyr was prepared using the procedure outlined by Staubli et al. [91] with a minor modification. Briefly, equimolar amounts of TMA and L-tyrosine were reacted at reflux in DMF under argon for three hours. The solution was cooled, filtered, and concentrated in vacuo at 60°C to obtain a viscous oil. Subsequently, TMA-Tyr was washed with excess warm water to remove impurities, followed by washing with excess 0.5 N HCl to remove unreacted tyrosine. The product is a white to slightly yellow powder. The yield was, in general, above 80%.

TMA-Tyr. ^{1}H NMR (DMSO-d_6): ∂ 3.17-3.4 (m, 2H, CH_2), 5.04 (m, 1H, CH), 6.53 (d, 2H, ArH), 6.92 (d, 2H, ArH), 7.98 (m, 1H, ArH), 8.20 (s, 1H, ArH), 8.36 (m, 1H, ArH), 9.17 (s, 1H, ArOH), 13.42 (s, 1H, OH), 13.68 (s, 1H, OH). IR (KBr, cm^{-1}): 3370 (OH phenol), 1777, 1723 (C=O imide), 1705 (C=O acid), 1608, 1595 (C=C aromatic), 1380 (C-N stretch). Anal. Calc: C, 60.9; H, 3.7; N, 3.9; O, 31.5. Found: C, 61.4; H, 4.0; N, 3.9; O, 31.7.

3.4.5 Preparation of Acylated Monomers

Acylation of TMA-Tyr. TMA-Tyr was added to excess acetic anhydride and heated at reflux under dry nitrogen for 15 minutes. The solution was cooled in an ice

bath, filtered, and concentrated under vacuum at 40°C. Excess acetic anhydride was extracted by swirling the product (acyl-TMA-Tyr) in anhydrous ethyl ether at room temperature. The product was left in excess anhydrous ethyl ether at -20°C overnight to allow complete precipitation. The product was then filtered and vacuum dried over calcium chloride to give a white solid (85-90 % yield). ^{1}H NMR ($CDCl_3$): ∂ 2.13, 2.28, 2.42 (s, 6H, CH_3), 2.23 (s, 3H, ester CH_3), 3.5-3.65 (m, 2H, CH_2), 5.26 (t, 1H, CH), 6.93 (d, 2H, ArH), 7.19 (dd, 2H, ArH), 7.92 (m, 1H, ArH), 8.42 (m, 1H, ArH), 8.48 (s, 1H, ArH). IR (KBr, cm^{-1}) 1824 (C=O anhydride), 1780, 1728 (C=O imide), 1609 (C=C aromatic), 1386 (C-N stretch). Anal. Calc: C, 60.1; H, 3.9; N, 3.2; O, 32.8. Found: C, 58.9; H, 4.1; N, 3.1; O, 33.5.

Acylation of SA. Purified SA was stirred into excess acetic anhydride and heated at reflux under dry nitrogen for 15 minutes. The solution was filtered and cooled in an ice bath immediately. Excess acetic anhydride was removed under vacuum at 40°C. Crude acylated SA (acyl-SA) was recrystallized from dry toluene. The crystals were then stirred in a 1:1 mixture of dry petroleum ether and ethyl ether to extract traces of acetic anhydride and toluene. The product was dried under vacuum over calcium chloride to give a white crystalline solid (75-88% yield).

^{1}H NMR ($CDCl_3$): ∂ 1.34 (m, 8H, CH_2), 1.66 (m, 4H, CH_2), 2.23 (s, 6H, CH_3), 2.45 (t, 4H, CH_2). Anal. Calc: C, 63.3; H, 8.5; N, 0.0; O, 28.3. Found: C, 62.9; H, 8.5; N, 0.0; O, 28.5.

Acylation of CPP. CPP was refluxed in excess acetic anhydride for 15 minutes under nitrogen, followed by removal of the unreacted diacid by filtration. The solution was cooled using an ice bath and concentrated under vacuum at 40°C. The product was stirred in dry ethyl ether to remove traces of acetic anhydride. Finally, acylated CPP (acyl-CPP) monomers were recrystallized from a 1:9 mixture of dimethylformamide (DMF) and ethyl ether at -20°C. Purified acyl-CPP was filtered, washed with dry ethyl ether and dried under vacuum over calcium chloride to give a white solid (40 - 50 % yield). ^{1}H NMR (DMSO-d_6): ∂ 2.25 (m, 2H, CH_2), 2.38 (s, 6H, CH_3), 4.29 (t, 4H, CH_2),

7.14 (d, 4H, ArH), 7.99 (d, 4H, ArH). Anal. Calc: C, 63.0; H, 5.0; N, 0.0; O, 32.0. Found: C, 63.4; H, 5.0; N, 0.0; O, 32.0.

3.4.6 Melt Polymerization

Acyl-TMA-Tyr, acyl-SA, and acyl-CPP were mixed in a defined ratio (with or without 1-5 mole percent catalyst) in a Kimax glass sidearm tube (2x20 cm) with a capillary nitrogen inlet. The melt polycondensation procedure outlined by Domb [92] was used to synthesize the polymers. Briefly, the tube was immersed in an oil bath at the selected temperature (120-200 °C), and the activated monomers were allowed to melt (approximately 1 minute). High vacuum was applied ($\leq 10^{-1}$ Torr) and the condensation by-product, acetic anhydride, was collected in a liquid nitrogen-chilled trap. Throughout the polymerization a strong nitrogen sweep with vigorous agitation of the melt was performed for 30 seconds every 15 minutes. At the end of the reaction, the crude polymer was removed from the glass tube and dissolved in methylene chloride. The solution was filtered to remove the heterogeneous coordination catalysts and any insoluble fractions and precipitated dropwise into excess stirred dry petroleum ether. The precipitate was collected by filtration, washed several times with anhydrous ethyl ether, and dried under vacuum at room temperature to constant weight. If the polymer was not soluble in methylene chloride, it was purified by stirring in anhydrous ethyl ether for 2 hours. ^{1}H NMR ($CDCl_3$): reported in text. IR (KBr, cm^{-1}): 2932, 2852 (C-H aliphatic), 1817 (C=O anhydride), 1784, 1727 (C=O imide), 1604, 1582 (C=C aromatic), 1380 (C-N stretch).

Poly(TMA-Tyr:SA:CPP) 20:80:0. Anal. Calc: C, 64.52; H, 7.74 ; N, 0.73 ; O, 26.55. Found: C, 62.57; H, 7.96; N, 0.69; O, 27.78.

Poly(TMA-Tyr:SA:CPP) 20:60:20. Anal. Calc: C, 65.87; H, 6.45; N, 0.84; O, 26.84. Found: C, 61.93; H, 6.47; N, 0.66; O, 30.94.

Poly(TMA-Tyr:SA:CPP) 20:50:30. Anal. Calc: C, 66.21; H, 5.75; N, 1.07; O, 26.97. Found: C, 64.38; H, 6.57; N, 0.83; O, 28.22.

Poly(TMA-Tyr:SA:CPP) 20:40:40. Anal. Calc: C, 66.68; H, 5.65; N, 0.73; O, 26.94. Found: C, 64.17; H, 5.74; N, 0.78; O, 29.31.

Poly(TMA-Tyr:SA:CPP) 20:20:60. Anal. Calc: C, 66.94; H, 5.09; N, 0.87; O, 27.10. Found: C, 65.07; H, 5.44; N, 0.84; O, 28.65.

Poly(TMA-Tyr:SA:CPP) 0:50:50. Anal. Calc: C, 66.86; H, 6.62; N, 0.0; O, 26.52. Found: C, 65.61; H, 6.64; N, 0.0; O, 27.75.

Poly(TMA-Tyr:SA:CPP) 10:80:10. Anal. Calc: C, 65.61; H, 7.40; N, 0.46; O, 26.53. Found: C, 64.93; H, 7.47; N, 0.50; O, 27.10.

Poly(TMA-Tyr:SA:CPP) 40:30:30. Anal. Calc: C, 65.97; H, 5.09; N, 1.59; O, 27.35. Found: C, 63.76; H, 5.47; N, 1.37; O, 29.40.

Poly(TMA-Tyr:SA:CPP) 60:20:20. Anal. Calc: C, 65.30; H, 4.44; N, 2.51; O, 27.75. Found: C, 62.78; H, 4.97; N, 2.13; O, 30.12.

Poly(TMA-Tyr:SA:CPP) 100:0:0. Anal. Calc: C, 63.89; H, 4.05; N, 3.36; O, 28.70. Found: C, 61.90; H, 4.02; N, 3.34; O, 30.74.

3.5 Poly(TMA-Tyr:SA:CPP) Microsphere Studies

3.5.1 Materials

Poly[trimellitylimido-L-tyrosine-*co*-sebacic acid-*co*-1,3-bis(carboxyphenoxy)propane] anhydride (abbreviated poly(TMA-Tyr:SA:CPP)) with different monomer ratios were synthesized as described in section 3.4. Poly(vinyl alcohol) (PVA; M_W = 77,000-79,000; 88 mole % hydrolyzed) was purchased from Aldrich Chemical Company, Inc., Milwaukee, WI. ^{14}C-labeled bovine serum albumin

(BSA) was obtained from Sigma Chemical Company, St. Louis, MO. All solvents were analytical grade.

3.5.2 Polymer Characterization

The molecular weight and polydispersity of the polyanhydrides were determined as described in section 3.4.2. Thermal analysis was also performed as described in section 3.4.2.

Thermal analysis was performed using a Perkin Elmer DSC-2 differential scanning calorimeter consisting of a DSC7 analyzer and TAC7/7 instrument controllers. UNIX software was used on a DECpc 433 data station. An average sample weight of 5-10 mg was heated at heating rates ranging from 5 to 10°C/min under a flow of N_2 (30 psi).

The extent of copolymer crystallinity was estimated using DSC and X-ray powder diffraction. Copolymer crystallinity was estimated from copolymer heats of fusion using the following relation [93]:

$$Xc = \frac{\Delta H_{obs}}{\sum_i W_i \Delta H_{i,\,pure}} \qquad (3\text{-}1)$$

where X_c is the percent crystallinity of the copolymers, ΔH_{obs} is the heat of fusion for each copolymer measured by DSC (calories/gram), W_i is the weight fraction of monomer i in each copolymer and

$$\Delta H_{i,\,pure} = \frac{\Delta H_{i,\,obs}}{X'_{c,\,i}} \qquad (3\text{-}2)$$

where $X'_{c,i}$ is the percent crystallinity of homopolymer i as determined by X-ray diffraction, and $\Delta H_{i,obs}$ is the heat of fusion for homopolymer i. Poly(TMA-Tyr) is completely amorphous (see Chapter 8) and therefore $\Delta H_{poly(TMA\text{-}Tyr),pure}$ is zero. For poly(SA) and poly(CPP), values obtained previously for $\Delta H_{i,obs}$ and $X'_{c,i}$ were used [93] to obtain $\Delta H_{i,pure}$: $\Delta H_{i,obs}$ = 36.6 and 26.5 cal/g and $X'_{c,i}$ = 67% and 61% for poly(SA) and poly(CPP), respectively.

3.5.3 Microsphere Preparation

Poly(anhydride-*co*-imide) microspheres were prepared by the solvent evaporation method using a double emulsion [13, 86] with minor modifications. Briefly, 100 μL of a 100 mg/mL aqueous BSA solution (W1) was pipetted into 1 mL methylene chloride containing 100 mg dissolved poly(TMA-Tyr:SA:CPP) (O). Both solutions were kept at 0°C in an ice bath prior to use. The primary emulsion (water-in-oil, W/O) was prepared by probe sonication (Model VC-250, Sonics & Materials Inc., Danbury, CT) at output 4 (50W) for 30 sec on ice. To the primary emulsion was added 2 mL of aqueous 1 % PVA solution saturated with methylene chloride, followed by vigorous mixing with a vortex mixer for 20 sec to form a double emulsion in which the W1 phase (containing the protein) is homogeneously dispersed in the O phase (containing the polymer). The resulting double emulsion was poured into 100 mL 0.1 % PVA solution and stirred for 2 hr at room temperature to allow the methylene chloride (CH_2Cl_2) to completely evaporate. Since the polymer is not soluble in water it precipitates as the CH_2Cl_2 evaporates, thereby trapping the inner water droplets (W1) containing the antigen. The hardened microspheres are subsequently collected by centrifugation (450 *g* for 5 min), washed several times with double-distilled water (dd-H_2O), suspended in 7-10 mL dd-H_2O, flash-frozen in liquid nitrogen, and freeze-dried (Freeze Dryer 8, Labconco Corp., Kansas City, MO) into a free-flowing powder

consisting of antigen homogeneously dispersed within polymer microspheres. Microspheres with different BSA loadings were prepared by changing the BSA concentration in the W1 phase.

3.5.4 Microsphere Characterization

Microsphere size distributions were determined as described in section 3.1.4. Microsphere morphology was observed by scanning electron microscopy (SEM) using a Stereoscan 250 MK3 microscope from Cambridge Instruments (Cambridge, MA) at 15-27 kV. Microspheres were freeze-dried, mounted on metal stubs with double-sided tape, and coated with gold prior to observation.

3.5.5 Microsphere Cross-Sectioning

Several milligrams of microspheres were suspended in approximately 1 mL of water, dropped onto metal stages (cryostat block holder) and frozen at -30°C. The sample was then sectioned using a cryostat (IEC Minot custom microtome, International Equipment Company, Needham Heights, MA). The shavings were collected and freeze-dried to obtain sectioned microspheres.

3.5.6 Protein Recovery from Microspheres

The amount of protein encapsulated in polymer microspheres (protein loading) was determined by digesting a known weight of microspheres in 1 N NaOH and counting the ^{14}C activity using a Liquid Scintillation Analyzer (Tri-carb 2000CA, Packard Instruments, Downers Grove, IL).

3.5.7 Microsphere Degradation Studies: GPC and IR Analysis

The rate at which the anhydride bonds were cleaved (defined as polymer *degradation*) was characterized by Infrared (IR) spectroscopy and GPC analysis. Microspheres were incubated in release buffer at 37°C at various pH. Periodically, the microspheres were collected by centrifugation, washed with dd-H_2O, and freeze-dried prior to analysis. IR spectroscopy was performed on degrading samples using a Nicolet Magna-IR 550 Spectrometer and Nicolet data station with OMNIC 1.20 software (Nicolet, Madison, WI). The samples were either film cast in chloroform onto an NaCl plate or ground and pressed into KBr pellets. In addition, the molecular weight distribution of degrading microspheres was followed using GPC.

3.5.8 *In Vitro* BSA Release Studies

For release experiments, poly(anhydride-*co*-imide) microspheres (5-10 mg) were suspended in 5.0 mL 0.1M phosphate-buffered solution (PB; pH 7.4) and incubated at 37°C on an orbital shaker. At various times the tubes were removed from the incubator, centrifuged, and the buffer collected and replaced with fresh medium. Samples were filtered using a low protein-binding, 0.22 μm filter unit (Millipore Corp., Bedford, MA) and their radioactivity was quantified using a liquid scintillation analyzer to determine the amount of BSA released. BSA release profiles from poly(TMA-Tyr:SA:CPP) microspheres were determined as a function of pH according to the same procedure. The microspheres were placed in 0.1M phosphate-buffered solution from pH 7.4 to pH 11.0, or 0.1M KCl/HCl buffer solution (pH 2.0). Release experiments were done in triplicate.

3.5.9 *In Vitro* Microsphere Weight Loss Studies

Overall microsphere erosion was quantified by following polymer weight loss with time. 30 mg of poly(anhydride-*co*-imide) microspheres were suspended in 5.0 mL 0.1M phosphate-buffered solution (PB; pH 7.4) and incubated at 37°C on an orbital shaker. At various times microspheres were collected by centrifugation, washed three times with double-distilled water, freeze-dried and weighed. Erosion experiments were done in triplicate.

3.5.10 Monomer Solubility Determination

The water solubilities of TMA-Tyr, SA, and CPP at 37°C were determined by incubating excess monomer in water with stirring. The pH was adjusted using 0.1 *M* NaOH or 0.1 *M* HCl as necessary. After 96 hours the tubes were centrifuged (5 min, 500 *g*) and the supernatant was collected and filtered with a 0.45 µm filter (Millipore Corp., Bedford, MA). The concentrations of the monomers were determined by HPLC as previously described [94].

3.5.11 Investigation of Microsphere Erosion by SEM

Microsphere morphology before, and at specific times during degradation in release buffer at 37°C, was observed by scanning electron microscopy (SEM) as described in section 3.5.4.

3.5.12 Determination of Monomer Release by HPLC

The concentrations of TMA-Tyr, SA, and CPP in release media were determined using an isocratic HPLC method described previously [94]. The mobile phase was

composed of 1200 mL acetonitrile, 1500 mL water, and 100 mL 1*M* HCl solution. The stationary phase consisted of a PRP-1 Hamilton 4.1 X 150 mm column with 5 μm particles (Rainin Instruments, Woburn, MA). SA was detected at 210 nm, CPP at 246 nm, and TMA-Tyr at 280 nm. The run time was 10 min at a flow rate of 0.8 mL/min on a Waters HPLC consisting of a M510 pump, M490 UV detector, and a Wisp 712 autosampler (Millipore).

3.6 Acute Toxicity of Poly(TMA-Tyr:SA:CPP)

3.6.1 Animals and Animal care

Preliminary biocompatibility studies of poly(TMA-Tyr:SA:CPP) polymer were performed using male Sprague-Dawley rats (Charles River Laboratories, Cambridge, MA). Animals were given laboratory rodent chow (Purina) and tap water ad libitum.

3.6.2 *In Vivo* Toxicity Study

For acute toxicity studies, 200 mg of poly(TMA-Tyr:SA:CPP) was compression molded (Carver Laboratory Press, Fred S. Carver, Inc., Menomonee Falls, WI) into 13 mm i.d. disks and implanted subcutaneously into Sprague-Dawley rats (n=4). Compression molded polymer disks were used in this study to determine the toxicity of the polymer itself, eliminating the possibility that an adverse effect could be due to incomplete removal of other molecules involved in the preparation of microspheres (e.g., polyvinyl alcohol and methylene chloride). Animals were anesthetized prior to surgery by an intraperitoneal injection of 87 mg/kg ketamine (Fort Dodge Labs, Inc., Fort Dodge, IA) and 13 mg/kg xylazine (Miles, Inc., Shawnee, KS). An area on the dorsum of the rat was shaved, swabbed with the antiseptics isopropyl alcohol and

Betadine, and draped with a sterile cloth. An incision in the dorsal flank region approximately 2.5 cm long was made using a No. 10 surgical blade and a subcutaneous pouch was opened medial to the incision using blunt-end scissors. A single polymer disk was implanted into the subcutaneous space and the wound closed with sterile wound clips (Autoclip, Clay Adams, NJ). Control rats underwent the same surgical procedure but were given no implant. Four days following implantation, the animals were sacrificed and the implant and surrounding tissue (skin, subcutis, and underlying muscle) were harvested. This polymer/tissue sample was fixed in 10% neutral buffered formalin (Mallinckrodt Specialty Chemicals). The samples were then embedded in paraffin, sectioned, and stained with hematoxylin and eosin using standard histological techniques. Histological evaluation was performed by pathologists at Biodevelopment Laboratories, Inc., Cambridge, MA.

4 PLGA Microsphere Preparation, Degradation, and Pulsatile Release of the Protein Antigen gp120

4.1 Introduction

Poly(lactic-*co*-glycolic) acid (PLGA) is the most advanced biodegradable polymer for biomedical applications as it has been used for years in degradable sutures [40, 41] and, more recently, to deliver a luteinizing hormone-releasing hormone (LHRH) peptide agonist in the form of polymer microspheres to treat prostate cancer, endometriosis, and precocious puberty (Lupron Depot®) [42, 95-97]. PLGA is very safe as it degrades in the presence of water into natural body constituents (lactic and glycolic acid). In addition, many people have studied the degradation of PLA and PLGA both *in vitro* and *in vivo* [98-101]. However, most of these studies were done on large implantable devices or on surgical sutures. Relatively little is known about the degradation of the more porous, micrometer-sized PLGA microspheres, especially in the context of macromolecule delivery [102].

Recently there has been an explosion in research utilizing degradable polymer microspheres for drug delivery applications [8, 103]. Due to advances in chemical synthesis and recombinant DNA technology, the focus of microsphere research has changed from the delivery of relatively simple low weight molecules such as steroids, to the more challenging problem of delivering complex high weight drugs such as cytokines, subunit antigens, and genetic material [8]. To be maximally effective, each molecule will require a unique formulation. In particular, molecule stability, delivery rate, and duration of delivery must all be optimized to maximize product efficacy. For example, some molecules (e.g. cytokines) may benefit from a continuous type of release,

whereas others (e.g. antigens) may require a pulsatile-type release in order to be maximally effective. Unfortunately, research aimed at understanding polymeric microsphere-based systems on a microstructural level has not kept pace with the development of new delivery systems for various molecules. As a result, most formulations are still done empirically on a trial and error basis with little a priori knowledge of the resultant microsphere degradation and protein release kinetics.

The goal of this chapter was to characterize PLGA microspheres after preparation and throughout their degradation process to advance the understanding of how polymer microspheres release therapeutic compounds. A combination of qualitative observations (microsphere morphology during degradation by SEM and drug distribution by confocal microscopy) and quantitative measurements (polymer molecular weight, glass transition temperature, degree of crystallinity, microsphere porosity and pore distribution, and macromolecule release) were performed to understand microsphere degradation and macromolecule release using PLGA copolymers. Furthermore, the analytical methods used here were chosen carefully to permit the development of a theoretical mathematical model [104] to describe microsphere degradation and release of water-soluble molecules. Recombinant glycoprotein 120 (gp120), the envelope glycoprotein of human immunodeficiency virus-1 currently under investigation as a prophylactic vaccine for HIV-1, was chosen as a model antigen in this study.

4.2 Results and Discussion

Degradation rates of PLGA microspheres depend on the ratio of lactic to glycolic acid in the polymer, polymer molecular weight and degree of crystallinity [100], and, as discussed in this chapter and in Chapter 5, microsphere porosity. As a result, various lactide/glycolide homo- and copolymers will degrade at different rates, however, the

degradation mechanism is likely the same. To more thoroughly understand this mechanism, and be able to predict microsphere degradation and polypeptide release, it is necessary to have a quantitative understanding of the physical changes the microspheres undergo during degradation. Changes in polymer molecular weight, crystallinity, thermal transition temperatures such as the glass transition temperature (T_g), polymer mass, and microsphere porosity are important and have been studied here. In addition, qualitative information about drug distribution by confocal microscopy and microsphere morphology by SEM as the particles degrade complements the quantitative analysis and helps form a clear picture of the mechanism of microsphere degradation and water-soluble drug release.

4.2.1 Microsphere Preparation and Characterization

Fig 4-1 shows an SEM image and size distribution of a typical batch of microspheres made by the double-emulsion procedure. The mass-mean diameter of this batch is 46.0 μm. The mass-mean diameter of repeat batches of spheres is 43.4 ± 5.3 μm (n=4). Notice the Gaussian size distribution, typical of microspheres made by the double-emulsion process, is interrupted around the 20 μm size. Most spheres with diameters smaller than 20 μm were removed by filtration with a 20 μm stainless steel mesh during microsphere collection. This step is performed to reduce the amount of protein released in the first few days *in vitro* (i.e., the initial burst). The yield of microspheres [= mass of microspheres / (initial mass of polymer + initial drug mass)] was 64 ± 6 % (n=4). Greater than 80 percent of the gp120 was encapsulated in every case.

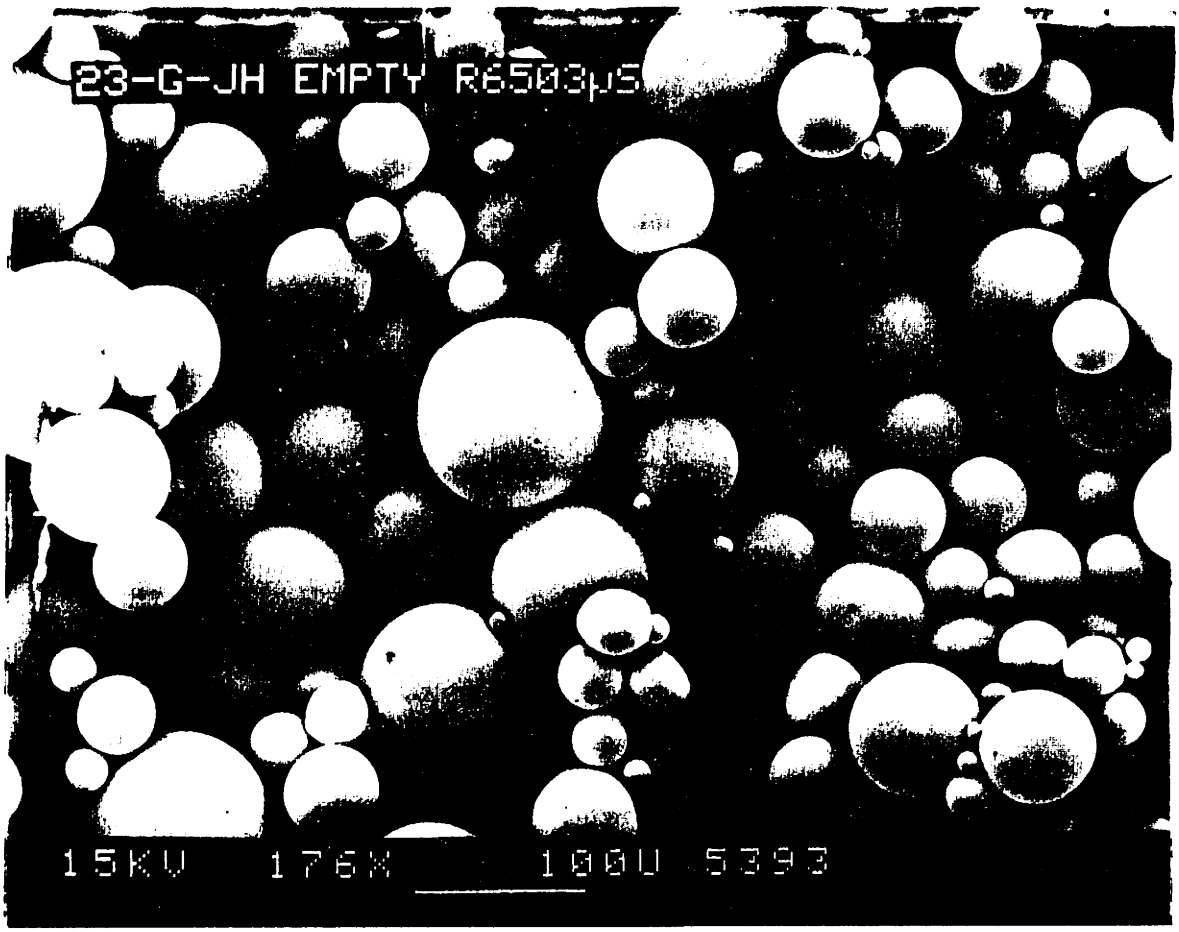

Fig 4-1a. Scanning electron microscopy photograph of a typical batch of PLGA 50:50 microspheres made by the double emulsion solvent evaporation procedure

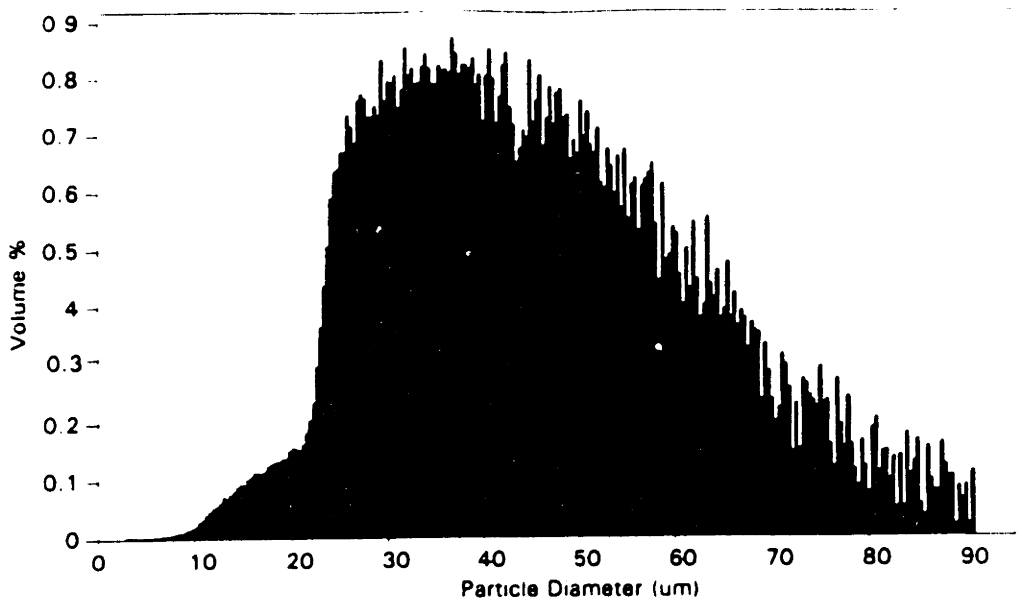

Fig 4-1b. Typical size distribution of PLGA 50:50 microspheres as determined using a Coulter Multisizer II. Notice the interruption in the Gaussian distribution around 20 μm due to filtering in the microsphere preparation process.

4.2.2 Initial Microsphere Porosity and Drug Distribution

The drug distribution within a single microsphere before any degradation has occurred is shown as a series of cross-sectional confocal microscopy images in Fig 4-2. The series was made by focusing the confocal microscope and recording images at 3.0 μm intervals throughout the sphere. The drug, in this case FITC-Dextran, is dispersed homogeneously in distinct occlusions formed during the first emulsification. The fact that dextran is distributed in distinct occlusions, as opposed to throughout the polymer matrix, suggests that the majority of pores leading away from the occlusions have diameters very near to or smaller than that of dextran (M_w = 71,000) initially.

The initial microsphere porosity (cc/g) and pore size distribution were determined by non-mercury porosimetry. Several populations of pore sizes exist within the microspheres initially. Fig 4-3 shows the volume of these pores as a function of pore diameter. Populations of pores exist at > 3 μm, 0.2 - 3 μm, 0.005 - 0.04 μm, 0.0015 - 0.005 μm, and < 0.0015. There are two populations of macropores[1] (pores with diameter > 0.3 μm) around 1 to 7 μm which most likely correspond to the internal drug occlusions. There is also a large population of mesopores (diameter 0.005 - 0.3 μm). Small mesopores, as defined here, have diameters on the order of typical polypeptides of low to moderate molecular weight. However, most importantly in terms of polypeptide release, a large volume of pores are due to micropores (diameter < 0.005 μm), pores with diameters too small to be entered by typical polypeptides such as gp120 (diameter approximately 0.012 μm). It is obvious that a single micropore takes up considerably less volume than either a meso- or macropore, however, a large percentage of the initial microsphere pore volume is due to these micropores (Table 4-1). Based on these

[1] Micro-, meso-, and macropores are terms that have been adopted to describe porous materials in the catalysis literature [105]. We have redefined these terms based on the observed porosity distribution of our microspheres and an implicit requirement that micropores possess diameters smaller than most polypeptides, including gp120.

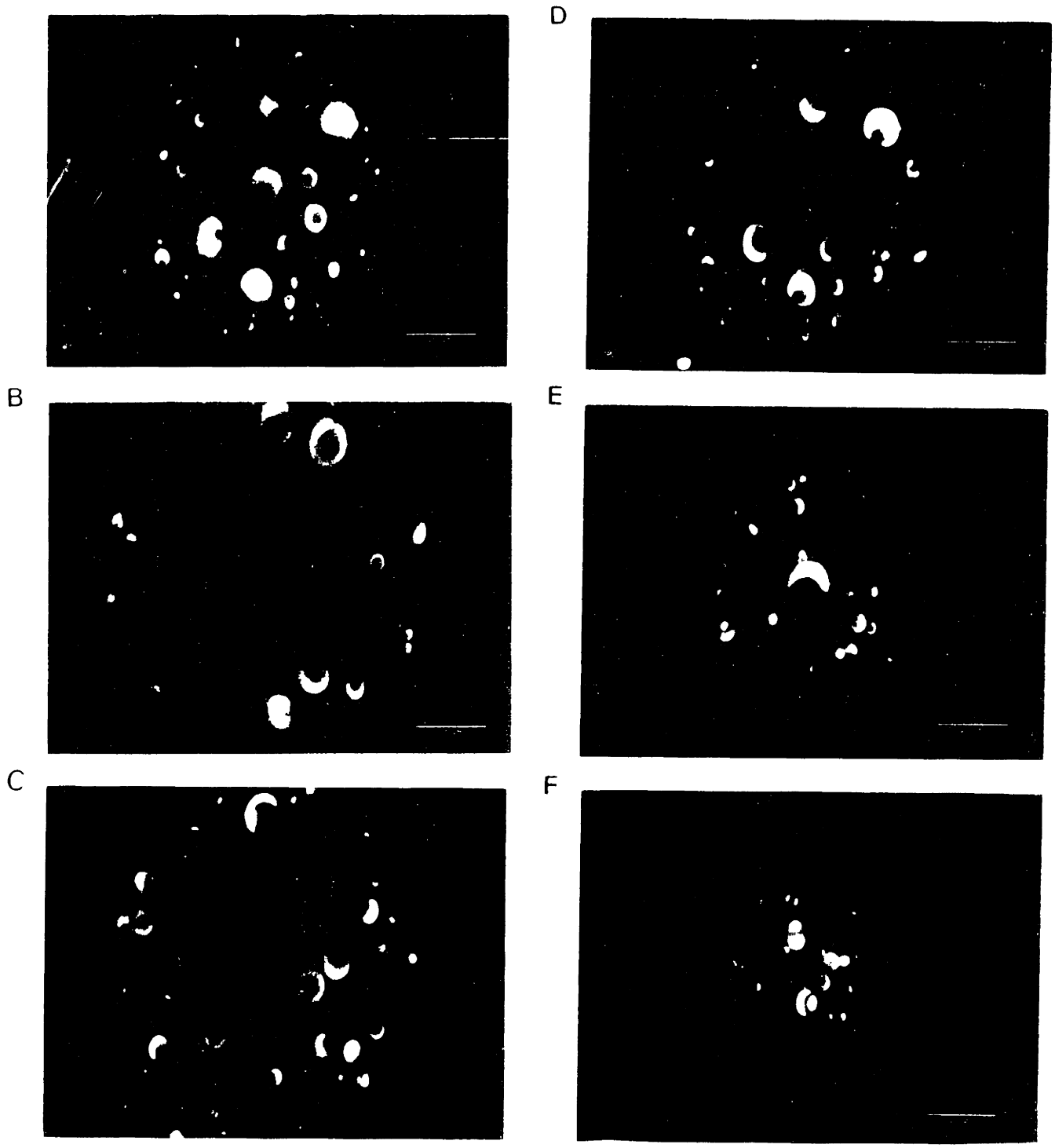

Fig 4-2. Series of confocal micrographs showing the *drug distribution in a single microsphere* before any degradation has taken place. The series was made by first focusing the microscope and recording the image at an arbitrary point in the microsphere (4-2a), and then continuing to focus and record images at 3 μm intervals throughout the sphere (4-2b-f). Only the drug, in this case FITC-Dextran, is visible in this confocal image.

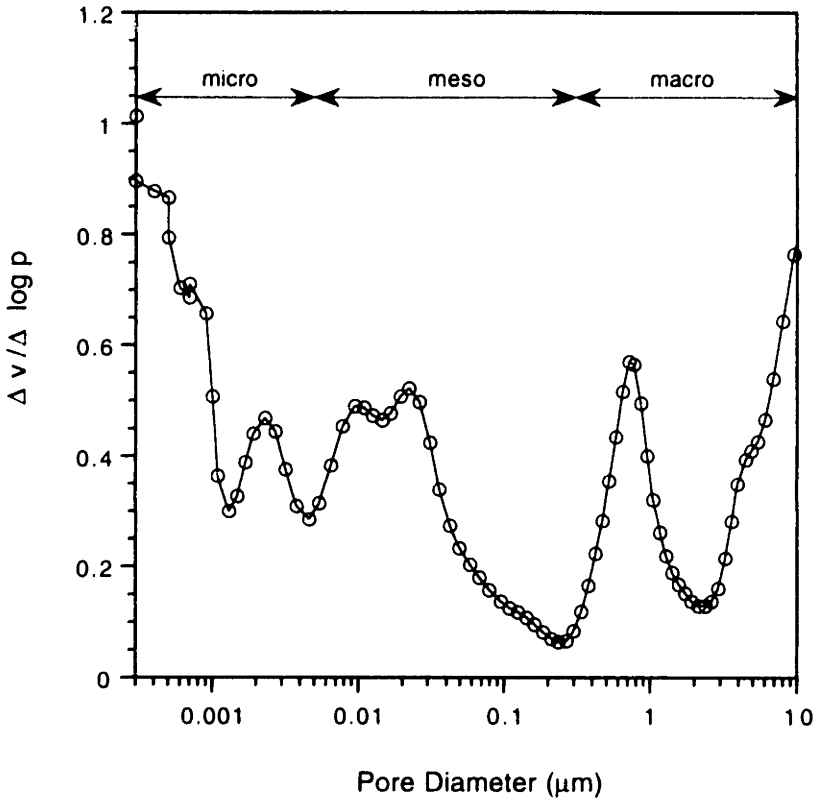

Fig 4-3. Non-mercury porosimetry plot showing the various populations (by volume percent) of pore sizes within the microspheres. Micro-, meso-, and macropores are defined as pores with diameters of < 0.005 μm, 0.005 - 0.3 μm, and > 0.3 μm, respectively. Pores smaller than 0.0003 μm were deemed too small to be accurately measured. "Pores" larger than 10 μm are due to spaces in between microspheres, as confirmed by confocal microscopy, and are therefore excluded from this analysis.

confocal and porosity experiments, Fig 4-4 shows a proposed model for the initial porosity of microspheres.

Table 4-1. Pore Size Distribution of the Initial Porosity of PLGA Microspheres[a]

Pore Classification	Pore Diameter (μm)	% of Initial Pore Volume[b]
Micro	0.0003 - 0.005	37.6
Meso	0.005 - 0.3	31.6
Macro	0.3 - 10	30.8

a Total intrusion volume initially = 1.6 cc/g. Initial microsphere porosity ≈ 50%.

b Pores larger than 10 μm were considered spaces in between microspheres (as confirmed by confocal microscopy) and pores smaller than 0.0003 μm were considered too small to be accurately detected. Therefore, these "pores" were not considered as part of microsphere porosity.

4.2.3 Microsphere Morphology During Degradation by SEM

Fig 4-5 shows scanning electron micrographs of a typical batch of PLGA microspheres during *in vitro* degradation in phosphate buffer, pH 7.2. Before any degradation has taken place the spheres have relatively dense inner cores and smooth external surfaces with few visible surface pores (N_0 = 1 x 10^{-4} μm^{-2}). It is important to point out that, in this study, visual resolution of surface pores using SEM pictures is confined to pore diameters approximately larger than 0.5 μm. At higher magnifications the intensity of the electron beam often distorts or destroys the microparticles. Also, it is important to realize that microparticles are coated with a layer of gold prior to

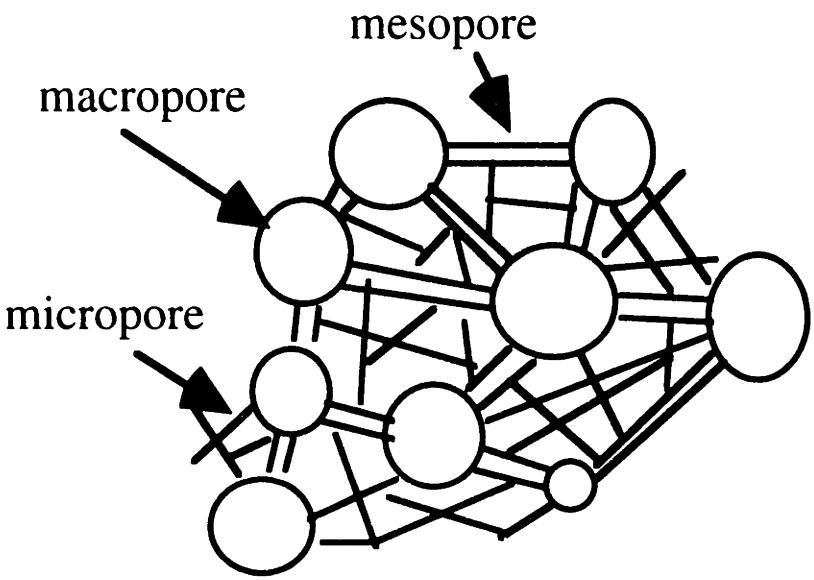

Fig 4-4. Schematic diagram of the proposed internal pore structure of a microsphere made by the double emulsion procedure. Macropores correspond to the occlusions formed by the first emulsification which contain the drug initially. Micropores <0.005 μm, Mesopores 0.005-0.3 μm, Macropores > 0.3 μm.

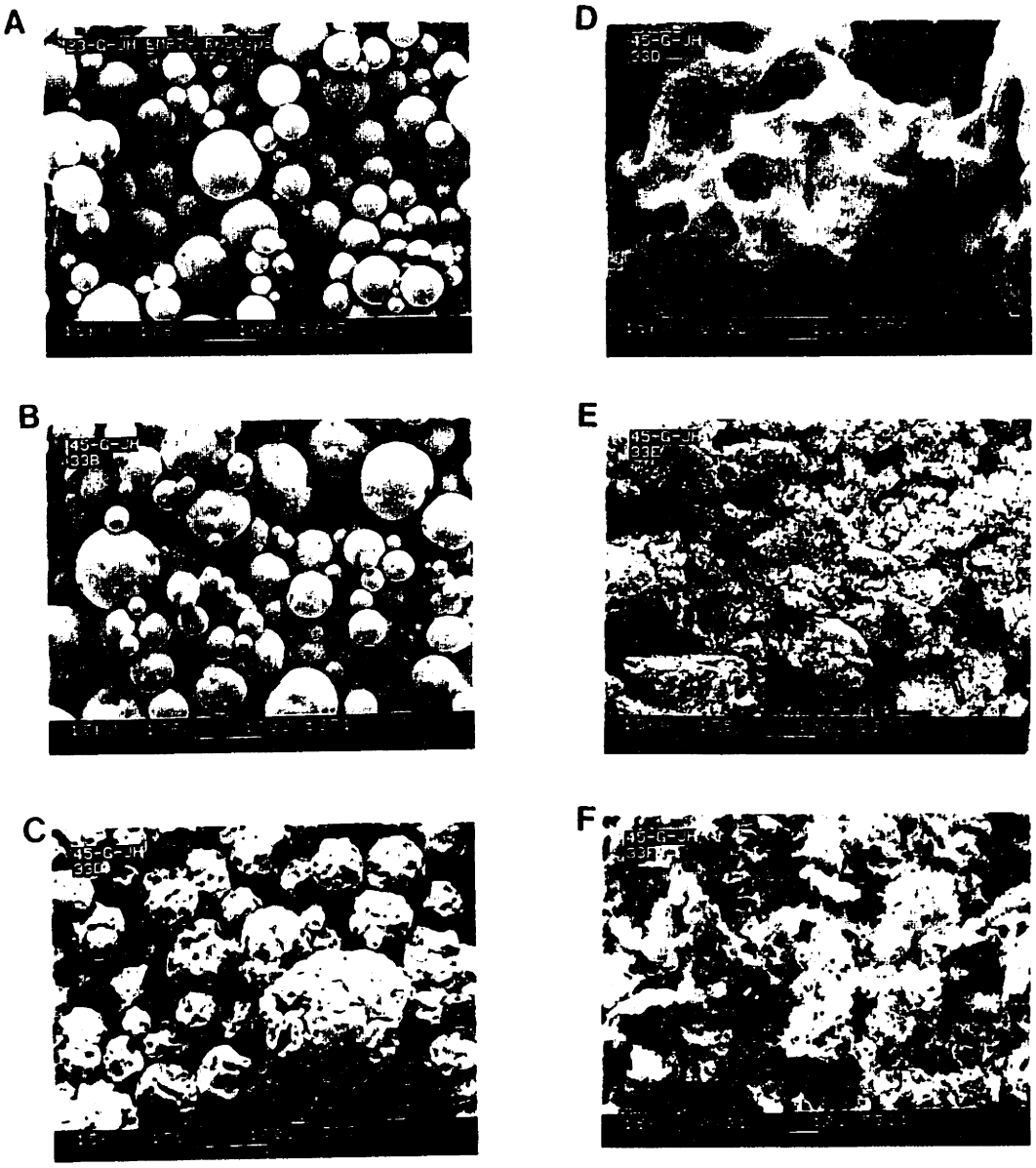

Fig 4-5. Series of SEM photographs showing the evolution of degrading PLGA microspheres: (a) microspheres before degradation; (b-f) microspheres after 4, 15, 15 (close-up), 26, and 37 days *in vitro* at 37°C. The microspheres are undergoing bulk-erosion characterized by a steady widening of pores present initially.

observation by SEM which can further obscure the existence of small meso- and micropores on their surface. Having said this, the *observable* surface pores have relatively small diameters initially compared with particles that have undergone various degrees of *in vitro* degradation (Fig 4-5). After five days in degradation medium the surfaces are still smooth, but the observable surface pores have grown noticeably in diameter and number (N_5 = 4 x 10^{-4} μm^{-2}, Fig 4-5 and 4-6). Diffusion of water toward the center of the particles through free molecular volume in the copolymer phase, or micro- and mesopores, accompanies a steady expansion or coalescence of pores as the polymer degrades and erodes. Thus, the increase in the number of observable pores per unit area is postulated to be due to the expansion and/or coalescence of pre-existing micro- and mesopores on the sphere surface which were originally too small to observe by SEM. This expansion and/or coalescence of pores is presumed to be occurring throughout the microspheres. By day 15 observable surface pores have grown appreciably in diameter and number (N_{15} = 11 x 10^{-4} μm^{-2}) as the particle begins the process of bulk erosion, that is, simultaneous degradation and erosion uniformly throughout the interior of the microsphere (Fig 4-5c). The invaginations on the sphere surfaces shown in Fig 4-5c may be caused in part by the collapse of vacuum-dried particles which have been partially eroded in their interior. After 26 days of degradation, very few distinct spheres are noticeable, even though a significant percentage of the polymer mass remains (Fig 4-5e). The polymer is of low molecular weight at this stage ($M_w \approx$ 10,000, PDI $\approx$ 1.3) and, as a result, has a low glass transition temperature. The polymer is also rubbery at this stage (T_g < 37°C, see thermal analysis section), enabling a large fraction of the spheres to fuse together (Fig 4-5e). By day 37, only skeletons of polymer spheres remain (Fig 4-5f).

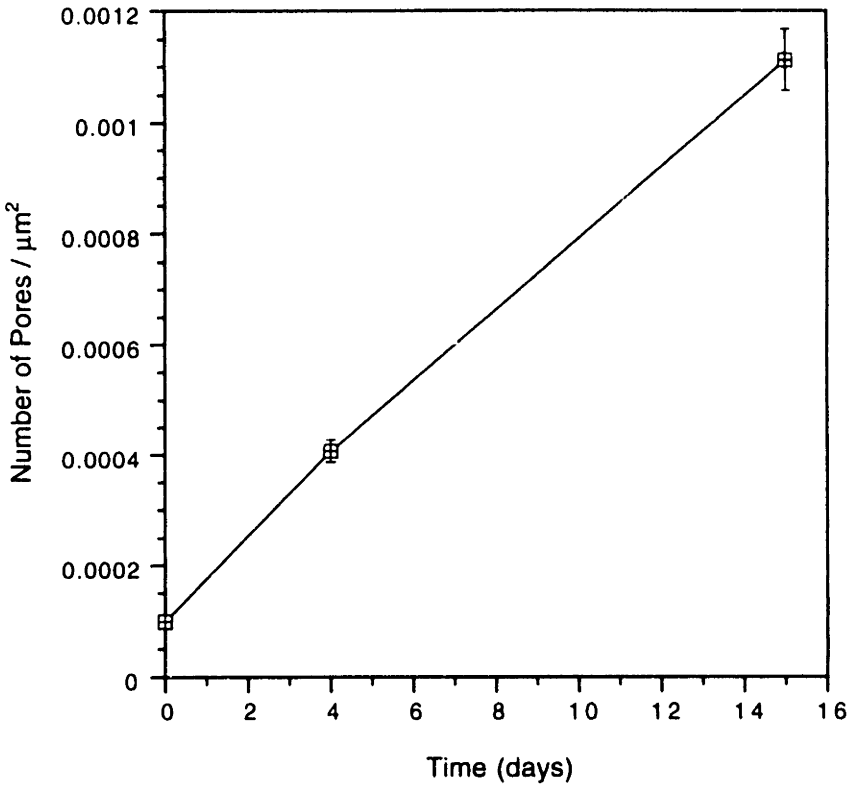

Fig 4-6. Number of pores visible by scanning electron microscopy on the surface of degrading microspheres at various times throughout degradation *in vitro* at 37°C. As degradation proceeds, preexisting pores on the surface (and throughout the microspheres) widen, explaining the increase in visible pores on the surface with time.

4.2.4 Drug Distribution During Microsphere Degradation by Confocal Microscopy

Fig 4-7 compares a series of confocal microscopy images to light microscopy images of a partially degraded microsphere (t = 7 days). The confocal images (on the left) show the drug distribution after 7 days in degradation/release media (only drug is visible), whereas the light microscopy images (on the right) show only the microsphere structure (drug not visible). It is apparent that after several days in release media the drug occlusions seen initially in Fig 4-2 are almost completely depleted of drug. The drug has apparently diffused from the occlusions into small water-filled mesopores, as evidenced by the fine distribution of FITC-Dextran throughout the sphere shown in Fig 4-7. Subsequent controlled release of macromolecular species is evidently controlled by the inability of protein to penetrate microporous barriers during its diffusion out of the microparticle.

4.2.5 Microsphere Degradation Analysis by GPC

As confirmed by GPC, preparation of the microspheres does not cause a loss in polymer MW. In fact, over the first day of "degradation", there was a modest increase in polymer M_w and M_n (Fig 4-8). This increase, although moderate, was consistently seen in these studies. This phenomenon is most likely explained by the dissolution and diffusion from the particle of monomers and low-weight oligomers present initially in pores (micro, meso, and macro) leading to the sphere surface. This is reflected in the increase in weight average molecular weight after one day in degradation medium. This explanation is supported by the accompanying decrease in M_w/M_n (the polymer polydispersity index) over the first day (from 1.85 to 1.71). Following this modest initial rise in MW, polymer MW decays slowly (Fig 4-8). The fact that significant polymer degradation occurs within only a few days of exposure to release buffer suggests that

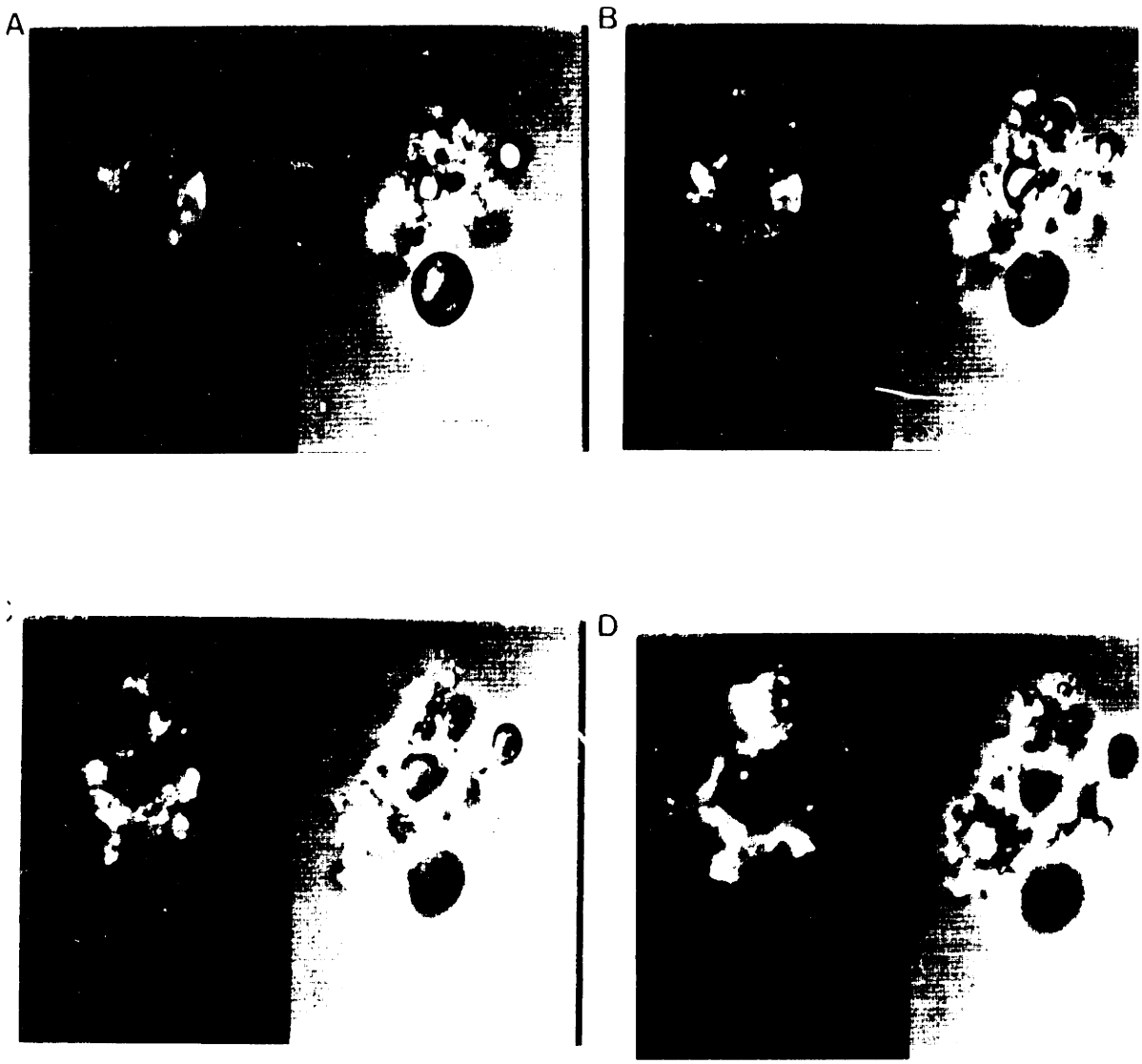

and light microscopy images showing the corresponding microsphere morphology (right), of a single microsphere (containing FITC Dextran as the drug) after 7 days in degradation release media at 37 C. The series was made as in Fig 4.2. Note that there is no drug (shown on left) in the position of large occlusions (shown on right) at this time.

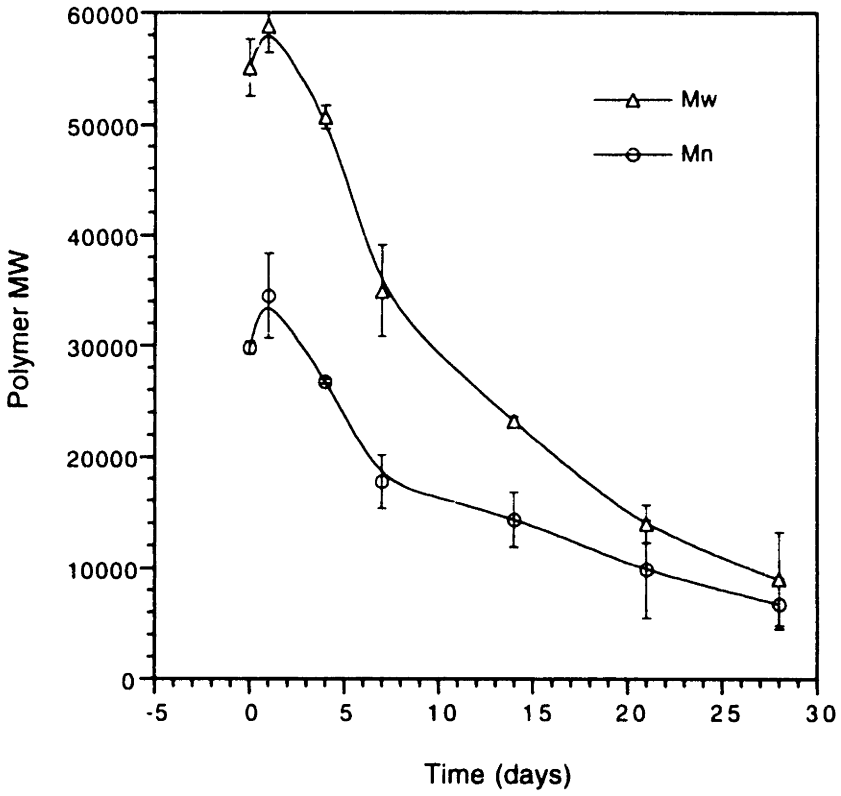

Fig 4-8. PLGA microsphere degradation profile *in vitro* at 37°C as determined by gel permeation chromatography.

water uptake by the spheres occurs quickly and, subsequently, ester bond hydrolysis is the rate limiting step in polymer degradation.

4.2.6 Thermal Analysis

Thermal transition temperatures of polymer microspheres and bulk PLGA polymer were characterized by differential scanning calorimetry (DSC) before, and at various times during, degradation in release buffer at 37°C. Bulk polymer (i.e., as received from manufacturer) was analyzed as a control (n=3) since it was relatively plentiful. Fig 4-9 shows that polymer T_g decreased as a function of degradation time. In the case of bulk polymer the decrease was approximately linear with time, corresponding with the decrease in polymer molecular weight. The T_g of the microsphere's polymer was slightly more variable, possibly due to the smaller sample and that each point represents a single experiment (n=1). Nevertheless, the values and trend of the data are similar to the bulk polymer case. DSC scans from 25°C to 200°C showed no evidence of melt transitions in any of the samples, indicating that the polymers were amorphous throughout degradation.

4.2.7 Polymer Mass Loss During *In Vitro* Degradation

Polymer mass loss during incubation in release buffer at 37°C is shown in Fig 4-10. A small weight loss in the first day confirms the presence of water-soluble monomers or oligomers in the polymer initially. There is a slight increase in weight of the solid phase over the next few days which is likely due to a combination of the addition of one molecule of water for every ester bond broken and the presence of residual water not removed during freeze-drying. There is very little polymer mass loss during the first 14 days of incubation (Fig 4-10) even though the polymer is decreasing

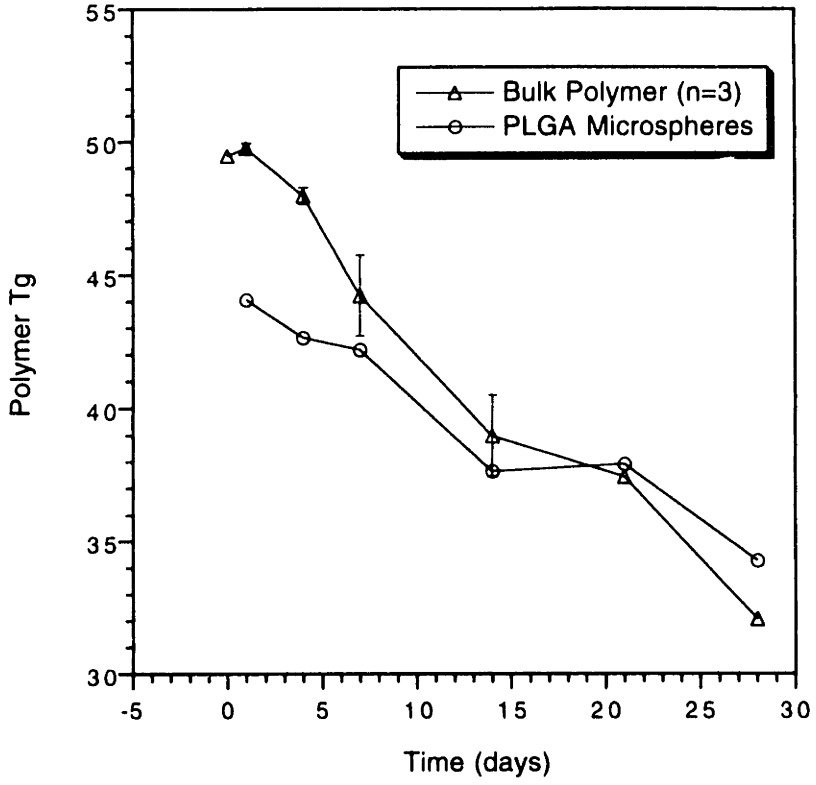

Fig 4-9. Polymer glass transition temperature of PLGA microspheres and of bulk PLGA polymer (i.e., polymer as received from the manufacturer) at various times during degradation *in vitro* at 37°C.

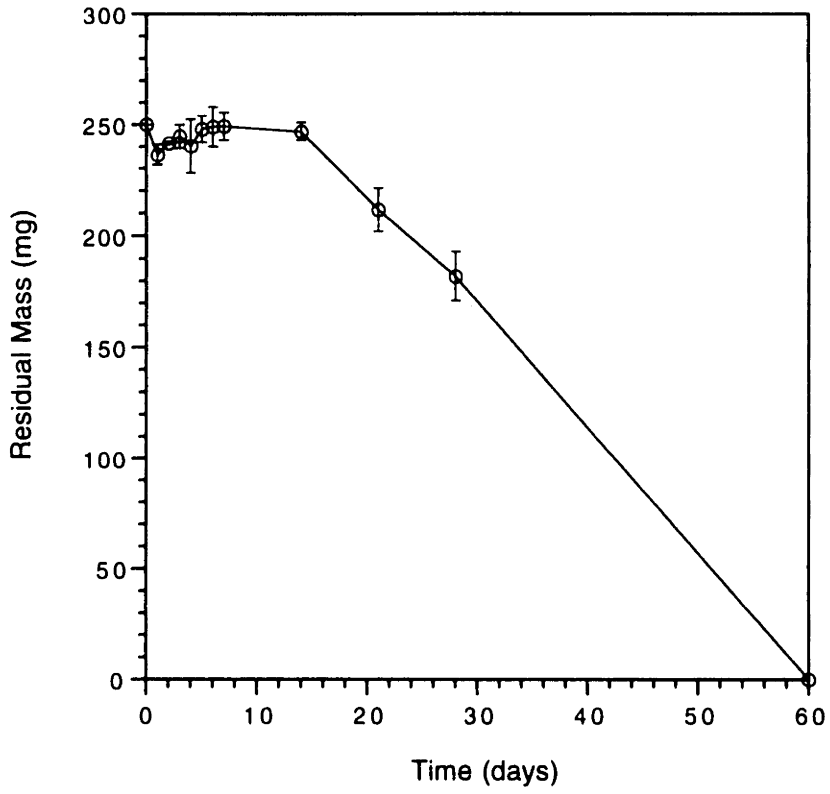

Fig 4-10. Polymer weight loss during degradation *in vitro* at 37°C.

in molecular weight (Fig 4-8). During this initial phase, ester hydrolysis of water-insoluble polymer chains produces two water-insoluble polymer chains the majority of the time and no mass is lost. Thus, the decrease in polymer molecular weight is not accompanied by a large loss of polymer mass initially. However, after several days the polymer reaches a critical molecular weight and subsequent ester bond hydrolysis leads to the formation of a fraction of water-soluble monomers and oligomers which are able to diffuse out of the spheres. At this time polymer weight loss begins to coincide with polymer degradation (Fig 4-10). In the polymer mass loss study, the critical molecular weight was reached at day 14 (M_w = 10,300). At this point polymer mass loss proceeds at an approximately constant rate until the polymer is completely degraded. As subsequently discussed, the delay in polymer mass loss is consistent with the observation of an induction period in gp120 release with microspheres whose pore volume is largely due to micropores.

4.2.8 *In Vitro* Macromolecule Release

To successfully deliver complex macromolecules for extended time periods *in vivo* it is essential to understand protein stability problems as well as the degradation mechanism of the microspheres. As a result, it is essential to study a macromolecule which is well characterized with respect to its stability in PLGA microspheres when attempting to correlate polymer degradation to macromolecule release [102, 106]. If unstable molecules are used the possibility of misinterpretation of results is increased which may lead to incorrect hypotheses and descriptions of the microsphere degradation and protein release processes. The drug that has been studied is gp120 (MW ≈ 104,000), a well-characterized protein antigen under investigation as a prophylactic vaccine for HIV-1 [107]. gp120 fit the macromolecule criteria for this study as it is known to be stable in PLGA microspheres for very long periods of time [107].

A typical *in vitro* release profile of gp120 from PLGA microspheres is shown in Fig 4-11. The profile is marked by a characteristic initial burst of vaccine (18 % of the total loaded gp120 in this case), followed by a period of very little or no release for several days, and then by a second period of rapid release.

4.2.9 Explanation for Pulsatile Macromolecule Release

Recently it has been reported that large PLGA implants degrade heterogeneously [108-110], degradation being faster on the interior relative to the surface of the device. This heterogeneous degradation was shown to be due to acid-catalyzed hydrolysis on the interior of the devices due to build-up of the acidic degradation products lactic and glycolic acid. This mechanism was also suggested for non-porous PLGA microspheres (containing no drug) made by a single-emulsion process [99]. The differential degradation in the interior versus the surface of the spheres was supported by the appearance of regions of crystallinity in originally amorphous polymers during microsphere degradation. In addition, two glass transition temperatures were observed in some polymers during degradation [99], further evidence of the existence of fast- and slow-degrading regions within the microspheres. However, the results reported here with porous PLGA 50:50 microspheres made by the double-emulsion procedure can not be explained by this hypothesis. There was no evidence of crystallinity or of two T_g's in the polymers studied here as microspheres degraded. Therefore, these types of polymer heterogeneities can not explain the existence of three phases of macromolecule release in this case. Furthermore, our particles appear to degrade at approximately equal rates on the interior and at the surface by SEM, perhaps due to their high initial porosity afforded by their preparation by the double-emulsion procedure.

As microsphere degradation proceeds and pores widen, more pores become visible on the surface of the particles. Micropores are defined as pores with diameters

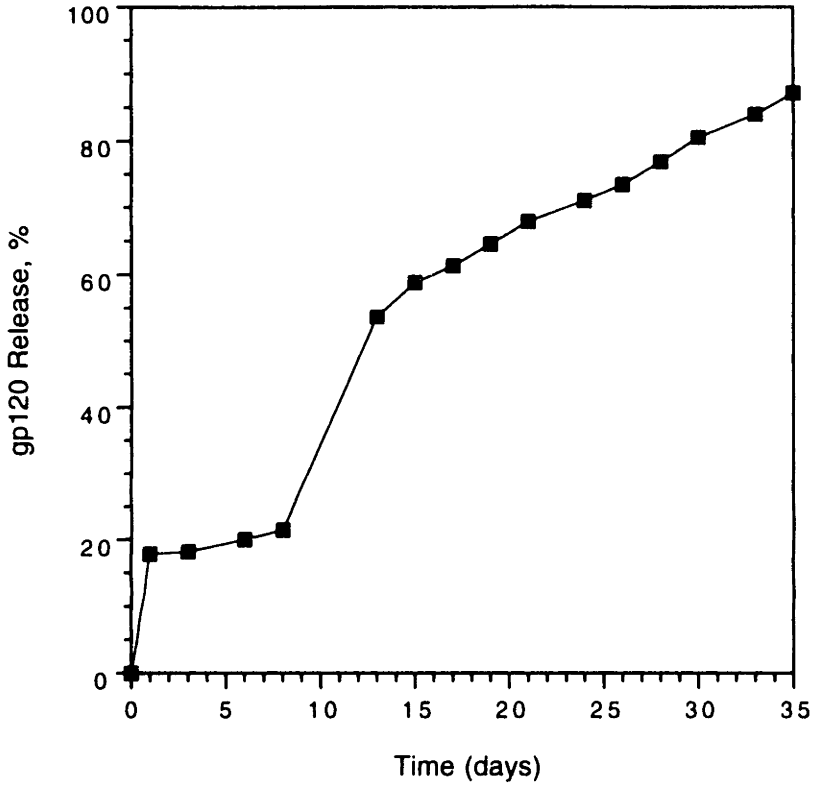

Fig 4-11. Typical gp120 release curve from PLGA microspheres *in vitro* at 37°C. The release process is characterized by an initial burst, followed by an induction phase, and finally a second release phase.

smaller than that of a small protein (< 50 Å). Protein-excluding micropores, which make up greater than 37 % of the total pore volume initially (Table 4-1), are thought to be distributed throughout the microparticles where they serve to hinder macromolecule diffusion from the particles. SEM studies showed that all pores, including micropores, widen steadily with time (Fig 4-5). It is proposed that the time it takes for widening and coalescence of micropores to the point where polypeptides or peptides can access them corresponds to the induction phase (or "lag-phase") observed in their release. This hypothesis is also consistent with a previous study in Dr. Langer's laboratory on the release of proteins from PLGA microspheres made by the double emulsion procedure [13]. In this study, the authors showed that they could control the length of the induction phase by changing the concentration of the polymer in the polymer phase during the preparation of microspheres. By increasing the polymer concentration they produced more dense (i.e., less porous) microspheres. More dense microspheres (less porous initially) showed an induction phase in protein release, whereas less dense (more porous) spheres showed little or no induction (i.e., continuous release).

Therefore, as an alternative explanation for macromolecule drug release from porous microspheres, it is proposed that molecule release is governed by diffusion through mesopores created as micropores grow and coalesce. That is, drug initially sequestered in meso- and macropores (including the initial drug occlusions as previously discussed) is prevented from release because it is separated from the external bath by microporous solid polymer. Protein released initially (i.e., the initial burst) is most likely due to desorption of protein absorbed to the surface of the spheres, or contained within meso- and macropores which have direct access to the surface of the particles. Following the initial burst, the induction phase (lag phase in protein release) may correspond to the time it takes for polymer degradation to result in micropore growth (by widening and coalescence with other micropores) into a sufficient number of mesopores with diameters greater than that of the drug. The

subsequent second release phase begins at the end of the induction period and lasts until drug has relatively unrestricted access to mesopores leading to the external bath. This final release phase is governed by protein diffusion through a tortuous network of water-filled pores.

4.3 Conclusions

The intermittent release of protein seen with porous PLGA microspheres may be well suited for the delivery of vaccines since it delivers an initial dose of vaccine at time zero, plus an additional dose a given time later (i.e., a built-in booster) from a single administration. In fact, it is possible to deliver several doses of vaccine antigen at appropriately spaced intervals using PLGA microspheres by varying the lactic/glycolic acid content or the molecular weight of the polymer, by changing the size of the microspheres, or by changing the procedure used to make the microspheres so as to control their initial porosity [12-14, 107]. A relatively fast-degrading polymer (PLGA 50:50, low MW) has been used in this study, leading to a relatively short lag phase between pulses. Longer lag phases can be obtained by increasing the lactic acid/glycolic acid ratio in the polymer backbone, by using higher molecular weight polymers, or by reducing the initial porosity of the spheres. The initial porosity of microspheres is controlled by factors such as the ratio of the volume of water/drug phase to the polymer/solvent phase in the primary emulsion, the polymer concentration used in the first step of microsphere preparation, and the rate at which the microspheres are dried. In Chapter 5 a mathematical model to describe PLGA microsphere degradation and release of macromolecules is developed based on the experimental results reported here.

5 Model of Erosion and Macromolecular Drug Release from PLGA Microspheres[2]

5.1 Introduction

Current theoretical understanding of polymer erosion and drug release primarily concerns the circumstance of a therapeutic molecule that is soluble in the polymer or copolymer phase---though perhaps loaded to a concentration exceeding the polymer solubility [111-113]. Recent interest in the encapsulation and ultimate controlled release of macromolecular, *insoluble* therapeutics (i.e., water-soluble as opposed to organic-soluble), makes this case of polymer erosion and drug release equally important as the *soluble* therapeutic case, and in some ways more challenging. From the theoretical point of view, complications arise with macromolecular drug release owing to the fact that the release of the water-soluble substance is intimately related to the "microporous" (i.e., angstrom- or nanometer-dimension) structure of the copolymer, which obviously evolves in time. While some success has been made in the past toward understanding the role of pore geometry on effective diffusion rates [114], no previous approach has succeeded in relating the *evolving* pore structure of an eroding polymer particle to the concomitant evolving transport properties of released species, and thereby to overall erosion and release rates.

In this chapter a theoretical framework is outlined that permits the prediction of (bulk-eroding) polymer erosion and macromolecular drug release as functions of time and various geometrical, physical, and chemical properties of the polymeric delivery

---

[2] This chapter was written in collaboration with Dr. Richard P. Batycky and Professor David A. Edwards at Penn State University, Department of Chemical Engineering, University Park, PA 16802. It is also reported in Batycky *et al.* [104].

system. An explicit microstructural model (based upon the hypothesis of coalescing micropores and evolving mesopores) is used to develop general expressions for the following [in each phase of the erosion/release process (hydration, induction and erosion phases)]: 1) the rate of polymer mass loss; 2) the rate of mean (mass- and number-average) molecular weight change; and 3) the rate of macromolecular drug release. Comparison of theoretical predictions are made with the experimental data of Chapter 4 in the special case of 50:50 poly(D,L-lactic-*co*-glycolic acid) (PLGA) microspheres encapsulating the protein gp120. The utility of the model for predicting erosion and release behavior in complex (e.g., *in vivo*) environments and possible future extensions are discussed.

5.2 Description of the Erosion and Release Process

Consider, for the sake of explicitness, the case of a poly(D,L-lactic-*co*-glycolic acid) microsphere, of radius r_0, that encapsulates a macromolecular hydrophilic substance, such as a protein or peptide drug. The hydrophilic drug is initially localized primarily in the vicinity of discrete, spherical (or nearly spherical) occlusions (or "macropores"), formed within the microparticle during the particle preparation process and remaining following the removal of water during the drying process. Depending upon the method of formation, the microparticle may contain a very large number of extremely small occlusions, or a smaller number of relatively large occlusions. Thus, the terminology "macropores" (versus the micro- and mesopores subsequently discussed) need not be literal. The volume of occlusions is denoted by V_0, and the volume fraction $\phi_0 = 4V_0/3\pi r_0^3$ is less than unity, $\phi_0 < 1$. Fig 5-1 provides an illustration of the spherical-occlusion structure of a single microsphere of the type under consideration as well as the localization of (fluorescently labeled) drug along the periphery of the occlusions.

In the process of polymer storage and microsphere formation and drying, a small

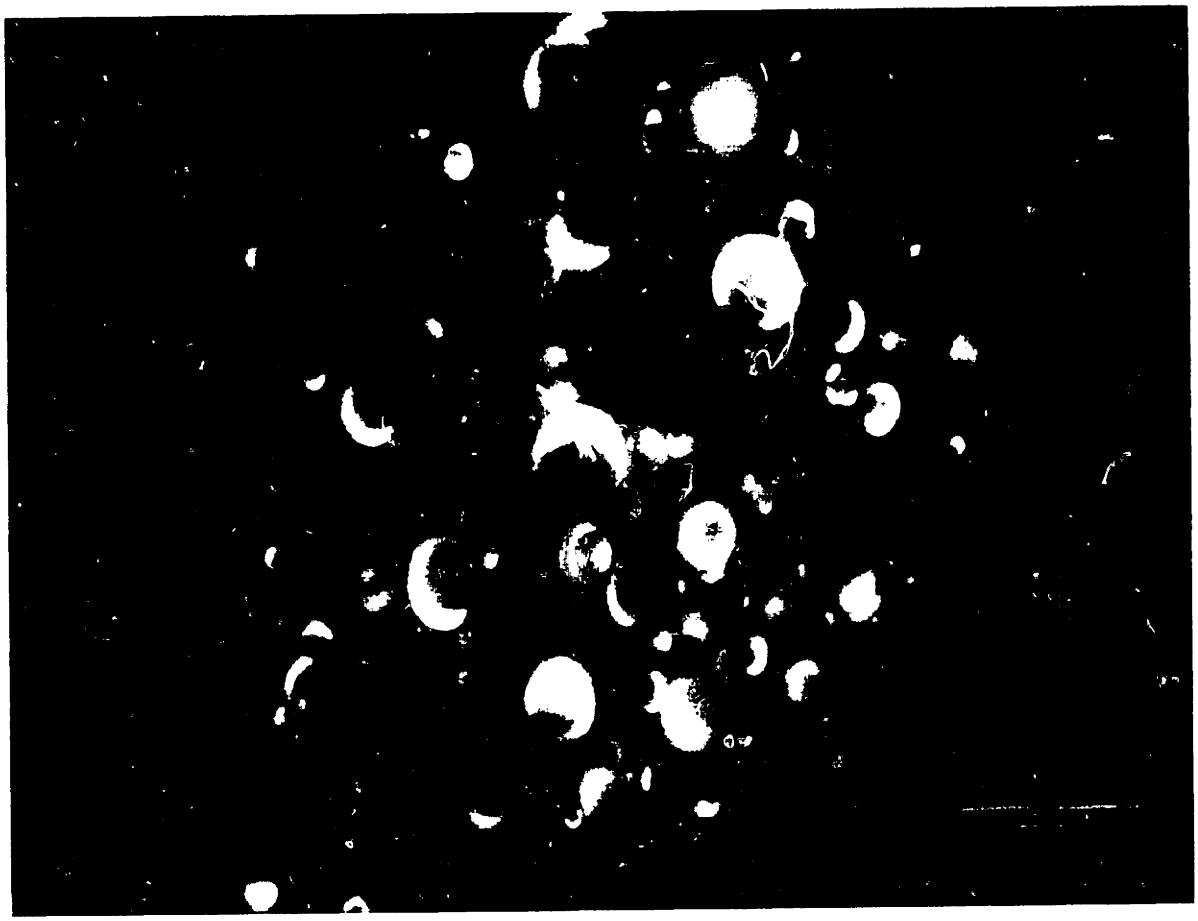

Fig. 5.1 Confocal microscopy photograph showing the spherical occlusion structure of a single PLGA microsphere and localization of (fluorescently labeled) drug along the periphery of the occlusions.

though finite amount of hydrolytic cleavage of PLGA ester linkages is anticipated to have occurred, particularly within the vicinity of the molecular-size pathways (the originating spatial domains of micropores, as next discussed) through which water has diffused out of the particle during the drying process.

Upon immersing the microsphere within an aqueous buffer, water starts to penetrate toward the microsphere's center. During this initial "hydration" phase the penetration of water into the microsphere is accompanied by the removal of predegraded monomers (and low oligomers) out of the particle and into the external bath. As the radius, $r_1(t)$, of the hydration front approaches the particle's center, the hydrated polymer begins to hydrolytically cleave [115].

At the conclusion of the hydration phase, degradation of PLGA copolymers is occurring throughout the microparticle volume. In this second, "erosion" phase, the micropores grow in size and coalesce owing to polymer erosion and oligomer solubilization, forming "mesopores", possessing mean characteristic radial dimension $R_M >> a_i$, where a_i are the Stokes-Einstein radii of released oligomers. In this phase, the erosion (and ultimate release of hydrophilic macromolecular drug) is controlled *not* by diffusion through the mesopores, but rather by the rate of appearance of monomers and oligomers into the mesopores via diffusion through the surrounding micro-porated matrix. From a modeling standpoint, the rate of "polymer erosion" or monomer release may *appear* to be (approximately) zeroth order (as further discussed subsequently), even though the mass transport process involves a diffusion-limited release of soluble substances from the (slowly eroding and vanishing) microporous zones of the microsphere to the growing mesoporous zones. On the other hand, the rate of release may be polymer-degradation controlled. In part, one of the aims of the subsequent analysis and comparison with experimental data will be to determine, via the *microscale* model of the *macroscopic* erosion process, which mechanism is truly rate-controlling, if any. It bears noting that the precise ratio of micro- to mesoporous zones within the

microsphere will depend intimately upon the extent of crystallinity (and therefore LA:GA ratio), polymer molecular weight, and the process used to prepare the microspheres.

Insofar as the macromolecular drug is concerned, its relatively large size $a_d >> a_i$, where a_d is the Stokes-Einstein radius of the protein or other macromolecular drug, will prevent release of the substance until the mesoscopic pores reach such numbers that the characteristic mean pore radius $\bar{R}(t) \approx a_d$. Thus, an "induction phase" can be expected for protein release, as commented upon in Chapter 4 and elsewhere [107, 116]. Although the primary macromolecular release will generally occur following the induction phase, protein absorbed to the surface of the microparticle and within preexisting mesopores may give rise to an initial "burst" of macromolecule release, controlled by the rate of macromolecule desorption.

It is also possible that some degradation or irreversible aggregation of macromolecular drug could occur owing to polymer-drug interactions as well as the acidity of released polymer degradation products [107, 116].

5.3 Model Equations

An internally consistent model of the foregoing views the molecular-size pore regions into which water initially diffuses, and from which predegraded soluble oligomers are released, as circular cylindrical micropores of radius R_μ.[3] Assuming these pores (which may, more explicitly, be viewed as localized regions, possibly of high monomer and oligomer concentration most prone to water penetration from the external bath) to be randomly distributed throughout the particle, the total number N_μ of such pores

[3] As pointed out in the discussion section, the general analysis outlined herein applies to far more general circumstances than those of microparticles into which water tunnels via straight, regularly shaped 'free molecular volume' cylindrical pores.

leading from the external particle surface can be related to the microparticle porosity ε (fractional volume containing no polymer) by

$$\varepsilon = \varepsilon_\mu + \varepsilon_M + \phi_0 \tag{5-1}$$

where

$$\varepsilon_\mu = N_\mu \frac{\pi R^2}{4\pi r_0^2} \tag{5-2}$$

is the fractional pore space of the micropores and

$$\varepsilon_M = N_M \frac{\pi R^2}{4\pi r_0^2} \tag{5-3}$$

is the pore space of mesopores (possessing a constant value ε_M^l throughout the hydration phase). The three pore populations may be measured by non-mercury porosimetry as shown in Chapter 4.

The rate of movement of the hydration front, $r = r_1(t)$, where r is a spherical coordinate localized at the center of the particle, is characterized by a balance of water diffusion into the polymer and solubilized monomer and oligomer (species i) diffusion out. It is convenient to consider the hydration front kinetics from the standpoint of monomer and oligomer diffusion. Solution of the associated pseudo-steady, Fickian-diffusion problem, permits determination of the following relationship between the radius $r_1(t)$ and time t during the initial hydration phase of the erosion process:

$$t = \frac{r_0^2}{A_1}\left[\frac{1}{6} - \frac{1}{2}\left(\frac{r_1}{r_0}\right)^2 + \frac{1}{3}\left(\frac{r_1}{r_0}\right)^3\right] \tag{5-4}$$

where A_I is a mass-transport constant defined by:

$$A_I \equiv \frac{\sum_i M_i \bar{D}_i^* (C_i^s - C_i^\infty)}{\alpha \rho^{bulk}} \tag{5-5}$$

depending notably upon the effective monomer and oligomer diffusion coefficients in the microparticle.[4] These latter can either be predicted on the basis of an explicit microscopic theory (as done later) or deduced experimentally by determination of the end of the hydration phase ($t = t_I$), or both. The time point characterizing the end of phase I is defined by

$$t_I = \frac{r_0^2}{6A_I} \tag{5-6}$$

Observation of the termination of "phase I" (hydration phase) at $t = t_I$ may involve measurement of several macroscopic quantities. The derivation of these quantities in terms of the microscale model constitutes the primary goal of this model. In the remainder of this section, the results of this derivation are reported.

The mass evolution during the hydration phase can be directly determined simply by accounting for mass loss from the micropores during hydration; this gives

$$\frac{m_p(t)}{m_p(0)} = 1 - \frac{\alpha \varepsilon_\mu^I}{1 - \phi_0 - \varepsilon_M^I - (1-\alpha)\varepsilon_\mu^I} \left[1 - \left(\frac{r_1}{r_0} \right)^3 \right] \tag{5-7}$$

where $m_p(t)$ is the net particle mass, ε_μ^I the fraction of the partially filled micropores, α the fractional amount of predegraded monomers and oligomer in the micropores relative to their bulk concentrations ($0 \le \alpha \le 1$), and r_1 is the hydration front radius and

[4] Further details of the theoretical developments outlined in this section---and of its physical basis---are described in Batycky *et al.* [104].

depends on time according to Eq. (5-4). This formula does not account for the added weight of water that has diffused into the particle---a contribution that is easily added by multiplying the right-most term by the difference between monomer and water masses, divided by $m_p(0)$.

For macromolecular drugs, as illustrated later, $a_d > R_\mu(0)$, i.e., the molecules are too large to diffuse out of the spherical occlusions (macropores) in which they are initially contained, absorbed to the occlusion walls, at least in the hydration phase of the erosion process. This gives rise to an *induction phase*, as previously noted. Nevertheless, a burst of drug release may occur owing to absorption to the external surface of the particle and in preexisting mesopores directly connected with the external bath. This initial release of protein is modeled as a first-order kinetic desorption process, giving

$$\frac{m_d(t)}{m_d(0)} = 1 - 4\pi r_0^2 \left[1 - \varepsilon_\mu^l - \varepsilon_M^l + \frac{2}{3}\varepsilon_M^l \frac{r_0}{R_M^l} \right] \frac{M_d C_d^s(0)}{m_d(0)} \left[1 - e^{-k_d t} \right] \tag{5-8}$$

where $C_d^s(0)$ is the surface concentration of absorbed drug, k_d the rate of desorption and $m_d(t)$ the total mass of drug remaining in the microsphere at time t. Given that the drug release in the initial "induction" phase (for the drug) is entirely a surface-release phenomenon, it is essentially independent of the hydration and ultimate erosion of the polymer.

In addition to the masses of drug and polymer particle, the mean (weight- and number-averaged) polymer molecular weights provide a wealth of information regarding the kinetics of phase I, and especially of the polymer degradation process itself.

Batycky *et al.* [104] provide general expressions for both weight- and number-averaged mean molecular weights. In this thesis attention is limited to the weight-averaged mean molecular weight as a function of time. In the initial hydration phase it is given by the following formula:

$$\overline{M}_w(t) = \overline{M}_w(0)\frac{1-\phi_0-\varepsilon_M^I-(1-\alpha)\varepsilon_\mu^I}{1-\phi_0-\varepsilon_M^I-(1-\alpha)\varepsilon_\mu^I-\alpha\varepsilon_\mu^I\left[1-\left(\frac{r_I}{r_0}\right)^3\right]} \tag{5-9}$$

This relation assumes that polymer degradation (prevented owing to the initial effect of solubilizing predegraded monomers and oligomers) does not begin until the erosion phase itself. Thus, by measurement of the mean molecular weight $\overline{M}_w$ at the start and conclusion of the hydration phase (during which the mean molecular weight potentially *increases* owing to removal of low-weight predegraded species), the time t_I can be known and hence the value of A_I determined (ultimately to be compared with the theoretical estimate of A_I.

It is important to note that measurement of $\overline{M}_w(t_I)$ provides knowledge of α (the fraction of predegraded monomers in the prepared microparticle)

$$\alpha = \frac{1-\phi_0-\varepsilon_M^I-\varepsilon_\mu^I}{\varepsilon_\mu^I}\left[\frac{\overline{M}_w(t_I)}{\overline{M}_w(0)}-1\right] \tag{5-10}$$

which (if α is independently measurable) can serve as a consistency check of the analysis. Other methods for determination of t_I are discussed in the next section, which provides a protocol for determination of all the transport constants appearing in the analysis.

In the second phase of the erosion process (the "erosion" phase, or phase II), the mass loss of the microparticle is linear with time:

$$\frac{m_p(t)}{m_p(0)} = 1-\frac{\alpha\varepsilon_\mu^I + A_{II}(t-t_I)}{1-\phi_0-\varepsilon_M^I-(1-\alpha)\varepsilon_\mu^I} \tag{5-11}$$

where $t \geq t_I$ and A_{II} is a second mass transport coefficient defined by:

$$A_{II} \equiv \frac{\sum_i M_i \bar{K}_i^*}{\rho^{bulk}} \tag{5-12}$$

A markedly different behavior is observed for the mass-averaged molecular weight in the erosion phase. Thus, for $t > t_l$:

$$\bar{M}_w(t) = \frac{\dfrac{1-\phi_0-\varepsilon_M^l-(1-\alpha)\varepsilon_\mu^l}{m_p(0)}\left[\sum_{i=1}^{\infty}\left(M_i^{bulk}\right)^2 n_i(t-t_l)\right] - M_1^{bulk} A_{II}(t-t_l)}{1-\phi_0-\varepsilon_M^l-\varepsilon_\mu^l-A_{II}(t-t_l)} \tag{5-13}$$

where M_i^{bulk} is the "apparent" molecular weight of a characteristic monomer and n_i is the total number of moles of polymer chains composed of i monomers and present in the bulk polymer. [A subtle point is that $n_1(t)$ is that amount of monomer which would be present if no monomers were removed from the bulk polymer.] The evolution of $n_i(t)$ is determined independently of the mass transport of solubilized erosion products by the particular degradation kinetics obeyed, as next discussed.

Although Batycky *et al.* [104] provide for more general cases, in comparisons with experimental data of Chapter 4, it will be assumed that the probability of cleavage of any given polymer chain is equal at every cleavage site along the length of the chain. The relation

$$n_i \equiv n_i\left[t,\, n_j(0)\right] \qquad \forall (j \geq i) \tag{5-14}$$

then depends on a single unknown, k_n, the "true" rate of hydrolytic cleavage. An explicit form of this equation is provided elsewhere [104]. Some properties of the initial distribution $n_i(0)$ within the bulk polymer during phase I can be computed in terms of other (known) quantities such as $m_p(0)$ and $\bar{M}_w(0)$. These expressions, along with the

short-time expansion of $n_i(t - t_l)$, allow an explicit relation between the observed trend in $\overline{M}_w(t)$ at the start of phase II and the rate of hydrolytic cleavage; that is [104]:

$$k_n = \frac{3A_{II}}{1-\phi_0-\varepsilon_M^l-\varepsilon_\mu^l} - \frac{3}{\overline{M}_w(0)}\frac{1-\phi_0-\varepsilon_M^l-\varepsilon_\mu^l}{1-\phi_0-\varepsilon_M^l-(1-\alpha)\varepsilon_\mu^l}\left(\frac{d\overline{M}_w(t)}{dt}\right)\Bigg|_{t=t_l^*} \tag{5-15}$$

This formula may be convenient for establishing a value for k_n from an experimentally observed $\overline{M}_w(t)$ profile. The evolution of $\overline{M}_w(t)$ can be approximated during phase II as:

$$\overline{M}_w(t) = M_l^{bulk} + \overline{M}_w(0)\frac{1-\phi_0-\varepsilon_M^l-(1-\alpha)\varepsilon_\mu^l}{1-\phi_0-\varepsilon_M^l-\varepsilon_\mu^l-A_{II}(t-t_l)}e^{-k_n(t-t_l)}\left[1+\frac{2}{3}k_n(t-t_l)\right] \tag{5-16}$$

It is worthwhile to note that these results are independent of the initial distribution $n_i(0)$.

Finally, the majority of macromolecular drug is prevented from escaping the microparticle in the first and second phases of the erosion process, at least until mesopores, assumed to be formed by the random coalescence of micropores at a rate determined by the zeroth-order rate constant, $k_{coal}(r_0)$, produce a mean pore radius $\overline{R}(t_l^d) = a_d$. That is, when a sufficient number of micropores will have coalesced by erosion to form mesopores, resulting in a mean pore radius R that is large enough for diffusive passage of macromolecules from their originating site in spherical occlusions, the induction phase is determined to have ended. A simple formula for t_l^d follows upon assuming a two-pore model (R_μ^l, R_M^l), where:

$$t_l^d - t_l = \frac{\varepsilon_\mu^l}{k_{coal}(r_0)}\frac{a_d}{R_M^l}\left(\frac{2r_0}{R_M^l}\right)^2 \tag{5-17}$$

Following the end of this "induction" phase for the drug ($t > t_l^d$), the net mass $m_d(t)$ of drug remaining in the microsphere decays in a classical Fickian manner:

$$\frac{m_d(t)}{m_d(0)} = \left\{1 - 4\pi r_0^2\left[1 - \varepsilon_\mu^I - \varepsilon_M^I + \frac{2}{3}\varepsilon_M^I \frac{r_0}{R_M^I}\right]\frac{M_d C_d^s(0)}{m_d(0)}\right\}\frac{6}{\pi^2}\sum_{j=1}^{\infty}\frac{e^{j^2\pi^2\bar{D}_d^*(t-t^d)/r_0^2}}{j^2} \qquad (5\text{-}18)$$

where $\bar{D}_d^*$ is the effective drug diffusion coefficient.

The preceding formulas permit explicit predictions of polymer mass, drug mass and mean molecular weights as functions of time.

5.4 Paradigm for Specific Calculations

In this section a paradigm is developed, on the basis of the preceding model, for interpretation of bulk polymer erosion and protein release data, to which attention is directed in the next section. A few simplifications have been made to permit an easily tractable paradigm. First, the initial micropore and mesopore distributions are assumed to be uniform (radii R_μ^I, R_M^I). No assumptions have been made regarding the initial polymer molecular weight distribution, nor the size or number of drug occlusions. Also, it is assumed that only monomers are released as degradation products.

Finally, although other degradable polymers may also be evaluated, it is useful to consider the case of PLGA microspheres, with drug initially localized in the macropores (occlusions) of the polymer particle. In this case, the coefficient A_I is given by

$$A_I = \frac{\bar{D}_{LA/GA}^*}{\alpha}\frac{M_{LA}C_{LA}^s + M_{GA}C_{GA}^s}{M_{LA}C_{LA}^p + M_{GA}C_{GA}^p} \qquad (5\text{-}19)$$

Assuming lactic acid (LA) and glycolic acid (GA) to be essentially infinitely soluble in the aqueous-filled micro- and mesopores, $C_i^s \equiv \alpha C_i^p$, hence $A_I \equiv \bar{D}_{LA/GA}^*$. The constants appearing on the right side of (5-19) are defined in Table 5-1. The diffusivity $\bar{D}_{LA/GA}^*$ may

either be predicted on the basis of free volume theory [117] or an equivalent averaging theory, such as macrotransport theory [118]. In the latter case,

$$\bar{D}^{\bullet}_{LA/GA} = D\left(\frac{1-\frac{a_{LA/GA}}{R^{I}_{\mu}}}{\frac{a_{LA/GA}}{R^{I}_{\mu}}}\right)^{5/2} \tag{5-20}$$

with $\bar{D}^{\bullet}_{LA/GA}$ the effective diffusion coefficient of monomers in the microporous matrix, $D = kT/6\pi\mu a_{LA/GA}$, and $a_{LA/GA}$ the Stokes-Einstein radius of LA and GA monomers (approximately identical: see Table 5-1). Equation (5-20) follows from consideration of pore diffusion of finite-size spherical molecules or colloids in the limit when the sphere radius is approximately that of the pore itself---the limit of interest here. The usefulness of (5-20) is that it permits determination of R^{I}_{μ} from experimental data. Other benefits to considering the effective diffusivity $\bar{D}^{\bullet}_{LA/GA}$ from a macrotransport or free volume point of view are later discussed.

In the remainder of this section, a paradigm is outlined on the basis of which the various constants appearing in the preceding equations can be determined (to the extent that they cannot be directly measured). The paradigm also identifies various consistency checks by which the accuracy of the model can be evaluated. The case of PLGA microspheres containing a macromolecular drug is considered. The preceding equations can be used to establish the following paradigm:

A) Measure the initial mean mass-averaged molecular weight $\bar{M}_w(0)$, the porosities ϕ_0, ε^{I}_{M}, ε^{I}_{μ} and the time $t = t_I$ at which the hydration phase ends. The latter may involve observation of a distinct change in molecular weight or mass kinetic behavior. Molecular weight will be an obvious indicator of the end of the hydration phase when a substantial predegradation has occurred (α finite), such that the mean molecular weight potentially increases during the hydration phase, attaining a

Table 5-1. Values of Variables Necessary for Theoretical Prediction of Microsphere Degradation and gp120 Release Properties

Variable	Description	Value
r_0	radius of microsphere	20 μm
M_{LA}, M_{GA}	monomer molecular weights	90.08, 76.05 g/mol
$\alpha_{LA/GA}$	monomer radius	2.3 Å
D	monomer diffusivity (Stokes-Einstein)	9.33×10^{-6} cm^2/s
ε_μ^I	initial microporosity	0.217 -
ε_M^I	initial mesoporosity	0.096 -
ϕ_0	occlusion porosity	0.173 -
R_M^I	initial mesopore radius	0.5 μm
$\rho^{bulk} = \sum_i M_i C_i^p$	bulk polymer density	0.634 g/cc
$\overline{M}_{w(0)}$	initial mass-averaged molecular weight of polymer	55113 g/mol
a_d	drug radius	62 Å
M_d	drug molecular weight	104 000 g/mol
$m_d(0)/[m_p(0)+m_d(0)]$	initial drug loading	18.5×10^{-3} -

maximum $\overline{M}_{w(t_I)}$ (see Chapter 4). In this case, one can predict from Eq. (5-10) the coefficient α. Otherwise, when the mean molecular weight does not (significantly) increase initially ($\alpha << 1$), the time t_I of phase I follows from (5-7) and (5-11) as the time at which the particle mass starts to diminish linearly.

B) Measure the rate of mesopore formation at the surface of the microparticles by visual observation at various times of degradation and deduce $k_{coal}(r_0)$.[5]

C) Predict the time of the induction phase t_I^d, given R_M^I, using (5-17). Compare this value with the experimental observed value as a *test of the analysis.*

D) Measure the fraction of drug released during the initial burst phase and the initial slope of the burst (or perhaps the time required for 95% of the burst to be complete) and use (5-8) to calculate both the surface concentration of absorbed drug $C_d^*(0)$ and the rate of desorption k_d.

E) Measure the time at which the mass of polymer vanishes and use Eq. (5-11) to determine from this time (t_{II}) the value of A_{II} and, via Eq. (5-12), the (apparent) polymer degradation rate constant, $\overline{K}^*_{LA/GA}$.

F) Determine the *true* polymer degradation rate, k_n, by either: i) measuring the rate of change of weight-average molecular weight at the start of phase II and using Eq. (5-15), or; ii) matching a specific point in the profile $M_w(t)$ (such as the time at which the molecular weight attains half of its initial value) and using Eq. (5-16).

---

[5]This method of measurement is obviously approximate. Distinct mesopores become apparent by visual inspection of electron microscopic photos (Chapter 4) when mesopores reach a radius of approximately $R_M^I \approx 1$ μm. Measuring the rate of growth of pores in the domain $R_M^I \geq 1$ μm may or may not be equivalent to measuring the rate constant $k_{coal}(r_0)$.

G) Measure the half-time of the drug mass released following the induction phase and deduce, via Eq. (5-18) and an iterative procedure, $\bar{D}_d^*$.

H) All of the necessary constants are now known. Predict $m_p(t)$, $m_d(t)$, and $\bar{M}_w(t)$ and compare with the experimental data. Depending upon the agreement of experimental data with theoretically predicted curves, as well as the absolute values of rate constants [$\bar{K}_d^*$, $\bar{D}_{LA/GA}^*$, k_n, $k_{coal}(r_0)$, $\bar{K}_{LA/GA}^*$], the diffusion-controlled or degradation-controlled nature of the erosion/release process can be analyzed, as well as the suitability of the model.

5.5 Comparison with Experimental Data of Chapter 4

In this section, the paradigm outlined in section 5.4 is used to deduce the transport and degradation rate constants describing the erosion of 50:50 PLGA microspheres and simultaneous release of the model protein gp120. The experimental data to which comparisons have been made are found in Chapter 4. Table 5-1 provides a list of pertinent physical and geometrical parameters characterizing the microspheres.

Fig 5-2 displays the mean weight-average molecular weight of the polymeric microspheres versus days in 0.1M phosphate buffer at 37°C. The initial rise in mean molecular weight is the signature of predegraded monomer released in phase I; hence, following step (A) of the paradigm, t_I = 1 day, with $\bar{M}_w(t_I)$ = 58787 g/mol. The termination time of phase I (t_I) corresponds to a value $A_I = 7.72 \times 10^{-12}$ cm^2/s from (5-6). This constant is the effective diffusion coefficient of the monomers within the microporous matrix, $\bar{D}_{LA/GA}^*$, a magnitude consistent with literature values for polymer diffusion coefficients. From (5-20) this gives a micropore radius of $R_\mu = a_{LA/GA}/0.996 \approx$ 2.3Å. The peak molecular weight $\bar{M}_w(t_I)$ combines with (5-10) to yield α = 0.158---i.e.,

the micropores initially contain LA and GA monomers with concentrations approximately 16% that of the bulk polymer concentrations.

The predicted % hydrated volume of the microsphere is $(\varepsilon_{\mu}^{l} + \varepsilon_{M}^{l}) \times 100 \approx 30\%$ at the end of the hydration phase, a result near to the hydration level of 50:50 PLGA slabs at the conclusion of their hydration phase, as reported by [115].

Visual observation of mesoscopic surface pores ($R_M^l \approx 1\mu m$) [step (B) of the paradigm] shows (Chapter 4) that the rate of pore coalescence is linear with a rate of mesopore formation of $k_{coal} = 0.36\ day^{-1}$.

Fig 5-3 shows the mass release of protein as a function of time in PBS buffer. The induction phase time is $t_I^d = 8$ days. Given the value of $k_{coal}(r_0)$ reported above, and using $R_M^l = 1\ \mu m$, following step (C) and using (5-17) one obtains $t_I^d = 9$ days, in close agreement with the experimental observation.

Approximately 1/5 of the initial mass of drug contained in the microparticle is released during the burst phase. Of this amount, 91% of this occurs in the first day. As described in step (D), from (5-8) and the value of R_M^l computed above, this corresponds to a desorption constant of $k_d = 2.40\ day^{-1}$ and a surface concentration of $C_d^s(0) = 4.22 \times 10^{-12}\ mol/cm^2$.[6]

The time of completion of the erosion process for the PLGA 50:50 copolymer matrices used in this study is approximately $t_{II} = 60$ days (data from Chapter 4; similar values appear elsewhere [100]). This corresponds to $A_{II} = 8.71 \times 10^{-3}\ day^{-1}$ from (5-11). Thus, as listed in step (E) of the paradigm, from Eq. (5-12) one finds $\bar{R}_{LA/GA}^{\bullet} = 3.85 \times 10^{-10}\ mol/cm^3/s$ upon assuming stoichiometric release of each monomer.

Following step (F), the mean molecular weight has a "half-life" of $\bar{M}_w(t = 11.4\ days) = 27557$, whence, from (5-16), this yields $k_n = 1.91 \times 10^{-6}\ s^{-1}$. The theoretical prediction of

---

[6]Embedded in the calculation of $C_d^s(0)$ are the initial masses of the polymer [$m_p(0) = 11.6$ ng] and the drug [$m_d(0) = 0.22$ ng] comprising a microsphere (from Chapter 4).

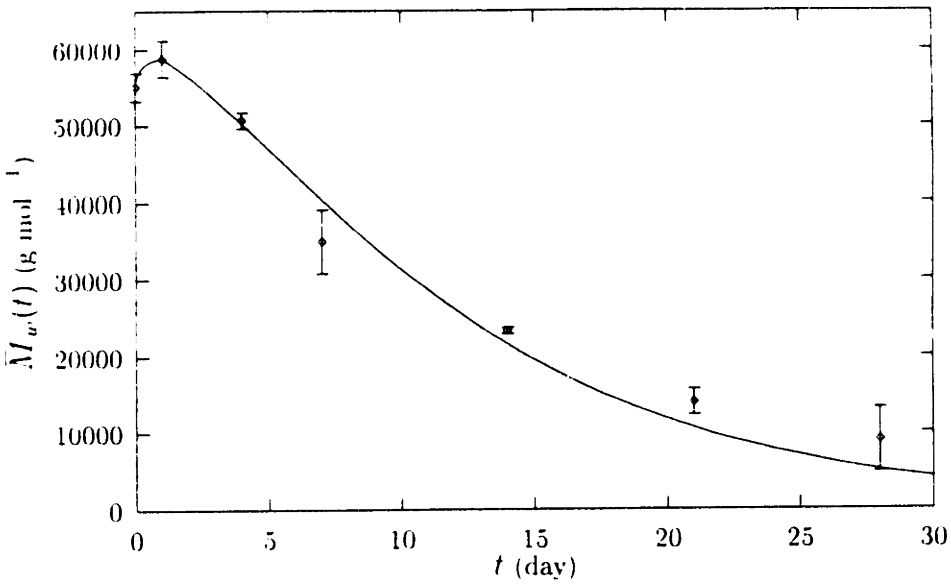

Fig 5-2. Microparticle mass-averaged mean molecular weight as a function of time comparing the theoretical prediction (solid line) with experimentally measured values from Chapter 4 (diamonds). Errors are ± S.E.M.

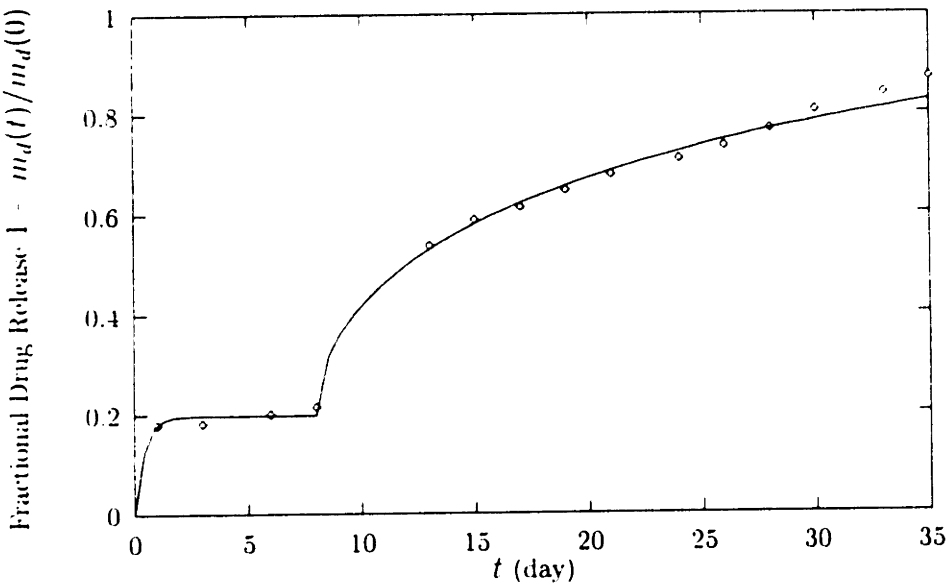

Fig 5-3. Fractional release of gp120 as a function of time comparing the theoretical prediction (solid line) with experimentally measured values from Chapter 4 (diamonds).

mean molecular weight behavior (solid line) is compared with the experimentally determined value in Fig 5-2.

Finally, following step (G) of the paradigm, from (5-18) one finds $\bar{D}_i^* = 1.79 \times 10^{-13}$ cm^2/s. The theoretical prediction (solid line) is compared in Fig 5-3 to the experimental data of Chapter 4.

Both molecular weight (Fig 5-2) and protein release (Fig 5-3) predictions closely match the experimental data of Chapter 4. Also, the values deduced for the physical and transport coefficients closely accord with expectations. Given this agreement, it is possible to determine whether the erosion process (phase II) is diffusion or reaction controlled. Note that the true degradation rate constant is

$$k_n = 1.91 \times 10^{-6}\ s^{-1}.$$

This represents the actual rate of polymer scission by hydrolysis. An *apparent* degradation rate constant can be defined in terms of the rate of "production" of soluble monomers in the external bath. Specifically, $\bar{K}_i^* = \bar{K}_{LA/GA}^*$ in the case of 50:50 LA:GA. $\bar{K}_{LA/GA}^*$ denotes a zeroth-order rate constant which can be related to the apparent degradation rate by $k_n^{app} = \bar{K}_{LA/GA}^* / C_{LA/GA}^p$. Assuming that, in the vicinity of aqueous pores, complete degradation has occurred ($C_{LA/GA}^p = C_i^p$) gives, $C_{LA/GA}^p = 3.82 \times 10^{-3}$ mol/cm^3. This gives

$$k_n^{app} = 1.01 \times 10^{-7}\ s^{-1}$$

a value that is within an order of magnitude of k_n. This shows that the rate of production of monomers into the external bath is near to (though less than) the rate of polymer degradation. That the polymer degradation rate is *faster* than the production rate may reflect the time scale of solubilization, among other possible effects.

If, on the other hand, it is assumed that monomer diffusion from the sites of hydrolysis to freely-diffusing mesopores is rate limiting the production of monomers, it is possible to estimate this "diffusion-limited" rate constant k_n^{diff} from $\bar{D}^{\bullet}_{LA/GA}$ (as deduced in the hydration phase). That is, $k_n^{diff} \approx \bar{D}^{\bullet}_{LA/GA}/h^2$, where h is a characteristic diffusion path length in the microparticle. In other words, monomers, following their formation must diffuse (even in the erosion phase) from the site of hydrolysis to a relatively large (meso or macro) pore, following which they rapidly appear in the external bath. The characteristic length $h \approx 1$ μm corresponds to the approximate distance between macropores (occlusions), and, it is assumed, between microporous domains of the eroding particle; thus

$$k_n^{diff} \approx 7.72 \times 10^{-4}\ s^{-1}$$

This rate constant far exceeds either the "true" (k_n) or "apparent" (k_n^{app}) degradation rate constants, meaning that, were the erosion process governed by molecular diffusion of solubilized monomers out of the polymer matrix, the disappearance of the polymer would occur *far more rapidly than observed.* Therefore, it may be concluded that the erosion of the particle is polymer-degradation-controlled in this case. This conclusion agrees with other experimental evidence appearing in the literature (e.g., Shah *et al.* [115]).

5.6 Discussion

The model of macromolecule release from bulk-eroding microspheres outlined in this chapter may serve a variety of purposes. Indirectly, the model specifies geometrical and other physical parameters that should be known or measured if the transport parameters controlling erosion and release are to be determined by implementation of

the paradigm. The requisite "input" data are those listed in Table 5-1, the values of which are either known from the literature or have been measured for the given system (in Chapter 4). Knowing these parameters, by measurement of $\overline{M}_w(t)$ and $m_d(t)$, and use of the paradigm, it is possible to determine:

i) the duration of the hydration phase (t_l);
ii) the polymer diffusivity(ies) of solubilized monomers or low oligomers ($\overline{D}_i^*$);
iii) the micropore coalescence rate constant (k_{coal});
iv) the true polymer degradation rate constant (k_n);
v) the monomer (and soluble oligomer) production rate ($\overline{K}_i^*$)---related to the "apparent" polymer degradation rate constant in the manner demonstrated in the preceding section;
vi) the effective diffusivity ($\overline{D}_d^*$) of the macromolecule through the eroding polymeric particle.

Having determined values for these parameters, predictions of weight- and number-averaged mean molecular weights ($\overline{M}_w$, $\overline{M}_n$), polymer mass (m_p) and drug mass (m_d) versus time can be made and compared with experimental data. It is essential to note that these deduced transport parameters are functions of copolymer composition, particle preparation method and macromolecular drug type---yet *not* functions of particle size or shape, or particle environment. That is, once the controlling transport parameters for a given microparticle system have been determined, predictions of erosion and release behavior in a variety of *in vitro* or *in vivo* environments, or for varying microparticle shapes and sizes, can be made. In addition, then, to the physical understanding that accompanies knowledge of the transport parameters ($\overline{D}_i^*$, k_n, $\overline{K}_i^*$, $\overline{D}_d^*$) (i.e., is the erosion process diffusion- or degradation-rate controlled?), a fully predictive theory is provided by knowledge of these same parameters, one that can be used to

predict particle performance in complex *in vivo* environments or for particle shapes and sizes unlike those that have been used to determine the parameters by comparison with experimental data using the paradigm.

There are, however, some limitations of the model as it has been outlined here, and that should ideally be removed in the future. For the purpose of arriving at a tractable theory, only two rate-controlling pore populations have been assumed (R_μ, R_M). In reality (see Chapter 4), the micro- and mesopore distributions are not tightly localized about mean radii (R_μ, R_M). In principle, broad distributions of pore radii can be included in a generalized model. Interactions between monomers (or oligomers) and pore walls have not been accounted for, nor have the effects of variable pH as may accompany solubilization of the acidic monomers of a bulk-eroding copolymer like PLGA (this effect, however, may be minimal due to buffering capacity of the release medium either *in vitro* or *in vivo*). The effect of pH on the scission rate constant (k_n) can, in the future, be taken into account. Perhaps most critical is the interaction between the encapsulated macromolecular drug and the polymer pore walls. Absorption of protein to pore walls, protein configuration changes caused by polymer interactions or low pH, and protein-protein interactions should all be accounted for, as many macromolecular drugs possess the potential to be altered by nonspecific interactions with the polymeric particle, low pH, etc. Nevertheless, the gp120 release data of Chapter 4 is well-described by the model in its present form.

It is highly desirable that formulation variables be related to the transport properties ($\bar{D}_i^*$, k_n, $\bar{K}_i^*$, $\bar{D}_d^*$), so that the latter need not be deduced from particle performance studies---rather might be estimated by choice of copolymer, preparation method, etc. One step in this direction might be to describe the monomer/oligomer diffusivities $\bar{D}_i^*$ by free volume theory [117], a predictive method highly developed for polymer diffusion processes, and that permits relation between polymer environment and the physicochemical nature of the diffusing substance.

6 Single Dose Antifertility Vaccine using PLGA Microspheres: Active Immunization Against Gonadotropin Releasing Hormone[7]

6.1 Introduction

Pet overpopulation is one of the critical problems in the field of animal protection. More than 5 million unwanted dogs and cats are destroyed each year in the United States (The American Society for the Prevention of Cruelty to Animals). Spaying and neutering are currently the most practical methods to control the pet population, however, factors such as cost and irreversibility make these surgical methods difficult to implement, creating the need for low-cost alternatives [119].

Vaccination of animals against gonadotropin releasing hormone (GnRH) has been under investigation as a non-surgical method of birth control [87, 119-121]. GnRH is a decapeptide hormone produced in both males and females which acts as the master reproductive hormone through regulation of the release of luteinizing hormone (LH) and follicle-stimulating hormone (FSH) from the pituitary [122]. In females, both LH and FSH are necessary for ovulation. In males, LH regulates testosterone production and FSH is necessary for spermatogenesis [123, 124]. Therefore, the absence of GnRH leads to a reduction in testosterone levels, sperm production, and testicular size, often resulting in immunological castration [119]. It has been shown that sufficiently high levels of antibodies against GnRH leads to suppression of reproductive behavior in both males and females [120]. However, a problem exists in that GnRH vaccines, even when conjugated to highly immunogenic molecules such as Tetanus toxoid (TT), are very

[7] The work described in this chapter was done in collaboration with Dr. Yun-Yen Tsong at The Population Council, Center for Biomedical Research, 1230 York Avenue, New York, NY 10021.

poorly immunogenic. As a result, it is necessary to immunize the animal several times in order to achieve long-lived high concentrations of antibodies capable of protecting the animal against pregnancy [119].

In this chapter, the possibility of reducing the number of shots necessary for successful immunization from 3 with the standard GnRH-TT vaccine preparation [119], to a single injection by using controlled-release PLGA 65:35 microspheres containing encapsulated GnRH-TT is demonstrated. PLGA 65:35 was chosen based on preliminary immunization studies done at the Population Council which showed that it resulted in the highest anti-GnRH antibody titers (compared with PLGA 50:50 and PLGA 75:25). Furthermore, while the GnRH-TT vaccine studied in this chapter may eventually be a useful tool in veterinary medicine, it also serves as a *model antigen* for the purposes of this thesis.

6.2 Results and Discussion

Fig 6-1 shows a scanning electron microscopy (SEM) photograph of a typical PLGA 65:35 microsphere containing 4.9 μg GnRH-TT per mg microspheres (0.49 wt %). The mass-average size of GnRH-TT microspheres is 45 μm as determined using a Coulter Multisizer II.

There were two groups of eight rats each used for immunization studies: (1) positive controls (Three-dose group) which received three doses of GnRH-TT at time 0, 4, and 8 weeks (soluble GnRH-TT); and (2) experimental group (microsphere group) which received a single injection of GnRH-TT encapsulated in PLGA 65:35 microspheres made by the double emulsion procedure. Fig 6-2 shows the results of the immunization experiment as measured by anti-GnRH antibody titer elicited by immunization. Antibody titers elicited by a single injection of GnRH-TT in

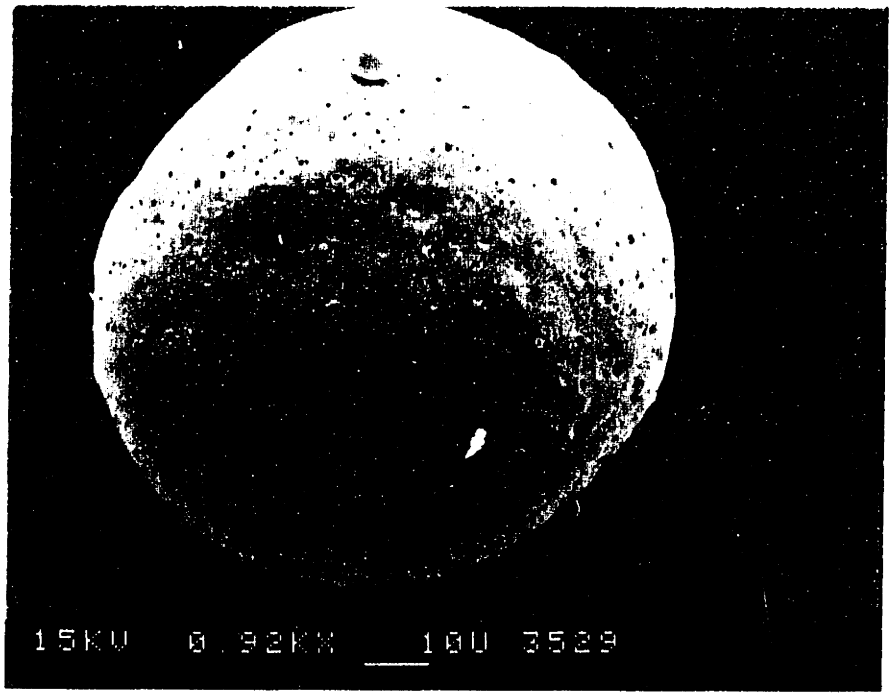

Fig 6-1. SEM photograph of a typical PLGA 65:35 microsphere containing entrapped GnRH-TT antigen.

microspheres were as high and lasted as long as those obtained using the standard three-immunization schedule. The only time point where antibody titers are significantly higher in the three-dose group was at week 6, the first bleed after this group of rats were given a booster shot of GnRH-TT (booster given at week 4). Thereafter, the titers for the three-dose controls and the single-dose microsphere groups were equivalent within the error of the experiment (Fig 6-2). Notice that there is a clear increase in antibody titers following each of the two booster doses in the three-dose group (i.e., between weeks 4 and 6, and between weeks 8 and 10). This sharp increase in specific antibody production is a typical response to the introduction of a bolus of antigen into an animal previously primed with antigen (i.e., boosters following the first injection of GnRH-TT) [11]. In the single-dose microsphere group there is a similar sharp increase in anti-GnRH-TT antibody production between weeks 6 and 10. This response is most likely due to an *"in vivo autoboost"* of antigen from the PLGA microspheres (i.e., a second release of antigen following an induction phase from the same dose of microspheres, see Chapter 4), consistent with the pulsatile release from PLGA microspheres shown in Chapter 4 and predicted in Chapter 5. This result shows the true power of a controlled release approach for vaccine administration.

Fig 6-3 shows the corresponding serum testosterone levels of the rats immunized with GnRH-TT. Initial testosterone levels in male rats typically ranges from 8 to 12 nmol/L. By the first bleed (4 weeks after initial injection) the levels of serum testosterone in the rats were reduced to less than 4 nmol/L with both the three-dose GnRH-TT and the microsphere GnRH-TT preparations. Since GnRH controls the production of testosterone (indirectly through control of LH production), decreased levels of testosterone following immunization indicates that antibodies with high specificity for GnRH are being produced. The microsphere vaccine preparation was able to maintain this testosterone production suppression throughout the 18 weeks of the study. Furthermore, the testosterone levels in rats immunized with GnRH-TT in

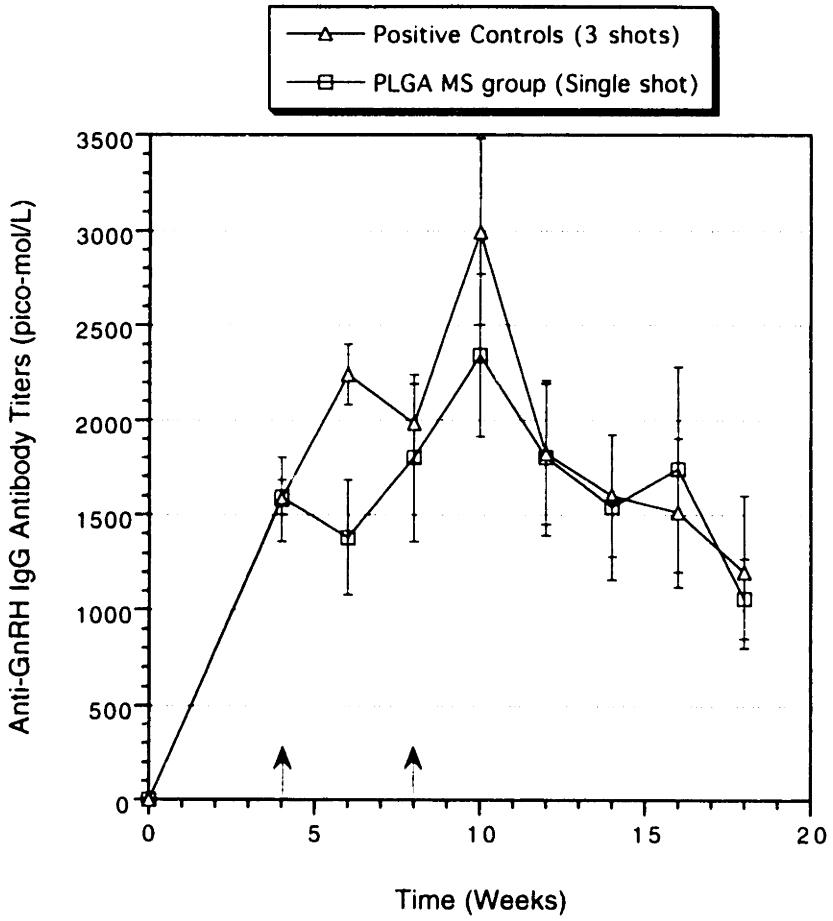

Fig 6-2. Anti-GnRH IgG antibody titers in male rats immunized with a standard three-dose GnRH-TT immunization regimen (Three-dose group, n=8, ± S.E.M.) and with a single-dose of GnRH-TT in PLGA 65:35 microspheres (PLGA MS group, n=8, ± S.E.M.). All rats received primary immunizations at t=0 weeks. Arrows denote the times at which control rats were given booster immunizations.

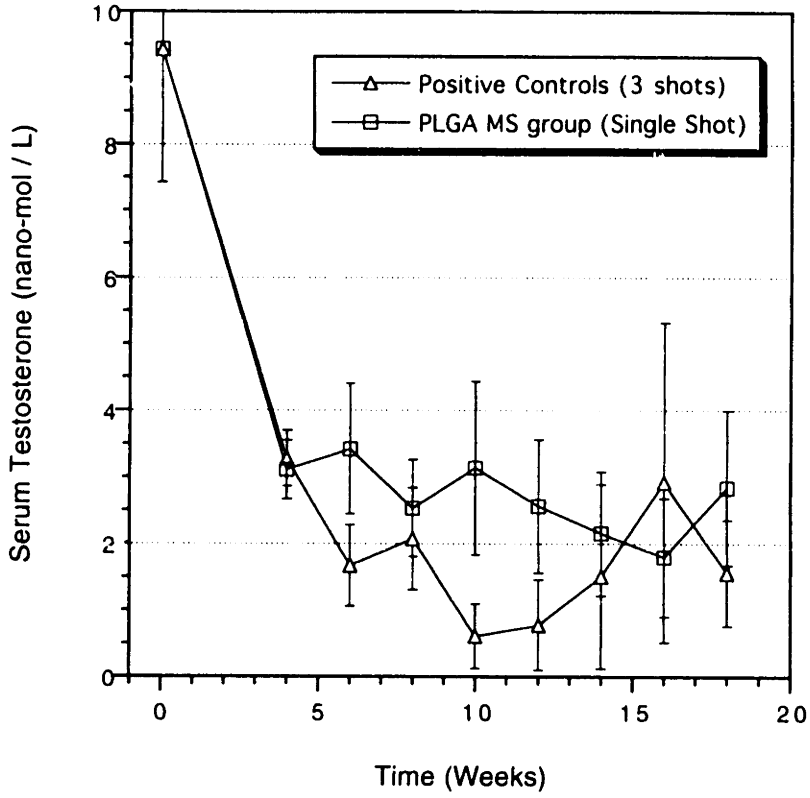

Fig 6-3. Serum testosterone levels in male rats (n=8, ± S.E.M.) following GnRH-TT immunization.

microspheres were essentially equivalent to those in rats that received the three-dose immunization schedule after 4, 8, and 14-18 weeks, a result consistent with the observed anti-GnRH-TT antibody response shown in Fig 6-2.

6.3 Conclusions

Controlled GnRH-TT release from a single dose of degradable polymer microspheres resulted in anti-GnRH immunity comparable to the standard three-dose GnRH-TT immunization schedule. This result was obtained without the use of additional adjuvants to complement the depot effect of PLGA microspheres. It is thought that higher and longer-lasting levels of immunity can be obtained by the addition of adjuvants and/or the use of polymers which degrade into adjuvant-active compounds [65]. Chapters 8-10 are dedicated to the development of new polymers for vaccine delivery which have the adjuvant L-tyrosine incorporated directly into their backbone.

7 PLGA Microspheres for Pulmonary Vaccine Delivery

7.1 Introduction

Controlled release drug delivery to the lung may simplify the way in which many drugs are taken [125, 126]. Pulmonary drug delivery is an attractive alternative to oral, transdermal, and parenteral administration because self-administration is simple, the lungs provide a large mucosal surface for drug absorption (comparable to the small intestine), there is no first-pass liver effect of absorbed drugs, there is reduced enzymatic activity and pH-mediated drug-degradation compared with the oral route, and it may eventually eliminate the need for several daily injections with drugs such as insulin. Owing to these and possibly other advantages, relatively high bioavailability of macromolecules such as protein antigens can be achieved via the inhalation route [127-129]. As a result, many aerosol formulations of therapeutic proteins and peptides are in use or are being tested for delivery to the lung [130-133], including vaccine antigens [21, 134].

In many cases, however, rapid absorption of molecules through lung epithelia leads to high drug concentrations in the blood, which can result in adverse side effects [135-137]. In addition, the duration of action of many drugs delivered to the lung can be very short (on the order of seconds to minutes in some cases [127]), necessitating repeat administration. This is particularly problematic when the patient would benefit from a sustained therapeutic effect, such as in the case of vaccine delivery. Controlled release formulations have shown promise in extending the therapeutic effects of drugs delivered via the lung while reducing side effects due to spikes of drug concentration in the circulation [126]. For example, liposomes have been used to extend the effectiveness

of drugs to hours that were previously only effective for minutes [138]. Liposomes are attractive controlled release vehicles in that they can be made using phospholipids endogenous to the lung, such as phosphatidylcholine dipalmitoyl (DPPC). DPPC is the principal constituent of lung surfactant, accounting for as much as 45 % of the material by weight [139]. However, a limitation with liposomes may be their instability during aerosolization [140] and *in vivo* due to macrophage phagocytosis [141, 142], limiting their effectiveness to relatively short periods of time (hours in most cases). In some cases, including vaccine delivery, patients would clearly benefit from longer sustained effects [143]. Controlled release polymer microspheres may offer a more stable alternative to liposomes for controlled drug delivery to the lung. PLGA microspheres have the additional advantage for pulmonary drug delivery that they can be made of virtually any size (nm to mm).

Although controlled drug delivery via the lung has shown promise for a wide variety of drugs, including cytokines and vaccine antigens, very few of these studies examine the aerosolization behavior of the formulation. Frequently, for example, carriers are placed in the lung by intratracheal (i.t.) instillation [21, 85, 135, 144, 145]. While this is an adequate method for the evaluation of the effect of controlled release on a particular dosage form in animals, i.t. instillation is not practiced clinically in humans. To facilitate its use in humans a dosage form such as a liquid aerosol or dry powder formulation (DPF) will be required.

Many drugs and excipients, especially proteins and peptides [146], and biodegradable carriers such as PLGA, are unstable in aqueous environments for extended periods of time. This can make storage as a liquid formulation problematic. In addition, protein denaturation can occur during aerosolization with liquid formulations [147]. Considering these and other limitations, DPF's are acquiring increasing attention as ideal aerosol formulations for pulmonary delivery [131, 133, 148]. Perhaps primary among disadvantages of DPF's is that powders of ultrafine

particulates usually have poor flowability and aerosolization properties, leading to relatively low respirable fractions of aerosol (fractions of inhaled aerosol that escape deposition in the mouth and throat) [143]. This is due to a number of factors, including particle aggregation, inappropriate particle size distributions, and deposition in the mouth and throat due to gravitational effects [149]. Aggregation is caused by particle-particle interactions (e.g., hydrophobic, electrostatic, and capillary) while deposition in the mouth due to gravity is exacerbated with dense aerosols. As a result, the optimization of the *aerosolization properties* of the DPF is essential to its eventual success.

Recently, we demonstrated that low mass density of DPF's contributes to the ability of relatively large aerosol particles (i.e., larger than the standard particle diameter limit of 5 μm) to deposit deep in the lung [150]. The inverse relation between particle size and particle density owes to the predominance of inertial and gravitational deposition mechanisms for inhaled aerosols [151]. The ability to create DPF's with large particle size translates furthermore into good flowability characteristics of the DPF (e.g., less aggregation) [152], easy aerosolization, and potentially longer-lived (non-phagocytosed) aerosols in the deep lung [37, 153]. In this chapter it is demonstrated that light aerosols (mass density less than 0.4 g/cc) containing a model drug can be made by double emulsification using PLGA. The porosity (or lightness) of the PLGA particles can be increased further by adding lung surfactant in the preparation of the PLGA particles, leading to even greater aerosolization efficiency. Since PLGA and DPPC are both biocompatible and currently used clinically in various ways, the particles described in this chapter may be ideal candidates for a variety of controlled-release pulmonary therapies, including vaccine antigen delivery.

7.2 Results and Discussion

Fig 7-1 shows SEM photographs of microspheres made with and without the lung surfactant, DPPC. In addition to its biocompatibility features, and the fact next demonstrated that DPPC renders microspheres more porous, it is possible that the release of DPPC from the slow eroding PLGA microspheres in the alveolar region of the lungs can more effectively insure the maintenance of normal surfactant fluid composition (the alveolar surfactant fluid layer is, on average, 10 nm thick) [154], thereby minimizing the possibility of local toxic side effects. As can be seen in Fig 7-1, microspheres made with and without DPPC have very similar surface characteristics and size distributions (as confirmed by size distribution measurements reported in Table 7-1).

Table 7-1. Characteristics of Microspheres (MS) used for *In Vitro* and *In Vivo* Aerosolization[a]

Sample	Mass-Mean (True) Diameter, (μm)	DPPC Load (μg/mg spheres)	DPPC Loading Efficiency, (%)	FITC-Dextran (Model Drug) Loading Efficiency, (%)
MS w/o DPPC	8.5 ± 0.76	0	N/A	95.8
MS w/ DPPC	8.2 ± 0.18	45 ± 6	83 ± 11	82.4

a Values are given ± standard deviation.

The external surfaces of the microspheres look almost identical for the two batches by SEM, an important point which allows direct comparison of their aerosolization behaviors. The efficient entrapment of DPPC within microspheres (83 % of theoretical ± 11% standard deviation, n=6) was confirmed by dissolving an aliquot of microspheres

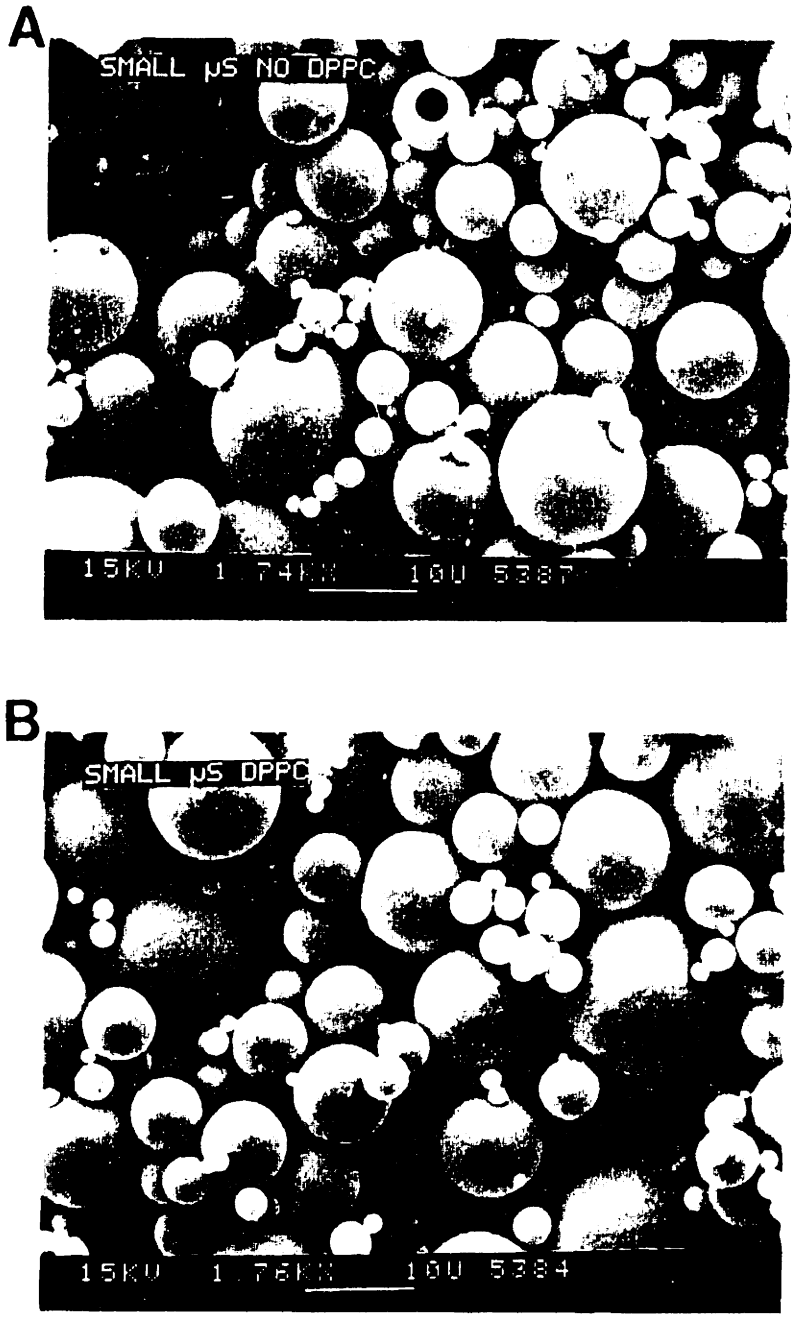

Fig 7-1. Scanning electron micrographs showing a typical batch of microspheres made (a) without DPPC and (b) with DPPC. Notice the external sphere morphologies and approximate particle size distributions appear very similar.

in chloroform and detecting the DPPC concentration in solution (Table 7-1). Particles made with and without DPPC are easily resuspended in aqueous solution after lyophilization and are lump-free when dry as determined by light microscopy.

Mercury intrusion measurements were performed to evaluate the total porosity, or mass density, of the microspheres. Table 7-2 summarizes the results of these studies. In addition to providing the mass density characteristics of the microspheres, with and without DPPC, Table 7-2 lists the mass density of bulk PLGA corresponding to the

Table 7-2. Comparison of Porous Microspheres (MS) with Bulk (PLGA 50:50) Polymer

Sample	Density, ρ_{MS} (g/cc)	Porosity (%)	Respirable Size Range, d_{resp} (μm)
Bulk PLGA	0.63 ± 0.03	0	1.0 - 5.9
MS w/o DPPC	0.37 ± 0.03	41 ± 4.0	1.3 - 7.7
MS w/ DPPC	0.27 ± 0.02	58 ± 3.3	1.55 - 9.13

polymer as it was received from the manufacturer (before processing). The mass density of PLGA 50:50 (and, therefore, the maximum density the microspheres could attain if they contained no porosity) is 0.63 ± 0.03 g/cc as determined by helium pyncnometry. In Table 7-2 it is apparent that both batches of microspheres are considerably porous *owing to their preparation by the double-emulsion procedure*. Moreover, the effect of DPPC is to render the microspheres even more porous. Microspheres without DPPC have a porosity of approximately 0.41 ± 0.04, whereas the porosity of microspheres with DPPC is 0.58 ± 0.03. Porosities (ε) were calculated by:

$$\varepsilon = 1 - (\rho_{MS})/(\rho_{PLGA}) \quad (1)$$

where ρ_{MS} is the density of the microspheres and ρ_{PLGA} is the density of PLGA 50:50.

Since the heightened porosity of the microspheres with DPPC is not readily apparent by surface morphology characteristics (Fig 7-1), a model drug, FITC-Dextran (M_W 19,000), was distributed throughout the microspheres to visualize the interior of the particles. Fig 7-2 shows a single microsphere made a) without DPPC and b) with DPPC. The light areas correspond to the fluorescent material, the intensity of the light indicating the relative amount of drug in a particular location. Dark areas are regions without drug, corresponding to solid polymer. Three observations may be made in Fig 7-2: (i) in each case the drug is evenly dispersed throughout the polymer matrix, a condition known to lead to prolonged delivery of macromolecules after placement in an aqueous environment (see Chapters 4 and 5); (ii) there appears to be, on average, less drug (lower light intensity) encapsulated in the DPPC microsphere. This was later confirmed by drug loading determination studies (Table 7-1), which revealed that DPPC-containing microspheres entrap 82.4% of theoretical FITC-Dextran compared with 95.8% encapsulation efficiency without the use of DPPC; and (iii) DPPC microspheres appear to be less dense (more porous) than microspheres made without DPPC, confirming the results of the mercury intrusion analyses (Table 7-2). The latter observation follows from the fact that the drug is dispersed more evenly throughout the DPPC particle, with very few regions of high concentration (i.e. high light intensity). Due to the large porosity of DPPC microspheres, drug initially sequestered in distinct drug pockets (due to the formation of the inner emulsion, see Chapter 4) is able to diffuse throughout the microsphere during its preparation and drying. Microspheres made without DPPC, on the other hand, have many more regions of high drug concentration (high light intensity) and also many more dark regions of solid polymer, where no drug has been able to diffuse. The fact that the loading efficiency of drug is decreased when DPPC is used appears due, therefore, to the increased porosity of these

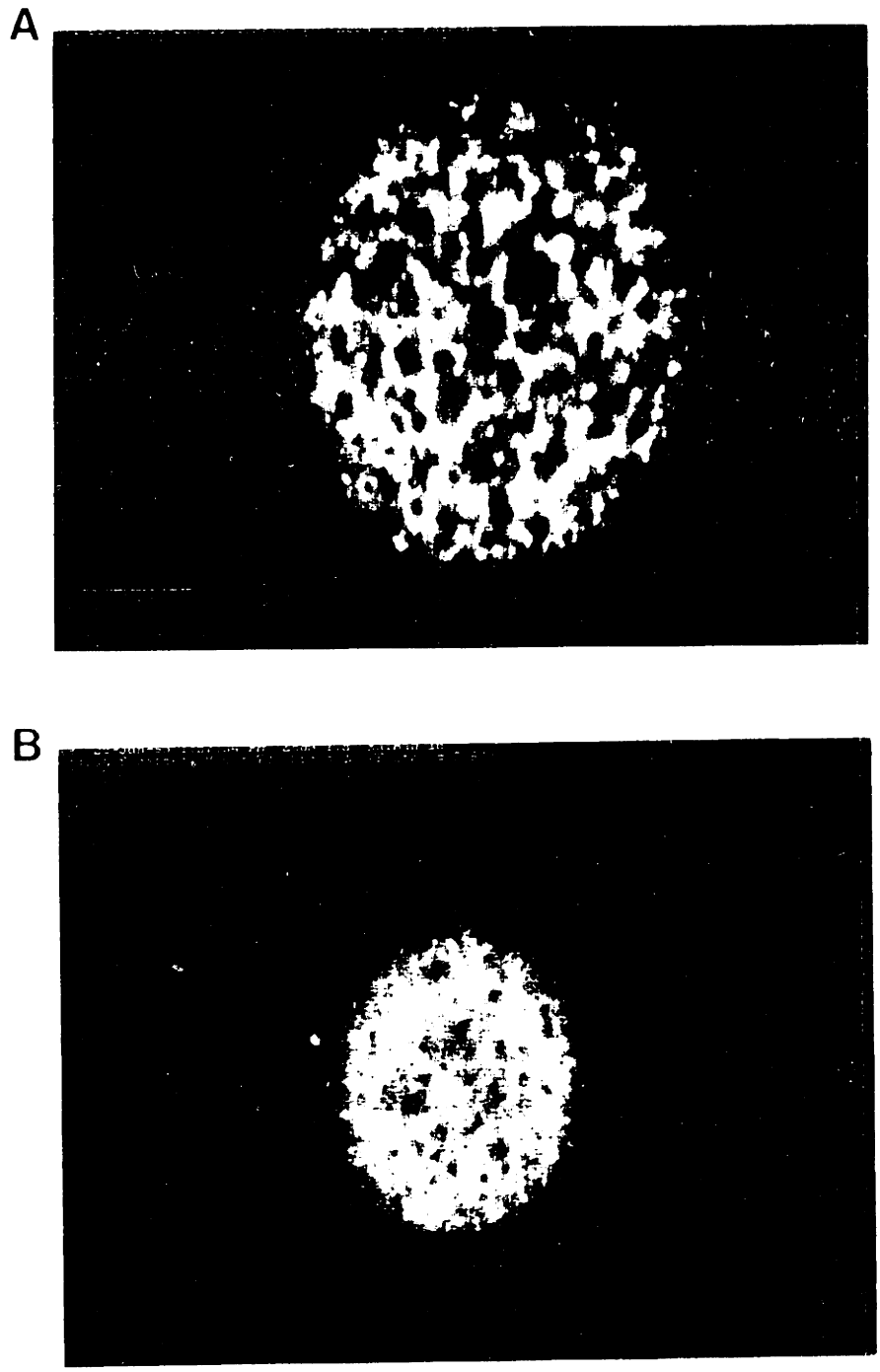

Fig 7-2 Confocal micrographs showing the distribution of the model drug, FITC-Dextran, throughout microspheres made a) without DPPC; and b) with DPPC.

particles, allowing a higher percentage of the drug to diffuse out of the particle during its preparation.

The advantage of relatively high particle porosity (microspheres mass density ≤ 0.4 g/cc) for inhalation therapies relates to the propensity for relatively large aerosol particles (of standard mass density, ρ_{MS} = 1 g/cc) to fall out of an inspiratory airstream prior to entering the airways, and for relatively small (respirable) aerosols to excessively aggregate [152]. For aerosols of standard mass density, the *respirable size range* (i.e., size of particles that enter and remain in the airways) is 0.8 to 4.7 μm [151]. However, aerosols in the size range 1-3 μm (ideal for maximal deep lung deposition [151]) tend to aggregate, leading to poor flowability and aerosolization characteristics [152]. By rendering microspheres porous, the upper respirable size limit can be increased, and therefore relatively large respirable aerosols can be made with excellent flowability and aerosolization features [150].

Using the concept of aerodynamic diameter [143], it is possible to determine the *respirable size range* of the microspheres given their mass density, ρ_{MS}. Specifically, it can be shown that:

$$\frac{0.8}{\sqrt{\rho_{MS}}} \leq d_{resp} \leq \frac{4.7}{\sqrt{\rho_{MS}}} \qquad (2)$$

where d_{resp} corresponds to the diameter of particles (in μm) able to enter and remain in the airways without inertial or gravitational deposition (particles smaller than this range are exhaled), and where ρ_{MS} is in units of g/cc. The theoretical respirable size range of the microspheres are shown in Table 7-2. Comparing the 'true' particle diameters (Table 7-1) with the theoretical respirable size limits (Table 7-2) reveals that a large fraction of the microspheres without DPPC are nonrespirable theoretically, whereas the microspheres with DPPC are near the upper limit of the respirable range. The optimal size range (i.e., d_{resp}) for a non-porous PLGA 50:50 microsphere is 1.0-5.9

μm (Table 7-2). The optimal respirable size range for microspheres without DPPC is 1.3-7.7 μm and, for microspheres with DPPC, 1.55-9.13 μm (Table 2)---the upper limit on size of respirable particles has increased from 5.9 to greater than 9 μm when DPPC is used in PLGA microsphere preparation. Therefore, the use of low density DPPC microspheres allows the use of larger particles for aerosolization, which may have advantages for drug delivery such as less particle-particle interaction due to decreased surface area to volume ratio, and lower susceptibility to phagocytosis by alveolar macrophages.

Fig 7-3 shows the results of an *in vitro* aerosolization of the microspheres as a dry powder released from a Spinhaler dry powder inhaler (DPI). Fig 7-3a shows the percentage of microspheres initially loaded into the DPI that were released upon simulated inhalation using an Andersen Mark I Cascade Impactor. DPI efficiencies approaching 80% were obtained with microspheres made with and without DPPC, a testament to the excellent flow properties and low aggregation of these spheres. Although the DPI efficiencies for the two batches were nearly the same, a great difference can be seen between microspheres made with and without DPPC when their deposition within the cascade impactor is observed (Fig 7-3b). Fig 7-3b shows the percent of aerosolized particles that reach stages 2-F of the Andersen impactor, considered the stages corresponding to the respirable fraction of PLGA microspheres in this study. It can be seen that a much greater percentage of microspheres make it to the latter stages of the impactor (considered deeper portions of the lungs) when DPPC is used in their preparation. Overall, greater than 35% (37.0 ± 2.1) of aerosolized particles made with DPPC are considered respirable compared with 13.2 ± 2.9 % without DPPC (Table 7-3). The primary reason for the relatively low respirable fractions (for both particle types) observed in Fig 7-3 is most likely the large particle size relative to the upper limit of the respirable range (Table 7-2). The large difference between the DPPC and non-DPPC particles shows, however, that the relatively low respirable fractions *in*

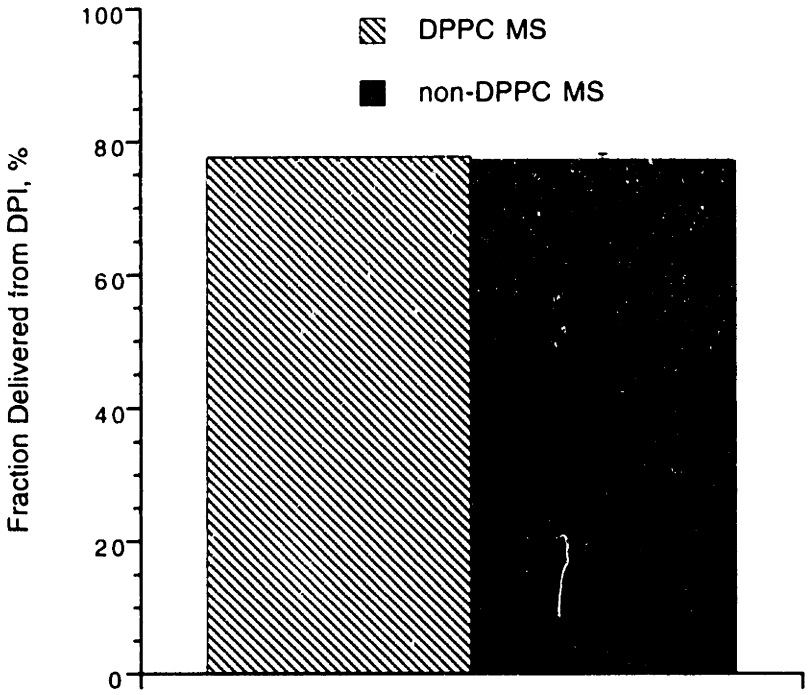

Fig 7-3a. Comparison of the *in vitro* aerosolization behaviors of PLGA microspheres made with and without DPPC showing the mass-fraction of the initial dose that is released from the dry powder inhaler device (DPI Efficiency).

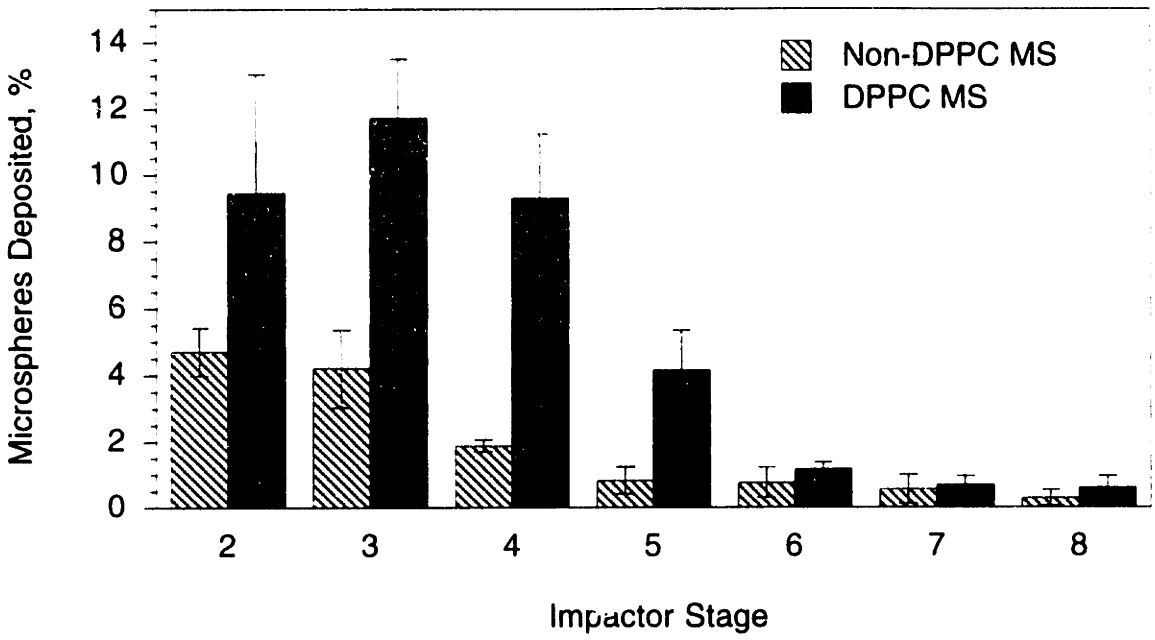

Fig 7-3b. Comparison of the *in vitro* aerosolization behaviors of PLGA microspheres made with and without DPPC showing the mass-fraction of the aerosolized dose that is deposited in stages 2 through filter (2-F) of the cascade impactor (considered the respirable fraction). Stages 0 and 1 correspond roughly to the mouth and throat, and to the upper airways of the lung, respectively. Stages 2-F correspond to successively deeper fractions of the lung.

vitro (compared with theoretical predictions based on d_{resp}) cannot be explained solely on the basis of particle size or density arguments, as next explained.

In order to estimate the *expected* respirable fraction (RF) of the microspheres, which could then be compared with *in vitro* and *in vivo* RF's, size distribution measurements were analyzed to determine the percentage of particles (by mass) of each type (DPPC and

Table 7-3. Comparison of Microsphere (MS) Aerosolization Properties *In Vitro*

Sample	Mass % of MS in Respirable Size Range[a]	Measured Respirable Fraction (%, *In Vitro*[b])
MS w/o DPPC	51 ± 6	13.2 ± 2.9
MS w/ DPPC	63 ± 2	37.0 ± 2.1

a Based on respirable size range (d_{resp}, Table 7-2) and size distribution analyses.

b Measured using an Andersen Mark I Cascade Impactor.

non-DPPC) that were within the theoretical respirable size range (i.e. d_{resp}, Table 7-2). As can be seen in Table 7-3, a higher percentage of particles made with DPPC are indeed expected to be respirable compared with non-DPPC particles (63 to 51%, respectively). This *expected* respirable fraction is based on the mass fraction of microspheres with diameters in the respirable size range, d_{resp}, as defined by Eq. (2), and therefore takes into account the different sizes and densities of the two batches of

microspheres. The significant difference observed between the theoretical respirable fraction and the actual respirable fraction measured *in vitro* (Table 7-3) indicates that aerodynamic diameter is not the sole factor influencing the experimental *in vitro* respirable fraction results.

To determine whether agglomeration forces during particle aerosolization from the Spinhaler device might be playing a role even after the particles enter the impactor system (i.e., primarily non-DPPC-particles remain agglomerated in the inspired stream, resulting in deposition in the first two impactor stages: stages 0 and 1), *in vivo* aerosolization experiments were performed in which particles were permitted to fall by gravity into the inspiration stream (see Methods) of a Harvard ventilator system joined with the trachea of an anesthetized rat. Approximately 63% of the inhaled DPPC-PLGA particles deposit in the airways and distal lung regions, whereas 57% of the non-DPPC particles are able to penetrate beyond the trachea in the lungs (Fig 7-4). These respirable fractions are much nearer to the predicted respirable fractions based upon particle diameter and mass density (Table 7-3). The total mass deferred to the lung in the *in vivo* experiments depended similarly on whether DPPC was associated with the PLGA microspheres. In the absence of DPPC, approximately 36% of the 50 mg dose reached the trachea and lung, whereas with DPPC, 39% of the original dose deposited in the trachea and lungs. Contrastingly, identical *in vivo* rat studies with *non-porous* PLGA particles of similar size (mean diameter of 6.9 μm ± 3.6 μm) reveal that only about 22% of non-porous particle mass reaches the airways at distal lung regions [150]. These results confirm that low particle mass density favors high respirable fractions of relatively large inhaled PLGA aerosols.

Comparing the *in vitro* and *in vivo* deposition results, it appears that particle aggregation may be less in the case of DPPC-containing PLGA particles than without DPPC, even though the particles are of identical size and similar surface morphological features. It is possible that DPPC lends to the PLGA particle surface a more

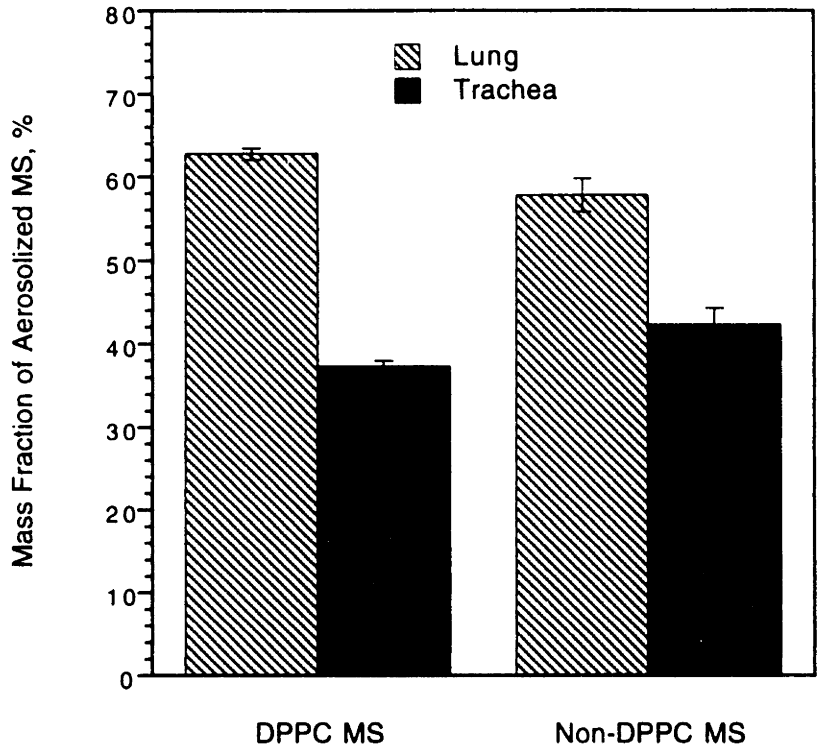

Fig 7-4. Comparison of the *in vivo* aerosolization behaviors of PLGA microspheres made with and without DPPC showing total particle mass deposited in the trachea and in the lungs (after the carina) of rats as determined using bronchoalveolar lavage.

hydrophobic character that minimizes particle aggregation caused by trace amounts of moisture absorption, although other interparticle attractions, such as van der Waals and electrostatic attractions, may also be affected. Future studies are aimed at the quantitative measurement of the contributions of the various forces of particle-particle attraction to particle aggregation. It is expected that these studies, combined with work to optimize particle size distributions, will lead to further improvements in the aerosolization efficiency of dry powder PLGA microsphere formulations.

8 Synthesis and Characterization of Anhydride-*co*-imide Terpolymers Containing Tyrosine for Vaccine Delivery

8.1 Introduction

As previously discussed, the polyesters based on lactide and glycolide have been the most widely studied degradable polymers for drug delivery applications [100]. Although these polymers may be acceptable for use in many medical applications, they may not always be the most suitable. For example, their poor immunostimulating properties may make them suboptimal depots for weakly immunogenic subunit antigens. As a result, antigens delivered via lactide/glycolide polymers often require the addition of an adjuvant to be maximally effective in initiating a protective immune response [30, 107].

The goal of this study was to synthesize and characterize a family of biodegradable polymers which could be used as a depot to deliver drugs, and more specifically, vaccine antigens. Initial studies in Dr. Langer's group focused on the use of degradable polyiminocarbonates based on *N*-benzyloxycarbonyl-L-tyrosyl-L-tyrosine hexyl ester (CTTH) [65], a dityrosine derivative, due to the inherent ability of L-tyrosine and many of its derivatives to stimulate a potent immune response to adsorbed antigens [57-60, 62, 155-157]. It was shown that vaccine release from poly(CTTH iminocarbonate) implants leads to enhanced levels of immunity compared with release from a similar polyiminocarbonate which is not based on a tyrosine derivative. However, these poly(CTTH iminocarbonates) were low molecular weight, brittle polymers which could not be used to fabricate microspheres suitable for *in vivo* injection in a reproducible manner. On the other hand, polyanhydride copolymers based on

sebacic acid (SA) and 1,3-bis(carboxyphenoxy)propane (CPP) are versatile drug delivery vehicles, having been used for years to deliver a variety of drugs from proteins to low molecular weight chemotherapeutic agents [86, 158]. CPP:SA copolymers are currently used clinically to deliver BCNU locally within the brain to treat patients with brain tumors [158]. They have a history of safe use in humans and animals [158, 159], and their erosion rate can be varied from hours to years depending on the ratio of SA to CPP in their backbone [160]. However, despite their usefulness for drug delivery applications, conventional polyanhydrides are expected to have limited inherent immunostimulatory properties. As a result, they may make only marginal delivery systems for vaccine antigens.

To improve the immunostimulatory effect of polyanhydrides, vaccine adjuvants such as tyrosine may be incorporated directly into their backbone. A class of polyanhydrides capable of incorporating tyrosine into their backbone is the poly(anhydride-*co*-imides) [91]. Such a polymer may be ideally suited for vaccine delivery by combining the adjuvanticity of tyrosine with the desirable controlled release properties of polyanhydrides. To achieve this goal, the objectives were: (i) incorporate a large percentage of tyrosine into the backbone of a biodegradable anhydride polymer which could be used to deliver vaccine antigens; and (ii) produce high molecular weight, amorphous polymers (crystallinity can lead to heterogeneous degradation and irreproducible drug loading and release) capable of delivering protein antigens for days to months. To achieve these objectives, the synthesis of a series of anhydride-*co*-imide terpolymers based on the mixed anhydrides of acetic acid and trimellitylimido-L-tyrosine (TMA-Tyr), SA, and CPP (Fig 8-1) was systematically optimized and the resulting polymers were thoroughly characterized . For the first time, high molecular weight polymers (M_W > 80,000) with appreciable TMA-Tyr content have been synthesized. Polymers were synthesized with a balance of CPP to allow for long-term release kinetics, SA to improve polymer solubility and processability, and tyrosine

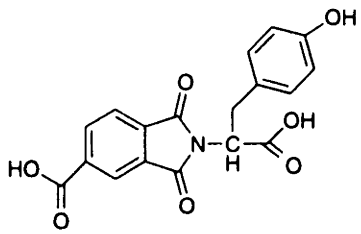

Trimellitylimido-L-tyrosine (TMA-Tyr)

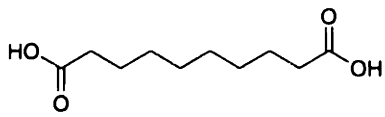

Sebacic Acid (SA)

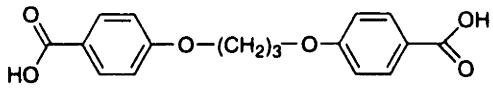

1,3-bis(carboxyphenoxy)propane (CPP)

Fig 8-1. Chemical structure of TMA-Tyr, SA, and CPP before acylation.

monomer (TMA-Tyr) for its possible adjuvanticity. Careful selection of the three monomers allowed the production of a series of amorphous polymers with a variety of monomer compositions which should allow a wide range of polymer erosion and drug release kinetics. In this chapter, the effect of various reaction conditions, as well as the effect of the various monomers and monomer ratios, on polymer molecular weight, polydispersity, glass transition temperatures, and crystallinity are reported.

8.2 Results and Discussion

8.2.1 Monomer Preparation

Purified monomers and acylated monomers were prepared and characterized by ^{1}H NMR, IR spectroscopy, elemental analysis, and gel permeation chromatography (GPC). Oligomers consisting of 1.2 to 1.7 units in average, based on GPC and ^{1}H NMR analysis, respectively, were synthesized from aromatic monomers (TMA-Tyr and CPP) compared with 4.7 to 5.0 units for the aliphatic monomer (SA) (Table 8-1). Oligomerization can occur during reflux in acetic anhydride, during subsequent acetic anhydride removal at high temperatures, and during purification by recrystallization. The use of long oligomers in the synthesis of copolymers leads to lower molecular weight polymers [92] and creates large aliphatic regions in the anhydrides (SA-rich regions) that are susceptible to faster degradation, resulting in heterogeneous polymer degradation. To avoid extensive oligomerization during the isolation step, unreacted acetic anhydride was removed at mild temperatures (40°C) under vacuum. By reducing the reaction time of TMA-Tyr, CPP, or SA in acetic anhydride (3 minutes under reflux), or lowering the reaction temperature (60°C for 2 hr), followed by filtration of unreacted diacid and evaporation of excess acetic anhydride at room temperature, primarily monomeric acylated monomers were produced. However, as the preparation of

monomeric prepolymer is time consuming and wasteful, short oligomers were used in this study.

Table 8-1. Characteristics of Acylated Monomers used in the Synthesis of Poly(TMA-Tyr:SA:CPP)

Monomer	Calculated MW	GPC Analysis			^{1}H NMR
		*M*w	*M*n	*Dp*[a]	*Dp*[b]
Acyl-TMA-Tyr	439.4	558	561	1.28	1.65
Acyl-SA	286.3	1513	1415	4.94	4.68
Acyl-CPP	400.4	460	492	1.23	1.09

a Degree of polymerization based on the M_n of GPC analysis

b Degree of polymerization based on ^{1}H NMR analysis

8.2.2 TMA-Tyr:SA:CPP Terpolymer Synthesis and Structure Confirmation

The reaction scheme used to synthesize the polymers is shown in Fig 8-2. In the first step, equimolar amounts of L-tyrosine and TMA were reacted at reflux in DMF. As a result of this condensation reaction, the amino terminus of tyrosine is incorporated into a cyclic imide bond. This reaction is performed for two reasons: first, the reactive amino terminus of tyrosine is protected by cyclicization, and is therefore not able to participate in side reactions during polymerization; and, second, the resulting monomer is a diacid suitable for condensation polymerization (after acylation) to make a linear polyanhydride. Once the monomers are made and purified, they are refluxed in acetic anhydride to acylate their carboxylic acid end groups. As confirmed by ^{1}H NMR and

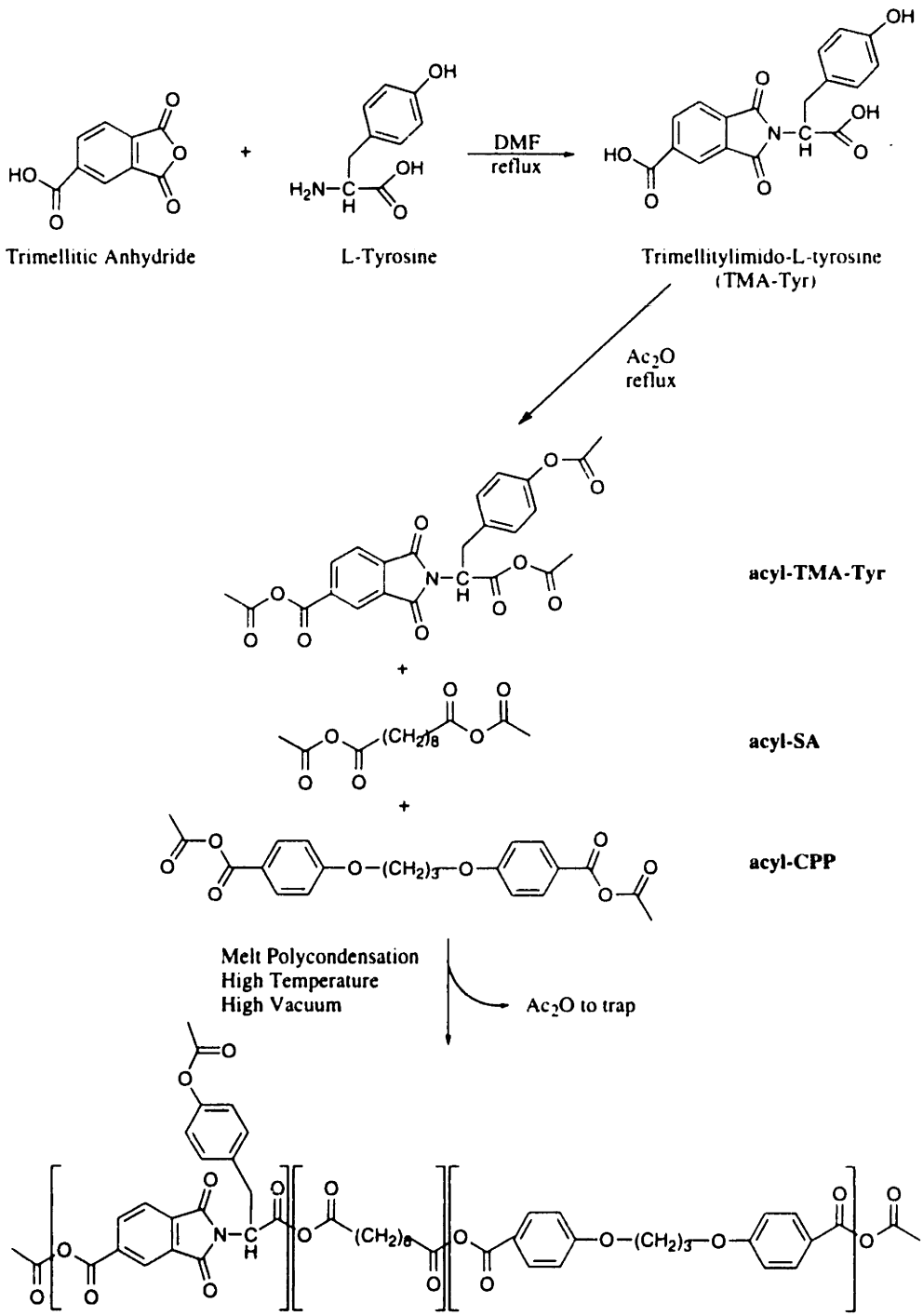

Poly(anhydride-*co*-imide) Terpolymer

Fig 8-2. Synthesis scheme of poly(TMA-Tyr:SA:CPP).

IR spectroscopy (see experimental section), the phenolic hydroxide of tyrosine also reacts with acetic anhydride to form an acetate ester, thereby protecting it from further reaction during polymerization. Subsequently, the acylated monomer powders are isolated and purified (see experimental section), and reacted in bulk at temperatures ranging from 120-200°C under high vacuum, with or without a heterogeneous catalyst.

IR and ^{1}H NMR spectroscopy were used to confirm the polymer composition and integrity. Of the three monomers used, two are symmetric (SA and CPP), and one is asymmetric (TMA-Tyr). As a result, ten diad sequences are expected in the polymer backbone. In the ^{1}H NMR spectra of poly(TMA-Tyr:SA:CPP) with a molar feed ratio of 20:50:30, multiplets for the SA-SA diad are found at 1.65 and 2.45 ppm, whereas multiplets for the CPP-CPP diad are at 2.35 and 8.08. Multiplets for the SA-CPP diad are at 1.74 and 2.60 attributed to protons of SA, and 6.97 and 7.98 attributed to CPP. Triplets for SA reacted with the tyrosine end of TMA-Tyr (SA-Tyr), and with the TMA end of TMA-Tyr (SA-TMA) are found at 2.48 and 2.65, respectively. Both triplets are attributed to protons of SA. Finally, multiplets attributed to TMA-Tyr corresponding to overlay signals for the remaining TMA-Tyr diads (TMA-CPP, Tyr-CPP, TMA-TMA, Tyr-TMA, and Tyr-Tyr), as well as for SA-Tyr and SA-TMA, are found at 3.59, 3.70, 5.25, 5.43, 7.18, 7.91, 8.42, and 8.52 ppm. Due to the complex overlapping in the ^{1}H NMR spectra when several monomers are used, especially in the regions of asymmetric monomers such as TMA-Tyr, it is difficult to assign the individual diads involving TMA-Tyr. Multiplets for the aliphatic protons of SA and CPP are found at 1.34 and 4.25 ppm, respectively. At 2.22 there is a multiplet representing a clear overlapping of the terminal -CH_3 signals of SA and TMA-Tyr. The signal for the terminal -CH_3 of CPP is contained in a multiplet at 2.35 which is overlapped by signals for the CPP-CPP and CPP-SA diads. It is already well established that copolymers of CPP and SA have a random distribution of the two monomers throughout their polymer backbone [161].

The fact that all three monomers of the terpolymers react with one another suggests that they are random copolymers as well.

For infrared analysis, in general, aliphatic carbonyls of anhydride polymers absorb around 1740 and 1810 cm^{-1} and those of aromatic polyanhydrides around 1720 and 1780 cm^{-1}. When the polymer contains both aliphatic and aromatic monomers (e.g., SA and CPP), the peaks at 1720-1740 cm^{-1} overlap. The results reported here agree with these generalities for polyanhydrides, showing an aliphatic carbonyl peak at 1817 cm^{-1}, and shoulders of low intensity around 1785 cm^{-1} for the aromatic carbonyl , and 1730 cm^{-1} for the overlap of aromatic and aliphatic carbonyls. These shoulders partially overlap distinct peaks for the imide carbonyls at 1784 and 1727 cm^{-1}. Extensive overlapping of anhydride and imide carbonyls in the 1700-1800 cm^{-1} region makes it difficult to readily assign some of the anhydride peaks. Characteristic peaks for aromatic C=C bonds (TMA-Tyr and CPP) are found at 1604 and 1582 cm^{-1}, those for aliphatic C-H stretches at 2932 and 2852 cm^{-1}, and a peak for the C-N stretch appears at 1380 cm^{-1}. The OH band for TMA-Tyr at 3370 cm^{-1} is not present in the polymer spectra, confirming the acylation of the phenol hydroxyl in the polymer structure.

8.2.3 TMA-Tyr:SA:CPP Terpolymer Synthesis Optimization

In this part of the study the factors affecting polymer molecular weight and polydispersity were systematically determined using a fixed TMA-Tyr:SA:CPP feed ratio of 20:50:30, the only exception being the initial reactions run to determine the effect of reaction temperature on the polymerization (Fig 8-3). The critical factors involved in achieving high molecular weight polymers were monomer purity, temperature of reaction, duration of polymerization, catalyst and catalyst concentration, and the removal of the condensation by-product, acetic anhydride. Fig 8-3 shows the effect of reaction temperature on the melt polymerization using a molar feed ratio of TMA-

Tyr:SA:CPP of 16:42:42. When the reaction was run for 1.5 hours without catalyst, the maximum weight average molecular weight obtained was 25,600 (at 180°C). By raising the reaction temperature from 120°C to 180°C, higher molecular weight polymers were produced. However, polymer polydispersity also increased with molecular weight. This result is consistent with previous studies on polyanhydrides containing CPP and SA, where 180°C was also the optimal reaction temperature [92]. Dark-colored, partially-insoluble products were observed at reaction temperatures higher than 190°C, probably as a result of decomposition and/or cross-linking reactions. Polymer cross-linking may be explained by the formation of free phenolic hydroxyl of TMA-Tyr which is then able to react with anhydride bonds in the polymer backbone. As a result, a reaction temperature of 180°C was used for subsequent synthesis optimization of the anhydride-*co*-imides in this study.

The effect of reaction time at 180°C on polymer molecular weight is shown in Fig 8-4. The results represent an average of three to five reactions, except for the three-hour time point which was run twice. Molecular weight increased with reaction time initially, reached a maximum at one hour, and decreased thereafter. Increasing the reaction time beyond 2 hours at 180°C (or 30 minutes at 200°C) yielded a rubbery gel that swelled extensively in chloroform. This product was partially solubilized after 24 hours, but had a lower molecular weight than that prior to cross-linking. The decrease in molecular weight with time may be explained by polymer depolymerization which occurs during excessive heating. It has been proposed that depolymerization of polyanhydrides is due to the formation of low molecular weight cyclic oligomers, which are in equilibrium with the high molecular weight linear polymer [162, 163]. Factors such as high viscosity of the polymer melt and steric effects due to chain folding may limit chain mobility and reactive end-group availability after one hour of reaction.

The effect of catalysts on the melt polymerization was also studied. Because the reaction is a transesterification that involves nucleophilic attack of an etheric oxygen on

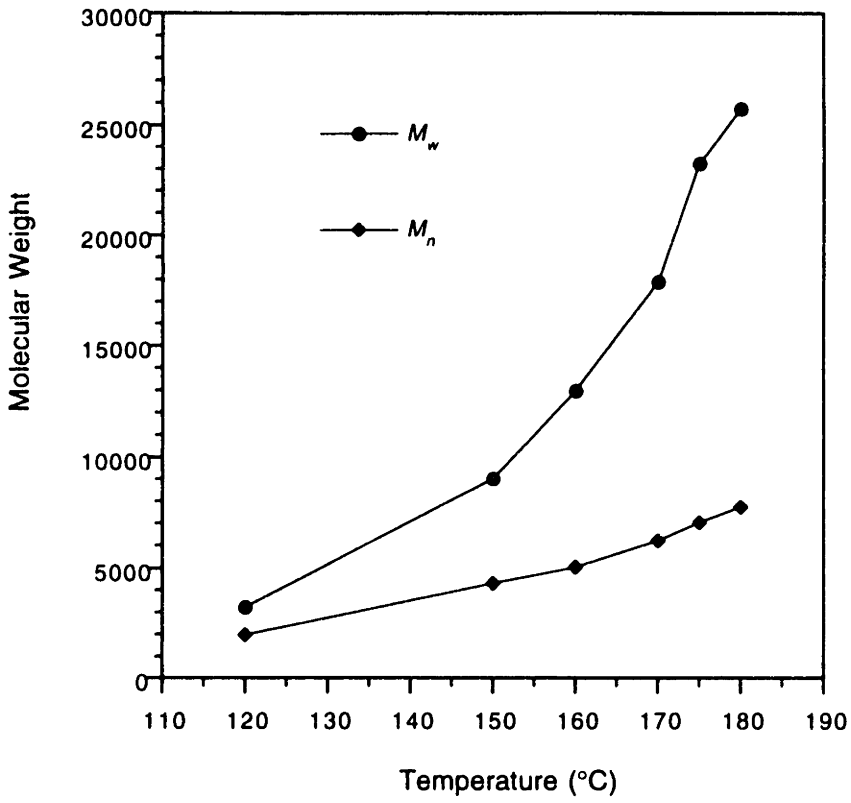

Fig 8-3. Molecular weight of poly(TMA-Tyr:SA:CPP) (molar feed ratio of 20:50:30) as a function of reaction temperature. The terpolymers were melt polymerized for 1.5 hours without catalyst.

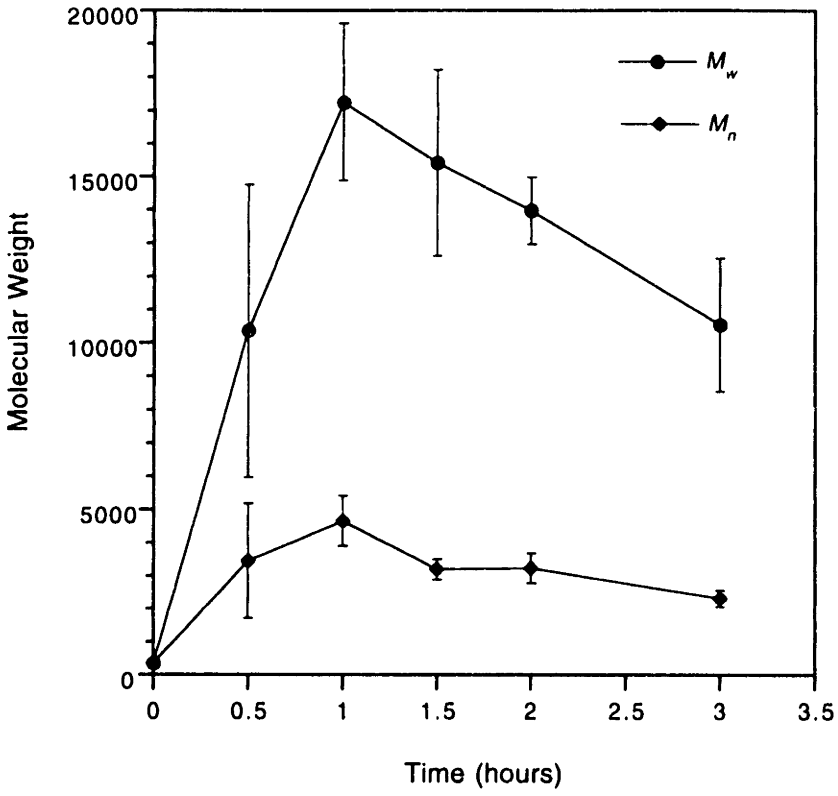

Fig 8-4. Molecular weight of poly(TMA-Tyr:SA:CPP) (molar feed ratio of 20:50:30) as a function of reaction time. The terpolymers were melt polymerized at 180°C without catalyst.

a carbonyl carbon, it was proposed that a catalyst that increases the electron deficiency of the carbonyl carbon should enhance the polymerization rate. Many coordination catalysts were suggested for the transesterification polymerization of polyesters [164]. Similar catalysts have been found active in ring-opening polymerization of epoxides due to metal-oxygen complexation [165]. More importantly, coordination catalysts, such as cadmium acetate ($CdAc_2$) and earth metal oxides, have previously been shown effective in producing high molecular weight polyanhydrides [92]. In this study the effect of several coordination catalysts on polymer molecular weight were characterized. Two mole percent catalyst was used because it was previously shown to be optimal in the synthesis of SA:CPP copolymers [92]. Fig 8-5 shows that higher molecular weights in shorter times were achieved when two mole percent $CdAc_2$ or earth metal oxides were used as catalysts. The weight average molecular weight reached a maximum of 62,000 in 30 minutes with $CdAc_2$ compared to 18,000 in 60 minutes without a catalyst. High molecular weights were also achieved using barium oxide (BaO) after slightly longer times (60 minutes) than with $CdAc_2$. The use of two mole percent calcium carbonate ($CaCO_3$) led to significantly higher molecular weights after 30 minutes compared with polymers synthesized without catalyst. However, after 60 minutes the molecular weights were not significantly different between the two groups. In general, the highest molecular weights in the shortest times were achieved using $CdAc_2$. Finally, the best catalysts ($CdAc_2$ and BaO) were less effective in large particle size (300 - 500μm) than in small particle size (< 50 μm), consistent with the assumption of a heterogenic type of reaction. It may be possible to use a much lower percentage of catalyst if its particle size distribution is very small (e.g., < 5 μm). Such particle size distributions may be achieved, for example, using spray drying. However, with very small catalyst particles it is difficult to ensure their complete removal by filtration after polymerization, a potential problem when toxic catalysts are used.

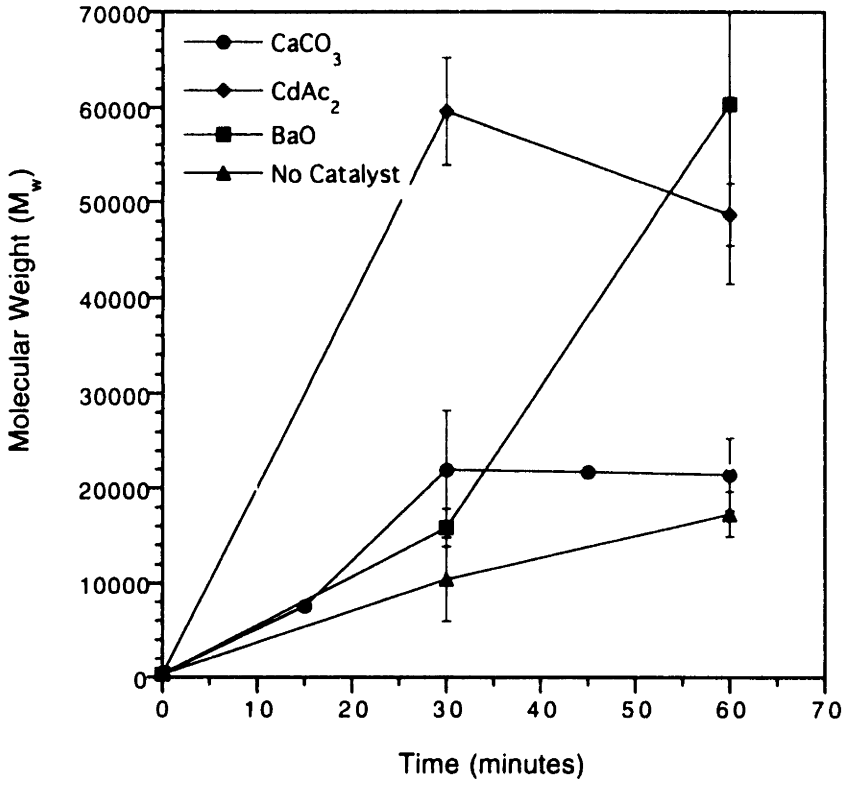

Fig 8-5. Melt polymerization of poly(TMA-Tyr:SA:CPP) (molar feed ratio of 20:50:30) with two mole percent of various heterogenic catalysts at 180°C.

Although high molecular weight polymers were obtained using two molar percent of $CdAc_2$ or BaO for 1 hour (M_W = 51,000 and 62,000, respectively), the polydispersity was not reduced (M_W/M_n = 4.2 and 6.3) compared to polymerizations without catalyst. In fact, the polydispersity of the poly(anhydride-*co*-imides) generally increased with increased molecular weight, regardless of the polymer composition (e.g., see Tables 8-2 and 8-3). The increase in polydispersity with M_W is consistent with the classical mechanism of condensation reactions [166].

Finally, the effect of catalyst concentration was determined for $CdAc_2$ and $CaCO_3$. $CdAc_2$ was chosen due to its effectiveness at a concentration of two mole percent, whereas $CaCO_3$ was selected because it is generally regarded as safe and therefore may be better suited for use with polymers intended for *in vivo* use. Optimal molecular weights for polymers synthesized using $CdAc_2$ and $CaCO_3$ were obtained after 30 and 60 minutes, respectively, regardless of catalyst concentration (Fig 8-6). Increasing the $CdAc_2$ concentration from zero to five percent led to polymers with weight average molecular weights in excess of 80,000. However, $CaCO_3$ did not appear to be an effective catalyst at any concentration under the conditions tested. Results similar to those shown in Fig 8-6 were obtained at different reaction times for each catalyst (i.e., 30 min for $CaCO_3$ and 60 min for $CdAc_2$; 1-5 mole % catalyst).

8.2.4 Effect of Monomer Ratio on TMA-Tyr:SA:CPP Terpolymers

The effect of TMA-Tyr:SA:CPP ratios on polymer characteristics was determined by synthesizing a series of polymers with various monomer ratios. For this part of the study, two mole percent cadmium acetate was used as a catalyst, and the reactions were run for 30 minutes at 180°C (optimized conditions). Highly aromatic polyanhydrides, which had greater than 80 percent TMA-Tyr or CPP content, were generally rigid and brittle and of low molecular weight (M_W < 5000). Higher molecular weights were

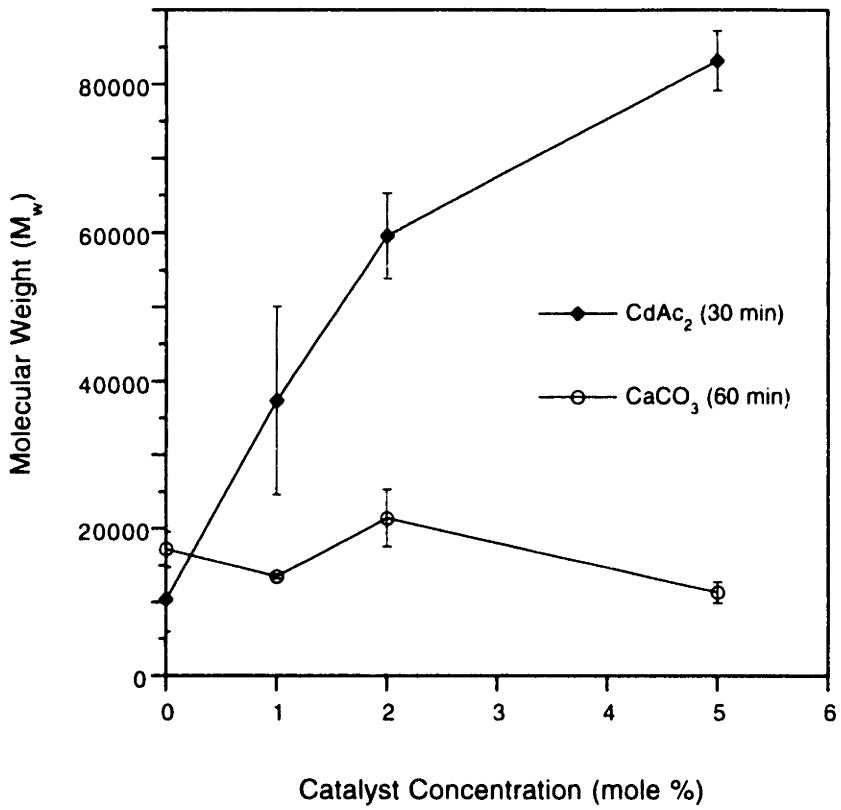

Fig 8-6. Melt polymerization of poly(TMA-Tyr:SA:CPP) (molar feed ratio of 20:50:30) with various concentrations of cadmium acetate ($CdAc_2$) or calcium carbonate ($CaCO_3$) at 180°C. Terpolymers synthesized using $CdAc_2$ and $CaCO_3$ were reacted for 30 minutes and 60 minutes, respectively, according to the optimal reaction conditions of the catalysts.

obtained by copolymerization with SA. Table 8-2 shows the characteristics of a series of polymers synthesized at a constant 20 mole percent acyl-TMA-Tyr and various ratios of SA:CPP in the reaction feed. Molecular weights in excess of 77,000 were obtained for

Table 8-2. Characteristics of Poly(TMA-Tyr:SA:CPP) Synthesized with Constant acyl-TMA-Tyr (20 mole %) in the Reaction Feed[a]

% TMA-Tyr:SA:CPP (reaction feed)	M_W	PDI	T_m (°C)	% TMA-Tyr:SA:CPP (^{1}H NMR)
20 : 80 : 0	77,842	5.82	67.0	10.5 : 89.6 : 0.0
20 : 60 : 20	80,358	6.80	44.2	13.9 : 64.5 : 21.6
20 : 40 : 40	45,400	4.13	*b*	13.4 : 41.7 : 44.9
20 : 20 : 60	21,803	2.93	*b*	17.2 : 26.6 : 56.2
20 : 0 : 80	4,082	2.02	188.3	*c*

a Polymers melt polymerized at 180°C with two mole percent cadmium acetate for 30 minutes. T_g's of these polymers reported in Fig 8-7.

b Not detectable

c Not tested

polymers with 0 to 20 percent acyl-CPP in the feed. Thereafter, the molecular weight decreases with increasing CPP content. However, polymers with up to 60 percent CPP (and 20 percent TMA-Tyr) in the feed with molecular weights in excess of 20,000 were achieved. Similarly, as shown in Table 8-3, when the SA:CPP feed ratio is kept constant at 1:1, high molecular weight polymers are obtained when the reaction feed contains 0

to 20 mole percent acyl-TMA-Tyr, with lower molecular weights as the amount of acyl-TMA-Tyr is increased. Polymers with molecular weights in excess of 17,000 were

Table 8-3. Characteristics of Poly(TMA-Tyr:SA:CPP) Synthesized with Constant SA:CPP Molar Feed Ratio of 1:1

% TMA-Tyr:SA:CPP (reaction feed)	M_W	PDI	T_m (°C)	T_g (°C)	% TMA-Tyr:SA:CPP (^{1}H NMR)
0 : 50 : 50	39,506	3.66	185.8	6.4	0.0 : 59.7 : 40.3
20 : 40 : 40	45,400	4.13	*b*	29.5	13.1 : 41.5 : 45.4
40 : 30 : 30	38,185	4.29	*b*	46.9	30.8 : 34.2 : 35.0
60 : 20 : 20	17,589	2.97	*b*	54.4	52.4 : 23.7 : 23.9
80 : 10 : 10	3,875	1.66	*c*	*c*	*c*
100 : 0 : 0	1,988	1.91	*b*	93.5	100 : 0.0 : 0.0

a Polymers melt polymerized at 180°C with two mole percent cadmium acetate for 30 minutes.

b Not detectable

c Not tested

synthesized that contained greater than 50 percent TMA-Tyr in their backbone as determined by ^{1}H NMR spectroscopy. Subsequently, it was determined that TMA-Tyr:SA:CPP terpolymers with molecular weights in this range are suitable for the encapsulation of drugs, including vaccine antigens, in injectable microspheres (see Chapter 9).

The decrease in molecular weight with increased percentages of either CPP or TMA-Tyr can be explained by the increased rigidity and steric hindrance of these two units compared with the flexible monomer, SA. A polymer chain which ends with an SA unit is able to react more readily with an additional monomer unit than a chain ending in either CPP or TMA-Tyr. Therefore, as the percentage of SA in the reaction feed is increased, the percentage of chains ending with an SA unit at any given time during the polymerization is also increased, and longer polymer chains are produced on average. Despite its effect on polymer molecular weight, CPP is copolymerized with TMA-Tyr and SA to enhance the hydrophobicity of the polymer. As a result, the presence of CPP in the polymer backbone slows down the polymer degradation and erosion process, allowing the release of drugs over longer periods of time compared with a polymer of TMA-Tyr and SA alone (see Chapter 9).

Long-term release is essential to the success of many applications involving the delivery of pharmaceuticals, especially vaccine antigens [167].

Tables 8-2 and 8-3 also show that the percentage of TMA-Tyr incorporated into the polymer backbone is consistently less than the percentage in the reaction feed (by 3 to 10 %). This is in agreement with elemental analysis data (experimental section) that show nitrogen levels in the polymers consistently below predicted values based on monomer feed ratios. This result is also consistent with data obtained in the synthesis of poly(anhydride-*co*-imides) containing glycine and alanine [168].

The solubility of these polymers in organic solvents was predominantly a function of polymer composition. Increasing solubility in common organic solvents, such as chloroform, methylene chloride, and N,N-dimethyl formamide, was observed with a higher SA content. In order to encapsulate drugs, including water-soluble vaccines, into microspheres via convenient solvent-evaporation processes, polymer solubility in low-boiling organic solvents is a necessity [167]. Therefore, it is difficult to

produce microspheres with TMA-Tyr:CPP polymers if SA is not included in the backbone.

8.2.5 Thermal Analysis

Glass transition temperatures (T_g) of the amorphous polymer fractions and melting temperatures (T_m) of the crystallites were determined by differential scanning calorimetry (DSC). In the case of polyanhydrides made up of three monomers, thermal behavior and extent of crystallization depend on the monomer make-up, polymer molecular weight, and the ability of the repeat units to pack into regular structures. Polymers containing greater than 60 % SA exhibit melting transitions (Tables 8-2 and 8-3), which suggests the presence of long range order in these polymers (i.e., regions of crystallinity). Regions of crystallinity were also observed when the polymer contained a high percentage of CPP (i.e., TMA-Tyr:CPP 20:80). However, polymers which contained all three monomers did not show any crystallinity, the only exception being a high molecular weight polymer (> 80,000) containing greater than 60 percent SA in its backbone. This result is expected since the appearance of several melting transitions, corresponding to sebacic acid-rich regions, has previously been observed in poly(anhydride-*co*-imides) with an appreciable SA content [169]. The lack of crystallinity in the terpolymers is primarily due to the presence of three structurally different monomers, especially the asymmetric TMA-Tyr moiety which does not allow for a regular structure. In Table 8-2 T_m's of 67.0 and 188.3°C for poly(TMA-Tyr:SA) 20:80 and poly(TMA-Tyr:CPP) 20:80, respectively (i.e., copolymers that contained 20% TMA-Tyr, and 80% SA or CPP) are reported. These values are similar to values reported elsewhere for CPP:SA copolymers which contain 80% SA (66-72°C), and 80% CPP (205°C), respectively [161]. This result, combined with the fact that the homopolymer of TMA-Tyr does not exhibit a melting transition, indicates that the

crystalline regions in TMA-Tyr:SA and TMA-Tyr:CPP copolymers are due to the excess of SA or CPP monomers in these polymers. The fact that terpolymers with appreciable percentages of all three monomers (Table 8-3) lack crystallinity is further evidence that the TMA-Tyr monomer is uniformly distributed throughout the polymer backbone where it serves to disrupt packing. For drug delivery it is desirable to use amorphous polymers with a uniform monomer distribution in order to achieve: a) homogeneous drug distribution in, and degradation of, the polymer matrix; and b) reproducible drug release kinetics.

Fig 8-7 shows T_g as a function of SA:CPP ratio in the reaction feed when the acyl-TMA-Tyr feed is held constant at 20 mole percent. As expected, polymer T_g goes through a minimum when the SA:CPP ratio is 1 (29.5°C), and increases as the polymer is enriched in either CPP or SA. In other words, as the polymer goes from a terpolymer with high percentages of all three repeat units (20% TMA-Tyr. 40% SA, 40% CPP), to a copolymer consisting of only two repeat units (20% TMA-Tyr, and 80% SA or CPP), the T_g approaches that of the homopolymers of SA or CPP. Poly(SA) has a reported T_g of 50-60°C [161, 169], compared with 46.6°C reported here for poly(TMA-Tyr:SA) 20:80. Similarly, poly(CPP) has a reported T_g of around 96°C [161], compared with 58.7°C for poly(TMA-Tyr:CPP) 20:80 reported here. Additionally, the polymer T_g increases steadily as the percent of imide monomer (TMA-Tyr) in the terpolymer backbone increases when the SA:CPP ratio is kept constant at 1 (Table 8-3). This trend has previously been reported for poly(anhydride-*co*-imides) containing glycine and alanine [168]. The increase in T_g with increased levels of TMA-Tyr is likely due to the high rigidity of the imide-containing monomer unit, which sterically hinders chain movement even though polymers rich in TMA-Tyr are typically low molecular weight. In general, the thermal transition temperatures of terpolymers were significantly reduced compared to the corresponding homopolymers. The reduced transition temperatures are probably a result of disrupted packing of neighboring polymer chains

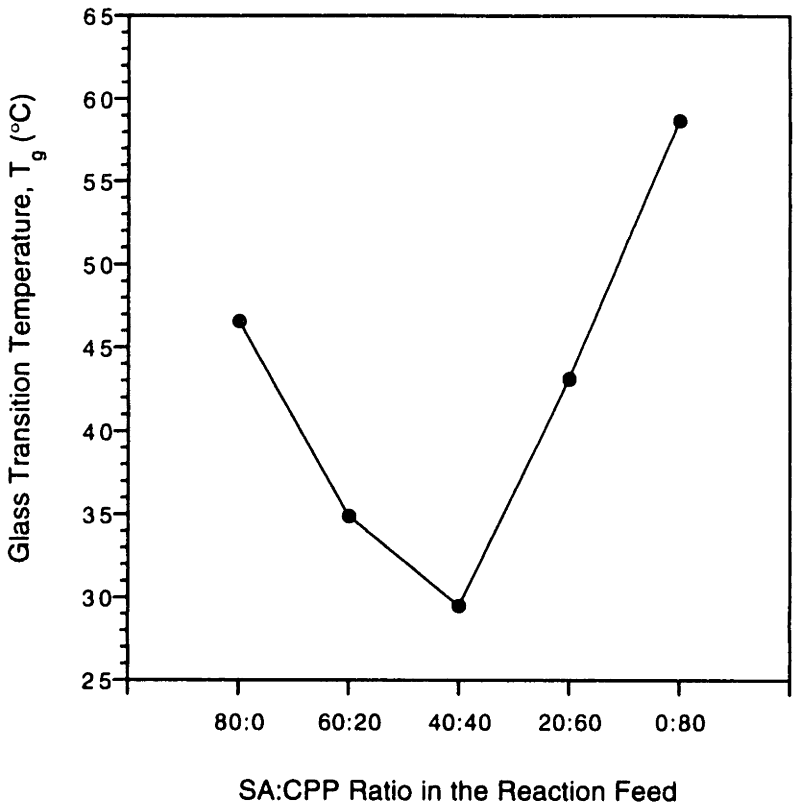

Fig 8-7. Effect of SA:CPP feed ratio on polymer glass transition temperature. The TMA-Tyr feed was held constant at 20 mole percent. Polymers were melt polymerized at 180°C with two mole percent cadmium acetate for 30 minutes.

caused by the use of several structurally different monomers. Finally, the appearance of a single T_g for each of the terpolymers (Tables 8-2 and 8-3) is further proof that monomers are randomly distributed in the polymer backbone.

8.2.6 Stability of TMA-Tyr:SA:CPP Terpolymers

The stability of TMA-Tyr:SA:CPP terpolymers, in a molar feed ratio of 20:50:30, was assessed in the solid state and as a 10 mg/mL solution in chloroform at different temperatures. The initial weight average molecular weight of the polymer used in this study was 23,500. Polymer samples were stored in the solid state and in $CHCl_3$ solution at -20, 4, and 25°C, and their molecular weight was followed with time by GPC (Fig 8-8). Whether stored as a solid or in solution, increasing depolymerization was observed at elevated temperatures. In addition, polymers were more stable in the solid state than in $CHCl_3$ solution. For example, in $CHCl_3$ at 20°C the polymer molecular weight decreases rapidly within a few days, however, polymer samples stored in the solid state at - 20°C showed only a slight decrease in molecular weight initially. The sharp initial decrease in M_W in solution may be explained by the increased mobility of the chains, enabling them to interact and react with each other by transesterification to form low molecular weight oligomers [162]. However, the presence of residual amounts of water in the chloroform may also play a role. After an initial drop in M_W, the polymers also show good stability for long times (greater than 20 days) at room temperature in the solid state (Fig 8-8).

8.3 Conclusions

The synthesis of biodegradable, poly(anhydride-*co*-imides) of high molecular weight and high tyrosine content was reported in this chapter. The use of three repeat

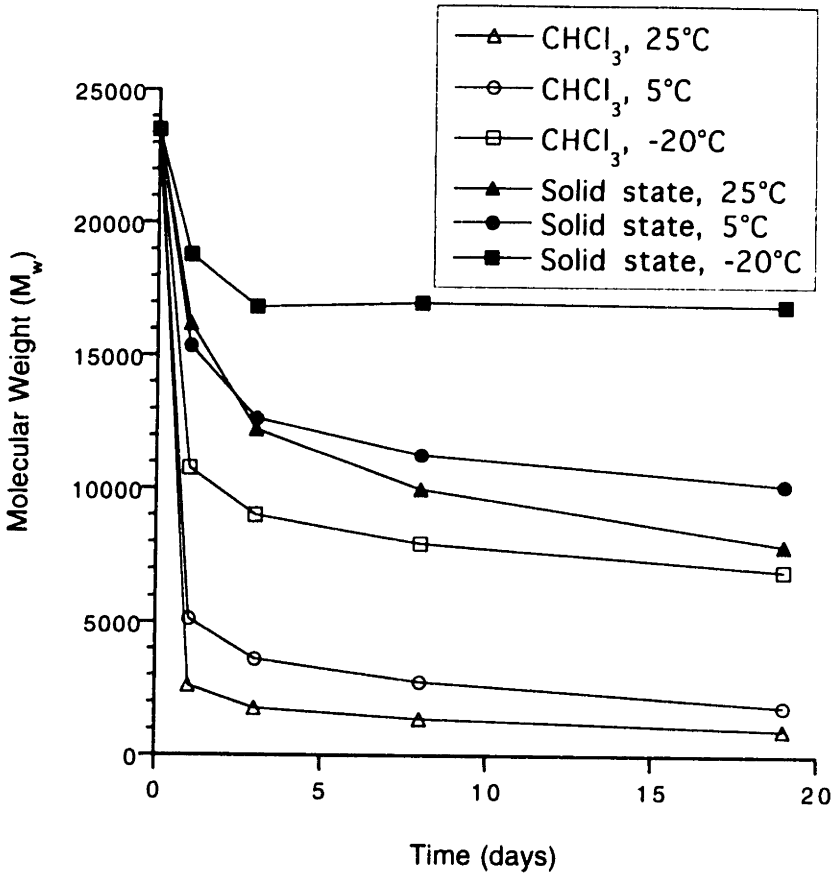

Fig 8-8. Stability of poly(TMA-Tyr:SA:CPP) (molar feed ratio of 20:50:30) in the solid state and as a 10 mg/mL solution in $CHCl_3$ at various temperatures. The initial terpolymer molecular weight was 23,500. The terpolymer was melt polymerized for 1.5 hours at 180°C without catalyst.

units allows the synthesis of amorphous polymers capable of a wide range of degradation times that may be useful in the delivery of pharmaceuticals, including vaccine antigens. The incorporation of tyrosine is important due to reports of its inherent ability to increase the immune response to adsorbed antigens. ^{1}H NMR spectroscopy and thermal transition temperature analysis suggest that the monomers of terpolymers are randomly distributed throughout the polymer backbone, thus allowing a more uniform degradation of the polymer, a distinct advantage for drug delivery applications. These polymers show good stability in the solid state at room temperature, making them potentially useful as carriers for antigens in regions of the world where refrigeration is difficult or expensive to maintain.

9 Controlled Protein Delivery from Poly(anhydride-co-imide) Microspheres

9.1 Introduction

Vaccination has eradicated or dramatically reduced the incidence of disease worldwide. It remains the most powerful, cost effective, and practical means of preventing infectious disease in the human population today. For example, it is estimated that infant and childhood deaths could be reduced by up to 50 % by immunization alone if vaccines currently being developed to prevent diarrheal diseases, acute respiratory infections, and malaria are eventually implemented in mass immunization programs [1, 170]. However, many challenges remain with respect to the effective administration of vaccines, especially in developing countries where they are needed most. In these countries, millions of people continue to die each year from diseases for which there already exists an effective vaccine, such as tetanus, pertussis and measles [1]. The majority of these deaths are due to poor patient compliance (i.e., patients do not return for their booster shots) and the enormous expense of administering literally millions of doses of vaccines. As a result, there is currently a global emphasis on the development of improved vaccine strategies to decrease the number of shots needed for protection against infection [171].

Considering the importance of a long-term depot effect in attaining and maintaining high antibody titers, it was hypothesized that the need for booster shots may be eliminated by using controlled release polymers to deliver protein antigens [34]. Initial studies in the late 1970's and early 1980's used a non-degradable ethylene-vinyl acetate copolymer implant to deliver model antigens in a continuous fashion [34, 35].

The result was a system which was, in most cases, as effective in a single dose as multiple doses of antigen in complete Freund's adjuvant, long considered the most potent vaccine adjuvant.

To be considered for mass- or routine-immunization in humans, however, the non-degradable polymer implant must be replaced with a biodegradable and injectable polymer system. In this chapter the production of injectable microspheres made with biodegradable tyrosine-containing poly(anhydride-*co*-imides) is reported. Depending on their monomer composition, this family of polymers is capable of releasing entrapped proteins in a continuous fashion for periods ranging from a few days to over a month, making them potentially useful as delivery systems for pharmaceutical proteins and vaccine antigens.

9.2 Results

9.2.1 Polymer Characterization

In order to achieve a range of polymer erosion and macromolecule release rates it was necessary to synthesize a family of polymers with a variety of monomer compositions. Table 9-1 summarizes the physical properties of the polymers used in this study. Weight average molecular weights (M_W) of polymers used exceeded 30,000 for this study, however, in general microspheres can be prepared using polymers with M_W's above 10,000 - 15,000 (see Chapter 10). In addition, the initial polymer molecular weight has very little effect on release kinetics with TMA-Tyr:SA:CPP terpolymers (see Chapter 10). The polymer characteristics that have the most profound effect are polymer composition and crystallinity. Crystalline regions of polymers show decreased rates of water absorption and therefore degrade and release proteins at slower rates than non-crystalline portions. As a result, amorphous polymers are often preferred for

controlled release due to their more homogeneous degradation and reproducible release kinetics [172]. The relative degrees of crystallinity of the copolymers used in this study were estimated using heats of fusion data (DSC measurement) as described previously [93]. TMA-Tyr:SA and SA:CPP copolymers have distinct crystalline regions (Table 9-1).

Table 9-1. Physical Properties of TMA-Tyr:SA:CPP Polymers

TMA-Tyr:SA:CPP (mole %)	M_W	PDI	T_m (°C)	T_g (°C)	ΔH (cal/g)	Crystallinity (%)
0 : 50 : 50[a]	39,506	3.66	185.8	6.4	3.5	7.5
20 : 80 : 0[a]	77,842	5.82	67.0	46.6	13.8	37.0
20 : 50 : 30[b]	33,000	6.64	*c*	17.3	*c*	*c*
40 : 30 : 30[a]	38,185	4.29	*c*	46.9	*c*	*c*
20 : 40 : 40[a]	45,400	4.13	*c*	29.5	*c*	*c*

a Prepared by hot-melt bulk polymerization at 180°C with two mole percent cadmium acetate for 30 minutes.

b Prepared by hot-melt bulk polymerization at 180°C for 60 minutes without catalyst.

c Not detectable

On the other hand, the terpolymers used in this study are amorphous (i.e., no crystallinity) as determined by DSC. The lack of crystallinity of the terpolymers is due to the random distribution of three monomers throughout the polymer backbone. This randomness makes crystallization more difficult, especially when the monomers have very different lateral and three-dimensional structures. In addition, the homopolymer of TMA-Tyr is amorphous. The fact that polymers containing TMA-Tyr consistently

have lower degrees of crystallinity (or no crystallinity) than those without this monomer is consistent with the result obtained by Flory [173] that the introduction of an uncrystallizable unit into a crystallizable monomer will lead to a decrease in polymer crystallinity.

9.2.2 Microsphere Preparation and Characterization

Fig 9-1 shows scanning electron micrographs of a typical batch of poly(TMA-Tyr:SA:CPP) 20:50:30 microspheres containing 7 wt % BSA. The microspheres are spherical and the external surfaces appear smooth without visible pores. The drug pockets within the microspheres corresponding to the first (inner) emulsion are clearly seen when the sphere is cross-sectioned prior to SEM observation (Fig 9-1c). The model protein is homogeneously distributed in dozens of internal pockets throughout each microsphere. The internal pockets have a distribution of sizes ranging from very small (nanometers) to large (> 5 μm). Size distribution measurements show that the microspheres also have a Gaussian distribution of sizes (Fig 9-2). More than 85 % of the microspheres had diameters ranging from 3 to 50 μm. In addition, the volume and number average diameters of this batch are 28.9 and 10.6 μm, respectively, facilitating their injection subcutaneously or intramuscularly with a normal 25-gauge needle. It is possible to control microsphere size (from a few microns to several millimeters), for example, by varying the intensity of mixing during the formation of the second emulsion (unpublished data). In this study, the second emulsion was always prepared in the same manner (vortex mixing) and microsphere size depended instead on the mixing method used in the inner emulsion preparation. When the inner emulsion was prepared by vortex mixing the resulting microspheres were larger with a large inner emulsion. When the primary emulsion was prepared by probe sonication, a fine inner emulsion was formed and the overall microsphere size was much smaller. The recovery

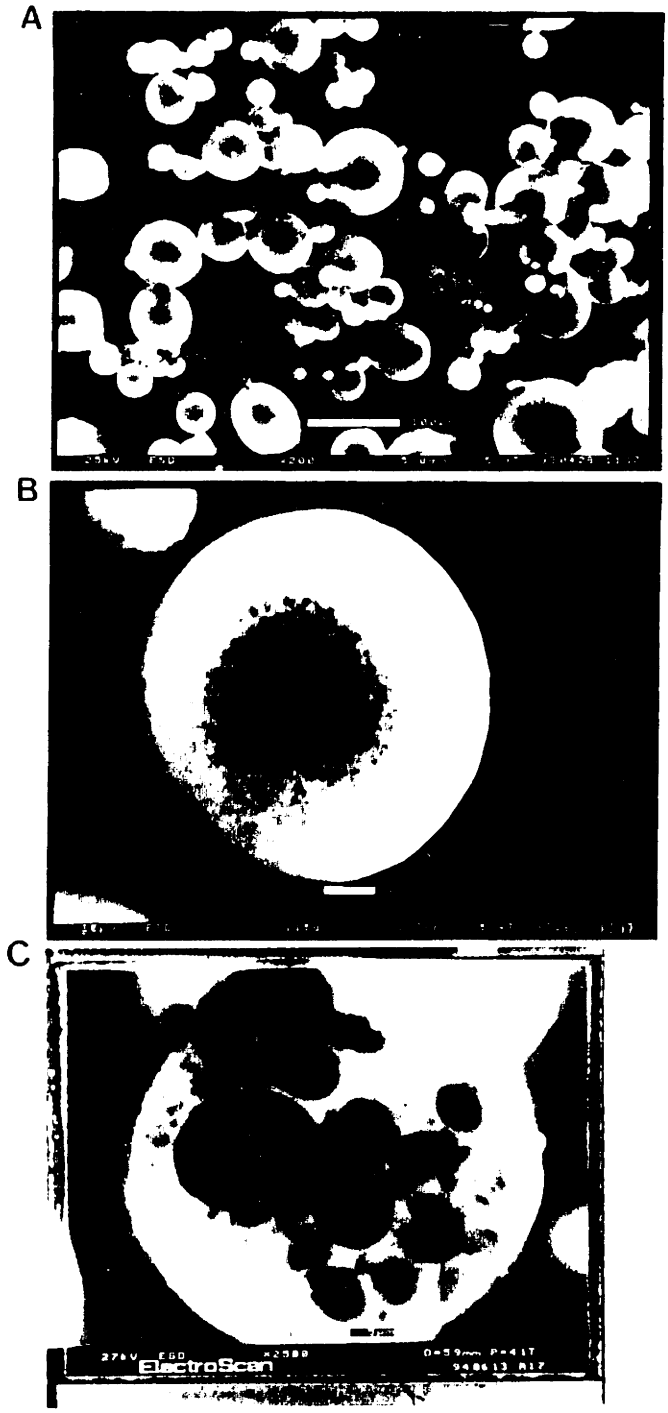

Fig 9-1 Scanning electron micrographs: a) typical batch of poly(TMA-Tyr:SA:CPP) microspheres containing 7% BSA by weight; b) close-up of a single sphere; c) cross-section showing the porous internal microsphere morphology. Proteins are trapped within the internal drug pockets shown here.

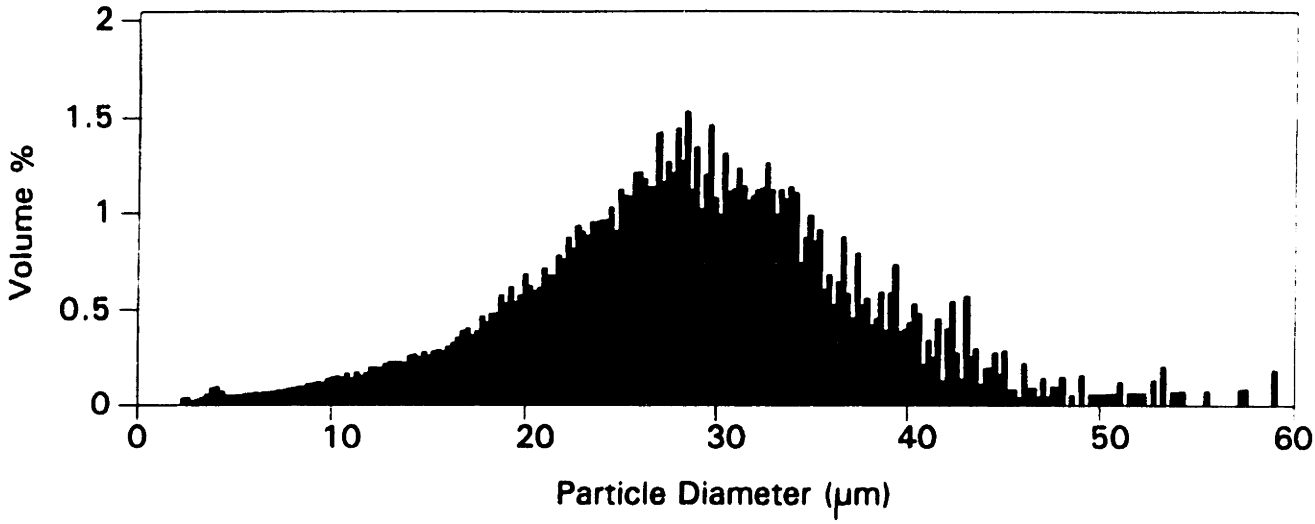

Fig 9-2. Size distribution of a typical batch of poly(TMA-Tyr:SA:CPP) 20:50:30 microspheres as determined using a Coulter Multisizer II. The microspheres contain /% BSA by weight.

of the microspheres was 75-85 % (n > 20), independent of the type of poly(anhydride-*co*-imide) used. The trapping efficiency of BSA was high and consistent from batch to batch (73.6 ± 2.8 %).

9.2.3 *In Vitro* BSA Release from Poly(TMA-Tyr:SA:CPP) Microspheres

A series of studies were performed to determine methods by which macromolecule release rates from poly(TMA-Tyr:SA:CPP) microspheres may be manipulated. As shown in Fig 9-3, changing the protein content of the microspheres (i.e., the BSA loading) can be used to achieve vastly different total BSA release rates. For example, over a 350-fold increase in total BSA dose can be achieved from poly(TMA-Tyr:SA:CPP) 20:50:30 microspheres by changing the BSA loading. The total BSA dose delivered over the period of 40 days increases from 0.35 to 131 μg BSA/mg spheres for spheres with initial BSA loadings of 0.08 wt % and 14.94 wt %, respectively. Of course, the difference in amount of protein that can be delivered is magnified if more spheres are used. For example, 10 mg of poly(TMA-Tyr:SA:CPP) 20:50:30 microspheres can control the release of total protein doses ranging from 3.5 μg to 1.3 mg of protein over the period of 40 days.

Fig 9-4 shows that the total BSA released from microspheres during a given length of time can be estimated as increasing linearly with their initial BSA content. For example, the total amount of BSA released during the initial release phase (first two days) increases linearly with the BSA loading of the microsphere. As shown in Fig 9-4, it is possible to estimate, based on initial percent BSA loading, the total amount of BSA that will be released from poly(TMA-Tyr:SA:CPP) 20:50:30 microspheres after any given time period (e.g. 2 days, 13 days, 40 days, etc.). This allows a great deal of flexibility in vaccine doses that can be achieved using poly(anhydride-*co*-imide) microspheres.

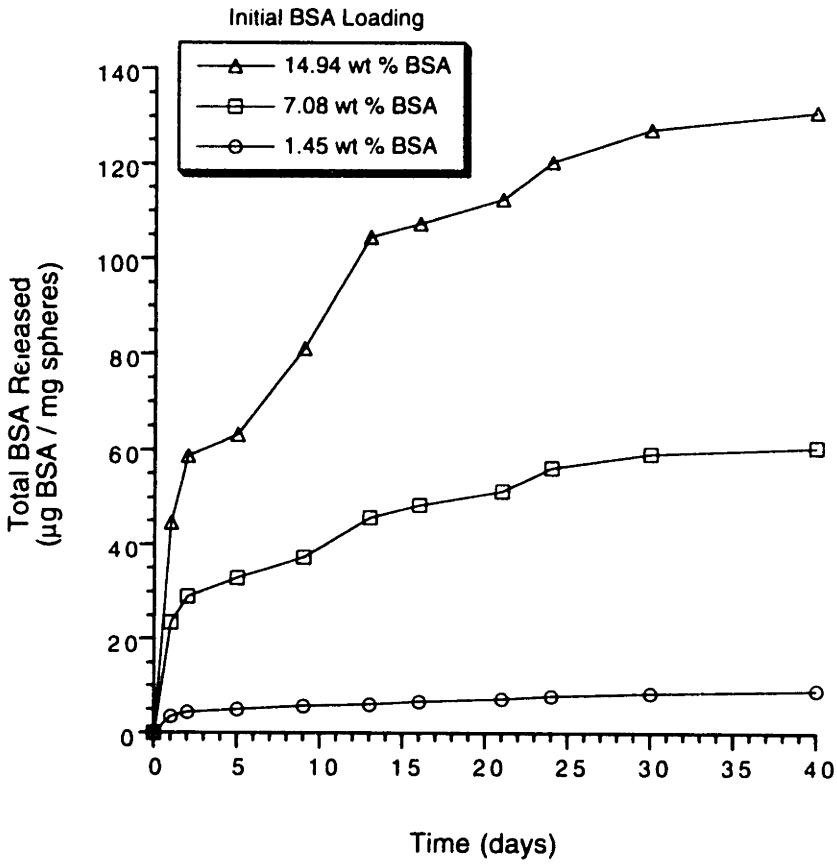

Fig 9-3a. Controlled release of a model protein, BSA, from poly(TMA-Tyr:SA:CPP) 20:50:30 microspheres containing various BSA loadings by weight: a) 14.94, 7.08, and 1.45 % BSA.

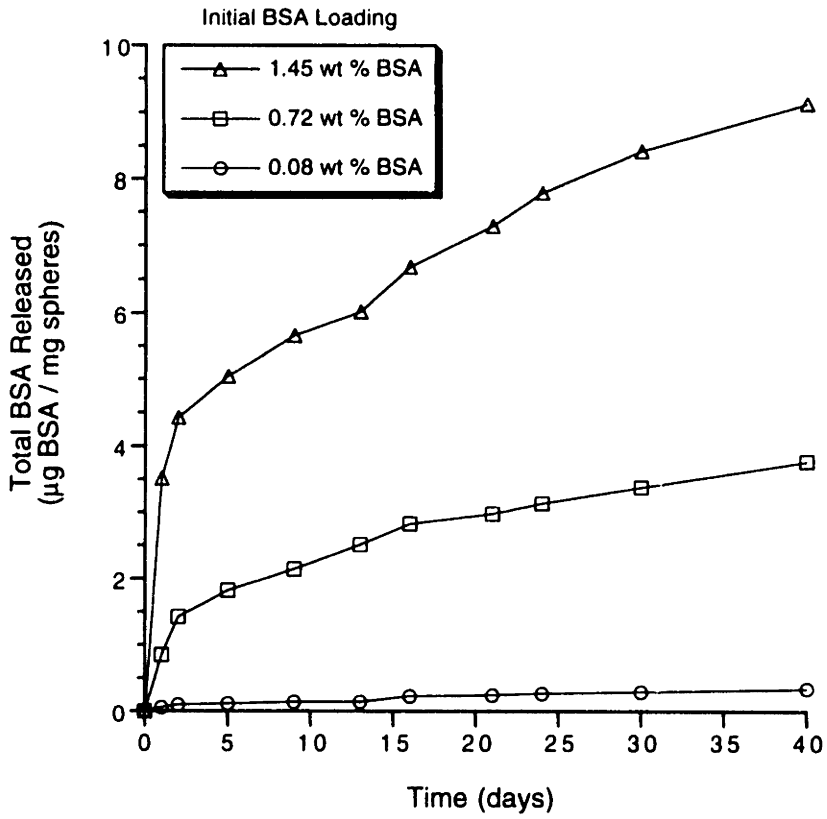

Fig 9-3b. Controlled release of a model protein, BSA, from poly(TMA-Tyr:SA:CPP) 20:50:30 microspheres containing various BSA loadings by weight: b) 1.45, 0.72, and 0.08 % BSA. Notice the difference in scale on the y-axes of Figures 9-3a and 9-3b.

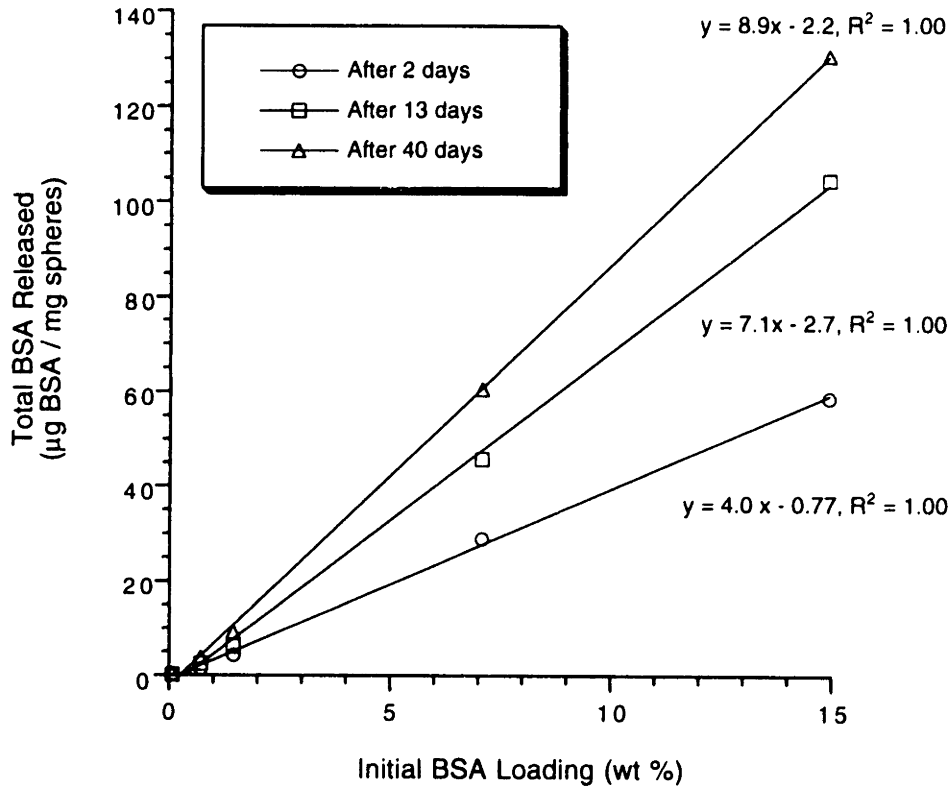

Fig 9-4. Amount of BSA released from poly(TMA-Tyr:SA:CPP) 20:50:30 microspheres after 2, 13, and 40 days as a function of BSA loading by weight.

Despite the large differences in the total BSA release doses from microspheres of different loadings, the average percentage of BSA released over time is very similar (with the exception of the BSA released during the first two days) (Table 9-2). As shown

Table 9-2. Release rates of a model protein, BSA, from poly(TMA-Tyr:SA:CPP) 20:50:30 microspheres as a function of protein loading

Wt % BSA Loading (μg BSA / μg polymer)	% BSA Released per day (days 0-2)	% BSA Released per day (days 2-24)	% BSA Released per day (days 24-40)
0.08	6.3	1.2	0.6
0.72	9.9	1.1	0.6
1.45	15.3	1.1	0.6
7.08	20.4	1.8	0.4
14.94	19.6	1.9	0.4

in Table 9-2, protein release from poly(TMA-Tyr:SA:CPP) 20:50:30 microspheres can be broken down into three phases: an initial release phase (days 0-2), an intermediate release phase (days 2-24), and a final release phase (days 24-40). The percent of BSA released during the initial release phase (total μg BSA released after two days / total μg BSA entrapped initially) increases with protein loading from roughly 6%/day for low BSA loadings, to a maximum of around 20%/day for microspheres with high BSA loadings. Indeed, slightly higher rates of protein release are observed over the first few weeks for microspheres with high BSA loadings (7.08 and 14.94 wt % BSA). The release mechanism of proteins from most polymers is controlled by protein diffusion, polymer

erosion, or a combination of the two (recall from Chapters 4 and 5 that gp120 release from PLGA microspheres is controlled by polymer erosion following the initial microsphere hydration phase). The increased release rates from poly(TMA-Tyr:SA:CPP) microspheres during the initial and intermediate release phases for microspheres with high BSA loadings indicates that BSA is being released by diffusion in addition to microsphere erosion. The protein released during the initial release phase is due to a combination of microsphere erosion and protein desorption and diffusion from the sphere surface, or from small pores near the surface of the microspheres. An increase in the percent protein loaded into the spheres likely is accompanied by a proportionate increase in protein on or near the microsphere surface, accounting for the higher BSA release rates initially. However, the effect of protein loading on polymer erosion rates was not determined and may be a factor in the extent of the initial release phase as well.

Polymer composition is another important tool by which to achieve vastly different macromolecule release rates and release durations from poly(TMA-Tyr:SA:CPP) microspheres. Polymer erosion and protein release periods from a few days to well over one month (> 10-fold increase) were achieved by increasing the percentage of the most hydrophobic monomer (CPP) in the polymer backbone (Fig 9-5). The overall BSA release rate, as well as the amount of protein released during the initial release phase, increased with increasing amounts of TMA-Tyr or SA monomer in the polymer backbone. The increased release rates are due to the less hydrophobic nature and higher water-solubility of TMA-Tyr and SA compared with CPP (see Chapter 10). As a result, polymers with high SA or TMA-Tyr contents erode more quickly than those with a high CPP content causing increased rates of protein release. It is theoretically possible to deliver drugs for periods ranging from hours to years just by changing the ratio of SA to CPP in the polymer [160]. In reality, however, one is limited by the stability of the protein at 37°C in a hydrophobic and, depending on the monomers used,

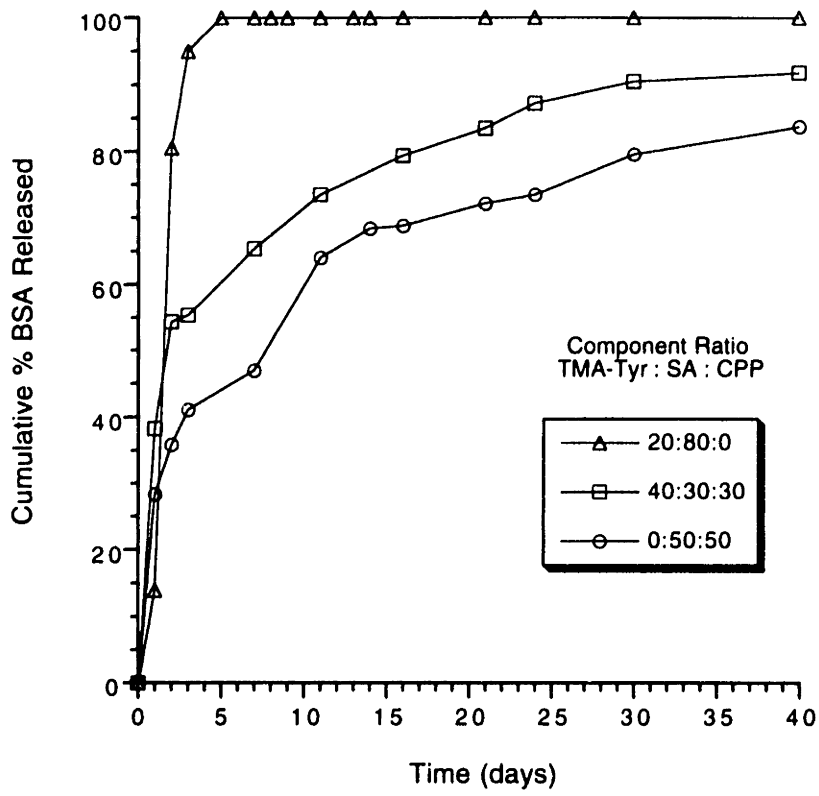

Fig 9-5. Controlled release of a model protein, BSA, from microspheres made with polymers of various TMA-Tyr:SA:CPP monomer ratios. The microspheres contain 7% BSA by weight. BSA release from microspheres is shown as a percentage of the initial amount encapsulated.

acidic environment [174]. In addition, polymers with greater than 60-70 % CPP in their backbone have limited solubility in low-boiling organic solvents and therefore are not good candidates for microencapsulation by solvent-evaporation processes. An alternative method of microencapsulation ("hot melt microencapsulation") has been developed for polyanhydride polymers which does not require dissolution of the polymer in organic solvents [175]. However, a disadvantage of this method may be the high temperatures to which the drug is subjected during processing.

BSA release profiles from microspheres (7 wt % BSA initially) are compared with microsphere erosion profiles for a family of TMA-Tyr:SA:CPP terpolymers in Fig 9-6. In the case of poly(TMA-Tyr:SA:CPP) microspheres, the *in vitro* release profile of BSA closely follows microsphere erosion as judged by polymer weight loss, indicating a release mechanism predominantly controlled by polymer erosion. In some cases, the model protein is initially released at a slightly higher rate than the microsphere erodes (however, usually only at high BSA loadings such as those shown in Fig 9-6). In this case, protein release is controlled by a combination of diffusion and polymer erosion initially, followed by erosion-controlled release at later times. The degradation and erosion properties of the poly(TMA-Tyr:SA:CPP) terpolymers are reported in more detail in Chapter 10.

Finally, the effect of pH on protein release profiles from poly(TMA-Tyr:SA:CPP) microspheres is shown in Fig 9-7. BSA release rates were significantly reduced at low pH and enhanced under basic conditions. In Chapter 10 it is shown that pH has little effect on the degradation rates of poly(anhydride-*co*-imides), but that polymer erosion and protein release are suppressed due to the decreased solubility of degraded diacid monomers under acidic conditions. The "stability" of poly(TMA-Tyr:SA:CPP) microspheres at low pH could be an advantage for oral drug delivery. It is particularly important for oral delivery of vaccines when mucosal immunity is desired since microspheres less than 10 μm in diameter are known to be taken up from the intestine

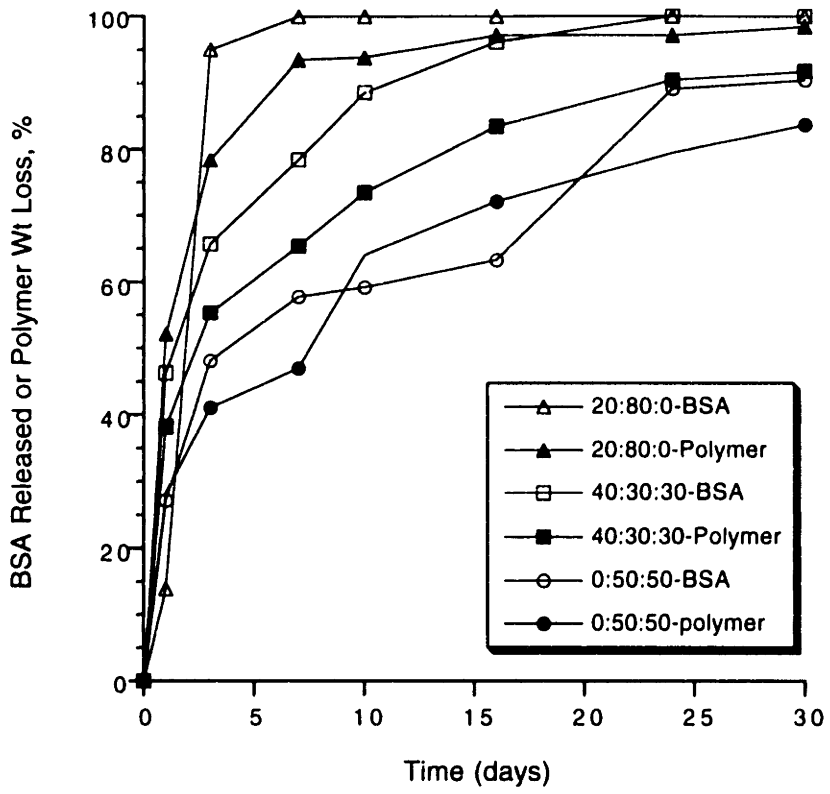

Fig 9-6. Microsphere erosion rates (filled-in symbols) compared with corresponding BSA release rates (open symbols) from microspheres made with polymers of various TMA-Tyr:SA:CPP monomer ratios. The microspheres contain 7% BSA by weight. Microsphere erosion patterns mirror BSA release patterns, indicating a release mechanism that is predominantly controlled by polymer erosion.

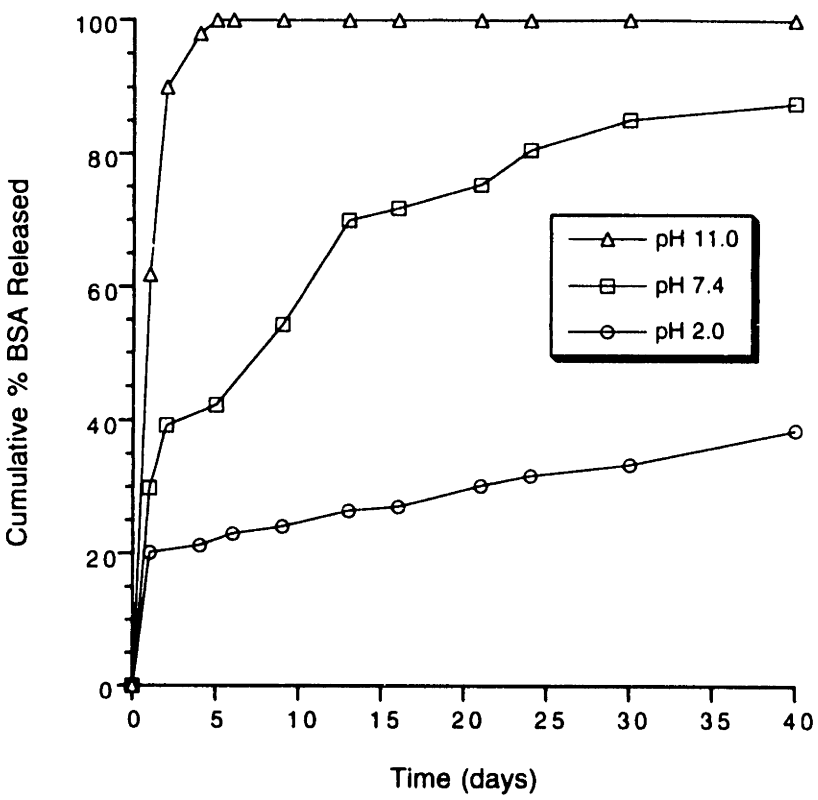

Fig 9-7. Controlled release of a model protein, BSA, from poly(TMA-Tyr:SA:CPP) 20:50:30 microspheres as a function of buffer pH. The microspheres contain 7% BSA by weight. BSA release from microspheres is shown as a percentage of the initial amount encapsulated.

into the Peyer's patches [15]. Before reaching the Peyer's patches the protein antigen is thought to be protected from the hazardous environment in the stomach and intestines (e.g., low pH and digestive enzymes) by the polymer matrix surrounding it [176]. Polyanhydrides may be particularly well suited for oral delivery because they are known to adhere to the mucosal lining in the intestine (i.e., they are bioadhesive), thereby increasing their residence time in the GI tract [177].

9.3 Discussion

A number of degradable polymers have been developed during the past several years for controlled release drug delivery, including polyanhydrides [178]. Polyanhydrides have been extensively studied for use in drug delivery systems due to their biocompatibility and ability to erode from their surface-inward (termed "surface-erosion") at rates ranging from days to years depending on the choice of monomer units [160]. In particular, poly(CPP:SA) has been used, both experimentally and clinically, for the treatment of neurological disorders and brain tumors [158, 179]. The anhydride-*co*-imides used in this study are similar to poly(CPP:SA) but also have an imide monomer, TMA-Tyr, incorporated into their backbone. The resulting terpolymers are amorphous and contain a derivative of a known adjuvant, L-tyrosine, in their backbone. Previously, Dr. Langer's group reported that the use of tyrosine-based poly(iminocarbonates) for antigen delivery can lead to increased levels of IgG antibody production compared with similar, but non-tyrosine-based, polymers [65]. However, these polymers were too brittle to use for microsphere fabrication and, being homopolymers, were not capable of providing a wide range of erosion rates similar to the polyanhydride copolymers.

Polymer microspheres are thought to enhance immunity to entrapped antigens by several mechanisms, the most obvious being their ability to provide a long-term depot effect. However, microspheres smaller than 10 μm are also known to be

phagocytosed by professional antigen presenting cells [37], resulting in efficient antigen processing and presentation to lymphocytes. In addition, recent reports have suggested that microsphere phagocytosis may provide an avenue for the induction of cell-mediated immunity [180, 181], the branch of the immune system thought important in riding the body of cancer and cell-associated pathogens, such as many viruses.

The current study shows that the double-emulsion solvent-evaporation method can be used for the efficient encapsulation of water-soluble drugs, including macromolecules into poly(anhydride-*co*-imides). More than one antigen may be incorporated into the same microsphere, or in separate batches of microspheres which may then be mixed prior to inoculation. This may facilitate immunization against several diseases, or several antigenic epitopes of a single disease, in one injection, thus reducing the number of vaccine doses necessary to fully immunize an individual. The microencapsulation procedure is reproducible with respect to yield and size distribution, and microsphere size can be controlled by the intensity of mixing in the preparation of both the primary and secondary emulsions. High protein encapsulation efficiencies (> 70 %) are a distinct advantage of the double-emulsion method, compared with the poor encapsulation efficiencies of hydrophilic drugs typical when using other methods, including coacervation and liposome-encapsulation. Furthermore, the encapsulation process may be performed at low temperature (e.g., in an ice bath) to minimize thermal drug inactivation.

The ability to achieve a wide range of release kinetics and total protein doses using poly(anhydride-*co*-imide) microspheres makes them flexible carriers for pharmaceutical proteins, including subunit antigens. As a frame of reference, the recommended dose and frequency of dosing for several human vaccines given in the United States is listed in Table 9-3. These doses are well within the range attainable using very small amounts of poly(TMA-Tyr:SA:CPP) microspheres (< 5 mg). In addition, the ability of the polymers to provide long-term antigen persistence at the site

Table 9-3. Dosing Schedule of Some Human Vaccines - Candidates for Encapsulation into Microspheres[a]

Disease	Vaccine Type	MW[b]	Typical Dosing Regimen	Total Dose
Hepatitis B (Source: Merck & Co., Recombivax HB®)	Recombinant Surface Antigen (adw subtype)	24,000[c]	10 μg/injection, adult 2.5 μg/injection, child at time 0, 1, 6 months	30 μg, adult 7.5 μg, child
Tetanus (Source: Connaught Laboratories)	Toxoid, combined with Diphtheria Toxoid and whole-cell Pertussis vaccines	150,000	5 Lf/injection (approx. 25 μg) given at 2, 4, 6, 12-18 months, and 4-6 years (then 5 Lf/injection given every 10 years)	125 μg for initial series of 5 injections
Diphtheria (Source: Connaught Laboratories)	Toxoid, combined with Tetanus Toxoid and whole-cell Pertussis vaccines	66,000	6.7 Lf/injection (approx. 30 μg) given at 2, 4, 6, 12-18 months, and 4-6 years (then 2 Lf/injection given every 10 years)	150 μg for initial series of 5 injections
Haemophilus b-related diseases (Source: Lederle-Praxis, HibTITER®)	Oligosaccharides conjugated to Diphtheria CRM_{197} protein (oligosaccharides derived from purified capsular polysaccharides)	*d*	35 μg/injection (10 μg saccharide, 25 μg Diphtheria protein) given at 2, 4, 6, and 15 months	140 μg total (40 μg saccharide, 100 μg Diphtheria protein)

a Additional source: Physicians' Desk Reference®, Edition 48, 1994, Medical Economics Data Production Co., Montvale, NJ.

b For comparison, the MW of the model protein (BSA) is 68,000.

c The subunits of Merck's hepatitis B antigen are polymerized into spheres of surface antigen 17-25 nm in diameter (approximately 40 subunits). Source: Merck & Co., Inc.

d Not reported.

of injection may obviate the need for repeated boosting. Furthermore, in contrast to alum-adjuvanted vaccines, microspheres are lyophilized and stored in the dry state. This is a major advantage for administration in developing countries where maintaining refrigeration is often a limiting factor in the effective administration of liquid vaccine formulations [1].

Preliminary tissue response and toxicological studies with poly(TMA-Tyr:SA:CPP) are encouraging (see Chapter 10). In addition, *in vivo* degradation studies in mice showed that the polymer eroded with time and the monomers (TMA-Tyr, SA, CPP) completely disappeared from the implantation site. The gross appearance of tissue around the injection site following complete polymer erosion was indistinguishable from the normal tissue, suggesting tissue healing (unpublished data). Poly(TMA-Tyr:SA:CPP) polymer microspheres are currently being evaluated as vaccine delivery vehicles in small animals and monkeys.

10 Degradation of Poly(anhydride-*co*-imide) Microspheres and Acute Toxicity of the Polymer

10.1 Introduction

Polymers have been used for years in medicine as materials in the artificial heart, dialysis membranes, prosthetic limbs and hips, and other applications [182]. For use in the body, degradable polymers have the advantage that they perform their function and then degrade, thus obviating the need for surgical removal. A degradable system also minimizes the risk of long term toxicity or immuno-rejection of the polymeric device compared with non-degradable systems. An example of possible complications with non-degradable polymers can be found in recent reports on silicone breast implants, a system previously considered safe and biocompatible [183]. Applications of degradable polymers include resorbable surgical sutures [41], matrices for the controlled time-release of drugs [8], scaffolds for tissue engineering [184], and resorbable orthopedic devices such as bone pins [185].

Over the past twenty years there has been an explosion in the field of controlled/targeted drug delivery using biodegradable polymeric vehicles [186]. The lactide/glycolide homo- and copolymers (PLA/GA), such as those discussed in Chapters 4 through 7 of this thesis, have been used in the majority of studies as relatively few new biodegradable polymers have progressed to phase III clinical trials for drug delivery applications. For new biodegradable polymers to be considered for medical use, it is necessary to have a thorough understanding of their degradation mechanism, ways in which their degradation times can be manipulated, and their biocompatibility. For example, there is a large body of literature on the degradation properties and safety of PLA/GA and polyanhydrides (for example, see reviews by

Lewis [100] and Göpferich [187]), and these are the only two degradable polymers with FDA-approved controlled drug release products. However, relatively few studies have examined the degradation of drug-containing injectable microspheres, with some exceptions in the case of PLA/GA polymers [97, 102, 188-190].

In Chapter 8, the synthesis and characterization of biodegradable anhydride-*co*-imide terpolymers was reported. These polymers are comprised of three monomers: trimellitylimido-L-tyrosine (TMA-Tyr), sebacic acid (SA), and 1,3-bis(carboxyphenoxy)propane (CPP). The use of three monomers allows the preparation of a family of degradable materials with good processability and which are capable of a wide range of degradation and macromolecule release properties. In Chapter 9, this family of polymers was used to entrap a model protein antigen, bovine serum albumin (BSA), into microspheres capable of releasing the protein for days to weeks at 37°C *in vitro*. Microsphere erosion and protein release times depended on the polymer composition and protein load. In this Chapter, the mechanism of polymer microsphere erosion (and protein release) with this family of anhydride-imide terpolymers is reported. The erosion process for microspheres made with a variety of TMA-Tyr:SA:CPP compositions has been characterized by gel permeation chromatography, infrared spectroscopy, monomer erosion rates, overall microsphere weight loss rates, scanning electron microscopy, and the effect of pH on monomer solubility and erosion. As is shown, the erosion process of porous microspheres made with terpolymers occurs in two phases: 1) water uptake accompanied by hydrolysis of the anhydride bonds (defined as polymer *degradation*), and 2) dissolution and diffusion from the sphere surface of sparingly-soluble monomers (defined as *dissolution*). Step 2 was found to be the rate limiting step in TMA-Tyr:SA:CPP terpolymer microsphere erosion. In a second study, the *in vivo* acute toxicity of poly(TMA-Tyr:SA:CPP) with a molar ratio of 40:30:30 is examined after subcutaneous implantation in rats. It is concluded that TMA-Tyr:SA:CPP terpolymers are promising candidates for *in vivo* drug delivery and thereby

warrant further study. They are currently being evaluated as controlled release systems for vaccine antigens in animals.

10.2 Results

10.2.1 Polymer Characteristics

The physical properties of the polymers used are summarized in Table 10-1.

Table 10-1. Physical Properties of TMA-Tyr:SA:CPP Polymers

TMA-Tyr:SA:CPP (mole %)	M_w	PDI	T_m (°C)	T_g (°C)	ΔH (cal/g)	Crystallinity (%)
0 : 50 : 50[a]	39,506	3.66	185.8	6.4	3.5	7.5
20 : 80 : 0[a]	77,842	5.82	67.0	46.6	13.8	36.2
20 : 50 : 30[b]	33,000	6.64	*c*	17.3	*c*	*c*
40 : 30 : 30[a]	38,185	4.29	*c*	46.9	*c*	*c*

a Prepared by hot-melt bulk polymerization at 180°C with two mole percent cadmium acetate for 30 minutes.

b Prepared by hot-melt bulk polymerization at 180°C for 60 minutes without catalyst.

c Not detectable

10.2.2 Poly(TMA-Tyr:SA:CPP) Microsphere Erosion

Microspheres made by the double-emulsion procedure were spherical and highly porous as shown in Fig 10-1. When the microspheres are coated with a thin layer of gold it is possible to see their internal structure by scanning electron microscopy (SEM) without cross-sectioning (Fig 10-1a). Internal occlusions corresponding to the first emulsion are readily identified in Fig 10-1a. It is thought that the majority of encapsulated drug is present in these internal occlusions initially, likely absorbed to the polymer surfaces, as shown elsewhere [188]. Although the microspheres are very porous internally, their surfaces are smooth with no noticeable porosity (Fig 10-1b). Their relatively dense outer shell is most likely responsible for limiting the extent of the initial release of macromolecules such as BSA (see Chapter 9).

Unlike many polymers, such as the lactide/glycolide polyesters, which degrade slowly over long periods of time, anhydride bonds are very water labile causing porous poly(anhydride-*co*-imide) microspheres to degrade (defined as anhydride bond hydrolysis) quickly. Fig 10-2 shows the weight average molecular weight (M_w) as a function of time for a family of TMA-Tyr:SA:CPP polymer microspheres of various composition when placed in aqueous release media at 37°C. The various polymer microspheres, regardless of polymer composition and initial molecular weight, degrade within a matter of several days. Degradation occurs most rapidly when amorphous polymers with low amounts of the most hydrophobic monomer, CPP, in their backbone are used. It is interesting to note, however, that the amorphous TMA-Tyr:SA:CPP 40:30:30 polymer microspheres (i.e., containing 30 % CPP in its backbone) degrade more rapidly than the highly crystalline TMA-Tyr:SA 20:80 copolymer (no CPP) microspheres (Table 10-1). This finding may be explained by the fact that crystalline regions of polymers degrade much more slowly than non-crystalline regions [93]. As expected, degradation occurs most slowly with the partially crystalline polymer containing the highest percentage of CPP in its backbone (TMA-Tyr:SA:CPP 0:50:50). The degradation rates of poly(anhydride-*co*-imide) microspheres were also confirmed by infrared (IR)

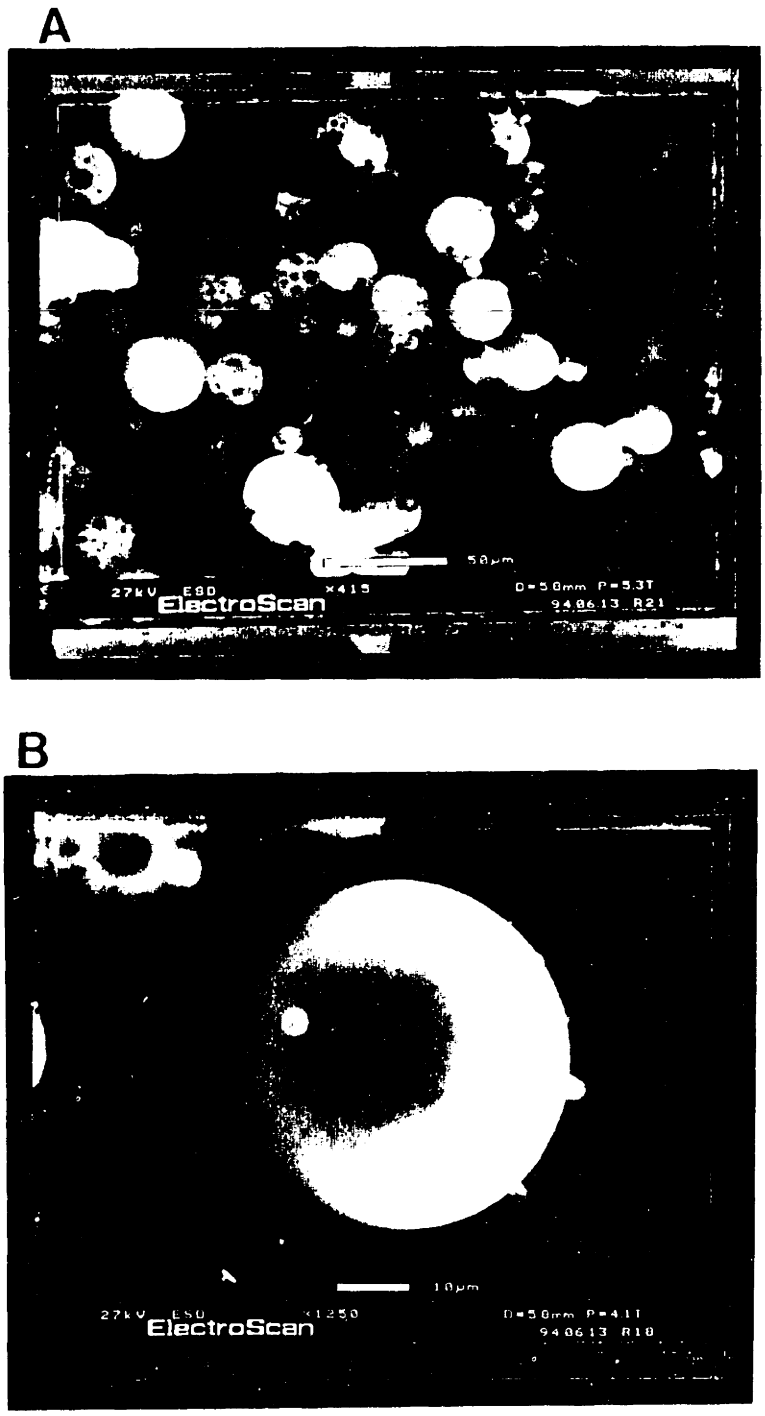

Fig 10-1. Scanning electron micrographs showing: (a) a typical batch of poly(TMA-Tyr:SA:CPP) 20:50:30 microspheres made by a double-emulsion solvent evaporation procedure and (b) a close-up of a single sphere showing its smooth, relatively non-porous outer shell.

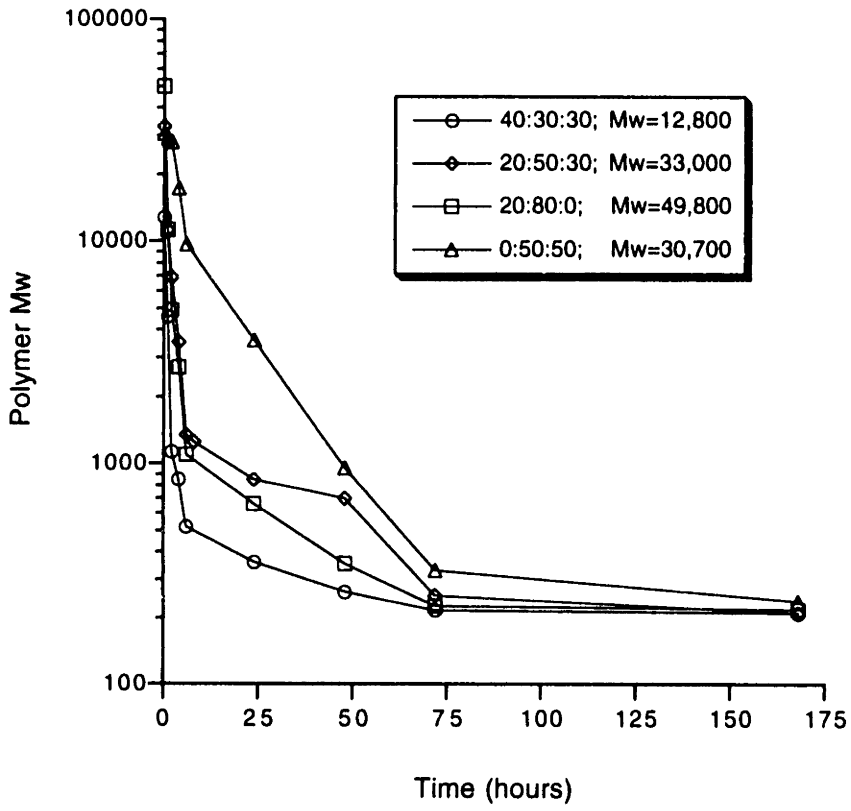

Fig 10-2. Poly(TMA-Tyr:SA:CPP) microsphere degradation profiles *in vitro* for a variety of polymer compositions as measured by gel permeation chromatography (GPC). Polymer compositions and initial M_w's are given in the figure legend.

spectroscopy: complete disappearance of characteristic anhydride IR peaks was observed after approximately 122 hours in release media at 37°C (data not shown).

Although polymer degradation occurs within several days of incubation in release media at 37°C, the microspheres do not always completely erode in this time. Figure 3 shows the rates at which microspheres lose weight over time in release buffer for a variety of polymer compositions. Although polymer degradation is complete with one week for all polymer compositions (Fig 10-2), the microspheres have not been completely eroded during this time (Fig 10-3). In fact, as the percentage of CPP in the polymer backbone is increased the microspheres can take over one month to completely erode. Once the microspheres are completely degraded, the rate limiting step for microsphere erosion becomes the slow dissolution of hydrophobic polymer degradation products (i.e., the original monomers) from the spheres into the external release media.

Further insight into the erosion mechanism of poly(TMA-Tyr:SA:CPP) microspheres was gained by scanning electron microscopy (SEM) observation of microspheres during their degradation in buffer at 37°C (Fig 10-4). Figs 4a and 4b show typical poly(TMA-Tyr:SA:CPP) 20:50:30 microspheres after four and seven days of *in vitro* degradation, respectively. After four days in buffer the microsphere has degraded significantly, however, it still maintains some structural integrity indicating that the polymer has not been completely hydrolyzed. However, after seven days in buffer the microsphere appears to have lost all structural integrity, indicating that the polymer is completely degraded at this point (i.e., complete hydrolysis of all anhydride bonds). However, a large proportion of the very poorly water-soluble monomers remain and appear to have collapsed into the interior structure of the microsphere (Fig 10-4b), which was initially very porous (Fig 10-1). This collapse may be caused by vacuum drying which precedes SEM observation. The erosion of the microsphere, and thereby the controlled release of macromolecules, from this point of complete polymer

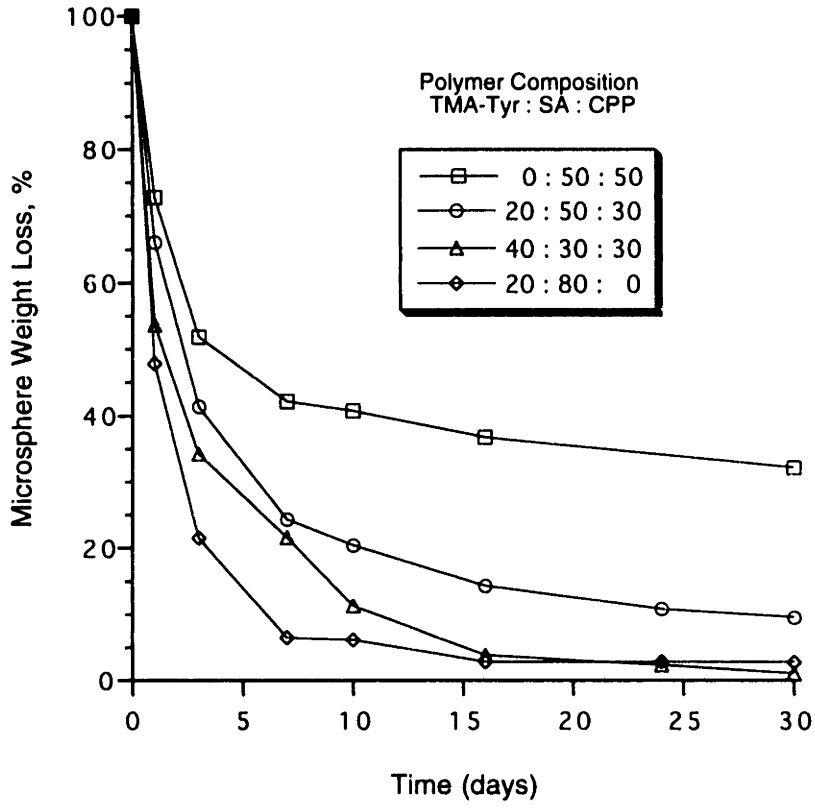

Fig 10-3. Poly(TMA-Tyr:SA:CPP) microsphere erosion rates *in vitro* as measured by microsphere weight loss.

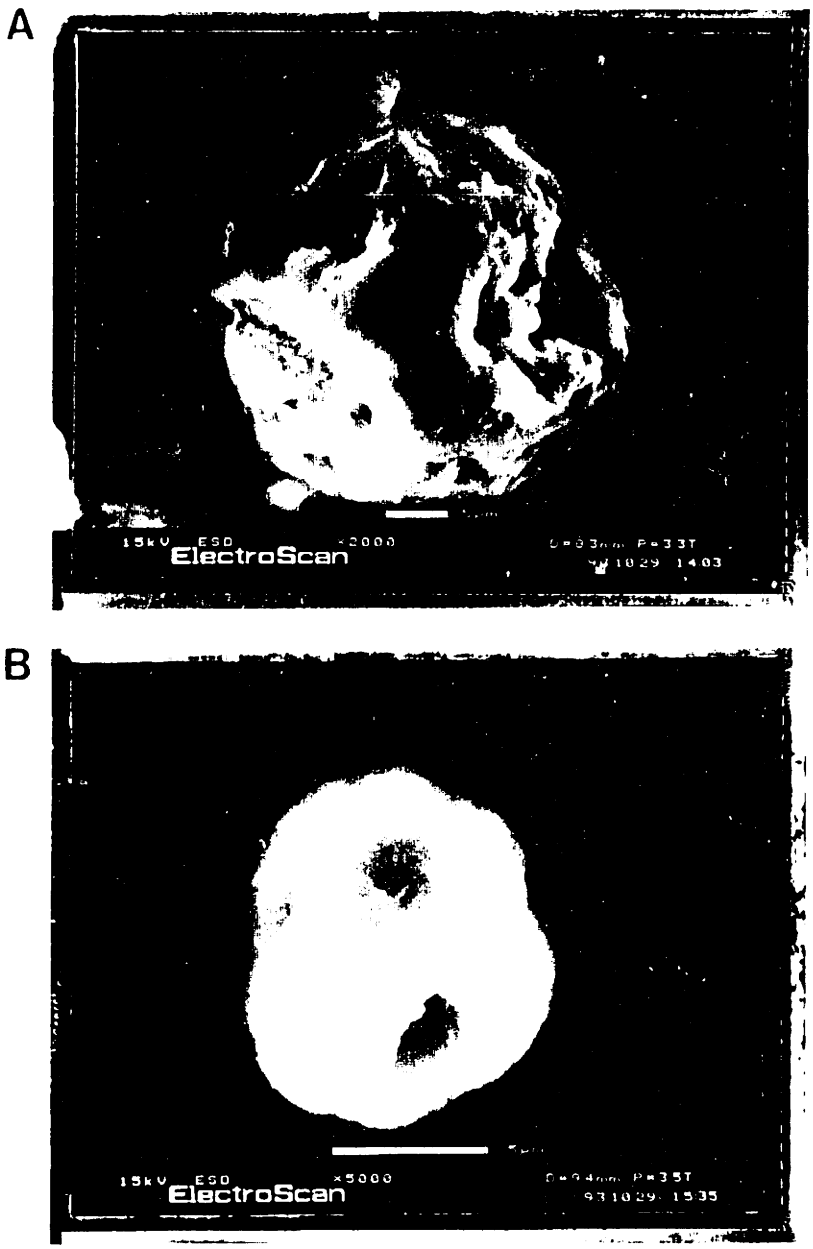

Fig 10-4. Scanning electron micrographs of poly(TMA-Tyr:SA:CPP) 20:50:30 microspheres during degradation *in vitro* after (a) four days and (b) seven days.

hydrolysis is controlled by the slow *dissolution* of hydrophobic monomers from the surface of the microsphere.

Owing to the fact that the various monomers have differing solubilities in water at pH 7.4 and 37°C (Fig 10-5), it was suspected that they would dissolve and diffuse from the surface of degraded microspheres at different rates. To understand the contribution of each monomer to the overall erosion of microspheres (and, therefore, to the release rates of macromolecules such as BSA), the appearance of each monomer in the release buffer was followed with time by HPLC. The release curves of each monomer from poly(TMA-Tyr:SA:CPP) microspheres of various compositions, and with a protein loading of 7 wt % BSA, are shown in Fig 10-6. The relatively hydrophilic monomers, TMA-Tyr and SA, were released at similar rates within a few days. Their fast release coincides with the relatively fast macromolecule (BSA) release in the first few days (i.e., the initial release phase) reported in Chapter 9. On the other hand, the hydrophobic monomer CPP was slowly released for greater than 30 days in each case (Fig 10-6b-d). This result may be explained in terms of the higher hydrophobicity and the lower water solubility of CPP compared with TMA-Tyr and SA. It is also possible that the more hydrophobic nature of polymers containing CPP slows microsphere hydration and, therefore, polymer hydrolysis. This is complicated, however, as is evident in Fig 10-2, by the existence of slow-degrading crystallites in polymers which do not contain high percentages of all three monomers.

Fig 10-7 shows the release profiles of a model protein, BSA, from poly(TMA-Tyr:SA:CPP) 20:50:30 microspheres made with polymers of various initial M_w's. The spheres initially had a BSA loading of 7 wt %. It can be seen that there is very little dependence of protein release rates on initial polymer molecular weight (i.e., MW preceding encapsulation). This finding confirms that polymer *degradation* occurs very rapidly with these polymer microspheres and that the subsequent *dissolution* of monomers is the rate-limiting step in microsphere erosion and, therefore, protein

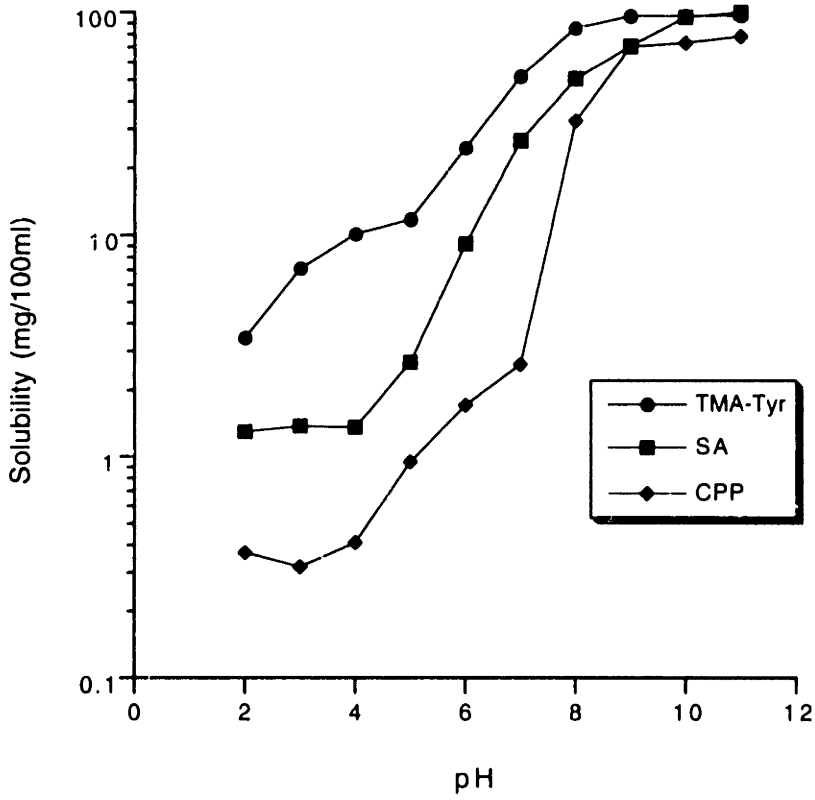

Fig 10-5. Solubilities of the monomers (TMA-Tyr, SA, and CPP) in water as a function of pH as determined by high pressure liquid chromatography (HPLC).

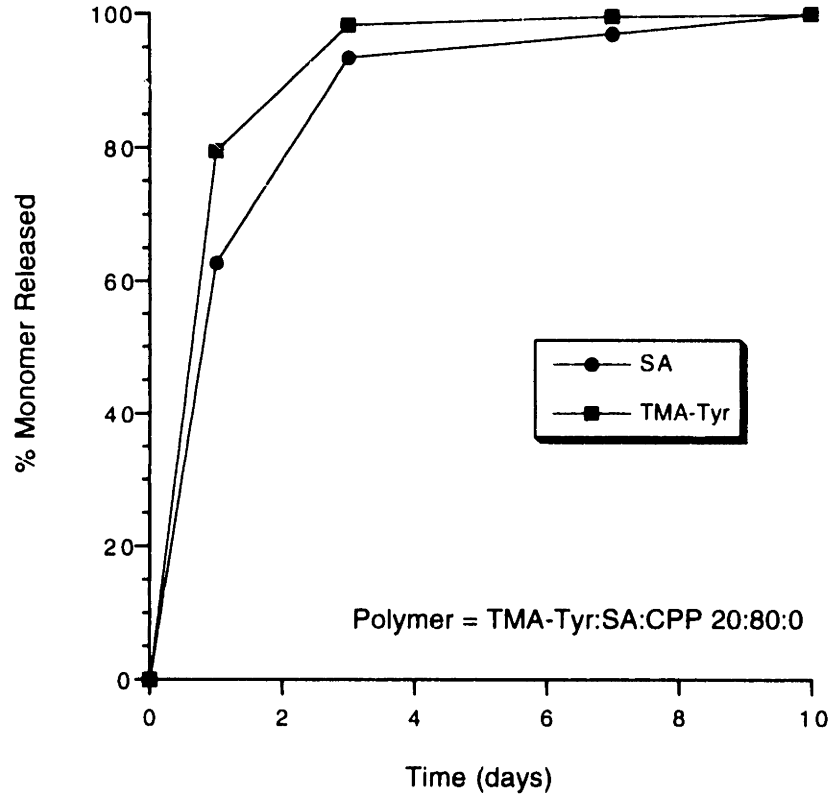

Fig 10-6a. Individual monomer release profiles *in vitro* from poly(TMA-Tyr:SA:CPP) microspheres of various compositions as measured by HPLC: (a) poly(TMA-Tyr:SA:CPP) 20:80:0.

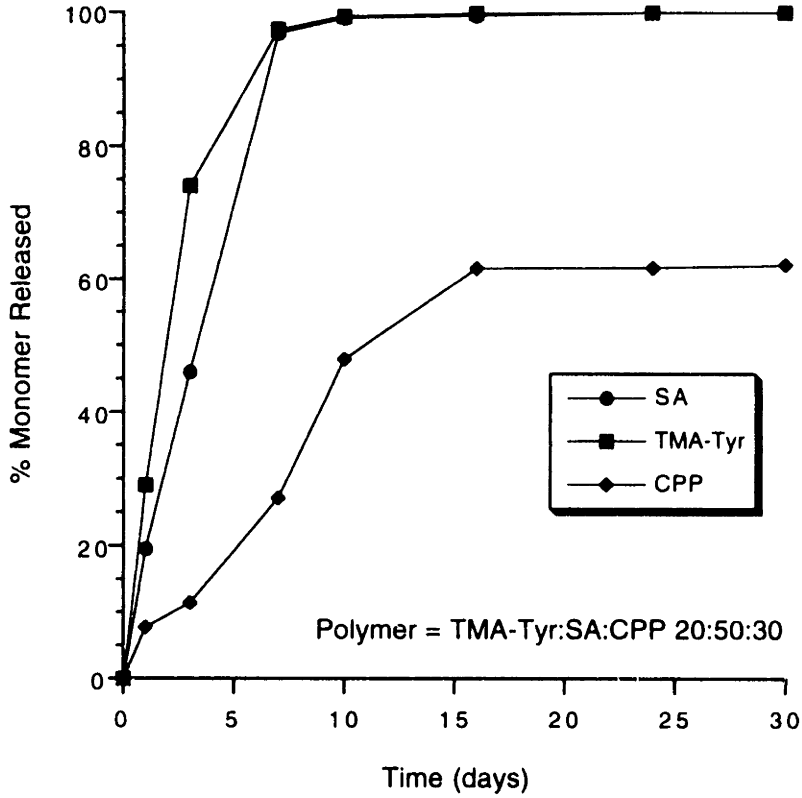

Fig 10-6b. Individual monomer release profiles *in vitro* from poly(TMA-Tyr:SA:CPP) microspheres of various compositions as measured by HPLC: (b) poly(TMA-Tyr:SA:CPP) 20:50:30.

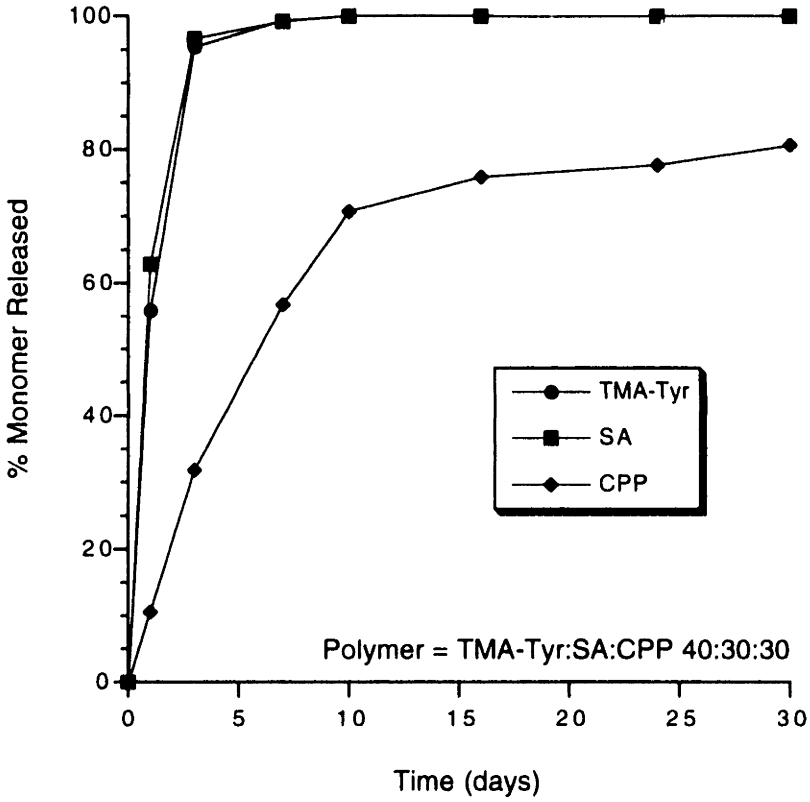

Fig 10-6c. Individual monomer release profiles *in vitro* from poly(TMA-Tyr:SA:CPP) microspheres of various compositions as measured by HPLC: (c) poly(TMA-Tyr:SA:CPP) 40:30:30.

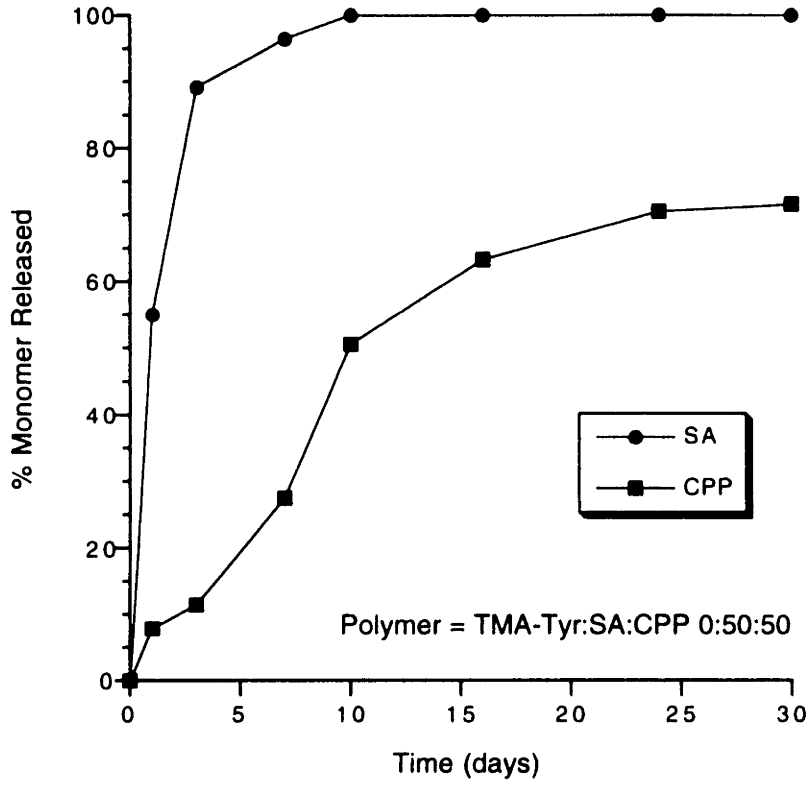

Fig 10-6d. Individual monomer release profiles *in vitro* from poly(TMA-Tyr:SA:CPP) microspheres of various compositions as measured by HPLC: (d) poly(TMA-Tyr:SA:CPP) 0:50:50.

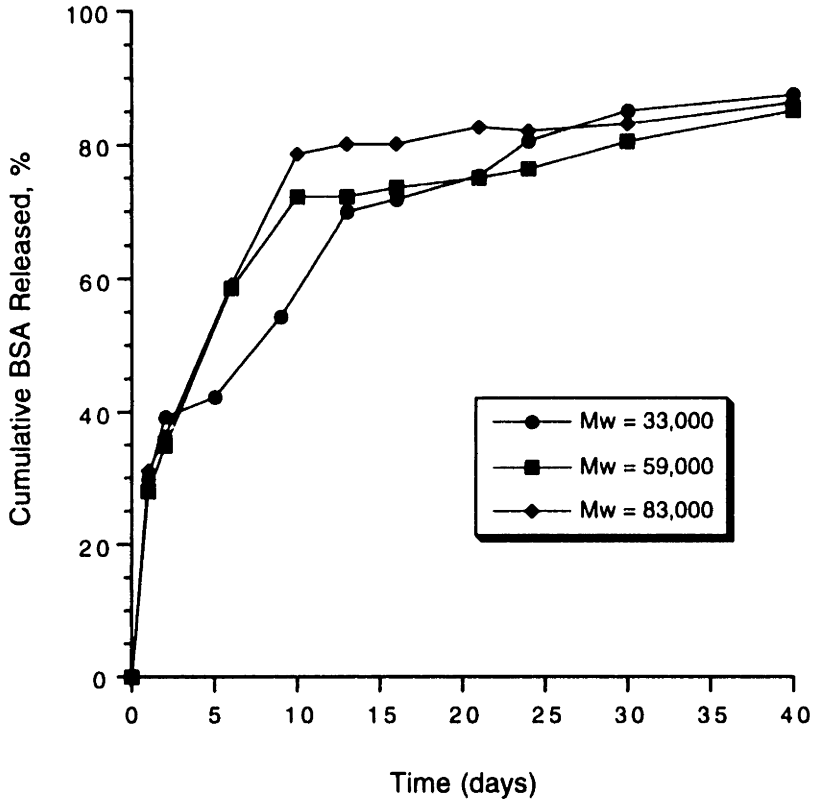

Fig 10-7. Controlled release profiles of a model protein, BSA, from poly(TMA-Tyr:SA:CPP) 20:50:30 microspheres made with polymers of various initial molecular weights.

release. This leads to release of proteins at rates approximately equal to the rate of microsphere weight loss, as shown in Chapter 9.

The effect of pH on polymer degradation and microsphere erosion was also examined. Fig 10-8 shows that pH does not have an effect on the degradation rates of poly(TMA-Tyr:SA:CPP) 20:50:30 microspheres; the polymers are completely degraded after a few days at pH's ranging from 2 to 11. This result, combined with the fact that following polymer degradation (fast) microsphere erosion is controlled by monomer dissolution (slow), suggested that the pH of the release medium may have a significant effect on erosion rates of microspheres (as confirmed in Fig 10-9). Fig 10-9 shows that poly(TMA-Tyr:SA:CPP) 20:50:30 microspheres erode much more slowly at low pH than at high pH. The reduced erosion rates of microspheres at low pH is due to the decreased solubility of the acidic monomers when their carboxylic acid groups are protonated (Fig 10-5). At high pH the monomers have relatively high solubilities (Fig 10-5) and microsphere erosion occurs more quickly (at a rate similar to the polymer degradation rate). At an intermediate pH (pH 7.4), significant microsphere erosion occurs in the first few days (corresponding to the time in which the majority of SA and TMA-Tyr are released), and is followed by a decreasing rate of erosion thereafter (when the polymer phase is mostly CPP; see Fig 10-6).

10.2.3 *In Vivo* Acute Toxicity of Poly(TMA-Tyr:SA:CPP) 40:30:30

Matrices of poly(TMA-Tyr:SA:CPP) were evaluated for tissue biocompatibility following subcutaneous implantation in rats. Compression molded polymer disks were used in this study to determine the toxicity of the polymer itself, eliminating the possibility that an adverse effect could be due to incomplete removal of other molecules involved in the preparation of microspheres (e.g., polyvinyl alcohol and methylene chloride). Control rats underwent the same surgical procedure but did not receive an

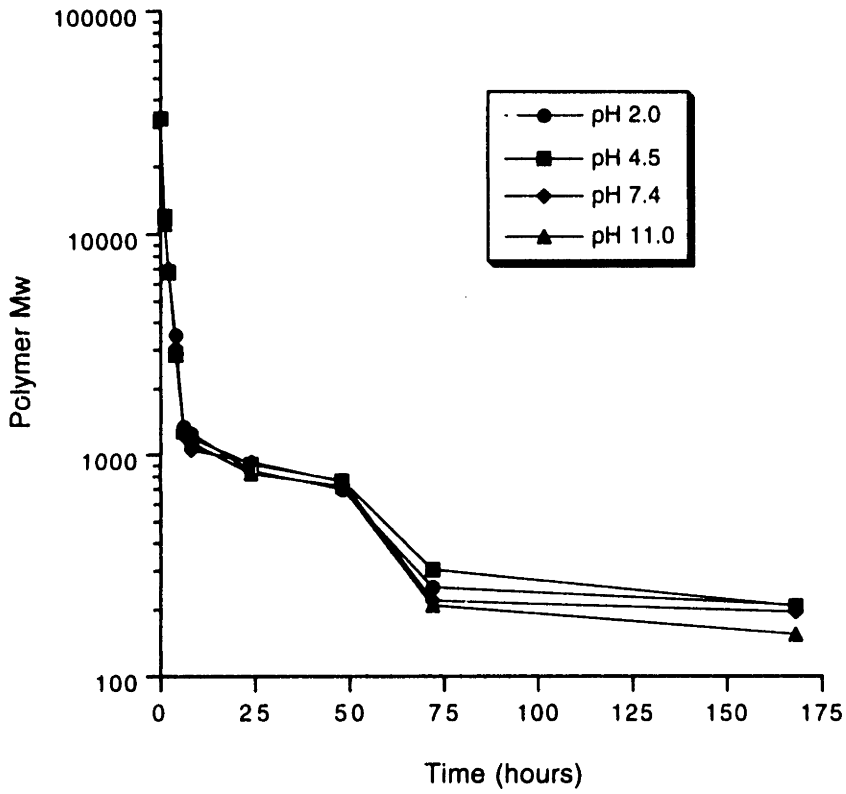

Fig 10-8. Poly(TMA-Tyr:SA:CPP) 20:50:30 microsphere degradation profiles *in vitro* as a function of buffer pH as measured by GPC.

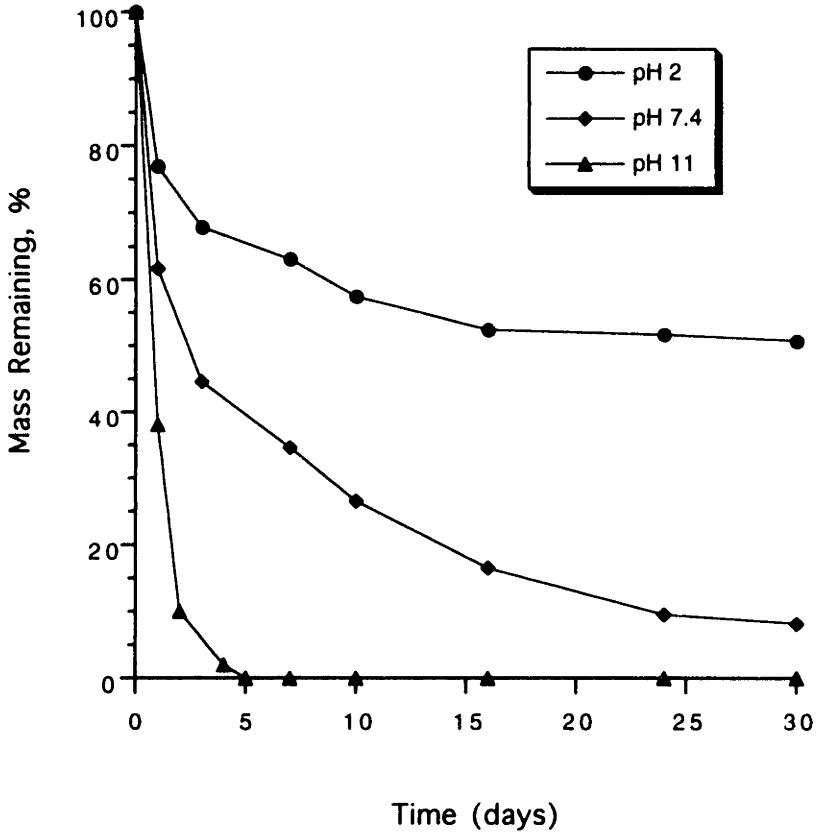

Fig 10-9. Poly(TMA-Tyr:SA:CPP) 20:50:30 microsphere erosion rates *in vitro* as a function of pH as measured by microsphere weight loss.

implant. In the control rats, the surgical area had a response that ranged from no inflammation to minimal chronic inflammation. The tissue reaction was typical of the normal progression to complete healing with no structural changes (i.e., return to normal with no persistent fibrosis). All four tissue sections with the polymer implant had similar microscopic appearances to each other. The reaction to the implant consisted of chronic inflammation characterized by moderate to marked infiltrates of predominantly macrophages and lymphocytes with some granulation tissue formation (Fig 10-10). Few or no neutrophils and little or no edema, necrosis or other adverse reactions were seen. No granuloma formation was observed (granuloma was defined as intense active inflammation with acute and chronic components including clusters of necrotic cells and debris with associated numerous lymphocytes). Granuloma formation is typical of tissues showing no progression to resolution of the lesion or healing around the implant site. Tissue surrounding poly(TMA-Tyr:SA:CPP) implants appears to be healing or progressing to fibrosis with incorporation of the implant. The reaction to the implant is typical of tissue reaction to sterile foreign material in contact with the host [191].

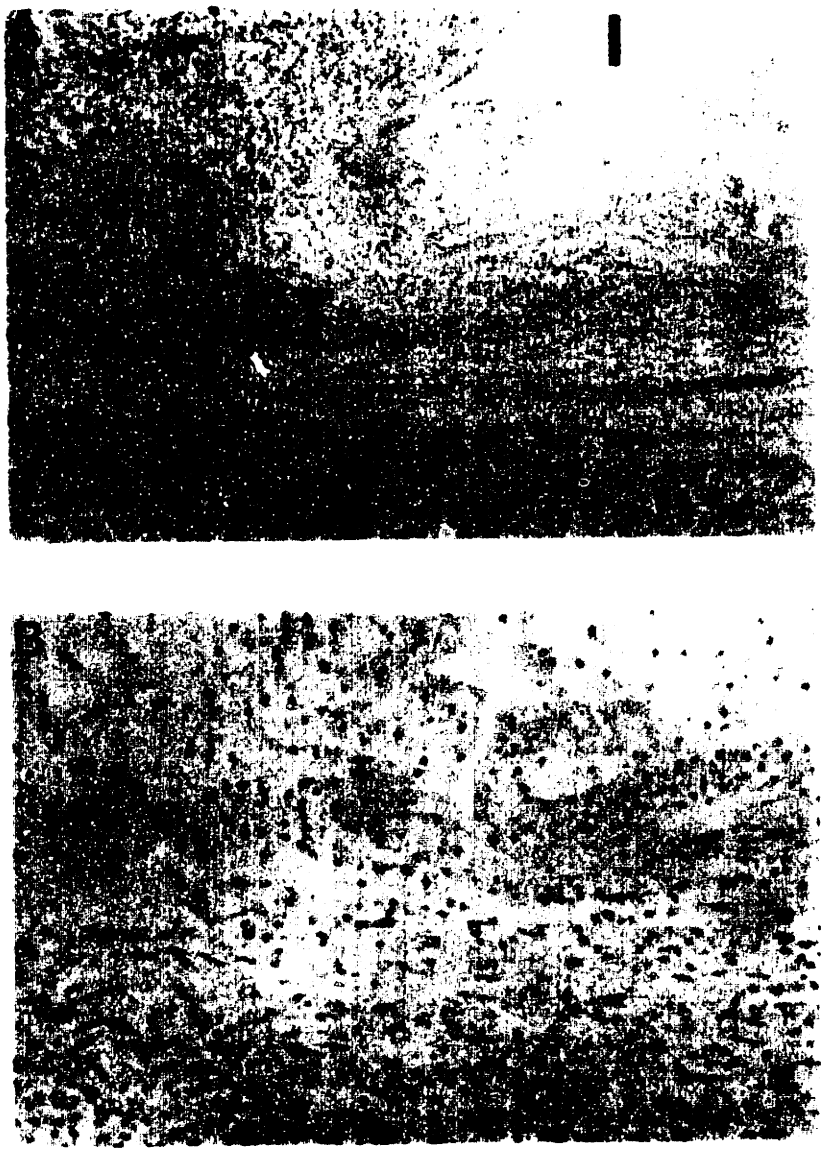

Fig 10-10. Histological examination of the implantation site after four days in Sprague-Dawley rats that received 200 mg poly(TMA-Tyr:SA:CPP) 40:30:30 implants: a) there is a loose connective tissue matrix surrounding the polymer with macrophages, lymphocytes, fibroblasts, and blood vessels (magnification: 100x); b) higher magnification of the granulation tissue region (magnification: 250x). The implant (I), muscle (M), and granulation tissue (GT) are indicated on the figure.

10.3 Discussion

The erosion of degradable polymers involves a number of steps, one or more of which may be rate controlling. In the first step, water contacts the water labile bond, by either direct access to the polymer surface or imbibition into the polymer matrix interior (microsphere hydration) [98]. The velocity of this process depends on the device porosity, the size of the device, and on the polymer composition (see Chapter 5). In the case discussed in this chapter, the small geometry of poly(TMA-Tyr:SA:CPP) microspheres combined with their high porosity results in a very rapid microsphere hydration. The next phase involves polymer degradation due to bond hydrolysis. The high reactivity of the anhydride bond with water leads to rapid degradation of poly(TMA-Tyr:SA:CPP), which constitutes the polymer phase of the microspheres. The resulting degradation products, either monomers or oligomers, then are able to dissolve and diffuse away from the sphere, thus completing the process of polymer erosion. The complete loss of TMA-Tyr and SA from microspheres after about 80 hr indicates that during this period water has penetrated the entire polymer matrix and reacted with all anhydride bonds involving TMA-Tyr and SA. All of the TMA-Tyr and SA monomers have apparently diffused to the surface of the spheres where they have been dissolved into the external bath. Moreover, complete disappearance of anhydride bonds was observed 122 hr after microsphere degradation by IR spectroscopy. Degradation studies confirmed that the remnants at this time were solid substances partially soluble in chloroform and their molecular weight was similar to that of CPP monomer. These findings suggested that at around 122 hr complete cleavage of anhydride bonds in the polymers occurred, leaving sparingly-soluble CPP monomers to control the release of protein.

Histology studies showed that tissue surrounding poly(TMA-Tyr:SA:CPP) implants appear to be healing or progressing to fibrosis with incorporation of the

implant. The reaction to the implant is typical of tissue reaction to sterile foreign material in contact with the host. These results are very encouraging, especially considering the dose of polymer given (200 mg/rat) is approximately 40-200 times the normal dose necessary for vaccine delivery (see Chapter 9).

11 Summary and Conclusions

11.1 Summary

The overall goal of this thesis was to develop polymeric controlled release delivery systems which could be administered either by injection or by inhalation that, by sustaining the delivery of vaccine antigens over extended periods of time, may reduce the number of vaccine doses required to achieve successful immunization (i.e., protection against infection).

Delivery via injection or inhalation requires the polymeric carrier matrix to degrade and be naturally resorbed by the patient. Based on this requirement, poly(D,L-lactic-*co*-glycolic acid) (PLGA) and poly(anhydride-*co*-imides) were chosen as two candidate biodegradable polymers to study for vaccine delivery. Each has its own particular advantages: PLGA is known to be very safe and is currently FDA approved for use in biodegradable surgical sutures and in various controlled release products, whereas poly(anhydride-*co*-imides) are able to incorporate derivatives of adjuvants (tyrosine-derivatives) into their polymeric backbone and therefore may be ideally suited as a matrix for vaccine antigen delivery.

In initial studies, PLGA microspheres containing a model vaccine were prepared and characterized with respect to their degradation process with the ultimate goal of gaining a more thorough understanding of polymer erosion and macromolecule release from porous bulk-eroding microspheres (see Chapter 4). Recombinant glycoprotein 120 (gp120, MW ≈ 104,000), a well-characterized protein under investigation as a prophylactic vaccine for HIV-1, was used as a model antigen. The microsphere degradation process is characterized with respect to microsphere morphology (SEM),

porosity (non-mercury porosimetry), drug distribution (confocal microscopy), polymer MW (GPC), polymer mass loss (weighing), polymer thermal transition temperatures and crystallinity (DSC), and protein release (*in vitro* incubation). gp120 release from PLGA microspheres was characterized by an initial burst, followed by an induction period of several days, and then a second release phase (i.e., pulsatile release). Studies showed that the microspheres contain an extensive network of pre-existing pores throughout the polymer matrix which grow over time. Understanding the evolution of these pores, most importantly nano- and sub-nano "micropores", is critical to understanding and predicting macromolecule release from PLGA microspheres, including the time between pulses.

A theoretical model based on these studies is subsequently outlined in Chapter 5 for predicting the time evolution of total mass, mean molecular weight and drug release for PLGA microspheres containing a macromolecular drug, such as a protein or peptide. Explicit analytical formulas are derived for calculating measurable macroscale characteristics (such as drug release or mean weight-averaged molecular weight) as functions of time and various transport coefficients. A general methodology for measuring the transport coefficients (such as polymer degradation rate constant) from erosion and release data is outlined. The use of this methodology is illustrated by comparison with erosion and release data from PLGA microspheres loaded with gp120. Very good agreement between theory and experiment is observed. Also, the rate coefficients deduced show that the erosion of the PLGA microspheres is degradation- (as opposed to diffusion-) controlled.

In Chapter 6, PLGA microspheres containing a model vaccine (gonadotropin releasing hormone conjugated to tetanus toxoid, GnRH-TT) were prepared and used to immunize rats to test the ability of controlled release microspheres to reduce the number of injections needed for successful immunization. Microspheres were as

effective in a single dose in eliciting systemic IgG antibody levels as the three-dose immunization schedule with standard human adjuvants.

To improve patient compliance and potentially decrease the cost of mass immunization programs we sought to develop vaccines that could be delivered without skilled medical personnel or the use of needles. To this end, porous PLGA microspheres were developed, some of which incorporate a major component of lung surfactant, L-α-phosphatidylcholine dipalmitoyl (DPPC), as an attractive method of antigen delivery to the lung via inhalation (see Chapter 7). A double emulsification preparation of PLGA microspheres renders the microspheres porous (mass density ~ 0.4 g/cc); the use of DPPC further improves the performance of dry powder PLGA microsphere formulations by rendering the PLGA microspheres even more porous (mass density < 0.3 g/cc). This property permits more efficient aerosolization and longer-lived, deep-lung-depositing PLGA aerosols. *In vivo*, 63% and 57% of double-emulsified particles (with and without DPPC), possessing mean diameters of approximately 8 μm, were delivered to the airways and deep lung of rats. By contrast, only 22% of single emulsion PLGA microspheres of comparable size were delivered beyond the trachea. *In vitro* aerosolization studies reveal that important differences between DPPC and non-DPPC PLGA microspheres can arise when the particles are aerosolized from a dry powder (Spinhaler) device. These studies show the great potential of pulmonary drug delivery using dry powder formulations involving safe, clinically proven PLGA polymers.

Many antigens are very poorly immunogenic, i.e., it is difficult to induce a strong immune response to them even with a well-designed controlled release system. Therefore, the final portion of this thesis was dedicated to the development of new polymers designed specifically for vaccine delivery in that they contain derivatives of adjuvants built into their backbone. To accomplish this goal, a series of anhydride-*co*-imide terpolymers based on trimellitylimido-L-tyrosine (TMA-Tyr), sebacic acid (SA),

and 1,3-bis(carboxyphenoxy)propane (CPP) [poly(TMA-Tyr:SA:CPP)] was synthesized by melt condensation polymerization (Chapter 8). It is desirable to incorporate tyrosine into the backbone of the polymer system due to its inherent ability to enhance the immune response to vaccine antigens. CPP and SA were copolymerized with the tyrosine derivative, TMA-Tyr, in order to develop a polymer with suitable material properties for drug delivery (e.g., high molecular weight, amorphous, and good solubility in low-boiling organic solvents), as well as to provide a series of polymers capable of a wide range of degradation and antigen release properties. A systematic series of studies was performed to evaluate and optimize the influence of monomer ratio, reaction time and temperature, reaction catalysts, and catalyst concentration on polymer molecular weight, percent TMA-Tyr incorporation, and crystallinity. Terpolymers were synthesized with weight average molecular weights in excess of 80,000 by using heterogenic catalysts and highly purified monomers with low degrees of oligomerization. In addition, the terpolymers had no crystalline regions, the only exception being polymers with greater than 60 percent SA in their backbone. Monomers and polymers were characterized by ^{1}H NMR and IR spectroscopy, elemental analysis, thermal transition temperature analysis, and gel permeation chromatography. The stability of these polymers in the solid state and in chloroform at various temperatures is also reported.

Subsequently, these new polymers were used to prepare polymer microspheres capable of the controlled release of macromolecules for periods ranging from days to over a month (Chapter 9). Microspheres were produced from a variety of polymer compositions using a double-emulsion solvent-evaporation technique, and tested for their ability to provide controlled release of a model protein, BSA, *in vitro*. The microspheres are spherical with smooth surfaces and encapsulate greater than 70% of the protein. Protein release rates from polymers of identical composition could be varied from 0.3 to over 125 μg/mg spheres/month by changing the amount of protein

encapsulated. This effect is magnified by using polymers with various monomer ratios. A close correlation between protein release and polymer weight loss was observed, suggesting a release mechanism controlled mainly by polymer erosion.

In Chapter 10, the degradation properties of poly(TMA-Tyr:SA:CPP) microspheres and *in vivo* acute toxicity of the polymer is reported. The microspheres erode from their surface-inward, termed surface-erosion, however, anhydride bond cleavage (polymer *degradation*) occurs on a much faster time scale with microspheres than with conventional larger delivery devices. Subsequent to bond cleavage, the ultimate erosion of the microsphere and release of macromolecules is due mainly to the slow *dissolution* of the individual hydrophobic monomers (TMA-Tyr, SA, and CPP) from the microsphere surface. TMA-Tyr:SA:CPP terpolymer degradation occurred rapidly (< 5 days) on the time scale of overall microsphere erosion (weeks to months) with most polymer compositions, regardless of polymer molecular weight. As a result, the initial polymer molecular weight does not have a significant effect on macromolecule release rates. Instead, monomer solubility correlated well with polymer erosion and BSA release time. Finally, TMA-Tyr:SA:CPP terpolymers were well-tolerated in acute toxicity studies in rats, and therefore show promise as biomaterials for vaccine delivery.

11.2 Conclusions

Due to their unique properties, microspheres show promise in achieving the lofty goals of single-step immunization with a heat-stable, non-toxic vaccine formulation which can be administered by injection to protect against a number of childhood diseases. In addition, by administering vaccines in microspheres of a size readily taken up by macrophages, it may be possible to evade antigen neutralization by maternal antibody. This would theoretically allow children to be vaccinated at a much earlier

age, which is of particular importance in developing countries where hundreds of thousands of children are infected before they are old enough to receive their first immunization.

The polyesters based on lactic and glycolic acid are likely to be the first polymers approved as vaccine vehicles. Controlled vaccine delivery from bioinert PLGA microspheres can lead to levels of immunity which are higher and longer lasting than those obtained by immunization with conventional adjuvants such as alum. This is most likely due to the ability of controlled release systems to provide a much longer-lasting antigen depot. However, polymers designed specifically to deliver vaccines, such as those with 'built-in adjuvanticity', may ultimately be better suited for the delivery of poorly immunogenic subunit vaccines.

The development of adjuvant-active microparticulate vaccine delivery systems seeks to combine the versatility in release profiles obtained with PLGA release systems with the additional adjuvant effect sometimes necessary for an effective immune response. Ideally, these "single-injection" vaccines would find widespread application in the place of existing conventional vaccines, whose protection is sometimes compromised by patient compliance or reproducibility, and in new subunit vaccines against illnesses such as Hepatitis B and HIV where the antigen is only weakly immunogenic. Besides their potential for clinical use, these vaccine systems are also being used to further probe the immune response to vaccination and find the optimum antigen and adjuvant release profiles.

As with any emerging technology, many formidable challenges in the design, formulation and manufacture of polymeric microparticulate vaccine systems for parenteral use remain to be addressed as promising candidates proceed further along the development process (see section 11.3). The end result, though, should be a new generation of vaccine systems which not only improve vaccination with existing

antigens but may very well make the difference between success and failure with poorly immunogenic subunit antigens.

11.3 Further Considerations in Microparticulate Vaccine Development

Since the primary purpose of immunization is to prevent disease rather than treat an existing one, a vaccine must be designed such that the risks of any adverse effects involved in receiving it are greatly outweighed by the risks involved in actually contracting the disease. And because a polymeric microparticulate vaccine system is more complex than a standard vaccine preparation, care must be taken to design a system which safely and efficaciously imparts protection against disease to the recipient. Furthermore, a method of manufacture for the vaccine must be developed to result in a reproducible, stable sterile product.

During the evaluation of candidate polymers, biocompatibility becomes an important issue. If a non-adjuvant polymer such as PLGA is to be used as a release matrix, the polymer is usually chosen to have minimal interaction with the body. Adjuvant-active polymers, though, have been designed to interact in some way with the immune system, antigen, or both, and the biocompatibility of these systems is no longer just a question of being bioinert. In non-erodible polymer systems, the persistence of microparticulates at the injection site or throughout the lymphatic system must be determined and its effect on the surrounding tissues evaluated. All aspects of the continuing presence of an immune-stimulating polymer surface in a living system must be thoroughly studied, especially potential links to autoimmune complications. One need only look to the ongoing controversy over the systemic health impact of silicone in breast implants and vascular devices to see the heightened awareness of this area of materials evaluation [183, 192, 193]. In the case where the polymer is bioerodible, its degradation products must be identified, quantified and characterized and their toxicity

determined. If the adjuvant-active polymer is composed of an adjuvant-active monomer, the activity of the degraded forms must be studied since small changes in a molecule (MDP, for example) can profoundly effect its adjuvant and inflammatory actions [194].

The formulation of a conventional vaccine generally involves the choosing of generally regarded as safe (GRAS) excipients and preparing them in a form which ensures the potency of the vaccine throughout its shelf life. These requirements often present quite a challenge in and of themselves; in the formulation of polymeric microparticulate vaccine system, the level of complexity raises additional safety and stability considerations.

If an existing polymer is used, a compendial grade should be used where possible. If none is available, a reputable manufacturing source must be found, and critical product parameters, such as polydispersity and contaminants levels, must be identified and their effects on the vaccine quantified. On the other hand, if a novel adjuvant-active polymer is to be used, the vaccine developer has the additional responsibility of determining a method for preparing it according to a well-controlled reaction and purification scheme that results in reproducible material over many batches.

The final form of the vaccine will dictate which stability considerations must be addressed during the formulation phase. An aqueous suspension is feasible if the antigen is adsorbed onto non-erodible polymer microparticles. In this case, the stability of the adsorbed antigen must be ensured. Desorption of the antigen from the microparticulate surface is to be avoided as this may alter the processing of the antigen after injection. An aqueous environment increases the likelihood of chemical degradations such as oxidation or deamidation [195, 196]. The adsorbed antigen, particularly proteins, should be stabilized toward conformational changes that may irreversibly disrupt three-dimensional epitopes or lead to insoluble aggregate formation

or altered desorption behavior. Ideally, the above stability considerations would also result in a product which is stable at ambient temperature or higher which allow it to be easily distributed and stored in geographical areas where immunization needs are great but refrigeration difficult.

Dry powder or lyophilized formulations are appropriate when bioerodible microspheres are used or the aqueous stability of adsorbed antigen is not sufficient. Generally, a molecule, once in a dried environment, tends to be relatively stable. However, the processing steps involved in getting to that low water content state are often themselves deleterious to antigen or polymer stability. Antigen-loaded polymer microspheres are usually prepared in the presence of organic solvents and lend themselves to forming dry powders. However, during the incorporation process, antigen in contact with organic phases may undergo denaturation or aggregation. Stabilizers used during this process will in many cases be incorporated in the final device, and their effect on product performance must be determined [80]. Lyophilization requires that an aqueous suspension of the vaccine be frozen, and the concentration of components during this process can cause pH shifts, icnic strength effects and aggregation [197]. The proper choice of cryoprotectant and buffer species will minimize these effects. The formulation of either dry powders or a lyophilized solid must also ensure that the vaccine preparation is efficacious upon reconstitution and that no harmful changes in antigen structure during the drying process have been introduced.

Finally, when the preceding requirements have been met, there will be further difficulties involved in manufacturing the microparticulate dosage form for parenteral administration. Among these, sterility assurance of the final product may be the most potentially troublesome. Unless the system consists of extremely small nanoparticles, the formulated vaccine will not be able to be aseptically filtered through a 0.22 μm sterilizing filter as is commonly done with most parenterals. Thus, the sterility will

have to be imparted either earlier in the manufacturing process, before the production of the microparticulates, or at the end by terminal sterilization. Formation of the microparticulates under aseptic conditions adds many levels of complexity as more product intermediates must be sterilized and their sterility after manufacturing and handling manipulations must be validated. From a unit operations standpoint, terminal sterilization would be the preferred method of product sterilization, but it carries its own liabilities. If a suspension formulation is used, moist-heat sterilization is viable, but the cycle must be carefully developed so that the desired sterility assurance level is guaranteed without affecting the stability of the polymer and the antigen. In the case of a heat-labile protein or peptide antigen, this may not be possible. The other option for sterilization is gamma irradiation, a process which forms free radicals that can lead to antigen degradation and aggregation, polymer reactions such as molecular weight decrease and crosslinking [198], and antigen-polymer reactions. Changes in polymer properties can lead to alteration of the release characteristics of a microparticulate [199] and this effect of radiation has been observed with poly(lactide-glycolide) microspheres [200]. For a detailed treatment of the manufacturing issues associated with microparticulate vaccines, the reader is referred to a description of the development of a polylactide microsphere vaccine system [80].

12 Challenges and Future Directions

Although a great deal of progress towards the development of polymeric controlled release systems as vaccine carriers has been made, several challenges remain. A primary concern is the issue of vaccine stability during device fabrication, storage, and use in the body. Many antigens are proteins with fragile three-dimensional structures vital to the immunogenicity of the vaccine. This three-dimensional structure may be compromised or lost as the antigen denatures or aggregates. Exposure to organic solvents, rehydration after lyophilization upon exposure to moisture, or complex chemical interactions with the polymer excipient or other chemicals in the preparation of the controlled release device may result in loss or reduction of immunogenicity of protein-based vaccines. For these reasons, studies aimed at stabilizing complex molecules will be important for the future success of some controlled release vaccine systems [146, 201, 202].

Another significant challenge is the further development of the mucosal route for vaccine administration [81]. Of particular concern is the low percent of vaccine uptake in the gastrointestinal (GI) tract. Because microspheres of the appropriate size (< 10 μm) and surface characteristics (hydrophobic) are taken up by the Peyer's patches in the intestine, they have been used as oral vaccine vehicles. Microencapsulated vaccines generally result in greatly increased mucosal as well as systemic immune responses over soluble antigen [20, 134]. However, vaccine uptake is still quite low.

Future vaccine systems for oral administration may be developed using novel strategies such as bioadhesive polymers. An appropriately designed bioadhesive polymer would adhere to the lumen of the intestine, preferably near the Peyer's patches, thereby increasing the bioavailability of vaccine through enhanced particle

uptake or increased uptake of released vaccine [203, 204]. The molecular and physicochemical properties found to be important in influencing the bioadhesive performance of polymers in the GI tract have been previously reviewed [205]. Alternatively, microspheres made of non-bioadhesive polymers may be linked to specific targeting ligands (e.g., anti-epithelial cell antibodies [206, 207] or lectins [208] to bring about an intimate and extended contact between vaccine vehicle and intestinal wall.

In another approach to increase uptake in the GI tract, vaccine delivery systems may be designed which target and stimulate receptors on M cells to increase particle uptake by mechanisms such as phagocytosis [209]. M cells are located on the dome epithelium of the Peyer's patches where they function as gatekeepers to the mucosal immune system, delivering antigens across the epithelium to lymphocytes and macrophages and exporting secretory antibodies for mucosal defense. The discovery of a molecular component unique to the membranes of M cells, which may then serve as a receptor, may lead to the possibility of targeting vaccine vehicles directly to M cells. This approach seems feasible since certain pathogenic bacteria and viruses are known to adhere selectively to M cells [210-215]. In fact, these organisms may be capable of serving as efficient delivery vehicles themselves for recombinant antigens [216]. Once the bacterial and viral molecules that mediate adherence to M cells have been identified, they could be used to target polymeric vaccine vehicles to the mucosal immune system.

Systems which target sites other than the GI tract may also prove useful for the mucosal delivery of vaccines in the future. Among these types of systems are nasal and intravaginal delivery systems which make use of bioadhesive polymer microspheres [217, 218], and polymer microspheres which may be administered by inhalation [85, 150, 219, 220] (also the subject of Chapter 7 of this thesis).

Another interesting challenge is the improvement of liposomal preparations for vaccine administration. Liposomes are concentric spheres consisting of phospholipid

bilayers separated by aqueous compartments. They can be made of non-toxic, immunologically-inert, biodegradable materials, and their composition and size can be varied to achieve various release rates. Since antigens or other materials can be incorporated into the aqueous or lipid phase, liposomes are versatile carriers [221].

Liposomes were originally rationalized as vaccine vehicles because they are avidly phagocytosed by macrophages [142, 222]. However, liposomes are often very unstable *in vivo*, most likely due to their rapid destruction by macrophages and high density lipoproteins [223], and therefore provide only a brief antigen depot when injected subcutaneously or intramuscularly [224, 225].

One approach to extending the *in vivo* lifetime of liposomes was demonstrated by Cohen *et al.* who used polymers to encapsulate vaccine-containing liposomes into microspheres, thereby protecting them from rapid destruction *in vivo* [45]. Fifty days after injection into rats, no radio-labeled bovine serum albumin (BSA) was detected at the injection site when liposomes alone were used as the carrier. On the other hand, almost 50% of the model vaccine was recovered on day 50 when the liposomal formulation was microencapsulated before injection. The increased antigen retention time correlated with the higher and longer lasting anti-BSA antibody titers seen with the microencapsulated liposome (MEL) formulation. At their maximal levels, antibody titers were 3-4 times higher with MELs than with non-encapsulated liposomes.

The further development of systems which are capable of providing pulsatile release also represents a significant challenge for future vaccine development. Examples of systems that can provide pulsatile release are externally and self-regulated systems reviewed elsewhere [226], and enzymatically activated microencapsulated liposomes [227].

Externally triggered systems are still in the early stages of development, however, their use is exciting for future vaccine administration due to their ability to release pre-programmed or self-controlled pulses of drug at any time following

administration. Thus, it may be possible to mimic a normal immunization regimen, consisting or several booster shots at spaced time intervals, by giving one injection of vaccine in a controlled release system and programming in custom bursts to match the normal schedule of boosters. However, should small portable triggering devices that can be preprogrammed become available, the clinical success of externally controlled systems for vaccination may be hindered by their associated cost and/or low patient acceptance.

Finally, a very important challenge for vaccine delivery from polymeric carriers is the intelligent development of new biomaterials which are engineered specifically for vaccine administration. The use of adjuvant-active polymers (see Chapters 8-10), or polymer systems which do not require the use of potentially harmful organic solvents during preparation [228, 229] are examples of this kind of system.

References

1. S.C. Arya. Human immunization in developing countries: practical and theoretical problems and prospects. *Vaccine* **12:**1423-1435 (1994).
2. B.R. Bloom. Vaccines for the third world. *Nature* **342:**115-120 (1989).
3. K.S. Warren. The biotechnology and children's revolutions. In R.K. Root, K.S. Warren, J. Griffiss and M.A. Sande (eds.), *Immunization*, Churchill Livingston, New York, 1989, pp. 1-9.
4. The National Vaccine Advisory Committee. The measles epidemic: the problems, barriers, and recommendations. *JAMA* **266:**1547-1552 (1991).
5. E.R. Zell, V. Dietz, J. Stevenson, S. Cochi and R. Bruce. Low vaccination levels of US preschool and school-age children: retrospective assessments of vaccination coverage, 1991-1992. *JAMA* **271:**833-839 (1994).
6. K.P. Goldstein, F.J. Kviz and R.S. Daum. Accuracy of immunization histories provided by adults accompanying preschool children to a pediatric emergency department. *JAMA* **270:**2190-2194 (1993).
7. A. Gibbons. A booster shot for children's vaccines. *Science* **255:**1351 (1992).
8. R. Langer. New methods of drug delivery. *Science* **249:**1527-1533 (1990).
9. A.T. Glenny, G.A.H. Buttle and M.F. Stevens. Rate of disappearance of diphtheria toxoid injected into rabbits and guinea-pigs: toxoid precipitated with alum. *J. Pathol. Bacteriol.* **34:**267-275 (1931).
10. J. Freund. The mode of action of immunological adjuvants. *Adv. Tuberc. Res.* **7:**130-148 (1956).
11. R. Edelman. Vaccine adjuvants. *Rev. Infect. Dis.* **2:**370-383 (1980).
12. J.H. Eldridge, J.K. Staas, J.A. Meulbroek, J.R. McGhee, T.R. Tice and R.M. Gilley. Biodegradable microspheres as a vaccine delivery system. *Mol. Immunol.* **28:**287-294 (1991).

13. S. Cohen, T. Yoshioka, M. Lucarelli, L.H. Hwang and R. Langer. Controlled delivery systems for proteins based on poly(lactic/glycolic acid) microspheres. *Pharm. Res.* **8:**713-720 (1991).

14. B. Gander, C. Thomasin, H.P. Merkle, Y. Men and G. Corradin. *Pulsed tetanus toxoid release from PLGA-microspheres and its relevance for immunogenicity in mice.* in *Proceed. Intern. Symp. Control. Rel. Bioact. Mater.* 1993. Washington D.C.: Controlled Release Society, Inc. pp. 65-66.

15. J.H. Eldridge, C.J. Hammond and J.A. Meulbroek. Controlled vaccine release in the gut-associated lymphoid tissues. I. Orally administered biodegradable microspheres target the Peyer's patches. *J. Controlled Release* **11:**205-214 (1990).

16. R. Edelman, R.G. Russell, G. Losonsky, B.D. Tall, C.O. Tacket, M.M. Levine and D.H. Lewis. Immunization of rabbits with enterotoxigenic *E. coli* colonization factor antigen (CFA/I) encapsulated in biodegradable microspheres of poly(lactide-*co*-glycolide). *Vaccine* **11:**155-158 (1993).

17. R.H. Reid, E.C. Boedeker, C.E. McQueen, D. Davis, L.-Y. Tseng, J. Kodak, K. Sau, C.L. Wilhelmsen, R. Nellore, P. Dalal and H.R. Bhagat. Preclinical evaluation of microencapsulated CFA/II oral vaccine against enterotoxigenic *E. coli*. *Vaccine* **11:**159-167 (1993).

18. C.E. McQueen, E.C. Boedeker, R. Reid, D. Jarboe, M. Wolf, M. Le and W.R. Brown. Pili in microspheres protect rabbits from diarrhoea induced by *E. coli* strain RDEC-1. *Vaccine* **11:**201-206 (1993).

19. Z. Moldoveanu, M. Novak, W.Q. Huang, R.M. Gilley, J.K. Staas, D. Schafer, R.W. Compans and J. Mestecky. Oral immunization with influenza virus in biodegradable microspheres. *J. Infect. Dis.* **167:**84-90 (1993).

20. D.T. O'Hagan, J.P. McGee, J. Holmgren, A.M. Mowat, A.M. Donachie, K.H.G. Mills, W. Gaisford, D. Rahman and S.J. Challacombe. Biodegradable microparticles for oral immunization. *Vaccine* **11:**149-154 (1993).

21. P. Marx, R. Compans, A. Gettie, J. Staas, R. Gilley, M. Mulligan, G. Yamshchikov, D. Chen and J. Eldridge. Protection against vaginal SIV transmission with microencapsulated vaccine. *Science* **260:**1323-1327 (1993).

22. R. Bomford. Aluminum salts: Perspectives in their use as adjuvants. In G. Gregoriadis, A.C. Allison and G. Poste (eds.), *Immunological Adjuvants and Vaccines*, Plenum Press, New York, 1988, pp. 35-41.

23. P. Frost and E.M. Lance. On the mechanism of action of adjuvants. *Immunology* **35:**63-68 (1978).

24. J.W. Mannhalter, H.O. Neychev, G.J. Zlabinger, R. Ahmad and M.M. Eibl. Modulation of the human immune response by the non-toxic and non-pyrogenic adjuvant aluminum hydroxide: Effect on antigen uptake and antigen presentation. *Clin. Exp. Immunol.* **61:**143-151 (1985).

25. J. Kreuter and I. Haenzel. Mode of action of immunological adjuvants: Some physicochemical factors influencing the effectivity of polyacrylic adjuvants. *Infect. Immun.* **19:**667-675 (1978).

26. S. Shirodkar, R. Hutchinson, D. Perry, J. White and S. Hem. Aluminum compounds used as adjuvants in vaccines. *Pharm. Res.* **7:**1282-1288 (1990).

27. S.L. Nail, J.L. White and S.L. Hem. Structure of aluminum hydroxide gel. II. Aging mechanism. *J. Pharm. Sci.* **65:**1192-1195 (1976).

28. W.J. Herbert. The mode of action of mineral-oil emulsion adjuvants on antibody production in mice. *Immunology* **14:**301-318 (1968).

29. H. Fukumi. Effectiveness and untoward reactions of oil adjuvant influenza vaccines. *Symposia Series in Immunobiological Standardization* **6:**237-240 (1967).

30. V.C. Stevens. Vaccine delivery systems: potential methods for use in antifertility vaccines. *Am. J. Reprod. Immunol.* **29:**176-188 (1993).

31. C.H. Stuart-Harris. Adjuvant influenza vaccines. *Bull. W.H.O.* **41:**617-621 (1969).

32. J. Freund, J. Casals and E.P. Hosmer. Sensitization and antibody formation after injection of tubercle bacilli and paraffin oil. *Proc. Soc. Exp. Biol. Med.* **37**:509-513 (1937).

33. F. Ellouz, A. Adam, R. Ciorbaru and E. Lederer. Activity of bacterial peptidoglycan derivatives. *Biochem. Biophys. Res. Commun.* **59**:1317-1322 (1974).

34. I. Preis and R. Langer. A single-step immunization by sustained antigen release. *J. Immunol. Methods* **28**:193-197 (1979).

35. S.M. Niemi, J.G. Fox, L.R. Brown and R. Langer. Evaluation of ethylene-vinyl acetate copolymer as a non-inflammatory alternative to Freund's complete adjuvant in rabbits. *Laboratory Animal Science* **35**:609-612 (1985).

36. Y. Tabata and Y. Ikada. Effect of the size and surface charge of polymer microspheres on their phagocytosis by macrophage. *Biomaterials* **9**:356-362 (1988).

37. Y. Tabata and Y. Ikada. Macrophage phagocytosis of biodegradable microspheres composed of L-lactic/glycolic acid homo- and copolymers. *J. Biomed. Mater. Res.* **22**:837-858 (1988).

38. J.H. Eldridge, J.A. Meulbroek, J.K. Staas, T.R. Tice and R.M. Gilley. Vaccine-containing biodegradable microspheres specifically enter the gut-associated lymphoid tissue following oral administration and induce a disseminated mucosal immune response. *Adv. Exp. Med. Biol.* **251**:192-202 (1989).

39. S. Cohen, M.J. Alonso and R. Langer. Novel approaches to controlled release antigen delivery. *International Journal of Technology Assessment in Health Care* **10**:121-130 (1994).

40. A.K. Schneider. Polylactide sutures. U.S. Patent 3,636,956, 1972.

41. D.K. Gilding and A.M. Reed. Biodegradable polymers for use in surgery: polyglycolic/poly(lactic acid) homo- and copolymers: 1. *Polymer* **20**:1459-1464 (1979).

42. H. Okada, Y. Inoue, T. Heya, H. Ueno, Y. Ogawa and H. Toguchi. Pharmacokinetics of once-a-month injectable microspheres of leuprolide acetate. *Pharm. Res.* **8:**787-791 (1991).

43. J.H. Eldridge, J.K. Staas, J.A. Meulbroek, T.R. Tice and R.M. Gilley. Biodegradable and biocompatible poly(DL-lactide-co-glycolide) microspheres as an adjuvant for staphylococcal enterotoxin B toxoid which enhances the level of toxin-neutralizing antibodies. *Infect. Immun.* **59:**2978-2986 (1991).

44. Y. Tabata, R. Nakaoka and Y. Ikada. *Potentiality of gelatin microspheres as an immunological adjuvant.* in *Proceed. Intern. Symp. Control. Rel. Bioact. Mater.* 1993. Washington, D.C.: Controlled Release Society, Inc. pp. 392-393.

45. S. Cohen, H. Bernstein, C. Hewes, M. Chow and R. Langer. The pharmacokinetics of, and humoral responses to, antigen delivered by microencapsulated liposomes. *Proc. Natl. Acad. Sci. USA* **88:**10440-10444 (1991).

46. J. Kreuter, R. Mauler, H. Gruschkau and P. Speiser. The use of new polymethylmethacrylate adjuvants for split influenza vaccines. *Exp. Cell Biol.* **44:**12-19 (1976).

47. J. Kreuter and P. Speiser. New adjuvants on a polymethylmethacrylate base. *Infect. Immun.* **13:**204-210 (1976).

48. J. Kreuter and P.Speiser. *In vitro* studies of poly(methyl methacrylate) adjuvants. *J. Pharm. Sci.* **65:**1624-1627 (1976).

49. J. Kreuter, U. Tauber and V. Illi. Distribution and elimination of poly(methyl-2-^{14}C-methacrylate) nanopartilce radioactivity after injection in rats and mice. *J. Pharm. Sci.* **68:**1443-1447 (1979).

50. J. Kreuter, M. Nefzger, E. Liehl, R. Czok and R. Voges. Distribution and elimination of poly(methyl methacrylate) nanoparticles after subcutaneous administration to rats. *J. Pharm. Sci.* **72:**1146-1149 (1983).

51. J. Kreuter, U. Berg, E. Liehl, M. Soliva and P.P. Speiser. Influence of the particle size on the adjuvant effect of particulate polymeric adjuvants. *Vaccine* **4:**125-129 (1986).

52. J. Kreuter, E. Liehl, U. Berg, M. Soliva and P.P. Speiser. Influence of hydrophobicity on the adjuvant effect of particulate polymeric adjuvants. *Vaccine* **6:**253-256 (1988).

53. H. Snippe, M.J. DeReuver, F. Strickland, J.M.N. Willers and R.L. Hunter. Adjuvant effect of non-ionic block copolymer surfactants in humoral and cellular immunity. *Int. Archs. Allergy Appl. Immun.* **65:**390-398 (1981).

54. R. Hunter, F. Strickland and F. Kezdy. The Adjuvant Activity of Nonionic Block Copolymer Surfactants. I. The Role of Hydrophile-Lipophile Balance. *J. Immunol.* **127:**1244-1250 (1981).

55. R.L. Hunter and B. Bennett. The Adjuvant Activity of Noionic Block Polymer Surfactants. II. Antibody Formation and Inflammation Related to the Structure of Triblock and Octablock Copolymers. *J. Immunol.* **133:**3167-3175 (1984).

56. R.L. Hunter and B. Bennett. The Adjuvant Activity of Non-Ionic Block Polymer Surfactants. III. Characterization of Selected Biologically Active Surfaces. *Scand. J. Immunol.* **23:**287-300 (1986).

57. A.C.M.L. Miller and E.C. Tees. A metabolisable adjuvant: Clinical trial of grass pollen tyrosine adsorbate. *Clin. Allergy* **4:**49-55 (1974).

58. A.W. Wheeler, D.M. Moran, B.E. Robins and A. Driscoll. L-tyrosine as an immunological adjuvant. *Int. Archs. Allergy Appl. Immunol.* **69:**113-119 (1982).

59. A.C.M.L. Miller, A.P. Hart and E.C. Tees. D. *pteronyssinus* -tyrosine adsorbate: Biological and clinical properties. *Acta Allerg.* **31:**35-43 (1976).

60. A.W. Wheeler, N. Whittall, V. Spackman and D.M. Moran. Adjuvant properties of hydrophobic derivatives prepared from L-tyrosine. *Int. Archs. Allergy Appl. Immunol.* **75:**294-299 (1984).

61. A. Nixon-George, T. Moran, G. Dionne, C. Penney, D. LaFleur and C. Bona. The adjuvant effect of stearyl tyrosine on a recombinant subunit hepatitis B surface antigen. *J. Immunol.* **144**:4798-4802 (1990).

62. C.L. Penney, D. Ethier, G. Dionne, A. Nixon-George, H. Zaghouani, F. Michon, H. Jennings and C.A. Bona. Further studies on the adjuvanticity of stearyl tyrosine and ester analogues. *Vaccine* **11**:1129-1134 (1993).

63. J.L. Maryanski, A.S. Verdini, P.C. Weber, F.R. Salemme and G. Corradin. Competitor analogs for defined T cell antigens: Peptides incorporating a putative binding motif and polyproline or polyglycine spacers. *Cell* **60**:63-72 (1990).

64. J. Kohn and R. Langer. Polymerization reactions involving the side chains of α-L-amino acids. *J. Am. Chem. Soc.* **109**:817-820 (1987).

65. J. Kohn, S.M. Niemi, E.C. Albert, J.C. Murphy, R. Langer and J.G. Fox. Single-step immunization using a controlled release, biodegradable polymer with sustained adjuvant activity. *J. Immunol. Methods* **95**:31-38 (1986).

66. J. Kohn and R. Langer. Poly(iminocarbonates) as potential biomaterials. *Biomaterials* **7**:176-182 (1986).

67. D.F. Kline, *Tyrosine-Based, Adjuvant-Active Polyiminocarbonates and Controlled Release of Antigen*, Ph.D. Thesis, Massachusetts Institute of Technology, Cambridge, MA, 1993.

68. D.R. Absolom, W. Zingg and A.W. Neumann. Protein adsorption to polymer particles: role of surface properties. *J. Biomed. Mater. Res.* **21**:161-171 (1987).

69. W. Norde and J. Lyklema. The adsorption of human plasma albumin and bovine pancreas ribonuclease at negatively charged polystyrene surfaces. I. Adsorption isotherms. Effects of charge, ionic strength, and temperature. *J. Colloid Interface Sci.* **66**:257-265 (1978).

70. F. MacRitchie. The adsorption of proteins at the solid/liquid interface. *J. Colloid Interface Sci.* **38**:484-488 (1972).

71. J. Kohn. The synthesis and characterization of pseudopoly(amino acids): New polymers for medical applications. *Polym. Preprints* **31:**178-179 (1990).

72. C. Li and J. Kohn. Synthesis of poly(iminocarbonates): Degradable polymers with potential applications as disposable plastics and as biomaterials. *Macromolecules* **22:**2029-2036 (1989).

73. S. Pulapura, C. Li and J. Kohn. Structure-property relationships for the design of polyiminocarbonates. *Biomaterials* **11:**666-678 (1990).

74. S. Pulapura and J. Kohn. Biomaterials based on "pseudo"-poly(amino acids): a Study of tyrosine derived polyiminocarbonates. *Polym. Preprints* **31:**233-234 (1990).

75. H.-Q. Mao, R.-X. Zhuo and C.-L. Fan. Synthesis and biological properties of polymer immunoadjuvants. *Polymer Journal* **25:**499-505 (1993).

76. M. Parant, F. Parant, L. Chedid, A. Yapo, J.F. Petit and E. Ledever. Fate of the synthetic immunoadjuvant, muramyl dipeptide (14C-labeled) in the mouse. *Int. J. Immunopharmacol.* **1:**35-47 (1979).

77. Y. Tabata and Y. Ikada. Activation of Macrophage *In Vitro* to Acquire Antitumor Activity by a Muramyl Dipeptide Derivative Encapsulated in Microspheres Composed of Lactide Copolymer. *J. Controlled Rel.* **6:**189-204 (1987).

78. V.C. Stevens, J.E. Powell, A.E. Lee, P.T.P. Kaumaya, D.H. Lewis, M. Rickey and T.J. Atkins. *Development of a delivery system for a birth control vaccine using biodegradable microspheres.* in *Proceed. Intern. Symp. Control. Rel. Bioact. Mater.* 1992. Orlando: Controlled Release Society, Inc. pp. 112-113.

79. C. Kensil, S. Soitysik, U. Patel and D. Marciani. Structure/Function relationship in adjuvants from Quillaja saponaria Molina. In F. Brown, R.M. Chanou, H. Ginsberg and R. Lerner (eds.), *Vaccines 92: Modern Approaches to New Vaccines including Prevention of AIDS*, Cold Spring Harbor Laboratory Press, Cold Spring Harbor, 1992, pp. 35-40.

80. J.L. Cleland. Design and production of single-immunization vaccines using polylactide polyglycolide microsphere systems. In M.F. Powell and M.J. Newman (eds.), *Vaccine Design: The Subunit and Adjuvant Approach*, Plenum Press, New York, 1995, pp. 439-462.

81. J.H. Eldridge, R.M. Gilley, J.K. Staas, Z. Moldoveanu, J.A. Meulbroek and T.R. Tice. Biodegradable microspheres: vaccine delivery system for oral immunization. *Curr. Topics Microbiol. Immunol.* **146**:59-65 (1989).

82. D.T. O'Hagan. Intestinal translocation of particulates - implications for drug and antigen delivery. *Adv. Drug Deliv. Rev.* **5**:265-285 (1990).

83. N. Santiago, S.J. Milstein, T. Rivera, E. Garcia, T.C. Chang, R.A. Baughman and D. Bucher. *Oral immunization of rats with influenza virus M protein (M1) microspheres.* in *Proceed. Intern. Symp. Control. Bioact. Mater.* 1992. Orlando: Controlled Release Society, Inc. pp. 116-117.

84. Z. Moldoveanu, J.K. Staas, R.M. Gilley, R. Ray, R.W. Compans, J.H. Eldridge, T.R. Tice and J. Mestecky. Immune responses to influenza virus in orally and systemically immunized mice. *Curr. Topics in Microbiol. Immunol.* **146**:91-99 (1989).

85. J.K. Staas, R.E. Hunt, P.A. Marx, R.W. Compans, J.F. Smith, J.H. Eldridge, J.W. Gibson, T.R. Tice and R.M. Gilley. *Mucosal immunization using microsphere delivery systems.* in *Proc. Intern. Symp. Control. Rel. Bioact. Mater.* 1993. Washington D.C.: Controlled Release Society, Inc. pp. 63-64.

86. Y. Tabata, S. Gutta and R. Langer. Controlled delivery systems for proteins using polyanhydride microspheres. *Pharm. Res.* **10**:487-496 (1993).

87. A. Ladd, P. Gopinath, Y.-Y. Tsong, T. Probst, W. Chung and R. Thau. Active immunization against GnRH combined with androgen supplementation is a promising antifertility vaccine for males. *Am. J. Reprod. Immunol. Microbiol.* **17**:121-127 (1988).

88. R.R.C. New. Characterization of liposomes. In R.R.C. New (ed.), *Liposomes: A Practical Approach*, IRL Press, New York, 1990, pp. 105-161.

89. J. Turner and S. Hering. Greased and oiled substrates as bounce-free impaction surfaces. *J. Aerosol Sci.* **18**:215-224 (1987).

90. A. Conix. Poly[1,3-bis(p-carboxyphenoxy)propane anhydride]. In J.R. Elliott (ed.), *Macromolecular Syntheses*, John Wiley & Sons, New York, 1966, pp. 95-99.

91. A. Staubli, E. Ron and R. Langer. Hydrolytically Degradable Amino Acid Containing Polymers. *J. Am. Chem. Soc.* **112**:4419-4424 (1990).

92. A.J. Domb and R. Langer. Polyanhydrides. I. Preparation of High Molecular Weight Polyanhydrides. *J. Polym. Sci.* **25**:3373-3386 (1987).

93. E. Mathiowitz, E. Ron, G. Mathiowitz, C. Amato and R. Langer. Morphological characterization of bioerodible polymers. 1. Crystallinity of polyanhydride copolymers. *Macromolecules* **23**:3212-3218 (1990).

94. A. Göpferich and R. Langer. The influence of microstructure and monomer properties on the erosion mechanism of a class of polyanhydrides. *J. Polym. Sci.* **31**:2445-2458 (1993).

95. Y. Ogawa, M. Yamamoto, H. Okada, T. Yashiki and T. Shimamoto. A new technique to efficiently entrap leuprolide acetate into microcapsules of polylactic acid or copoly(lactic/glycolic) acid. *Chem. Pharm. Bull. (Japan)* **36**:1095-1103 (1988).

96. Y. Ogawa, M. Yamamoto, S. Takada, H. Okada and T. Shimamoto. Controlled-release of leuprolide acetate from polylactic acid or copoly(lactic/glycolic)acid microcapsules: Influence of molecular weight and copolymer ratio of polymer. *Chem. Pharm. Bull. (Japan)* **36**:1502-1507 (1988).

97. Y. Ogawa, M. Yamamoto, H. Okada, T. Yashiki and T. Shimamoto. *In vivo* release profiles of leuprolide acetate from microcapsules prepared with polylactic

acids or copoly(lactic/glycolic) acids and *in vivo* degradation of these polymers. *Chem. Pharm. Bull. (Japan)* **36**:2576-2581 (1988).

98. J.A. Tamada and R. Langer. Erosion kinetics of hydrolytically degradable polymers. *Proc. Natl. Acad. Sci. USA* **90**:552-556 (1993).

99. T. Park. Degradation of poly(lactic-*co*-glycolic acid) microspheres: Effect of copolymer composition. *Biomaterials* **16**:1123-1130 (1995).

100. D.H. Lewis. Controlled release of bioactive agents from lactide/glycolide polymers. In M. Chasin and R. Langer (eds.), *Biodegradable Polymers as Drug Delivery Systems*, Marcel Dekker, Inc., New York, 1990, pp. 1-41.

101. S.J. Holland, B.J. Tighe and P.L. Gould. Polymers for Biodegradable Medical Devices, I. The Potential of Polyesters as Controlled Macromolecular Release Systems. *J. Controlled Release* **4**:155-180 (1986).

102. T. Park, W. Lu and G. Crotts. Importance of *in vitro* experimental conditions on protein release kinetics, stability, and polymer degradation in protein encapsulated poly(D,L-lactic acid-*co*-glycolic acid) microspheres. *J. Controlled Release* **33**:211-222 (1995).

103. M. Donbrow. *Microcapsules and Nanoparticles in Medicine and Pharmacy*, CRC Press, Inc., Boca Raton, 1992.

104. R.P. Batycky, J. Hanes, R. Langer and D.A. Edwards. Model of erosion and macromolecular drug release from biodegrading microspheres. Manuscript in Preparation.

105. J. Rouquerol, D. Avnir, D. Everett, C. Fairbridge, M. Haynes, N. Pernicone, J. Ramsay, K. Sing and K. Unger. Guidelines for the characterization of porous solids. In J. Rouquerol, F. Rodriguez-Reinoso, K. Sing and K. Unger (eds.), *Characterization of Porous Solids III: Studies in Surface Science and Catalysis*, Elsevier Science B.V., 1994, pp. 1-9.

106. J. Cleland and R. Langer. Formulation and delivery of proteins and peptides: Design and development strategies. In J. Cleland and R. Langer (eds.), *Formulation and Delivery of Proteins and Peptides*, American Chemical Society, Washington D.C., 1994, pp. 1-21.

107. J. Cleland, M. Powell, A. Lim, L. Barron, P. Berman, D. Eastman, J. Nunberg, T. Wrin and J. Vennari. Development of a single shot subunit vaccine for HIV-1. *AIDS Res. Human Retrovirus* **10**:S21-S26 (1994).

108. S. Li, H. Garreau and M. Vert. Structure-property relationships in the case of the degradation of massive aliphatic poly(α-hydroxy acids) in aqueous media, part I: poly(DL-lactic acid). *J. Mater. Sci.: Mater. Med.* **1**:123-130 (1990).

109. S. Li, H. Garreau and M. Vert. Structure-property relationships in the case of the degradation of massive aliphatic poly(α-hydroxy acids) in aqueous media, part II: degradation of lactide-glycolide copolymers: PLA37.5GA25 and PLA75GA25. *J. Mater. Sci.: Mater. Med.* **1**:131-139 (1990).

110. M. Therin, P. Christel, S. Li, H. Garreau and M. Vert. *In vivo* degradation of massive poly(α-hydroxy acids): Validation of *in vitro* findings. *Biomaterials* **13**:594-600 (1992).

111. T. Higuchi. Mechanism of sustained-action medication. Theoretical analysis of rate of release of solid drugs dispersed in solid matrices. *J. Pharm. Sci.* **52**:1145-1149 (1963).

112. P.I. Lee. Diffusional release of a solute from a polymeric matrix - approximate analytical solutions. *J. Membrane Sci.* **7**:255-275 (1980).

113. A. Joshi and K.J. Himmelstein. Dynamics of controlled release from biodegradable matrices. *J. Controlled Release* **15**:95-104 (1991).

114. W.M. Saltzman, S.H. Pasternak and R. Langer. Microstructural models for diffusive transport in porous polymers. In P.I. Lee and W.R. Good (eds.),

Controlled-Release Technology: Pharmaceutical Applications, American Chemical Society, Washington D.C., 1987, pp. 16-33.

115. S.S. Shah, Y. Cha and C.G. Pitt. Poly(glycolic acid-*co*-D,L-lactic acid): Diffusion or degradation controlled drug delivery? *J. Controlled Release* **18**:261-270 (1992).

116. Y. Cha and C.G. Pitt. A one-week subdermal delivery system for L-methadone based on biodegradable microcapsules. *J. Controlled Release* **7**:69-78 (1988).

117. J.L. Duda and J.M. Zielinski. Free-volume theory. In P. Neogi (ed.), *Diffusion in Polymers*, Marcel Dekker, New York, 1996, pp. 143-171.

118. H. Brenner and D.A. Edwards. *Macrotransport Processes*, Butterworth-Heinemann, Boston, 1993.

119. A. Ladd, Y.-Y. Tsong, A. Walfield and R. Thau. Development of an antifertility vaccine for pets based on active immunization against luteinizing hormone-releasing hormone. *Biology of Reproduction* **51**:1076-1083 (1994).

120. A. Ladd. Progress in the development of anti-LHRH vaccine. *Am. J. Reprod. Immunol.* **29**:189-194 (1993).

121. I. Robertson, H. Fraser, G. Innes and A. Jones. Effect of immunological castration on sexual and production characteristics in male cattle. *Vet. Res.* **111**:529-531 (1982).

122. V. Schally, A. Arimura and A. Kastin. Hypothalamic regulatory hormones. *Science* **179**:341-350 (1973).

123. C. Paulsen. The testes. In R. Williams (ed.), *Textbook of Endocrinology*, Saunders, Philadelphia, 1974, pp. 323-367.

124. E. Steinberg. Hormonal control of mammalian spermatogenesis. *Physiol. Rev.* **51**:1-10 (1971).

125. I. Gonda. Preface. Major issues and future prospects in the delivery of therapeutic and diagnostic agents to the respiratory tract. *Adv. Drug Del. Rev.* **5**:1-9 (1990).

126. X. Zeng, G. Martin and C. Marriott. The controlled delivery of drugs to the lung. *Int. J. Pharm.* **124:**149-164 (1995).

127. D.A. Wall. Pulmonary absorption of peptides and proteins. *Drug Delivery* **2:**1-20 (1995).

128. J. Patton and R. Platz. Pulmonary delivery of peptides and proteins for systemic action. *Adv. Drug Del. Rev.* **8:**179-196 (1992).

129. P. Byron. Determinants of drug and polypeptide bioavailability from aerosols delivered to the lung. *Adv. Drug. Del. Rev.* **5:**107-132 (1990).

130. J.S. Patton, P. Trinchero and R.M. Platz. Bioavailability of pulmonary delivered peptides and proteins: α-interferon, calcitonins and parathyroid hormones. *J. Controlled Release* **28:**79-85 (1994).

131. B. Damms and W. Bains. The cost of delivering drugs without needles. *Nature Biotechnology* In Press.

132. R.W. Niven, K.L. Whitcomb, L. Shaner, A.Y. Ip and O.B. Kinstler. The pulmonary absorption of aerosolized and intratracheally instilled rhG-CSF and monoPEGylated rhG-CSF. *Pharm. Res.* **12:**1343-1349 (1995).

133. S. Kobayashi, S. Kondo and K. Juni. Pulmonary delivery of salmon calcitonin dry powders containing absorption enhancers in rats. *Pharm. Res.* **13:**80-83 (1996).

134. J. Eldridge, J. Staas, J. Meulbroek, J. McGhee, T. Tice and R. Gilley. Disseminated mucosal anti-toxin antibody responses induced through oral or intrathecal immunisation with toxoid-containing biodegradable microspheres. In T.T. MacDonald, S.J. Challacombe, P.W. Bland, C.R. Stokes, R.V. Heatley and A.M. Mowat (eds.), *Advances in Mucosal Immunology*, Kluwer Academic Publishers, Boston, 1989, pp. 375-378.

135. F. Liu, Z. Shao, D. Kildsig and A. Mitra. Pulmonary delivery of free and liposomal insulin. *Pharm. Res.* **10:**228-232 (1993).

136. P.R. Wyde, H.R. Six, S.Z. Wilson, B.E. Gilbert and V. Knight. Activity against rhinoviruses, toxicity and delivery in aerosol of enviroxine in liposomes. *Antimicrob. Agents Chemother.* **32:**890-895 (1988).

137. H. Schreier, K. McNicol, M. Ausborn, D. Soucy, H. Derendorf, A. Stecenko and R. Gonzalez-Rothi. Pulmonary delivery of amikacin liposomes and acute liposome toxicity in the sheep. *Int. J. Pharm.* **87:**183-193 (1992).

138. I. Kellaway and S. Farr. Liposomes as drug delivery systems to the lung. *Adv. Drug Del. Rev.* **5:**149-161 (1990).

139. J.A. Clements and R.J. King. Composition of the surface active material. In R.G. Crystal (ed.), *The Biochemical Basis of Pulmonary Function*, Marcel Dekker, Inc., New York, 1976, pp. 363-387.

140. K.M.G. Taylor, G. Taylor, I.W. Kellaway and J. Stevens. The stability of liposomes to nebulisation. *Int. J. Pharm.* **58:**57-61 (1990).

141. R.J. Gonzalez-Rothi, J. Cacace, L. Straub and H. Schreier. Liposomes and pulmonary alveolar macrophages: Functional and morphological interactions. *Exp. Lung Res.* **17:**687-705 (1991).

142. C.R. Alving. Delivery of Liposome-Encapsulated Drugs to Macrophages. *Pharmacological Therapy* **22:**407-424 (1983).

143. I. Gonda. Physico-chemical principles in aerosol delivery. In D. Crommelin and K. Midha (eds.), *Topics in Pharmaceutical Sciences 1991*, Stuttgart: Medpharm Scientific Publishers, 1992, pp. 95-117.

144. Y. Li and A.K. Mitra. Effects of phospholipid chain length, concentration, charge, and vesicle size on pulmonary insulin absorption. *Pharm. Res.* **13:**76-79 (1996).

145. Y. Lai, R. Mehta, A. Thacker, S. Yoo, P. McNamara and P. DeLuca. Sustained bronchodilation with isoproterenol poly(glycolide-*co*-lactide) microspheres. *Pharm. Res.* **10:**119-125 (1993).

146. R. Liu, R. Langer and A.M. Klibanov. Moisture-induced aggregation of lyophilized proteins in the solid state. *Biotechnol. Bioeng.* **37**:177-184 (1991).

147. M. Mumenthaler, C.C. Hsu and R. Pearlman. Feasibility study on spray-drying protein pharmaceuticals: Recombinant human growth hormone and tissue-type plasminogen activator. *Pharm. Res.* **11**:12-20 (1994).

148. M. Timsina, G. Martin, C. Marriott, D. Ganderton and M. Yianneskis. Drug delivery to the respiratory tract using dry powder inhalers. *Int. J. Pharm.* **101**:1-13 (1994).

149. W. Li, M. Perzl, J. Heyder, R. Langer, J. Brain, K. Englmeier, R. Niven and D. Edwards. Aerodynamics and aerosol particle deaggregation phenomena in model oral-pharyngeal cavities. *J. Aerosol Sci.* In Press (1996).

150. D. Edwards, G. Caponetti, J. Hrkach, N. Lotan, J. Hanes, A. Ben-Jebria, M. Eskew, J. Ultman and R. Langer. Porous polymeric aerosols for pulmonary drug delivery. Submitted (1996).

151. J. Heyder, J. Gebhart, G. Rudolf, C. Schiller and W. Stahlhofen. Deposition of particles in the human respiratory tract in the size range 0.005-15 μm. *J. Aerosol Sci.* **17**:811-825 (1986).

152. J. Visser. Van der Waals and other cohesive forces affecting powder fluidization. *Powder Technology* **58**:1-10 (1989).

153. S. Rudt and R.H. Muller. *In vitro* phagocytosis assay of nano- and microparticles by chemiluminescence. I. Effect of analytical parameters, particle size and particle concentration. *J. Controlled Release* **22**:263-272 (1992).

154. E.R. Weibel. *Morphometry of the Human Lung*, Academic Press, New York, 1963.

155. P.J. Moloney and G. Wojcik. Synthetic Adjuvants for Stimulation of Antigenic Responses. Canadian Patent 325,670, 1979.

156. B.G. Overell. U.S. Patent 4,428,932, 1984.

157. C. Penney. Stearyl tyrosine: An organic equivalent of aluminum-based immunoadjuvants. In M. Powell and M. Newman (eds.), *Vaccine Design: The Subunit and Adjuvant Approach*, Plenum Press, New York, 1995, pp. 611-624.

158. H. Brem, S. Piantadosi, P.C. Burger, M. Walker, R. Selker, N.A. Vick, K. Black, M. Sisti, S. Brem, G. Mohr, P. Muller, R. Morawetz and S.C. Schold. Placebo-controlled trial of safety and efficacy of intraoperative controlled delivery by biodegradable polymers of chemotherapy for recurrent gliomas. *Lancet* **345**:1008-1012 (1995).

159. C. Laurencin, A. Domb, C. Morris, V. Brown, M. Chasin, R. McConnell, N. Lange and R. Langer. Poly(anhydride) administration in high doses *in vivo:* Studies of biocompatibility and toxicology. *J. Biomed. Mater. Res.* **24**:1463-1481 (1990).

160. K.W. Leong, B.C. Brott and R. Langer. Bioerodible polyanhydrides as drug-carrier matrices. I: Characterization, degradation, and release characteristics. *J. Biomed. Mater. Res.* **19**:941-955 (1985).

161. E. Ron, E. Mathiowitz, G. Mathiowitz, A. Domb and R. Langer. NMR characterization of erodible polymers. *Macromolecules* **24**:2278-2282 (1991).

162. A.J. Domb and R. Langer. Solid-state and solution stability of poly(anhydrides) and poly(esters). *Macromolecules* **22**:2117-2122 (1989).

163. J.W. Hill and W.H. Carothers. Studies of polymerization and ring formation. XIV. A linear superpolyanhydride and a cyclic dimeric anhydride from sebacic acid *J. Am. Chem. Soc.* **54**:1569-1579 (1932).

164. R.E. Wilfong. Linear polyesters. *J. Polym. Sci.* **54**:385-410 (1961).

165. J. Furukawa and T. Saegusa. *Polymerization of aldehydes and oxides*, Wiley-Interscience, New York, 1963.

166. G. Odian. *Principles of Polymerization*, Wiley-Interscience, New York, 1981.

167. J. Hanes, M. Chiba and R. Langer. Polymer microspheres for vaccine delivery. In M.F. Powell and M.J. Newman (eds.), *Vaccine Design: The Subunit and Adjuvant Approach*, Plenum Press, New York, 1995, pp. 389-412.

168. K. Uhrich, A. Gupta, T. Thomas, C. Laurencin and R. Langer. Synthesis and Characterization of Degradable Poly(anhydride-*co*-imides). *Macromolecules* **28**:2184-2193 (1995).

169. A. Staubli, E. Mathiowitz, M. Lucarelli and R. Langer. Characterization of Hydrolytically Degradable Amino Acid Containing Poly(anhydride-*co*-imides). *Macromolecules* **24**:2283-2290 (1991).

170. Ghana Health Assessment Project Team. A quantitative method of assessing the health impact of different diseases in less developed countries. *Int. J. Epidemiol.* **10**:73-80 (1981).

171. M.F. Powell and M.J. Newman (eds.), *Vaccine Design: The Subunit and Adjuvant Approach*, Plenum Press, New York, 1995.

172. E. Mathiowitz and R. Langer. Polyanhydride microspheres as drug delivery systems. In M. Donbrow (ed.), *Microcapsules and Nanoparticles in Medicine and Pharmacy*, CRC Press, Boca Raton, 1992, pp. 99-123.

173. J.P. Flory. Thermodynamics of crystallization in high polymers. I. Crystallization induced by stretching. *J. Chem. Phys.* **15**:397-408 (1947).

174. J.L. Cleland and R. Langer (eds.), *Formulation and Delivery of Proteins and Peptides*, American Chemical Society, Washington, D.C., 1994.

175. E. Mathiowitz and R. Langer. Polyanhydride microspheres as drug carriers I. Hot-melt microencapsulation. *J. Controlled Release* **5**:13-22 (1987).

176. D.T. O'Hagan. Microparticles as oral vaccines. In D.T. O'Hagan (ed.), *Novel Delivery Systems for Oral Vaccines*, CRC Press, Boca Raton, 1994, pp. 175-205.

177. D.E. Chickering, W.P. Harris and E. Mathiowitz. A microtensiometer for the analysis of bioadhesive microspheres. *Biomed. Instrum. Technol.* **29**:501-512 (1995).

178. M. Chasin and R. Langer (eds.), *Biodegradable Polymers as Drug Delivery Systems*, Marcel Dekker, Inc., New York, 1990.

179. M.A. Howard, A. Gross, M.S. Grady, R. Langer, E. Mathiowitz, R. Winn and M.R. Mayberg. Intracerebral drug delivery in rats with lesion-induced memory deficits. *J. Neurosurg.* **71:**105-112 (1989).

180. M. Kovacsovics-Bandowski, K. Clark and B. Benacerraf. Efficient major histocompatibility complex class I presentation of exogenous antigen upon phagocytosis by macrophages. *Proc. Natl. Acad. Sci. USA* **90:**4942-4946 (1993).

181. A. Moore, P. McGuirk, S. Adams, W.C. Jones, J.P. McGee, D.T. O'Hagan and K.H.G. Mills. Immunization with a soluble recombinant HIV protein entrapped in biodegradable microparticles induces HIV-specific $CD8^+$ cytotoxic T lymphocytes and $CD4^+$ Th1 cells. *Vaccine* **13:**1741-1749 (1995).

182. N. Peppas and R. Langer. New challenges in biomaterials. *Science* **263:**1657-1804 (1994).

183. D. Kessler. The basis of the FDA's decision on breast implants. *New England J. Med.* **326:**1713-1715 (1992).

184. R. Langer and J. Vacanti. Tissue Engineering. *Science* **260:**920-926 (1993).

185. P. Rokkanen, O. Bostman, S. Vainionpaa, E. Makela, E. Hirvensalo, E. Partio, K. Vihtonen, H. Patiala and P. Tormala. Absorbable devices in the fixation of fractures. *J. Trauma* **40:**S123-S127 (1996).

186. Controlled Release Society. *Proc. 22nd Int. Symp. Control. Release Bioact. Mater.* 1995. Seattle, WA: Controlled Release Society, Inc.

187. A. Göpferich, R. Gref, Y. Minamitake, L. Shieh, M. Alonso, Y. Tabata and R. Langer. Drug delivery from bioerodible polymers: Systemic and intravenous administration. In J. Cleland and R. Langer (eds.), *Formulation and Delivery of Proteins and Peptides*, American Chemical Society, Washington D.C., 1994, pp. 242-277.

188. J. Hanes, P. Hildgen, R. Batycky, S. Coleman, J. Cleland, D. Edwards and R. Langer. Poly(D,L-lactic-*co*-glycolic acid) microsphere degradation and pulsatile release of the protein antigen gp120. Manuscript in Preparation.

189. H. Sah and Y. Chien. Degradability and antigen-release characteristics of polyester microspheres prepared from polymer blends. *J. Appl. Polym. Sci.* **58:**197-206 (1995).

190. Y. Cha and C. Pitt. The acceleration of degradation-controlled drug delivery from polyester microspheres. *J. Controlled Release* **8:**259-265 (1989).

191. J. Anderson. Inflammatory response to implants. *Trans. Am. Soc. Artif. Intern. Organs* **34:**101-107 (1988).

192. R. Goldblum, R. Pelly, A. O'Donell, D. Pyron and J. Heggers. Antibodies to silicone elastomers and reactions to ventriculoperitoneal shunts. *Lancet* **340:**610-613 (1992).

193. N. Touchette. Silicone implants and autoimmune disease: Studies fail to gel. *Journal of NIH Research* **4:**89-92 (1992).

194. F. Audibert, L. Chedid, P. Lefrancier and J. Choay. Distinctive adjuvanticity of synthetic analogs of mycobacterial water soluble components. *Cell. Immunol.* **21:**243-249 (1976).

195. Y. Wang and M. Hanson. Parenteral formulations of proteins and peptides. *J. Parenter. Sci. Technol.* **42:**S2 (1988).

196. M.C. Manning, K. Patel and R.T. Borshardt. Stability of protein pharmaceuticals. *Pharm. Res.* **6:**903-917 (1989).

197. M. Pikal. Freeze-drying of proteins. II. Formulation selection. *Biopharmaceutics* **3:**26 (1990).

198. I. Horacek and L. Kudlacek. Influence of molecular weight on the resistance of polylactide fibers by radiation sterilization. *J. Appl. Polym. Sci,* **50:**1-5 (1993).

199. R. Langer and N. Peppas. Chemical and physical structure of polymers as carriers for controlled release of bioactive agents: a Review. *J. Macromol. Sci.* **23**:61-125 (1983).

200. S.R. Hartas, J.H. Collett and C. Booth. *The influence of gamma-irradiation on the release of melatonin from poly(lactide-coglycolide) microspheres.* in *Proceed. Intern. Symp. Control. Rel. Bioact. Mater.* 1992. Orlando. pp. 321-322.

201. D.B. Volkin and A.M. Klibanov. Minimizing protein inactivation. In T.E. Creighton (ed.), *Protein Function: A Practical Approach,* IRL Press, Oxford, 1989, pp. 1-24.

202. A.M. Klibanov. Stabilization of enzymes against thermal inactivation. *Adv. Appl. Microbiol.* **29**:1-28 (1983).

203. M. Helliwell. The use of bioadhesives in targeted delivery within the gastrointestinal tract. *Adv. Drug Delivery Rev.* **11**:221-251 (1993).

204. A. MacAdam. The effect of gastro-intestinal mucus on drug absorption. *Adv. Drug Delivery Rev.* **11**:201-220 (1993).

205. J.-M. Gu, J.R. Robinson and S.-H.S. Leung. Binding of acrylic polymers to mucin/epithelial surfaces: Structure-property relationships. *Crit. Rev. Ther. Drug Carrier Syst.* **5**:21 (1988).

206. A.B. MacAdam, G.P. Martin, S.L. James and C. Marriott. Preparation and characterisation of anti-porcine gastric mucus antibodies. *J. Pharm. Pharmacol.* **43**:62P (1991).

207. A.B. MacAdam, G.P. Martin, S.L. James and C. Marriott. *Development of a novel delivery system for targeting the gastro-intestinal tract.* in *Proc. Intern. Symp. Control. Rel. Bioact. Mater.* 1992. Orlando: Controlled Release Society, Inc. pp. 277-278.

208. C.-M. Lehr, F.G.J. Poelma, H.E. Junginger and J.J. Tukker. An estimate of turnover time of intestinal mucus gel layer in the rat in situ loop. *Int. J. Pharm.* **70**:235 (1991).

209. M.R. Neutra and J.-P. Kraehenbuhl. Transepithelial transport and mucosal defence I: the role of M cells. *Trends Cell Biol.* **2**:134-138 (1992).

210. P. Sicinski, J. Rowinski, J.B. Warchol, Z. Jarzabek, W. Gut, B. Szczygiel, K. Bielecki and G. Koch. Poliovirus type 1 enters the human host through intestinal M cells. *Gastroenterology* **98**:56-58 (1990).

211. J.S. Wassef, D.F. Keren and J.L. Mailloux. Role of M cells in initial antigen uptake and in ulcer formation in the rabbit intestinal loop model of shigellosis. *Infect. Immun.* **57**:858-863 (1989).

212. R.L. Owen, N.F. Pierce, R.T. Apple and W.C. Cray, Jr. M cell transport of vibrio cholerae from the intestinal lumen into peyer's patches: a Mechanism for antigen sampling and for microbial transepithelial migration. *J. Infect. Dis.* **153**:1108-1118 (1986).

213. S. Kohbata, H. Yokobata and E. Yabuuchi. Cytopathogenic effect of Salmonella Typhi GIFU 10007 on M cells of murine ileal peyer's patches in ligated ileal loops: An ultrastructural study. *Microbiol. Immunol.* **30**:1225-1237 (1986).

214. L.R. Inman and J.R. Cantey. Specific adherence of Escherichia Coli (strain RDEC-1) to membranous (M) cells of the peyer's patch in Escherichia Coli diarrhea in the rabbit. *J. Clin. Invest.* **71**:1-8 (1983).

215. J.L. Wolf, R.S. Kauffman, R. Finberg, R. Dambrauskas, B.N. Fields and J.S. Trier. Determinants of Reovirus interaction with the intestinal M cells and absorptive cells of murine intestine. *Gastroenterology* **85**:291-300 (1983).

216. J.-P. Kraehenbuhl and M.R. Neutra. Transepithelial transport and mucosal defence II: secretion of IgA. *Trends Cell Biol.* **2**:170-174 (1992).

217. E. Bjork, K. Holmberg, B. Bake and P. Edman. *Effect of degradable starch microspheres on the human mucociliary clearance.* in *Proc. Intern. Symp. Control. Rel. Bioact. Mater.* 1992. Orlando: Controlled Release Society, Inc. pp. 417-418.

218. D.T. O'Hagan, D. Rafferty, S. Wharton and L. Illum. Intravaginal immunization in sheep using a bioadhesive microsphere antigen delivery system. *Vaccine* **11**:660-664 (1993).

219. D.B. Bennett, J. Miller, M. Madonna-Langan, H. Ellens, R. Kirsh, R.C. Rathi and J. Kopecek. *Uptake of HPMA-Mannose copolymers by human macrophages and targeting to alveolar macrophages*. in *Proc. Intern. Symp. Control. Rel. Bioact. Mater.* 1992. Orlando: Controlled Release Society, Inc. pp. 66-67.

220. J. Hanes, C. Evora, A. Ben-Jebria, M.L. Eskew, D.A. Edwards and R. Langer. Poly(D,L-lactic-*co*-glycolic acid) microspheres for pulmonary drug delivery. In Preparation (1996).

221. A.C. Allison. Mode of action of immunological adjuvants. *J. Reticuloendothel. Soc.* **26**:619-630 (1979).

222. G. Gregoriadis. Immunological adjuvants: a Role for liposomes. *Immunol. Today* **11**:89-97 (1990).

223. H. Schreier, M. Levy and P. Milhalko. Sustained release of liposome-encapsulated gentamicin and fate of phospholipid following intramuscular injection in mice. *J. Controlled Release* **5**:187-192 (1987).

224. A.L. Weiner, S.S. Carpenter-Green, E.C. Soehngen, R.P. Lenk and M.C. Popescu. Liposome-collagen gel matrix: a novel sustained drug delivery system. *J. Pharm. Sci.* **74**:922-925 (1985).

225. D.A. Eppstein, Y.V. Marsh, M.A. van der Pas, P.L. Felgner and A.B. Schreiber. Biological activity of liposome-encapsulated murine interferon gamma is mediated by a cell membrane receptor. *Proc. Natl. Acad. Sci. USA* **82**:3688-3692 (1985).

226. J. Hanes and R. Langer. Polymeric controlled release vaccine delivery systems. In R.A. Bronson, N.J. Alexander, D. Anderson, D.W. Branch and W.H. Kutteh (eds.), *Reproductive Immunology*, Blackwell Science, Cambridge, MA, 1996, pp. 647-664.

227. P. Kibat, Y. Igari, M. Wheatley, H. Eisen and R. Langer. Enzymatically activated microencapsulated liposomes can provide pulsatile drug release. *FASEB J.* **4**:2533-2539 (1990).

228. A.K. Andrianov, R. Langer, L.G. Payne, B.E. Roberts, S.A. Jenkins and H.R. Allcock. *Polyphosphazene ionotropic gel microcapsules for controlled drug delivery.* in *Proceed. Intern. Symp. Control. Rel. Bioact. Mater.* 1993. Washington D.C.: Controlled Release Society, Inc. pp. 26-27.

229. A.K. Andrianov, L.G. Payne, K.B. Visscher, H.R. Allcock and R. Langer. Hydrolytic degradation of ionically crosslinked polyphosphazene microspheres. *J. Appl. Pol. Sci.* In Press